

Institut für Organische Chemie und Biochemie
der Technischen Universität München

**Carbohydrate-Based Mimetics in Drug Design:
Sugar Amino Acids as Structural Templates and
Key Residues of Bioactive Peptidomimetics**

Sibylle Annette Wunnedta Gruner

Vollständiger Abdruck der von der Fakultät für Chemie der Technischen Universität
München zur Erlangung des akademischen Grades eines

Doktors der Naturwissenschaften

genehmigten Dissertation.

Vorsitzende: Univ.-Prof. Dr. S. Weinkauff

Prüfer der Dissertation: 1. Univ.-Prof. Dr. H. Kessler
2. Univ.-Prof. Dr. W. Hiller
3. Univ.-Prof. Dr. O. Nuyken

Die Dissertation wurde am 12. Dezember 2001 bei der Technischen Universität München
eingereicht und durch die Fakultät für Chemie am 24. Januar 2002 angenommen.

From November 1998 to November 2001, the work for this PhD thesis has been carried out in the working group of Prof. Dr. Horst Kessler at the “Institut für Organische Chemie und Biochemie der Technischen Universität München”.

I would like to thank Prof. Dr. Horst Kessler for the interesting and challenging project, which gave me insight into carbohydrate, peptide, and medicinal chemistry as well as into NMR based structure determination. I thank him for his continuous interest in my work, for his constant assistance of my scientific work as well as supporting my efforts to give talks and presentations at international and national scientific conferences. I very much enjoyed the great scientific freedom, excellent working conditions, and the inspiring, and amicable atmosphere at the Institute.

I would like to thank all my colleagues in the working group of Professor Kessler, especially:

- The people from my laboratory: Mona Wolff and Martin Sukopp, for the excellent working atmosphere;
- Elsa Locardi for the good collaboration in the area of sugar amino acids and the teamwork in writing the Chemical Reviews article, for inspiring scientific discussions, and for being a great friend;
- Mona Wolff, for synthetic contributions, (and for working overtime to help me meet deadlines);
- Martin Sukopp, Ulrich Hersel, Manuel Tönnis, Dr. Claudia Biro, Matthias Stöckle and Niko Schmiedeberg for inspiring discussions;
- Vientent Truffault, and Dr. Gerd Gemecker for introducing me to NMR-structure determination and the “personalities” of our 600 MHz spectrometers;
- Christian Rölz and Georg Voll for teaching me distance geometry calculations.
- Georg Voll for the MD calculation of compound **113**.
- Prof. Dr. György Kéri, Dr. Richard Schwab, and Dr. Aniko Venitiner for the biological testing of the somatostatin analogues.
- My students Thorsten Poethko, Jens Schiener, Martin Paulus, Andreas Enthart, Thomas Quelle, Benjamin Roßbach, Stefan Mitschke, Peter Kaden, Clemens

Wagner, Karin Lüdtke, Linda Valis, Wolfgang Kleist, Alexander Schriewer, and Anita Miess for synthetic contributions to this work;

- The Novaspin Biotech GmbH team for its support, especially Dr. Holger Lüttgen;
- Ulrich Hersel, Martin Sukopp and Dr. Christian Spindler for the critical inspection and reading of this manuscript,
- Dr. Rainer Haeßner for his support of NMR, hardware and software problems, and many hot chocolates,
- Maria Kranawetter for preparative HPLC purifications,
- Burghard Cordes and Dr. W. Spahl for recording MS-spectra.
- Evelyn Bruckmaier and Marianne Machule for secretarial assistance
- And all mentioned and unmentioned co-workers, who have become my close friends;

My special thanks go to Dr. Christian Spindler and to my parents for their understanding and lasting support.

All this contributed to the success of this work.

dedicated to my parents and Christian

1	INCENTIVE	1
2	STATE OF THE ART: SUGAR AMINO ACIDS, AND β-PEPTIDES IN DRUG DESIGN	3
2.1	The Concept of Sugar Amino Acids in Drug Design	3
2.2	Naturally Occurring Sugar Amino Acids	5
2.3	Synthesis of individual SAA building blocks	7
2.3.1	Furanoid SAAs	7
2.3.1.1	α -SAAs	7
2.3.1.2	β - and γ -SAAs	8
2.3.1.3	d-SAAs	10
2.3.2	Pyranoid SAAs	12
2.4	Carbohydrates and SAAs as Scaffolds	14
2.5	Carbohydrate Mimetics	16
2.5.1	Linear Oligomers	16
2.5.2	Cyclic SAA-Oligomers	21
2.5.3	Glucosidase Inhibitors	23
2.6	Peptidomimetics	25
2.6.1	Carbohydrate-Based Peptidomimetics	25
2.6.1.1	Linear SAA Homooligomers and Their Structures	25
2.6.1.2	Turn Mimetics and Model Peptides Containing SAAs	26
2.6.2	β -Peptides	29
2.6.2.1	Helices	30
2.6.2.2	The β -sheet structure	36
2.6.2.3	Tube-like Structures	37
2.7	Biologically Active Peptides Containing SAA Building Blocks	39
2.7.1	Somatostatin Analogues	39
2.7.2	SAAs in enkephalin analogs	40
2.7.3	Protein:Farnesyltransferase	42
2.7.4	Integrin-Ligands	43
3	RESULTS AND DISCUSSION	46
3.1	Synthesis of Two New Furanoid SAAs ^[22, 118-121, 184, 185]	46
3.2	Foldamers ^[22, 118, 119, 184]	48
3.2.1	Solid Phase Synthesis of the Linear Mixed SAA-AA-Oligomers 113 and 115	49
3.2.2	Synthesis of the Cyclic Mixed [f-SAA106- β -hGly] ₃ Oligomer 114 in Solution	51
3.2.3	Structural Analysis	52

3.2.3.1	CD Spectroscopy	52
3.2.3.2	NMR Analysis and MD-Calculations	55
3.2.4	Conclusions	68
3.3	Somatostatin Analogues Containing f-SAA 106 and f-SAA 107 as Structure-Inducing Templates	70
3.3.1	Somatostatin – General Introduction	70
3.3.1.1	Physiological Activity of Somatostatin	70
3.3.1.2	Non-peptidic Somatostatin Analogues	72
3.3.1.3	Somatostatin Receptors	75
3.3.2	Somatostatin Analogues and Cancer	77
3.3.2.1	Chemotherapy	77
3.3.2.2	Somatostatin Analogues in Clinical Use	78
3.3.2.3	Apoptosis	78
3.3.2.4	Concept, Strategy and Design of SAA Containing Somatostatin Analogues	79
3.3.2.5	Synthesis of SAA Containing Somatostatin Analogues on Solid Phase	85
3.3.2.6	Antitumor Activity of the f-SAA Containing Compounds	86
3.3.2.7	Conclusions and Outlook	92
3.3.3	Neurogenic Inflammation – Inflammatory Diseases	94
3.3.3.1	General Introduction	94
3.3.3.2	Biological Test on Anti-inflammatory Activity of Compounds 142-145	98
3.3.3.3	Conclusions	99
4	SUMMARY	100
5	EXPERIMENTAL SECTION	102
6	REFERENCES	134

1 Incentive

The impressive development of molecular biology, biophysical methodology, and computer based molecular modeling and design in the last two decades has caused considerable change in the approach to target and pharmacological lead identification. Unfortunately, the “de novo design” of new biologically active compounds, based on structure activity relationships, has failed to meet expectations. Therefore, in the 90’s combinatorial chemistry paired with robot aided high-throughput screening for certain biological activities and thus lead identification, has emerged as the method of choice. However, it soon became obvious that generating tremendous libraries of millions of randomly chosen compounds, followed by high-throughput screening has also major draw backs.

As a consequence, the combination of rational design and combinatorial chemistry has gained more and more interest. Now, the design of smaller, rationally designed libraries has become the state of the art.

Carbohydrates as well as peptides and proteins are essential biopolymers of life. They are involved in complex biological processes such as catalysis and highly selective molecular recognition. In order to perform these functions, the correct folding of the biopolymers creating the active site is crucial, since any kind of interaction is observed only if the reactive groups are positioned in the correct spatial orientation to each other. Thus, the development of small, easy-to-functionalize building blocks and oligomers with backbones of discrete and predictable folding patterns (“foldamers”) is required in order to design and develop molecules with useful biological functions. Nevertheless, for a successful application, their structural properties have to be scrutinized.

SAs are sugar moieties containing at least one amino as well as at least one carboxyl group. Thus, they may be considered as monomeric building blocks of chimeras between carbohydrates and proteins. They allow among other modifications the

replacement of the naturally occurring, but synthetically difficult to generate, O-/N-glycosidic bonds by peptidic bonds. This not only increases the enzymatic stability, but facilitates the assembly of large, diverse oligomer carbohydrate or peptidomimetic libraries by solid phase techniques as well. Their use as structural templates in peptides, is also a very attractive application of SAAs.

The aim of this work was therefore the development of new SAA building blocks suitable for rational combinatorial synthesis and spatial screening. To meet our demands the SAAs had to full fill a number of requirements:

- They had to be obtainable by a fast, easy to scale up, high yielding and cheap synthetic route.
- They had to have secondary structure inducing properties
- They should introduce chiral diversity
- They ought to be compatible to solid phase synthetic techniques
- and were supposed to enhance enzymatic stability.

The basic structural properties of these new SAA building blocks, the folding patterns and secondary structures induced, were to be investigated by synthesis and structural analysis of several SAA oligomers. Finally, the insights gained were then intended to be applied and evaluated in biologically active systems by implementation of the SAA building blocks in small rational combinatorial libraries of biological active peptides.

2 State of the Art: Sugar Amino Acids, and β -Peptides in Drug Design

2.1 The Concept of Sugar Amino Acids in Drug Design

Among the major classes of biomolecules carbohydrates, allow almost unlimited structural variations due to their chiral diversity and high density of easy to functionalize groups. The molecular diversity of carbohydrates offers a valuable tool for drug discovery in the areas of biologically important oligosaccharides, glycoconjugates and molecular scaffolds by investigating their structural and functional impact. Chimeras of the three big classes of biopolymers, that is, nucleic acids, proteins and carbohydrates, have attracted great interest as both functional, and structural analogues in recent years, also because of their potential application in drug design. However, Sugar Amino Acids^a (SAAs) and their oligomers, which bridge carbohydrates and proteins, have only recently been investigated.^[3, 5, 14-22] SAAs are sugar moieties containing at least one amino as well as at least one carboxyl group (Figure 1).

Besides their immediate intrinsic different pharmacological properties, SAAs can be used as building blocks for the preparation of modified analogs of biologically

^a The term "sugar amino acid", SAA, as a functional, succinct classification term, was introduced by our group and is widely accepted, although a plethora of terms have been proposed in the literature for compounds derived from SAAs. These include saccharide-peptide hybrids, glycosamino acids and glycotides,^[1] peptidosaccharides,^[2] saccharopeptides,^[3] amide-linked carbohydrates, tetrahydro-furan (pyran) amino acids and carbopeptoids,^[4-7] although the latter compounds most often do not have a peptoid functionality (IUPAC definition). The term saccharopeptides has also been used to describe oligosaccharides in which the glycosidic linkage has been replaced by an amide bond.^[8, 9] Some publications use the term "sugar amino acids" for glycosylated amino acids,^[10, 11] for a disaccharide based on an amino- and carboxyl cyclopropyl-carbohydrate derivative,^[12] or in one case even for conjugates based on the Michael addition of C-terminally protected amino acids to 2,3-dideoxy-hex-2-enopyranos-4-uloses.^[13] In some cases the SAAs are linked to each other, in other cases to amino acids. Herein the term SAA is used for compounds with two immediate linkages of the amino and carboxy functionalities to the carbohydrate frame. Further elongations with one connectivity, that is a carbon chain, are considered glycosylated amino acids or glycopeptides.

active peptides and/or oligosaccharides. The difference in ring size allows modification of the conformations of the peptides and carbohydrates.

SAs can as well be used as starting compounds for different oligomers. They are potential pharmaceutical compounds, are valuable for the synthesis of natural products or analogs, and also as building blocks in drug design and drug research.

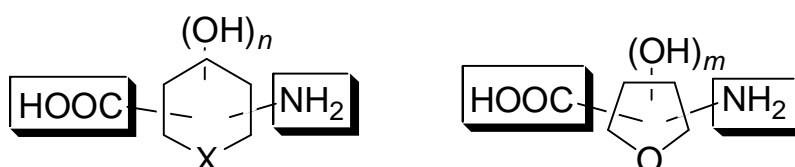


Figure 1: *Sugar amino acids as structural scaffolds, as carbohydrate mimetics, and as peptide mimetics.*

In the following the state of the art of SAA synthesis, with emphasis on furanoid SAs, their incorporation in peptidic or saccharidic structures, and their potential use in medicinal chemistry is described.

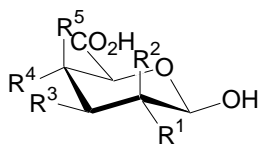
2.2 Naturally Occurring Sugar Amino Acids

Some sugar amino acids can be found in nature largely as construction elements. The most prominent and abundant example is sialic acid often located peripherally on glycoproteins. This family of natural SAAs consists of *N*- and *O*-acyl derivatives of neuraminic acid **1** (Figure 2). The main substituents on nitrogen are the *N*-acetyl and *N*-glycosyl groups. Glycosaminuronic acids (**2-5**) are more common in form of their derivatives. For instance 2-acetamido-2-deoxy-glucuronic acid is found in bacterial cell walls^[23] and 2-acetamido-2-deoxygalacturonic acid is one component of bacterial Vi antigen of *Escherichia coli*.^[24] Derivatives of glucosaminuronic acid were also detected in the cancomycin family of antibiotics similar to vancomycin.^[25]

Interestingly, natural SAAs can be found in nucleoside antibiotics.^[26] Two different 3-amino-3-deoxy uronic acids, derivatives of 3-amino-3-deoxy-D-gulopyranuronic acid and 3-amino-3,4-dideoxy-D-xylohexopyranuronic acid, were found in ezomycin A **6**.^[26, 27] 4-Amino-4-deoxy-glucuronic acid **5**, can be found in gougerotin,^[28-32] a antibiotic from *Streptomyces* bacteria, as the carbohydrate residue of the nucleoside.

The naturally occurring furanoid SAA (+)-hydantocidin **7** (Figure 2), which represent a spirohydanthion derivative,^[33-35] exhibits herbicidal activity.

Siastatin B **8** (Figure 2) is among the class of SAAs, in which the nitrogen is located within the pyranoid ring structure. This inhibitor for both β -glucuronidase and *N*-acetylneuraminidase was isolated from a *Streptomyces* culture.^[36]



Glycosaminuronic acids		R ¹	R ²	R ³	R ⁴	R ⁵
glucosaminuronic acid	2	NH ₂	H	OH	OH	H
galactosaminuronic acid	3	NH ₂	H	OH	H	OH
mannosaminuronic acid	4	H	NH ₂	OH	OH	H
4-amino-4-deoxy-glucuronic acid	5	OH	H	OH	NH ₂	H

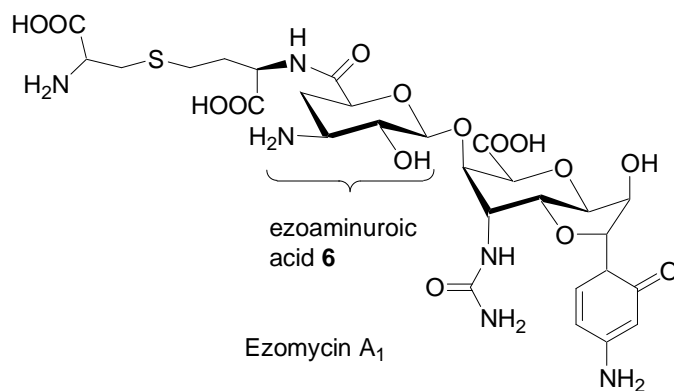
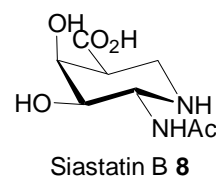
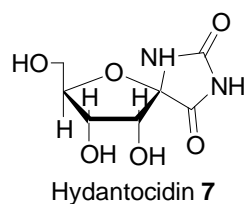
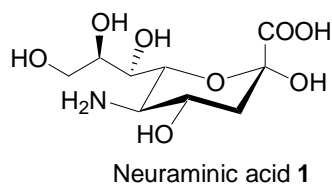


Figure 2: Naturally occurring sugar amino acids.

2.3 Synthesis of individual SAA building blocks

The synthesis of sugar amino acids is accomplished starting from commercially available, or easy accessible monosaccharides, i.e., glucose, glucosamine, diacetone glucose, galactose, etc. The amino functionality of the SAA is usually introduced as an azide, cyanide or nitromethane equivalent, followed by subsequent reduction. The carboxylic function is introduced directly as CO₂, or as a hydrolyzable cyanide, by a Wittig reaction and subsequent oxidation or by selective oxidation of a primary alcohol.

2.3.1 Furanoid SAAs

2.3.1.1 α -SAAs

Several derivatives with an α -amino acid moiety at the anomeric position of the sugar were synthesized by Fleet et al. including glucose,^[37] rhamnose,^[38] galactose,^[39] and mannose^[6] (Figure 3) derivatives. The various routes developed by Fleet's group and Dondoni's group have recently been summarized.^[11]

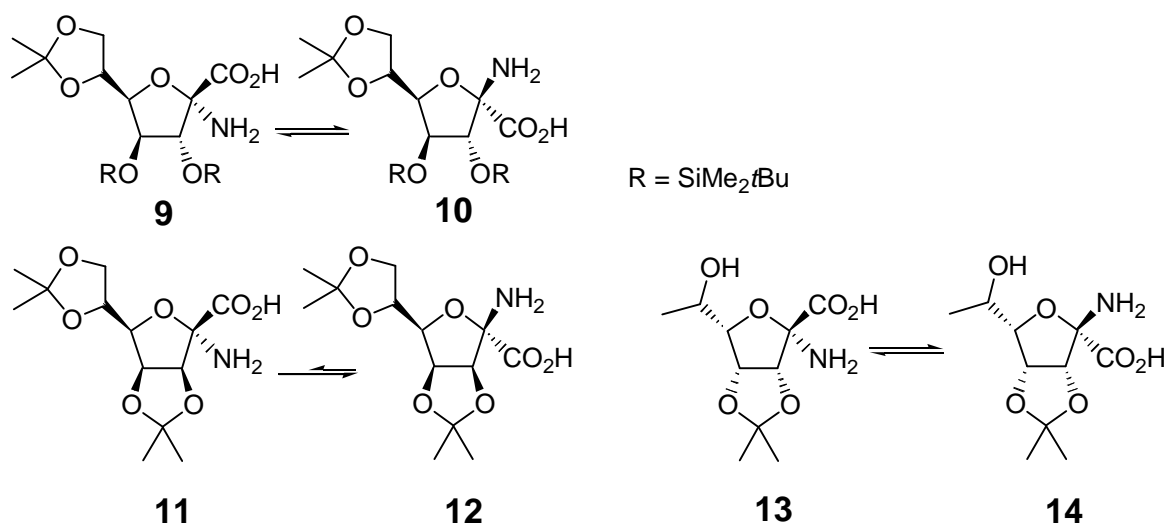


Figure 3: Some of Fleet's α -SAAs.

Fleet's azide precursors and N-protected SAAs are stable against epimerization; however, all free SAAs (also the pyranoid derivatives) and their respective esters equilibrate to a mixture of α - and β -anomers in solution.

This class of SAAs has also been employed as precursors to five- and six-membered spiroheterocyclic derivatives of carbohydrates such as the rhamnose functionality, required for enhanced activity analogs of hydantocidin.^[38-40] The naturally occurring (+)-hydantocidin **7**^[33-35] (see Figure 2) exhibits herbicidal activity. Those spirodiketopiperazine derivatives are considered as potential inhibitors of carbohydrate processing enzymes and thus might be useful in elucidating the biosynthesis of the cell walls of mycobacteria.

2.3.1.2 b- and g-SAAs

Fleet et al. published the synthesis of several azide precursors to β - and γ -SAAs shown in Figure 4.^[41, 42]

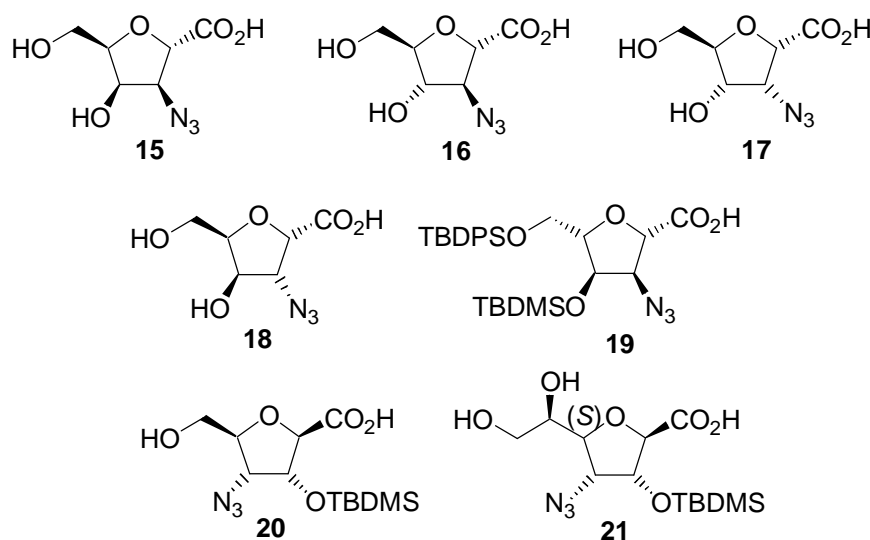
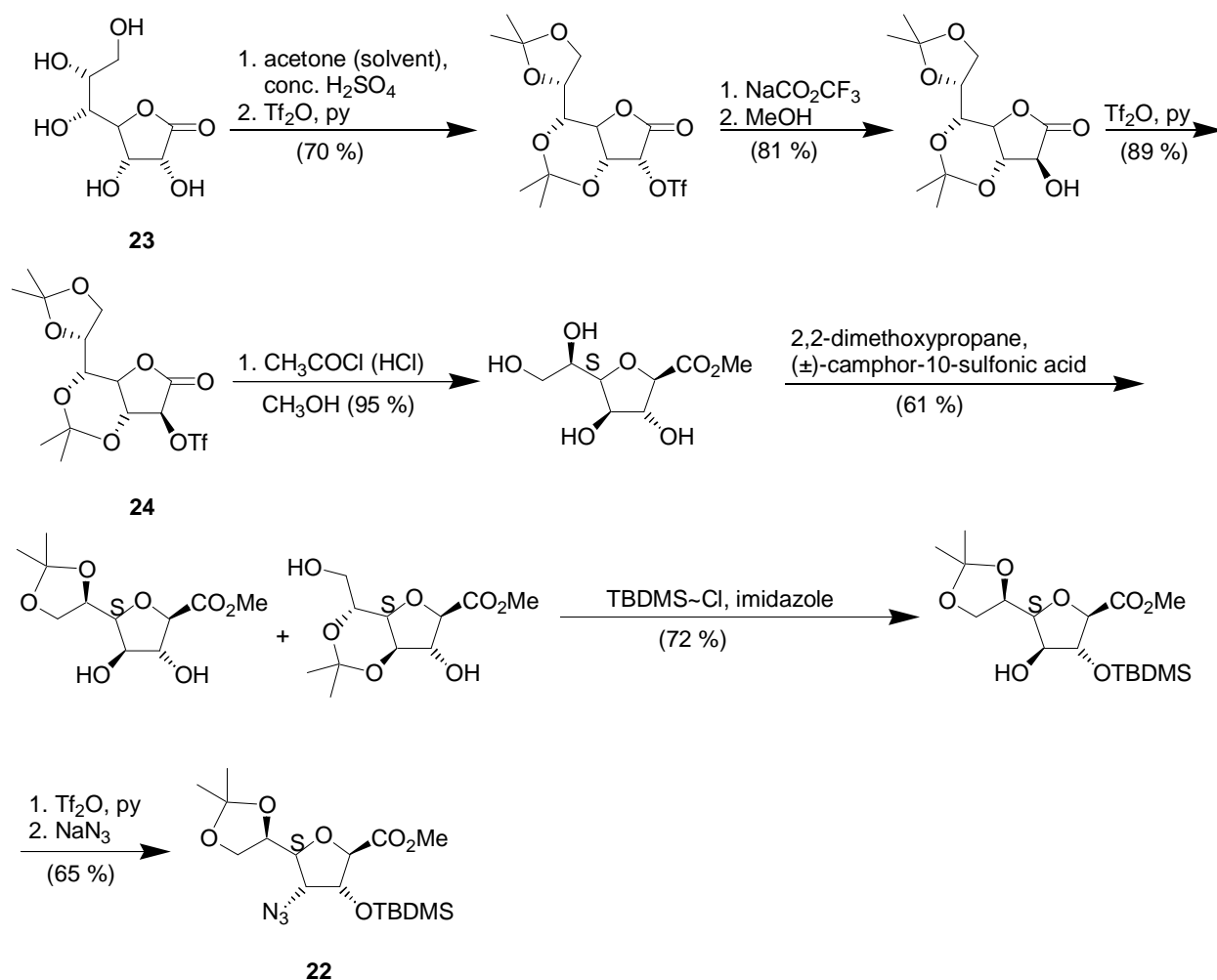


Figure 4: Some of Fleet's large collection of azides, used as **b**- and **g**-SAA precursors.

They synthesized the β -SAA precursor **19** and the γ -SAA precursors **20** and **21** via **22**, which was obtained by the route described in Scheme 2.^[42-46] Key step of the

synthesis of **22** was the hydrolysis of the side-chain acetonide of **24** and methanolysis of the lactone with intramolecular displacement of the triflate at C-2 by 5-OH.^[43, 46] Side-chain hydrolysis of the acetonide of **22** afforded the γ -SAA precursor **21**, subsequent periodate cleavage, followed by immediate cyanoborohydride reduction of the resulting aldehyde in acetic acid yielded the γ -SAA precursor **20**. Overall yields for **20** and **21**, starting from *D-glycero-D-gulo*-heptono-1,4-lactone **23**, were 10 % and 13 %, respectively. Sodium borohydride reduction of the ester function in **22**, followed by a series of protection deprotection steps and subsequent oxidation of the diol moiety with sodium periodate in the presence of catalytic amounts of ruthenium(III) chloride led to the β -SAA precursor **19** in an overall yield starting from **23** of about 3%.



Scheme 2: Synthesis of protected \mathbf{g} -SAA precursor **22**.

2.3.1.3 d-SAAs

As dipeptide isosteres for the incorporation into peptide based drugs Le Merrer and co-workers synthesized **25** and **28** (Figure 5).^[47] The benzylated derivatives were designed as mimics for hydrophobic, the unprotected SAAs as mimics for hydrophilic amino acids (see also chapter 2.7).

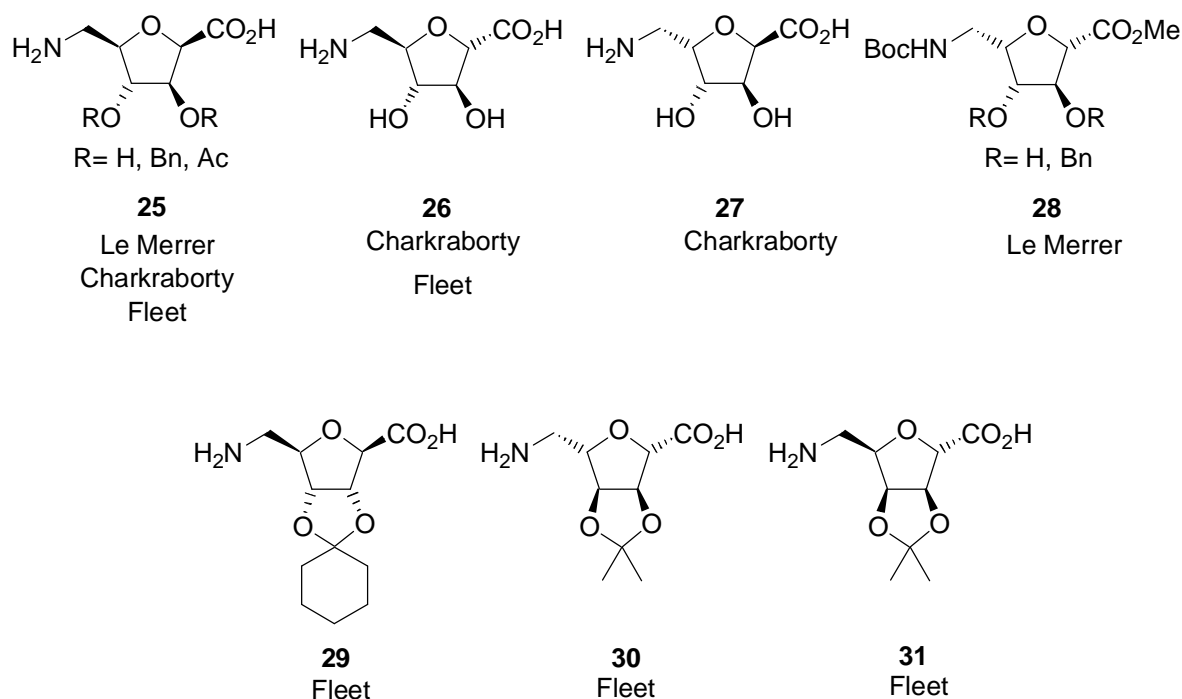
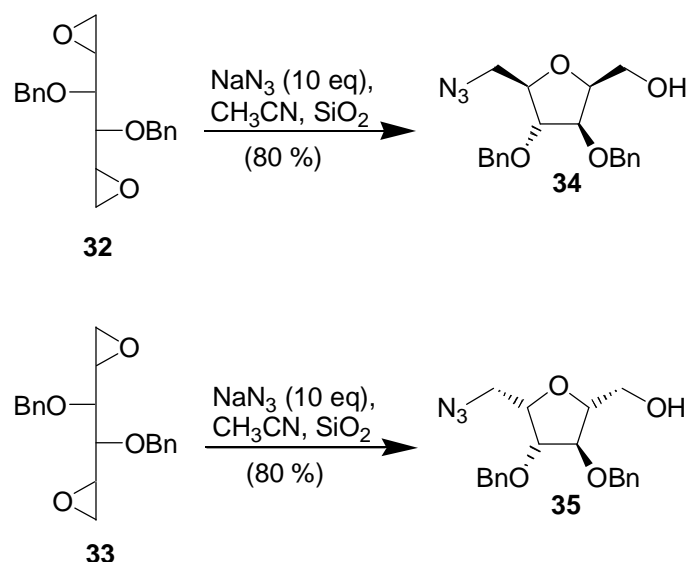


Figure 5: Some of Le Merrer's, Fleet's and Charkraborty's furanoid d-SAAs.

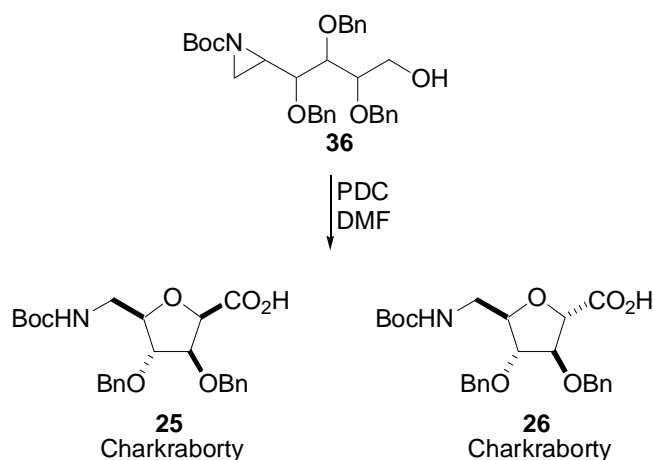
Key step of their synthesis was the one-pot silica gel assisted azidolysis followed by *O*-ring closure of the bis-epoxides **32** and **33** (Scheme 3) to yield **34** and **35** respectively. Sodium dichromate oxidation of the primary hydroxyl group, treatment with an excess of diazomethane, followed by a one pot conversion of the respective azidoesters by hydrogenolysis in presence of di-*tert*-butyldicarbonate, yielded the N-Boc protected, fully benzylated SAA methylesters of **25** and **28**.



Scheme 3: Key step of Le Merrer's synthesis of **25** and **28**.

SAA **25** was also synthesized by Chakraborty's and Fleet's groups, using different reaction pathways.^[48-51]

Furthermore, also for the use as dipeptide isosteres, Chakraborty et al. synthesized several new δ -SAAs (Figure 5).^[48, 49] The key step of their synthesis of SAA **25** and SAA **26** followed a different reaction path, in which an intramolecular 5-*exo* opening of the terminal aziridine ring (Scheme 4) of the hexose-derived substrate **36** (with the respective stereochemistry) by the γ -benzyloxy oxygen with concomitant debenzoylation occurred during pyridinium dichromate (PDC) oxidation of the primary hydroxyl group with complete stereocontrol.



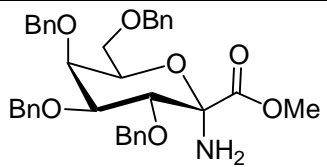
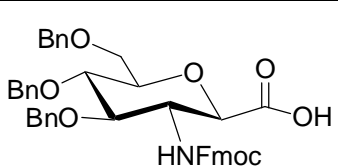
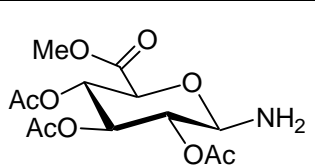
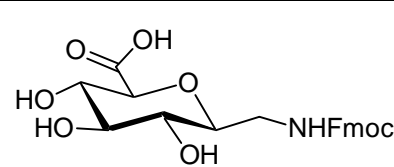
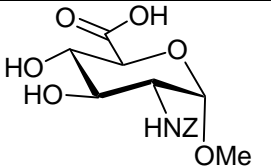
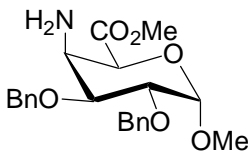
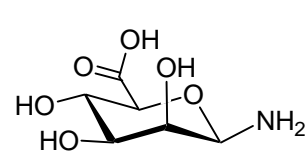
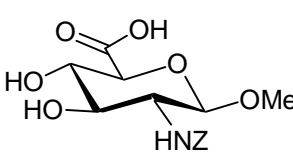
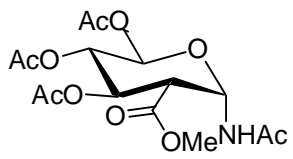
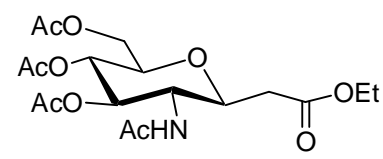
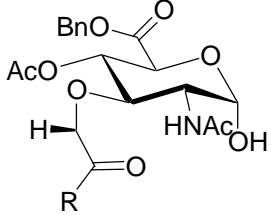
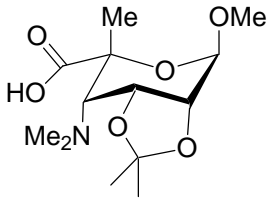
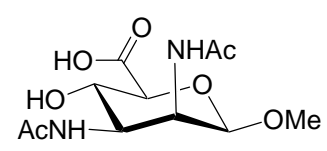
Scheme 4: Synthesis of **25** and **26** starting from **36**. The stereochemistry of **36** determines, if the synthesis results in **25** or **26**.^[49]

At about the same time Fleet et al. synthesized a wide range of different δ -SAAs including also **25**, to study the influence of the SAA's stereochemistry and that of the hydroxyl protecting groups on the secondary structure of their linear homooligomers.^[19, 20, 50-54] A few representative examples are shown in Figure 5.

2.3.2 Pyranoid SAAs

The most obvious approach for the synthesis of pyranoid SAAs is the oxidation of amino sugars for example glucosamine. Thus, Heyns and Paulsen described the first synthesis of the SAA, glucosaminuronic acid, in 1955 by catalytic oxidation of the primary hydroxyl group,^[55] in an effort to elucidate the structure of bacterial cell wall components and synthesize analogues. The oxidation of the amino sugar was also used by Paulsen et al. in the early synthesis of D-galactosaminuronic acid to confirm the structure of isolated components of bacterial Vi antigen.^[24] Since then a large number of pyranoid α -, β -, γ -, d-, and e-SAAs have been synthesized using various, sometimes very elegant methods (Table 1).^[18, 21, 22, 56]

Table 1: Some pyranoid SAAs and references for their synthesis.

a-SAAs	β -SAAs	?-SAAs	d-SAAs	e-SAAs
 <p>37^[11, 57, 58]</p>	 <p>38^[22]</p>	 <p>39^[22]</p>	 <p>43^[14, 22, 59]</p>	 <p>47^[55]</p>
		 <p>40^[60]</p>	 <p>44^[61, 62]</p>	 <p>48^[63, 64]</p>
		 <p>41^[65]</p>	 <p>45^[66]</p>	 <p>49^[67]</p>
		 <p>42^[68]</p>	 <p>46^[69]</p>	

2.4 Carbohydrates and SAAs as Scaffolds

Carbohydrates represent an attractive source of readily available, stereochemically defined scaffolds as they contain well-defined and readily convertible substituents with a rigid pyran ring or the more flexible furan ring.^[70-73] The functional pharmacophoric groups can thus be presented in a distinct arrangement.

The genesis of carbohydrate privileged structures was first described by Hirschmann and co-workers.^[74] A somatostatin agonist was discovered which contained a deoxyglucose nucleus carrying the key amino acid side chains of a cyclic hexapeptide agonist (Figure 6).^[70] Successively, a NK-1 receptor antagonist was identified by modification of the deoxyglucose-based somatostatin agonist.^[75, 76]

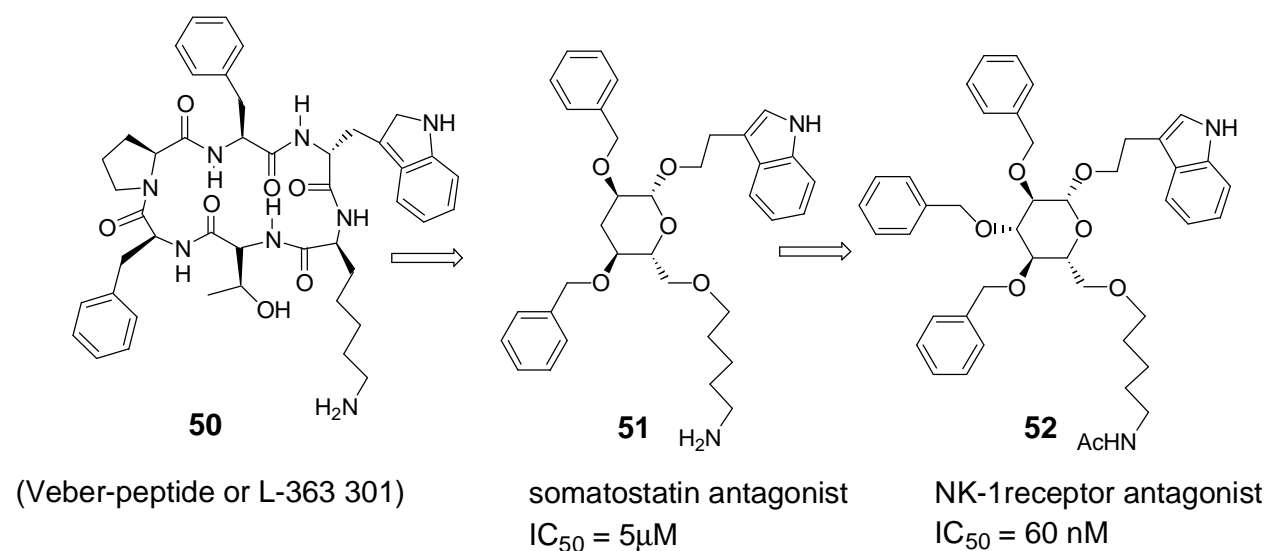


Figure 6: Glucose-based scaffold for the cyclic hexapeptide.

The tetrasubstituted xylofuranose **53** was synthesized by Papageorgiou et al. as a potential nonpeptide mimic of somatostatin (Figure 7).^[77] The scaffold was designed based on molecular dynamics simulations and the results from Hirschmann et al.^[70] The biological activity of the mixture of the α and β anomers in a ratio of 2:3 revealed a rather low $IC_{50} = 16\mu M$. They did show a similar conformational behavior as the Hirschmann scaffolds.

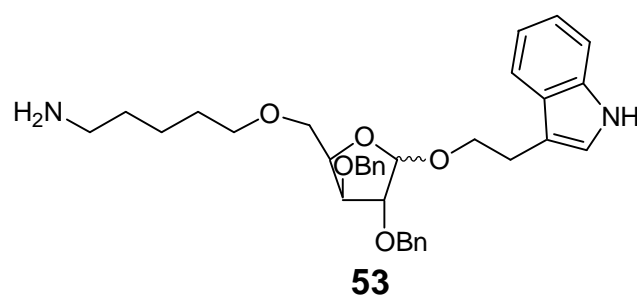


Figure 7: Somatostatin scaffold based on xylose by Papageorgiou et al.^[77]

Sugar amino acids in particular are also ideal peptidomimetic scaffolds, as they may function as structural pharmacophores depending on their substituents in addition to the imperative amino and carboxyl function.^[14] Smith III et al. reported the design of an inhibitor of mammalian ribonucleotide reductase (mRR) **54** based on the bound conformation of the heptapeptide N-AcFTLDADF **55** using a pyranoid SAA scaffold (Figure 8).^[78] This SAA was employed to mimic a β -turn present in the peptidic precursor and to carry, *via* ether linkage, the pharmacophores, Leu and Asp side chains, present in the $i+1$ and $i+2$ positions of the turn, respectively. The tetrahydropyran-based mimetic **54** was found to inhibit mRR, though considerably less well than the peptidic N-AcFTLDADF (K_i of 400-500 μ M for **54** vs. K_i of 15-20 μ M for **55**).

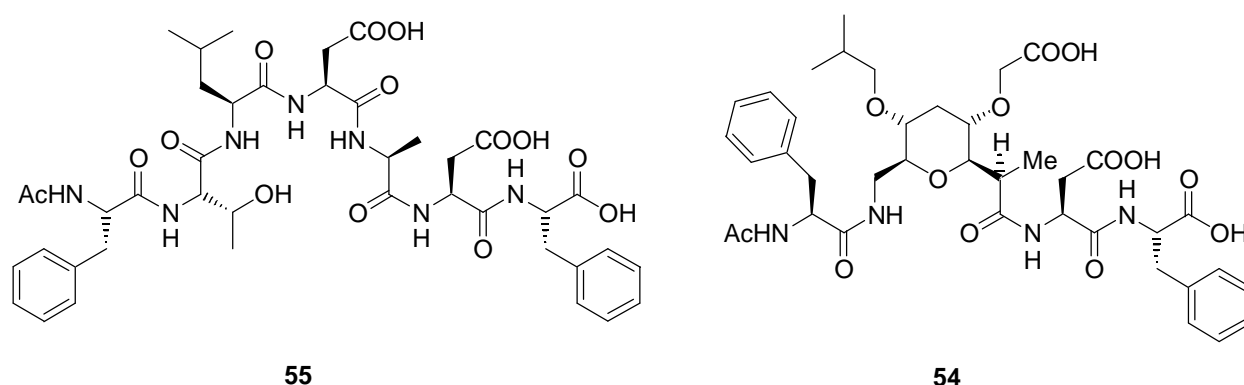


Figure 16: SAA-derived inhibitor **54** of mammalian ribonucleotide reductase.^[78]

2.5 Carbohydrate Mimetics

SAs have been used as analogs of biopolymer building blocks to mimic oligo- and polysaccharide structures *via* amide bond linkages.^[79, 80] In fact, the assembly of synthetic polysaccharide libraries in solution or on solid-phase is difficult in spite of the recent progresses using chemical and enzymatic techniques.^[81, 82] Taking advantage of the well-established chemistry of peptides many homooligomers from SAs and hybrid sequences containing natural amino acids (AAs), carbohydrates and SAs have been synthesized. The resultant oligomers represent useful drug candidates, since they may overcome the problems associated with oligosaccharide and peptide libraries such as the susceptibility towards glycosidases due to the altered peptide backbone, and such as their resistance to many proteases due to their resemblance to carbohydrates.

2.5.1 Linear Oligomers

The first oligomers were synthesized in solution by Fuchs and Lehmann, although they only characterized the individual products by mass spectroscopy.^[83-86] The first dimers were synthesized from D-glucosaminuronic acid and D-mannosaminuronic acid by coupling with DCC by Tsuchida et al. in 1976.^[87]

More recently oligomers were synthesized both in solution^[3, 5, 16] and on solid phase,^[17, 88] and have been proposed to mimic oligosaccharides^[4] and oligonucleotides (so called GNA, Glucopyranosyl Nucleic Amide) (Figure 9).^[89, 90] The aim of GNA development was to improve the properties of the presently most useful class of antisense agents, the phosphorothioates. Hence, to find more stable agents, less toxic and more selective binders than the phosphorothioates. After the discovery, that peptide nucleic acid (PNA) is a selective binder of DNA and RNA, the idea of replacing the phosphodiester linkages with amide bonds was advisable. Following this idea Goodnow et al. presented oligomers of **43** (Gum) as novel antisense agents with

the nucleobases attached *via* N-glycosidic linkage at the anomeric center.^[89, 90] The GNAs showed similar selectivity and binding affinities as DNA and RNA.

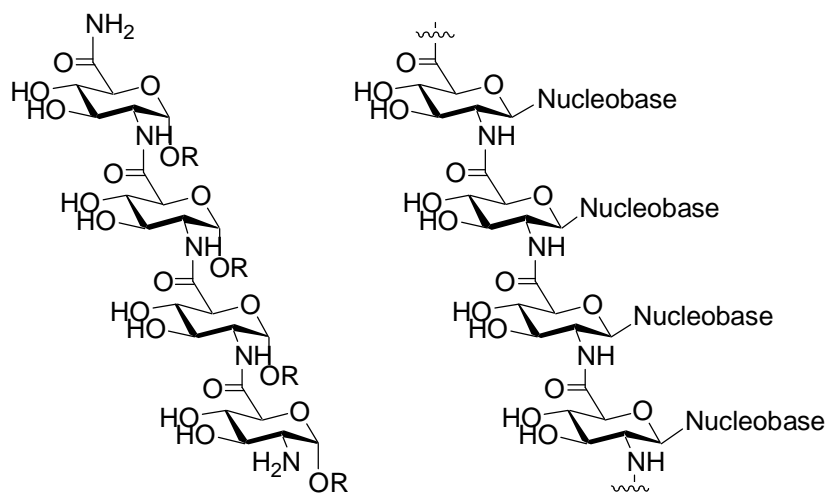


Figure 9: Oligomers of Gum; $R=Me$,^[91] $R=Bn$ ^[88] and with nucleobases.^[89, 90]

Wessel and co-workers, who first introduced in 1995 the synthesis of amide-linked oligomers in solution (Figure 9), used a [2+2] block synthesis.^[3] In their synthetic protocol benzyloxycarbonyl (Z) was employed as amine protecting group and carboxylic acids were protected as *tert*-butyl ester. The two monomer building blocks were coupled *via* mixed anhydrides and the so obtained dimer after *tert*-butyl deprotection was activated *via* 2-chloro-4,6-dimethoxy-1,3,5-triazine (CDMT). No protection of the hydroxyl groups was needed.

Fügedi et al. presented several oligomers, which were evaluated in glycosidase inhibitor assays with moderate activities (Figure 10).^[91-94]

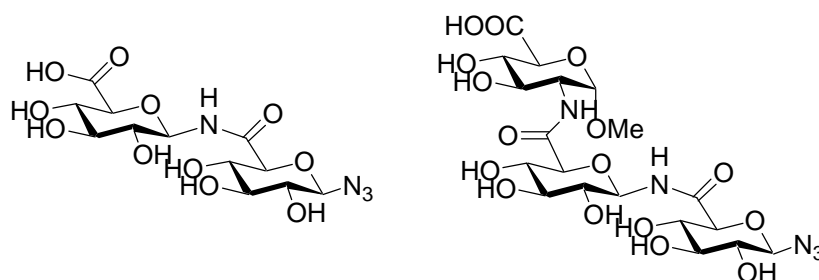


Figure 10: Oligomers by P. Fügedi's group.^[92, 94]

In the field of carbohydrate mimetics sialic acid analogs have received particular attention. Sabesan reported the peptide linked sialoside **56** mimicking an α -D-NeuAc(2 \rightarrow 6) β -D-Gal unit which is found in numerous glycoproteins and glycolipids, and as well as a receptor ligand for influenza virus hemagglutinin and as a substrate for neuraminidase (Figure 11).^[2] The inhibitory activity of **56** was not reported.

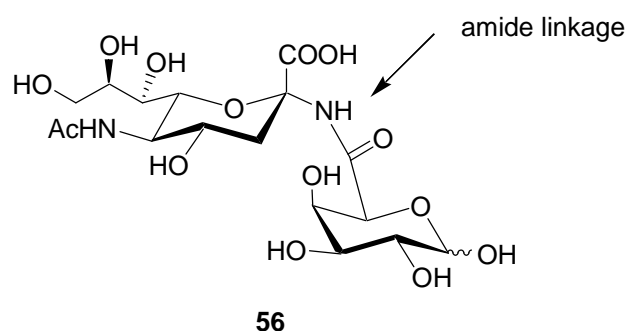


Figure 11: SAA-galactose conjugate **56** with an amide linkage replacing the natural ether linkage.^[2]

Gervay et al. described the synthesis of amino acid conjugates to *N*-acetylneuraminic acid^[95, 96] and later that of amide-linked dimeric sequences in solution.^[97] Oligomer **57** (Figure 12) however was synthesized using solid-phase techniques. To determine whether it adopted the same conformation as its glycosyl-linked cognate, its solution structure was analyzed.^[17] Although the conformational preferences of these structure were not completely resolved and were dependent on chain-length, amide proton NH/ND exchange rates determined by NMR and circular dichroism spectra can be interpreted as evidence for a preferred secondary structure.

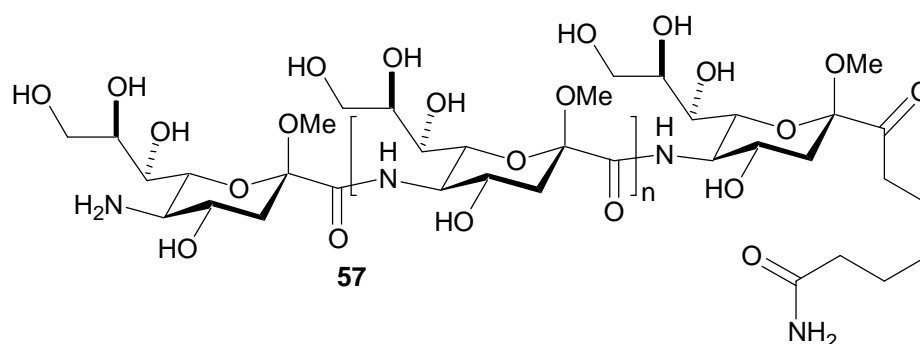


Figure 12: Amide-linked sialooligomers by Gervay et al.^[17, 95]

SAA oligomers were sulphated as reported by the Ichikawa group (Figure 13) to mimic and replace natural sulphated polysaccharides such as dextran sulfate and heparin, well-known inhibitors of HIV replication, in order to overcome the poor absorption, instability and anticoagulant activity of their precursors. A sulphated tetrameric analogue linked *via* the C-1 β -carboxylate and the C-2 amino groups fully blocked syncytium^b formation caused by HIV infection to CD4 cell at 50 μ M concentration,^[5] and the sulphated β -1,6 amide-linked analogue showed micromolar activity in the protection of MT2 cells from HIV infection.^[16]

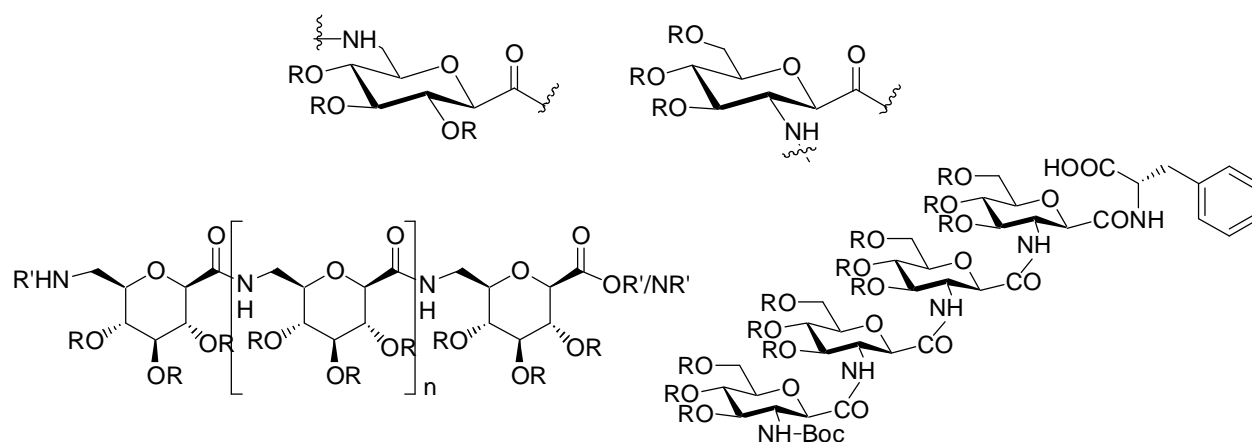


Figure 13: SAA oligomer building blocks and general structures of the oligomers by Ichikawa *et al.* ($R=H, SO_3Na$)^[5, 16]

Hybrid molecules with alternating SAAs and β -amino acids were also designed (Figure 14).^[98] The objective was to create another class of non-natural peptide or carbohydrate molecules and to screen them in an *in vitro* assay system involving highly metastatic tumor cell lines. An inhibitory activity towards cell adhesion (Chemotaxis) and invasion was observed with an $IC_{50} = 10 \mu$ M.

^b *syncytium*: Multinucleated masses produced by the fusion of many cells; often associated with viral infections.

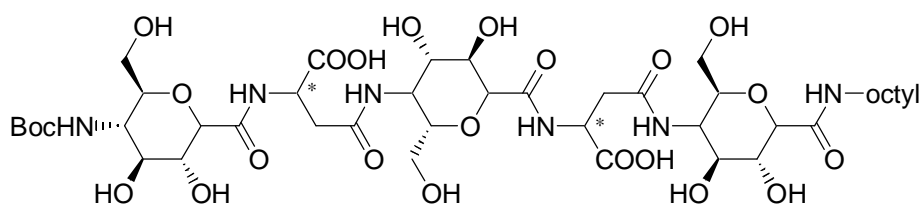


Figure 14: SAA-amino acid conjugates by Ichikawa et al.^[98]

The work of van Boom et al. introduced a new aspect to the synthesis of SAA oligomers. For the first time glycosylated SAAs or disaccharide SAAs were used to assemble the branched oligosaccharide mimetic **58** as a mimetic of the phytoalexin elicitor branched α -methyl heptaglucoside **59** (Figure 15). In **58** four amide bonds replace the β -1,6-acetal linkages of the pentasaccharide backbone of **59**.^[99] The building blocks for oligomer **58** were readily accessible by glycal chemistry. They attributed the lack of phytoalexin-elicitor activity shown by the β -1,6-glucuronosylamide oligomer to the reduced flexibility of the amide bond with respect to the native acetal bond or to a different molecular structure and hydrogen-bonding potential.

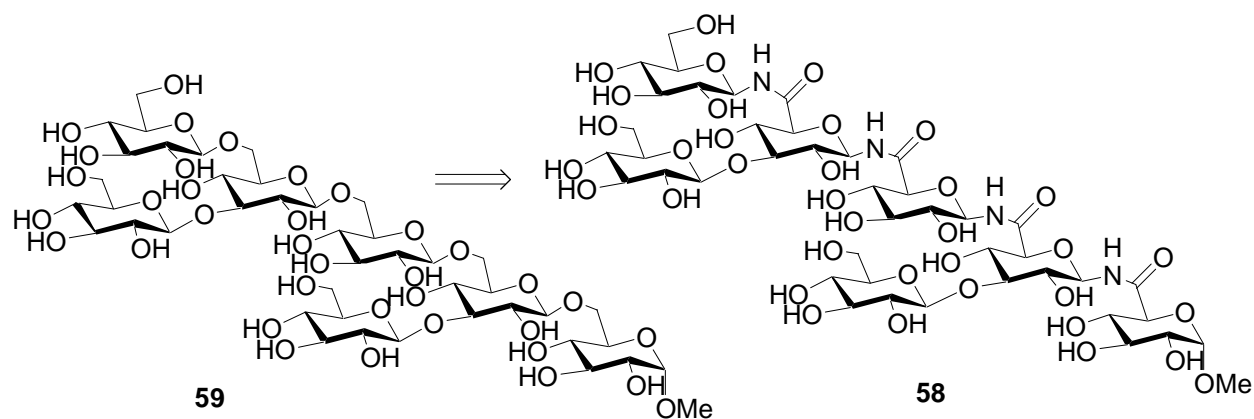


Figure 15: Structures of the $3^2,3^4$ -di-**b**-D-glucopyranosylgentiopentaoside **59** exhibiting phytoalexin-elicitor activity and the SAA-oligomer **58**.^[99]

With the aim of designing artificial glycoclusters with specific functions, Nishimura and co-workers^[100] reported the synthesis of poly(SAAs) **60** able to self-assemble to form stable monomolecular layers (Figure 16). Polymerization of 1-*O*-

dodecyl-Gum, derived from the readily available D-glucofuranurono-6,3-lactone, was accomplished using diphenylphosphoryl azide (DPPA).

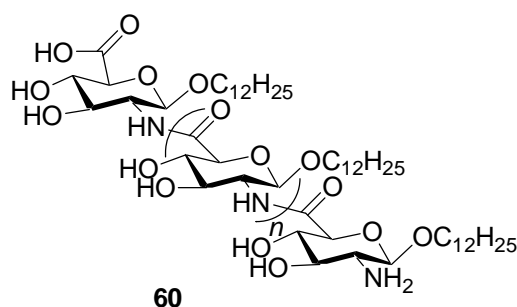


Figure 16: Poly(SAAs) able to self-assemble.

2.5.2 Cyclic SAA-Oligomers

Recently, mixed cyclic oligomers containing SAAs have been proposed by van Boom et al.^[101] and by us as potential molecules for host guest chemistry (Figure 17).^[102, 103] 2D NMR data suggests preferred secondary conformations for oligomers **61**^[101] and **62**.^[102, 103]

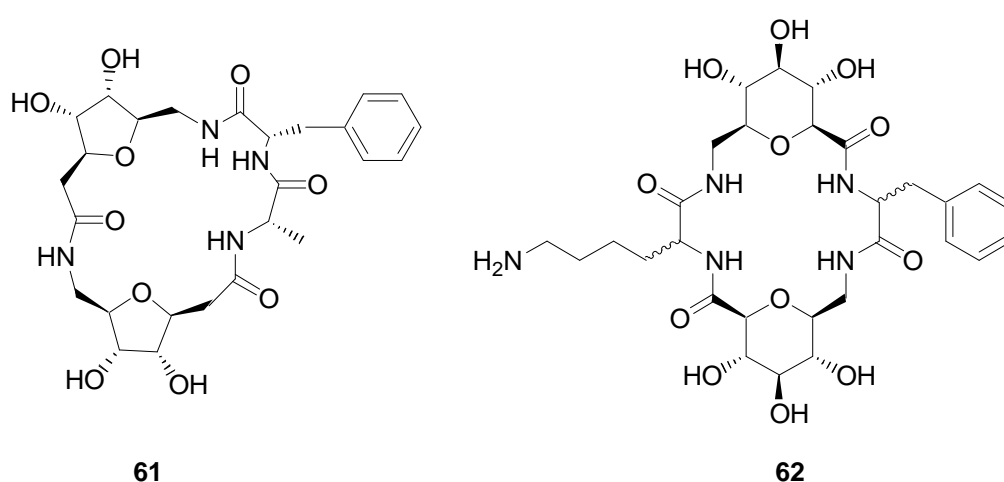


Figure 17: Mixed cyclic oligomers **61**^[101] and **62**.^[102]

The parallel solid-phase synthesis of cyclic sugar amino acid/amino acid hybrid molecules containing furanoid SAAs was carried out by van Boom et al. using Boc *N*-protection strategy and BOP/DIPEA as coupling reagents.^[101] The first amino acid was anchored on an oxime resin in order to employ acid catalyzed cyclization and cleavage from the resin.

In recent work, we introduced cyclic homooligomers of SAAs as novel cyclodextrin-like artificial receptors (Figure 18).^[59] This idea was based upon the assumption that a cyclic array of carbohydrate moieties and amino acid functional groups may lead to exquisite specificity of recognition and catalysis.

By exploiting standard solid and solution phase coupling procedures linear and cyclic homooligomers containing Gum were synthesized.^[59] High yields and very short coupling times for the oligomerization and cyclization of sequences containing 2, 3, 4 and 6 units were achieved. The conformational preferences in aqueous solution of the cyclic derivatives and their applications as potential host molecules were described. Taking into consideration the *trans* configuration of the amide bonds and the ⁴C₁ conformation of the pyranoid ring, confirmed *via* coupling constants and ROE data, two low energy structures were found for the SAA unit which differ in the relative orientation (*syn* or *anti*) of the C-H⁵ and C=O bonds. Stereoviews of the all-*syn* and all-*anti* conformations of the cyclic trimer are depicted in Figure 18. The molecular structure of the cyclic oligomers in the all-*syn* conformation generates a hydrophilic exterior surface and a nonpolar interior cavity which resemble the cyclodextrin molecular shape. Indeed, the complexation of the cyclic hexamer with two model guest molecules (*p*-nitrophenol, benzoic acid) was proved from titration studies using NMR the spectroscopic parameters: chemical shifts, longitudinal relaxations (T₁) and diffusion coefficients. All of them showed different values for host and guest molecules measured independently and in the presence of each other.

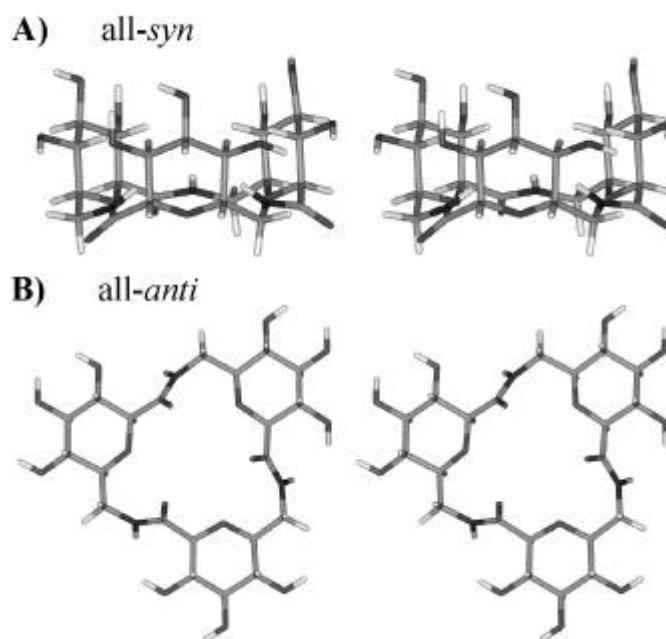


Figure 18: *Stereoviews of the all-syn and all-anti conformations of the cyclic trimer.*

2.5.3 Glucosidase Inhibitors

Sugar mimics in which the ring oxygen has been replaced by nitrogen have gained considerable interest as inhibitors of glycosidase, enzymes which are involved in numerous biological processes. The nitrogen substitution renders the compounds metabolically inert, but does not prevent their recognition by glycosidases and other carbohydrate-recognizing proteins. They inhibit glycosidases by mimicking the pyranosyl and furanosyl moiety of the corresponding substrates. The realization that amino-sugar glycosidase inhibitors might have enormous therapeutic potential in many disease or protective mechanisms by altering the glycosylation or catabolism of glycoproteins, or by blocking the recognition of specific sugars, has led to a tremendous interest and demand of these compounds. Thus, glycosidase inhibitors are potential antiviral, anticancer and antidiabetic drugs. As the extraction and isolation of naturally occurring glycosidase inhibitors from often rather scarce sources is both time-consuming and costly, many natural products and analogues have been synthesized.^[104-106]

Many of them, may be considered as SAAs, like the examples shown in Figure 19. The analogue **63** of deoxymannonojirimycin was isolated from *Lonchocapus seciceus*, and has been shown to be a potent and specific inhibitor for both a glucoprotein^c-processing mannosidase and a bovine α -L-fucoside.^[107] (2*S*,3*R*,4*R*,5*S*)-3,4,5-Trihydroxypipelic acid **64** was isolated from *Raphia racemosa*^[108] as a glucuronidase and iduronidase inhibitor.^[109] Siastatin B (**8**) is a potent neuraminidase inhibitor, and was first isolated in 1974 from *Clostridium perfringens*,^[36] its absolute configuration was proven by total synthesis.^[110] The inhibitory activity of those isolated natural SAAs, sparked extensive research in that field and many synthetic derivatives were synthesized.^[111, 112] Using **63** as a lead structure Ichikawa et al. developed the potent ($K_i = 79$ nM) β -glucuronidase inhibitor **68**.^[113]

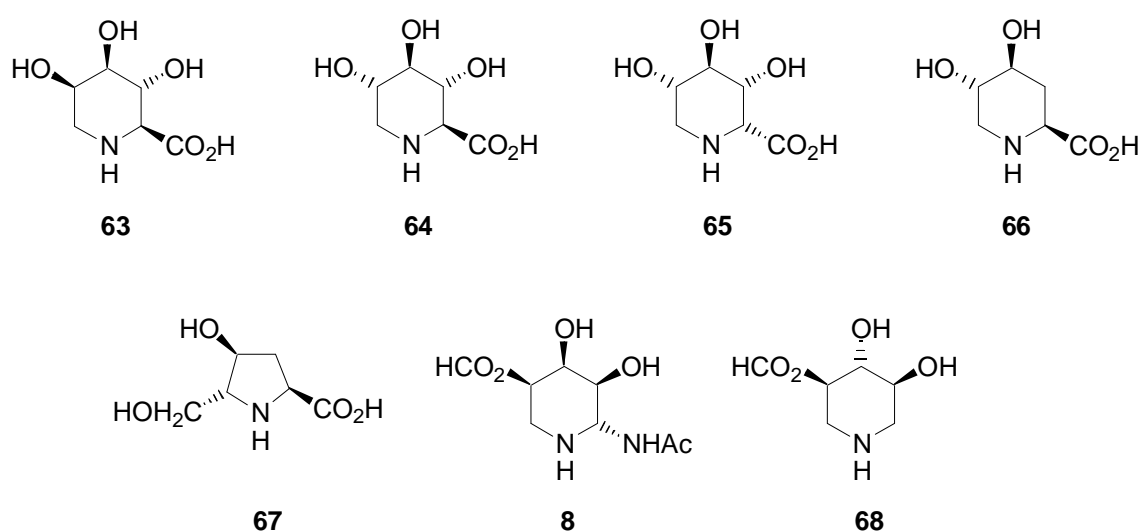


Figure 28: Some of the SAA, which are glucosidase inhibitors; their names and references: **63** (2*S*,3*R*,4*R*,5*R*)-3,4,5-Trihydroxypipelic acid,^[107] **64** (2*S*,3*R*,4*R*,5*S*)-3,4,5-Trihydroxypipelic acid,^[108, 109, 112] **65** (2*R*,3*R*,4*R*,5*S*)-3,4,5-Trihydroxypipelic acid,^[112] **66** (2*S*,4*S*,5*S*)-3,4-dihydroxypipelic acid,^[112] **67** bulgencinine,^[112] **8** siastatin B,^[36, 110] **68** (3*S*,4*R*,5*R*)-4,5-dihydroxy-3-piperidinecarboxylic acid.^[113]

Among the many ring nitrogen containing glycosidase inhibitors, most are synthesized by reductive cyclic amination. The hydrogenation of pyridine ring is seriously hampered by the lack of crucial stereoselective hydrogenation.^[104-106]

^c *Glucoproteins*: Glycoproteins with a molecular weight of approximately 620,000 to 680,000

2.6 Peptidomimetics

2.6.1 Carbohydrate-Based Peptidomimetics

Since proteins tend to exert their biological activity through only small regions of their folded surfaces, their functions could in principle be reproduced in much smaller designer molecules that retain these crucial surfaces. There are many options for modifications, such as steric constraints, cyclization, and/or replacement of the peptidic backbone or part of it to stabilize the bioactive conformation and fine tune bioavailability. Carbohydrates in general and SAA in particular can provide just that. SAAs, their mixed linear and cyclic oligomers, and homooligomers can adopt robust secondary turn structures or helices and thus may allow one to mimic structural elements of natural biopolymers. They can be used as substitutes for single amino acids or as dipeptide isosters. If used as replacement of hydrophobic residues, the sugar can also be functionalized with hydrophobic side chains (e.g. they may be benzylated), however if hydrophilic residues are replaced, or if solubility should be improved the sugar hydroxyl groups are unprotected or functionalized with hydrophilic residues.

2.6.1.1 Linear SAA Homooligomers and Their Structures

For the peracetylated tetramers of SAA **25** (Figure 5) as well as for the SAAs **29** and **30** Fleet et al. observed a repeating β -turn like bond structure by a combination of solution NMR and IR techniques.^[7, 20, 51, 114] All of the oligomers adopt a repeating 10-membered hydrogen-bonded ring structure. These results show, that protecting groups and substitution patterns of the hydroxyl groups in the sugar ring do not significantly influence the secondary structure of their homooligomers.

Based on their solution NMR studies Fleet et al. propose a left-handed helical structure for the octamer of **31** (Figure 5).^[51, 53, 115]

The tetramer of **26** shows no secondary structure.^[51] The NMR signals are not dispersed. For all three amide protons the chemical shifts are indistinguishable, while for the oligomers above with defined secondary structures dispersed chemical shifts were observed. Chakraoborty and co-workers investigated several protected and unprotected oligomers of **26**. The unprotected octamer shows a strong positive band in its circular dichroism (CD) spectra in MeOH and TFE, which might hint at a possible presence of a distinct secondary structure. However, the ¹H-NMR spectra in various polar solvents, did not show dispersed chemical shifts for the amide protons.^[116]

2.6.1.2 Turn Mimetics and Model Peptides Containing SAAs

We explored the conformational influence of a large number of SAAs on the peptide backbone by incorporation of SAA **43**, **47**, **48** and **69-73** respectively into several different model peptides as well as in biologically active peptides.^[15, 18, 21, 117-21]

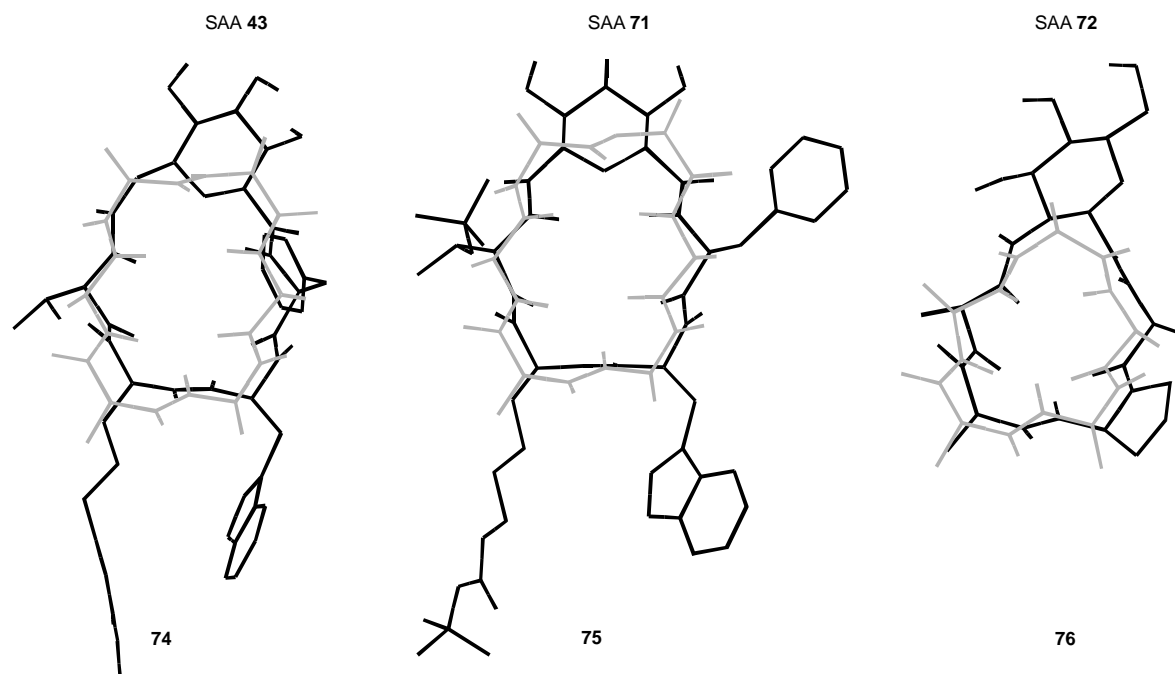


Figure 20: Superposition of **74** (black) and an idealized **bII'/bII'**-turn arrangement (gray); superposition of **75** (black) and an idealized **bII'/bII'**-turn arrangement (gray); superposition of **76** (black) and an idealized **bII'/g**-turn arrangement (gray).

The cyclic and linear peptides were investigated by NMR spectroscopy, distance geometry, and subsequent MD calculations to determine the potential of the turn-inducing and stabilizing potential of SAAs as both local and global constraints. As can be seen in Figure 20 the SAAs can adopt defined turn arrangements in cyclic peptides.

This resulted, in a SAA construction kit for predetermined constrained local conformations in synthetic peptides containing a series of SAAs (Figure 21).^[18, 21, 22] These units offer possibilities as mimetic structures for both, amino acids and dipeptide isosters.

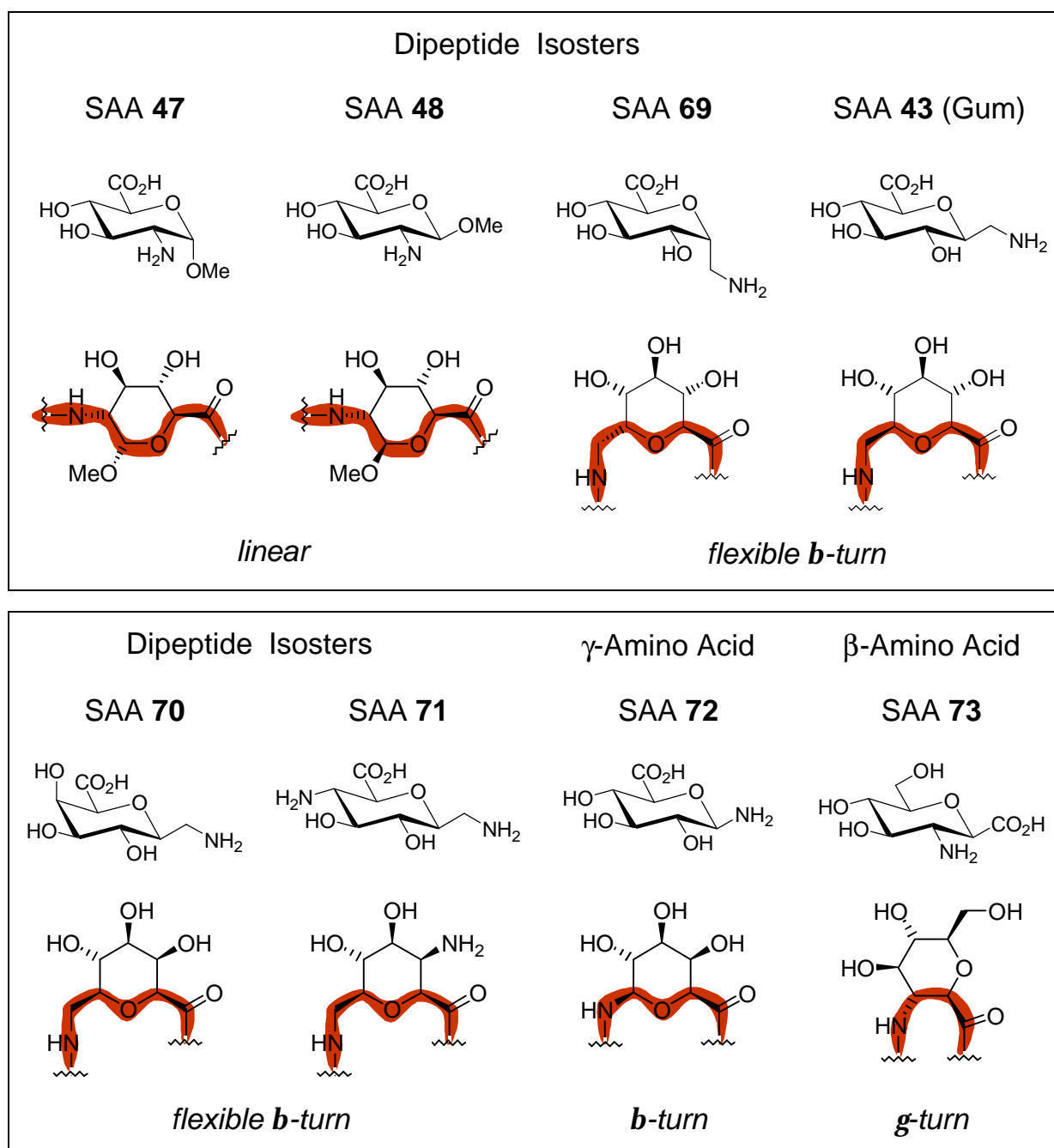


Figure 21: Extended SAA construction kit.

SAA 43 and 69-72 induce β -turns independent of the substitution pattern of the sugar ring while SAA 73 mimics a γ -turn.

The first non-cyclic, peptidic β -hairpin structure containing a SAA, proven by CD and NMR spectroscopy, was recently reported by van Boom et al. They used SAA 77, to stabilize a β -turn in the polypeptide chain AcKKYTVSI-SAA 77-KKITVSI (Figure 22).^[122]

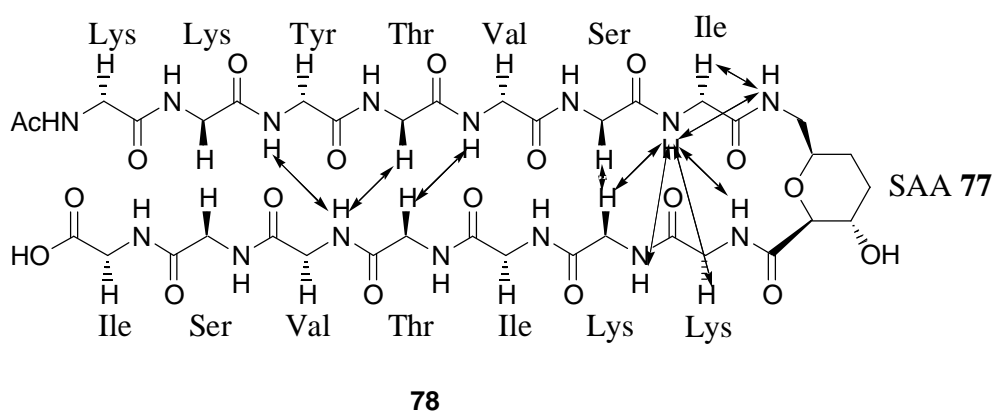


Figure 22: Relevant long range and turn region NOEs of 78.^[122]

2.6.2 β -Peptides

β -peptides are oligomers formed of β -amino acids. β -Amino acids are not unknown in nature. Some simple β -amino acids are found in the metabolism of mammals.^[123] More complicated and highly active ones are found for instance in β -lactam-antibiotics,^[124] in macrocyclic peptides from marine organisms,^[125] in microorganisms and in the anticancer agent paclitaxel (taxol).^[126]

The structure of several polydisperse poly- β -amino acids, the so called nylon-3 derivatives, have been studied in both the solid state and in solution. However, there do exist quite controversial reports on whether poly(α -isobutyl-L-aspartate) forms a helical^[127, 128] or a β -sheet^[129] structure. Until 1995, no structure of a β - or γ -peptide was known. However Gellman et al. concluded in 1994 from IR studies of β -di-peptides, that compact and specific folding patterns will be most likely adopted by β -peptides, when intramolecular hydrogen bonds are unfavorable between nearest neighbor amide groups on the polymer backbone.^[130] It was assumed that the extra methylene group adds additional degrees of rotational freedom, thus making the formation of a stable secondary structure less favourable than for the analogous α -peptide. However, further work of Seebach's and Gellman's groups demonstrated the opposite: Already a β -hexapeptide can form a stable helical structure in solution. α -Peptides only form distinct stable secondary structures in solution, when they consist of at least 15-20 amino acids.^[131-135]

2.6.2.1 Helices

Up to now four different types of β -peptide-helices are known.^[136] The 14-helix, also called 3_1 helix^[137-139] the 12/10/12 helix,^[139, 140] and the 12-helix, also called 2.5_1 helix.^[141-145]

2.6.2.1.1 The 14-Helix

The 14-helix (also called 3_1 helix^d) depicted in Figure 23 was discovered almost simultaneously by Gellman's and Seebach's groups.^[137, 138] Short oligomers of the β -amino acid trans-2-aminocyclohexanecarboxylic acid (trans-ACHC)^[137] and the hexa- β -peptide TFA·H-(β^3 -hVal- β^3 -hAla- β^3 -hLeu- β^3 -hVal- β^3 -hAla- β^3 -hLeu)-OH^e **79** already form that helix.^[149] It is characterized by a 14-membered ring hydrogen bond between an amide proton and a carbonyl. The side chains of the β -amino acids i and $i + 3$ reside above each other in close proximity on the outside of the helix.

The helicity and the dipole of the homologous L- β -peptides are inverse to that of the α -helix formed by the corresponding α -peptides (Figure 23). Only three β -amino acids are needed per full turn of a 14-helix, while 3.6 α -amino acids are required for a single winding of the α -helix. The pitch of an α -helix is 5.4 Å wide and its diameter 4.3 Å, whereas the pitch of the 14-helix is only 5.0 Å wide, however the diameter is 4.7 Å.

^d Crystallographic nomenclature according to ref.[146].

^e The notation β -HXaa for a homolog of the α -amino acid Xaa was introduced by Ondetti and co-workers^[147] and has been used and refined by Seebach and co-workers to β^2 - and β^3 -HXaa, where the numbers indicate the position of the side chains in the β -amino acids.^[148]

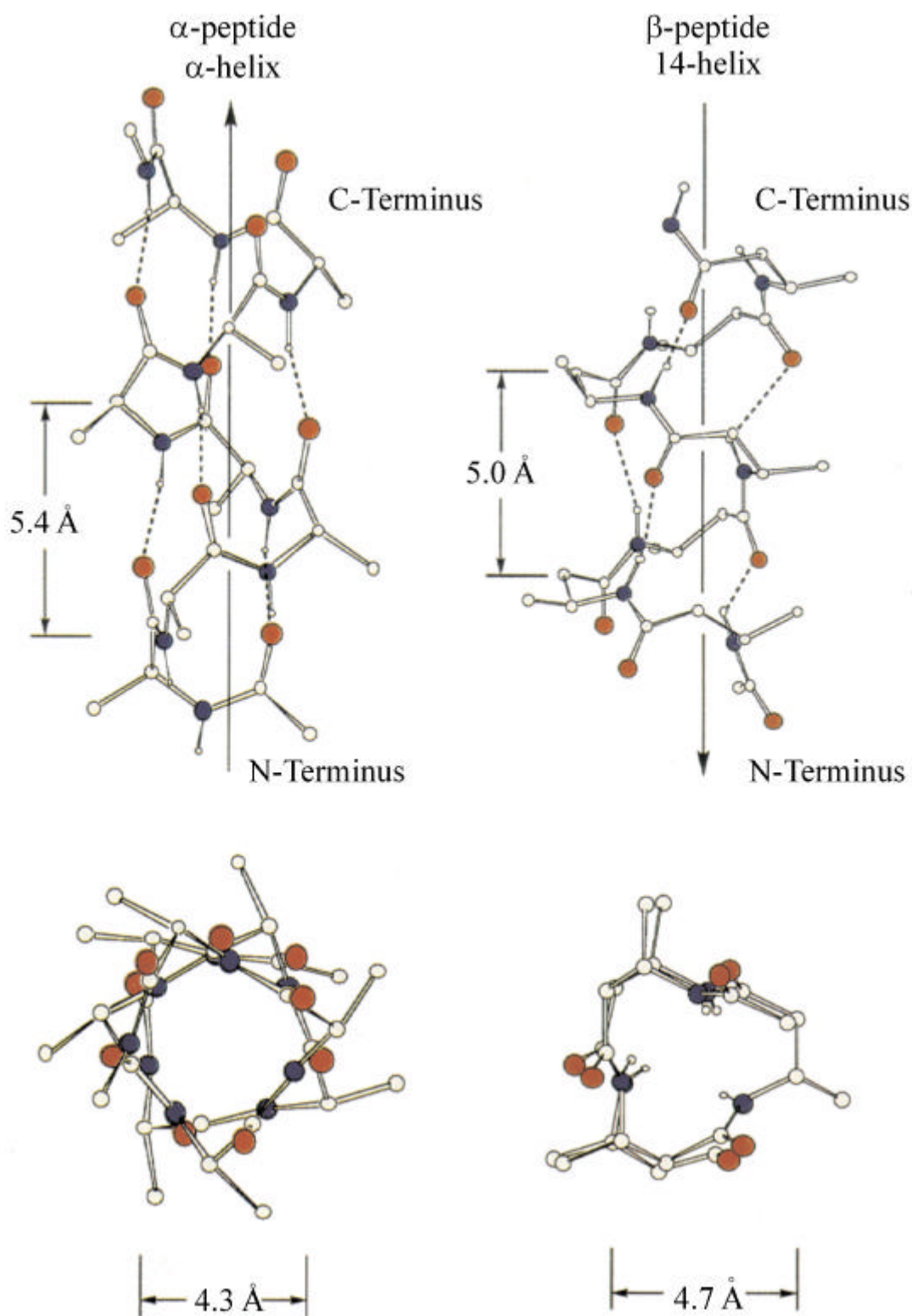


Figure 23: Comparison of the side and top views of the α -helix ($3_6{}_{13}$ -helix) formed by α -L-peptides (left) and the 14-helix (3_{14} -helix) formed by the homologous β -peptides (right).^[138, 149] From the side view the opposite dipoles, and opposite helicities are distinctly visible. The top view clearly reveals the different diameters and the different relative arrangements of the side chains.

There does also exist a right-handed 14-helix formed for instance by the β^2 -peptide $\text{CF}_3\text{CO}_2\text{H}\cdot\text{H}\cdot(\beta^2\text{-hVal}\text{-}\beta^2\text{-hAla}\text{-}\beta^2\text{-hLeu}\text{-}\beta^2\text{-hVal}\text{-}\beta^2\text{-hAla}\text{-}\beta^2\text{-hLeu})\text{-OH}$ **80** with *all*-R-configuration. The CD spectra of **80** is almost an exact mirror image of the one of **79** (Figure 14). The CD pattern is characteristic for the presence of an left- or right-handed 14-helix.

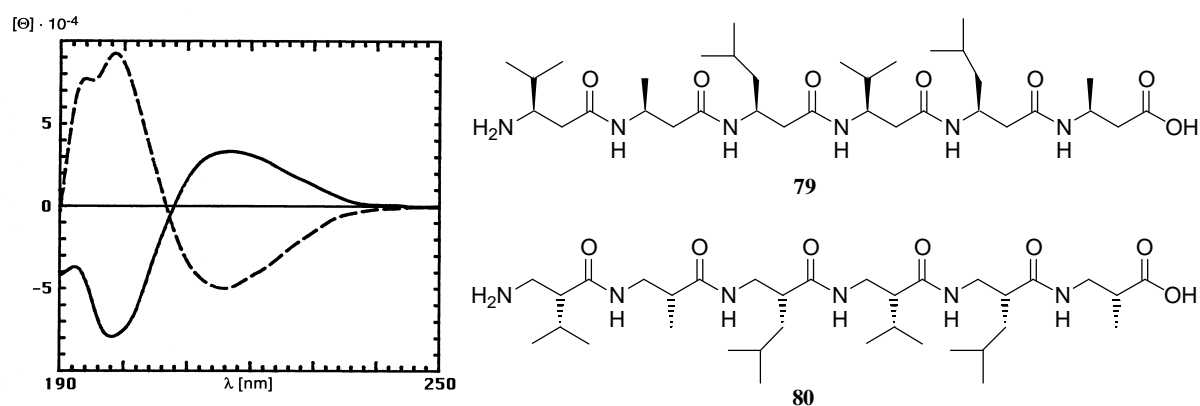


Figure 14: CD-spectra of the β^3 -hexapeptide **79** (- - -) forming a left-handed 14-helix and of the β^2 -hexapeptide **80** (—) forming a right-handed 14-helix in methanol (concentration $2 \cdot 10^{-4}$ M, molar ellipticity [?] in $10 \text{ deg cm}^2 \text{ mol}^{-1}$).

2.6.2.1.2 The 12/10/12-Helix

Seebach and co-workers discovered this new type of β -peptide helix in 1997.^[150] β -hexapeptides constructed from alternating β^2 - and β^3 -amino acid building blocks as the hexapeptide **81** (Figure 25) were designed to form a 14- but they formed a 12/10/12-helix, which consists of a central 10-membered and two terminal 12-membered hydrogen-bonded rings (Figure 25). The C=O and N-H bonds point alternatively up and down along the axis of the helix, thus the net dipole is almost zero. As in the 14-helix, side chains of the β -amino acids i and $i+3$ reside above each other.

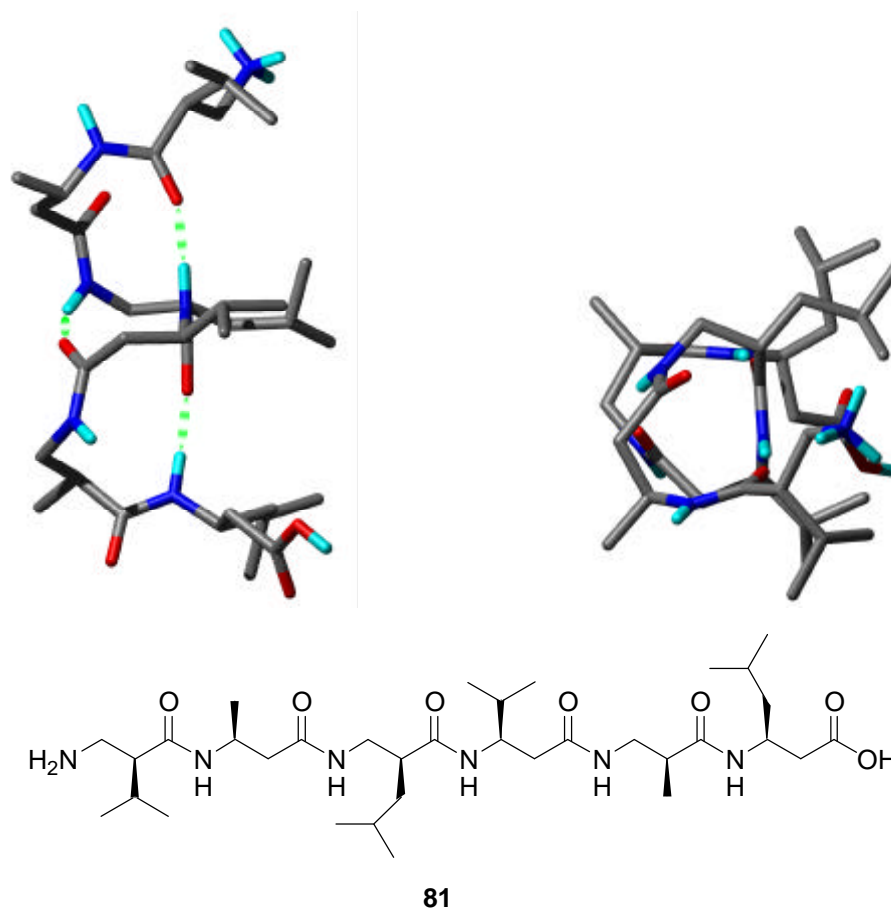


Figure 25: Side and top view of the low energy model of β -peptide **81**, obtained by a long, 10 ns MD simulation without any experimental restraints in vacuo at 50 K using the AMBER* molecular model and force field. All carbon-bound hydrogens have been omitted for clarity. The figures were generated by MolMol^[151] and raytraced by POV-Ray.^[140]

The 12/10/12-helix shows a new type of CD pattern with a strong maximum at 205 nm, different from that of the 14-helix, with a maximum at 200 nm and a minimum at 215 nm (Figure 26).

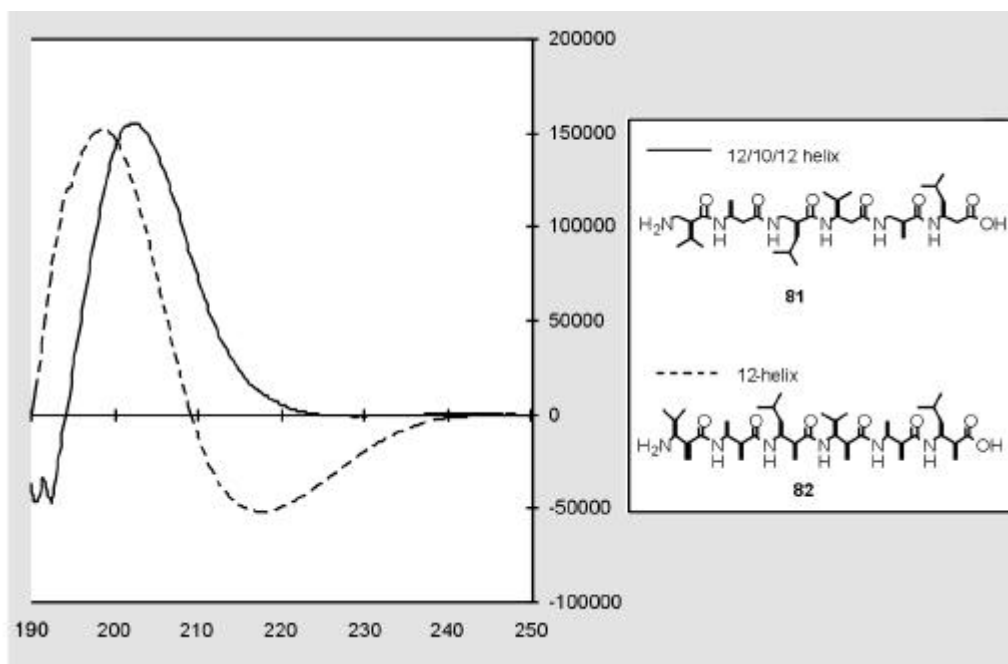


Figure 26: Circular dichroism (CD) spectra of β -peptides **81** and **82**. Comparison of the typical CD pattern assigned to the 12/10/12 helix (— **81**), and to the 14-helix (- - - **82**).

Seebach and co-workers argued that hydrophobic interactions of the aliphatic side chains as well as hindrance of solvent accessibility were the reasons why the 12/10/12 helix rather than the 14-helix is formed in alternating β^2/β^3 -peptides.

The major difference between those two helices is the polarity: The 12/10/12 helix has almost no resulting dipole moment of the molecule, while the 14-helix has one with the positive end at the C- and the negative at the N-terminus. The 14-helix consists of only one type of 14-membered turn whereas in the 12/10/12 helix we have two different turns, the central 10-membered- and the two terminal 12-membered turns.

2.6.2.1.3 The 12-Helix

Gellman and his group reported β -peptides with a different secondary structure, a left-handed 12-helix (also called 2.5₁-helix) (Figure 27).^[141, 145] They synthesized a series

of oligomers of (R,R)-trans-2-aminocyclopentanecarboxylic acid (trans-ACPC). The two longest oligomers, a hexamer **83** and the octamer, have been examined by X-ray crystallography^[145] and NMR spectroscopy in pyridine.^[141, 144] The CD-spectra of hexamer **83** show a maximum at about 204 nm, zero crossing at about 214 nm and a minimum at 221 nm.

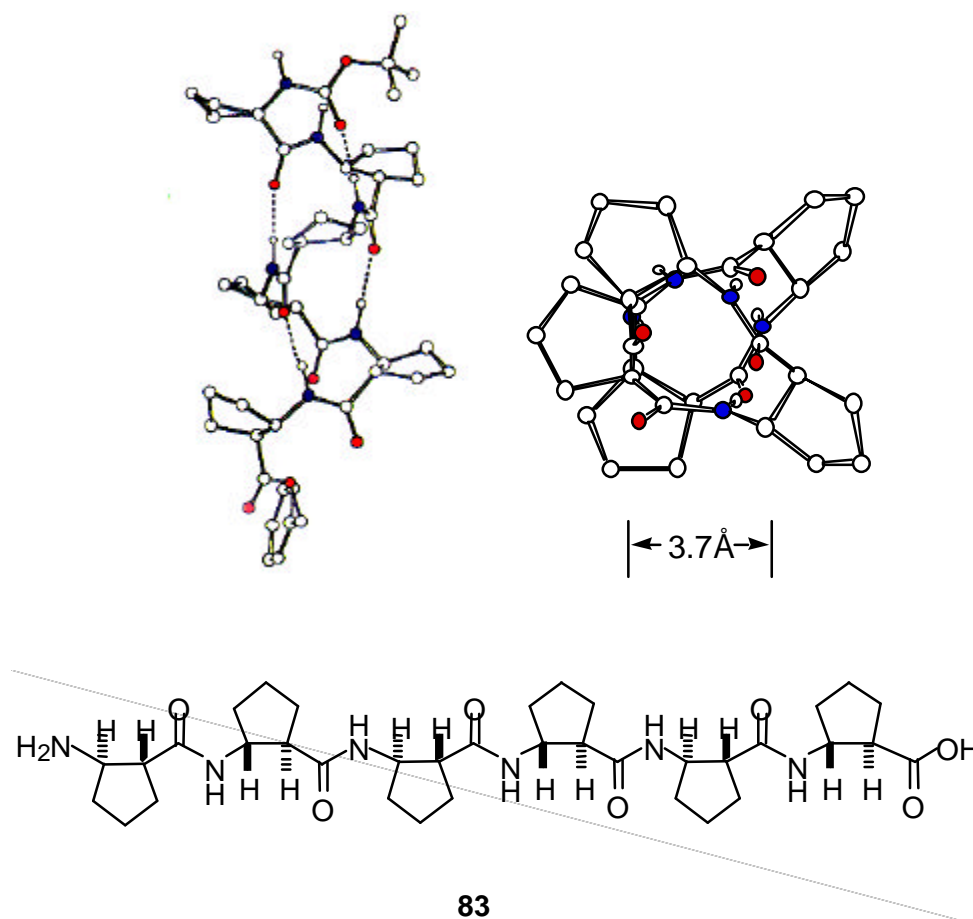


Figure 27: Model of the 12-helix and structure of the hexapeptide **83**.^[141]

Both crystal structures show that the β -peptide backbone adopts a regular helix that is defined by a series of interwoven 12-membered ring hydrogen bonds. Each hydrogen bond links an amide proton to a carbonyl oxygen three residues towards the N-terminus. The resulting dipole of this helix, has the same direction as that of the α -helix of α -peptides. CD data suggest that the conformational preference of trans-ACPC oligomers in methanol is strongly length-dependent, which implies that 12-helix formation is a cooperative process, as seen for the α -helix formed by conventional peptides.

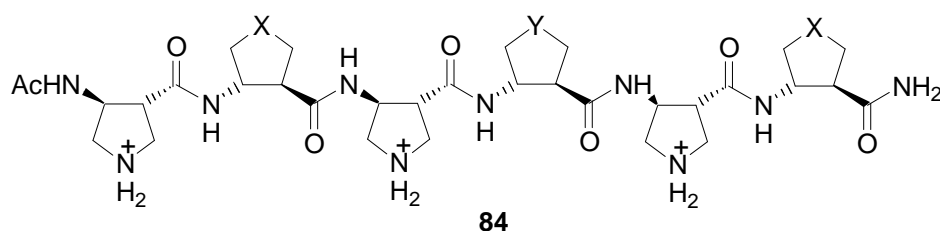


Figure 28: Hexameric β -peptides **84**: **84a**) ($X = \text{NSO}_2\text{CHMe}_2$, $Y = \text{NSO}_2\text{C}_6\text{H}_4\text{OMe-4}$; **84b**) $X=Y = \text{NSO}_2\text{CHMe}_2$; **84c**) $X=Y = \text{NSO}_2\text{C}_6\text{H}_4\text{OMe-4}$) containing *N*-sulfonylated *trans*-3-aminopyrrolidine-4-carboxylic acid (*S*-APC). 12-helix confirmed in aqueous solution by CD and NMR spectroscopy.^[142]

Recently Gellman and co-workers succeeded in designing water-soluble β -peptides forming the 12-helix.^[142, 143] Hexameric β -peptides **84 a-c** (Figure 28) contains *N*-sulfonylated *trans*-3-aminopyrrolidine-4-carboxylic acid (*S*-APC). The *S*-APC residue represent Gellman's group's general strategy for introducing specific side chains at defined positions along the surface of 12-helical β -peptides.^[142]

2.6.2.2 The β -sheet structure

The first β -peptide sheet-type structure was discovered by Seebach and co-workers^[138] for the fully protected tripeptide Boc- β -hVal- β -hAla- β -hLeu-OMe. Only recently they succeeded in obtaining an X-ray structure of the *N*-deprotected derivative **85**, which adopts also a sheet-type structure (Figure 29).^[152]

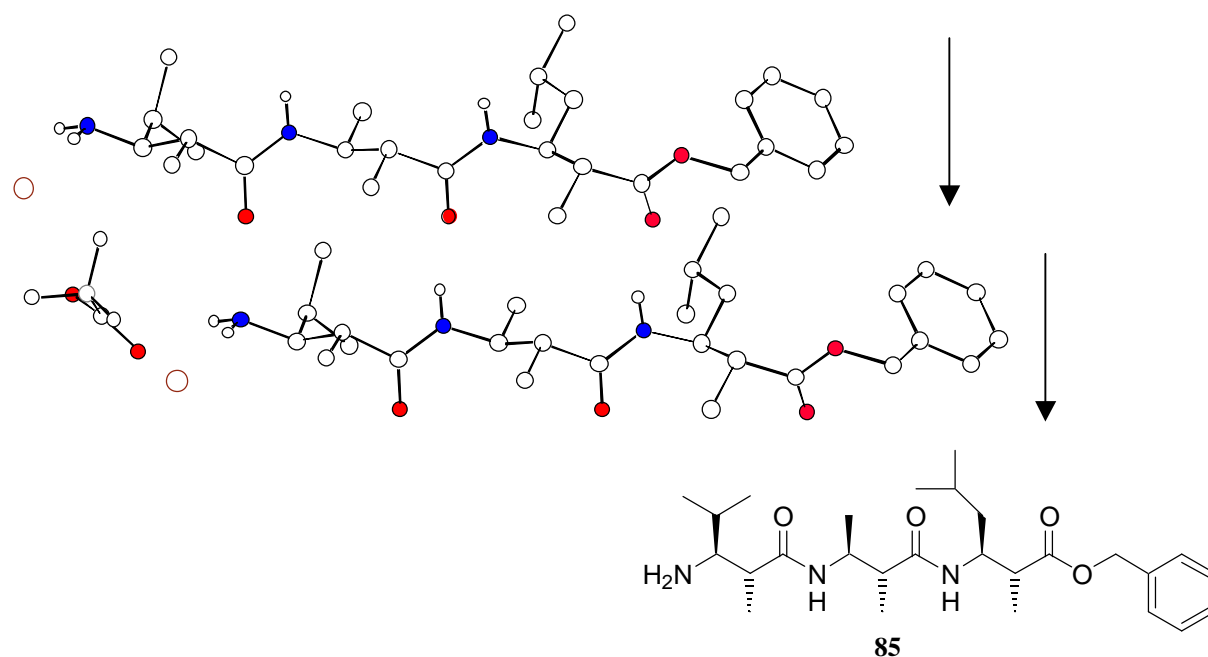


Figure 29: X-Ray structure and formula of the sheet-forming tripeptide **85**^[152]

It is different from the known pleated sheet of α -peptides, where C=O and N-H bonds point up and down alternatively. The β -peptide pleated sheet is polar, since all carbonyls point in one direction, while all N-H bonds point in the opposite direction. The peptides are linked by a 14-membered H-bonded ring.

2.6.2.3 Tube-like Structures

The β^3 -HAla-derived cyclic oligomers **86-88** form supramolecular, tubular structures similar to that of certain cyclo- α -peptides,^[153] as was determined by powder diffraction experiments (Figure 30). Those 16-membered rings are linked by four non-linear C=O \cdots H-N intermolecular H-bonds.

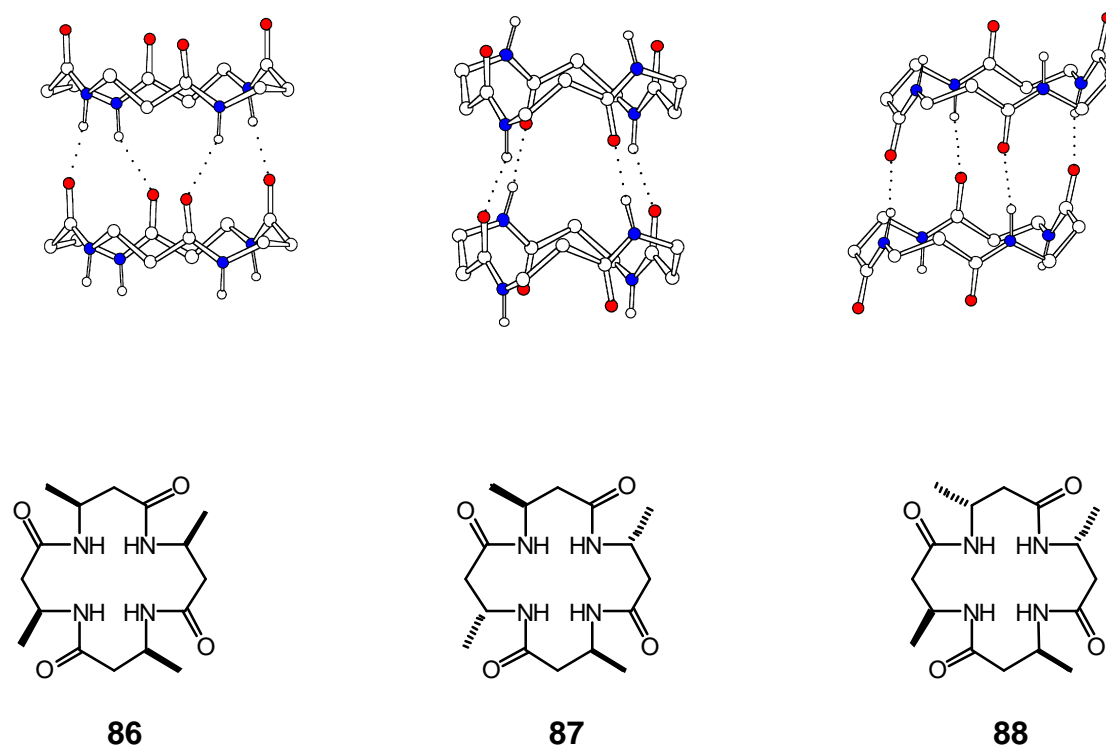


Figure 30: X-ray and molecular structure of the cyclic oligomers **86-88**.^[153]

2.7 Biologically Active Peptides Containing SAA Building Blocks

After verifying the conformational influence of the SAAs in cyclic peptides as compared to the backbone of model peptides our group, as well as several other groups focused the attention on the synthesis, conformational and biological evaluation relative to biologically active peptides. SAAs were used as turn mimetics and local constraints,^[14, 15, 18, 21, 47-49, 56, 117, 120, 121, 154] but also to improve pharmacokinetics,^[117, 155] to introduce a radioactive label for imaging^[156] or to glycosylate a peptide.^[157] The opioid, integrin and somatostatin receptors were some of the pharmacologically interesting targets, which were chosen to investigate. Two structurally cyclic peptides, such as the "Veber-Hirschmann" peptide *cyclo*(-Phe-Pro-Phe-D-Trp-Lys-Thr-) **50** (Chapter 2.4.1, Figure 6; Chapter 3.3., Table 4)^[158, 159] and our *cyclo*(-Arg-Gly-Asp-D-Phe-Val-) peptide^[160] as well as linear LH-RH analogs, were selected as a platform to determine the pharmacological potential of SAA scaffolds. Soon other groups started using SAAs in various biologically active peptides as well.

2.7.1 Somatostatin Analogues

Somatostatin is a 14-residue cyclic peptide hormone formed in the hypothalamus. Like its precursor somatostatin-28 it plays an important role in a large number of physiological actions. For instance it inhibits the release of growth hormone (GH),^[161, 162] and plays a role in the inhibition of insulin secretion.^[163, 164] Somatostatin analogues were shown to inhibit tumor cell growth and induce apoptosis.^[165, 166]

The first SAA introduced into a bioactive peptide was glucosyluronic acid methylamine (Gum) **43** (Chapter 2.6.1.2, Figure 21).^[14, 15] We introduced it as a dipeptide isoster into a cyclic hexapeptide of the "minimal" somatostatin sequence^[158, 167] *cyclo*[SAA **43**-Phe-D-Trp-Lys-Thr-]. By various NMR techniques and subsequent distance geometry calculations and molecular dynamic simulation it was shown, that SAA **43** induces a β -turn.^[15] (Figure 20)

The growth hormone release was inhibited with an IC₅₀ value in the sub- μ M range.

2.7.2 SAAs in enkephalin analogs

In order to explore the effect of the dipeptide isomers SAA **47** and SAA **43** on the conformation of linear peptides by NMR spectroscopy we synthesized the Leu-enkephalin analogs H-Tyr-SAA **47**-Phe-Leu-OMe (**89**) and H-Tyr-SAA **43**-Phe-Leu-OMe (**90**) (Figure 31).^[14, 15] The SAAs replace the Gly-Gly dipeptide of the natural sequence H-Tyr-Gly-Gly-Phe-Leu-OH, where Gly-Gly serves as a spacer in enkephalin between the messenger amino acid Tyr which is essential for the activity and the address sequence Phe-Leu responsible for the selectivity.^[168, 169]

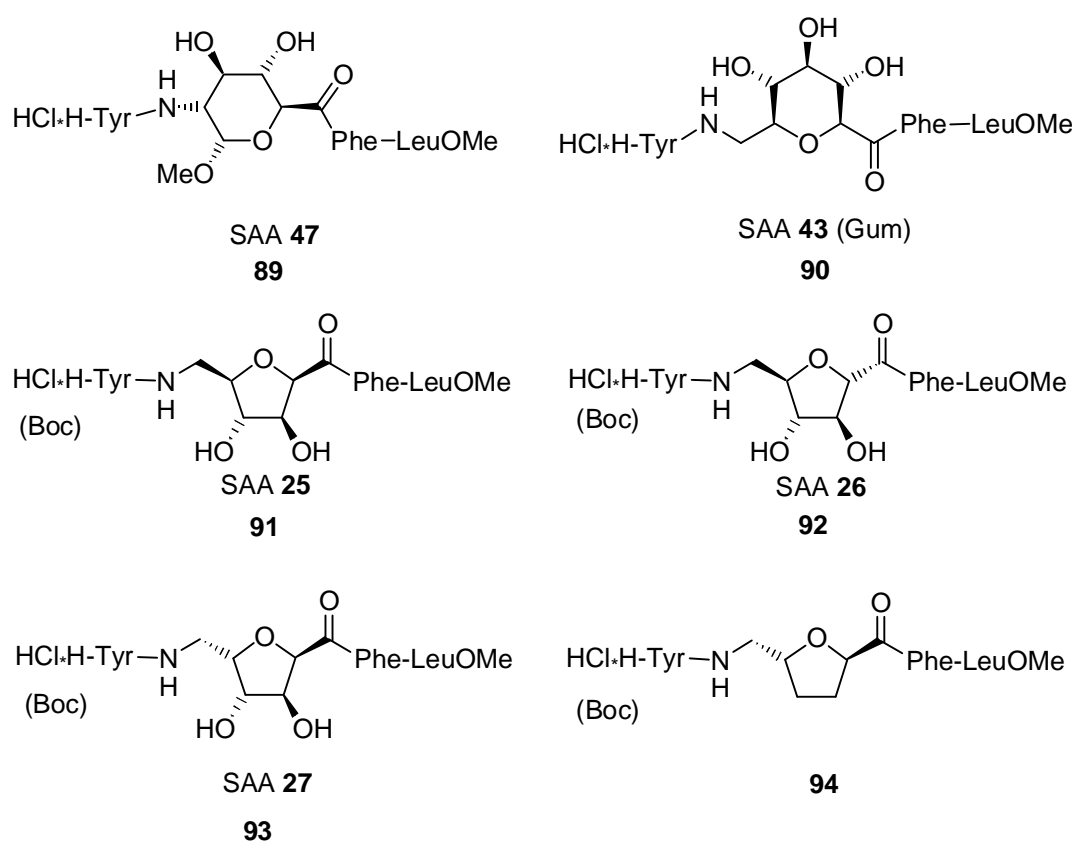


Figure 31: Leu-enkephalin analogues, in which Gly-Gly is replaced by SAAs.^[14, 15, 49]

Due to the functionality of the SAAs, these building blocks can be synthesized as Fmoc-derivatives and then be employed under standard SPPS^[170] conditions using the Fmoc strategy and TBTU/HOBt^[171] as a coupling reagents. The two enkephalin analogs **89** and **90** showed no biological activity in the guinea pig ileum assay (GPI).

However, when Chakraborty et al. incorporated their furanoid SAAs **25**, **26**, **27** and dideoxy-**27** analogously into Leu-enkephalin, the analgesic activity of the resulting compounds **91-94** (Figure 31) was in the same range as that of Leu-enkephalin methyl ester.^[48, 49] The N-terminally Boc protected analogues of **91-94** showed comparable activities as the unprotected ones. For synthesis of their peptidomimetic compounds they employed standard solution Boc strategy, using EDCI and HOBt as coupling agents.^[172] Extensive CD and NMR studies, followed by constrained molecular dynamics simulations revealed, that the Boc-protected **91** and Boc-protected **93** have folded conformations composed of an unusual nine-membered pseudo β -turn-like structure with a strong intramolecular H-bond between LeuNH \rightarrow sugarC3-OH. This turn moves the two aromatic rings of Tyr and Phe in close proximity, a prerequisite for biological activities of all opioid peptides. From analysis of the 3-D structures of **91-94**, they concluded, that a *cis-b*-hydroxycarboxyl moiety anchored on a five-membered ring was the essential structural motif, whose presence in some of these analogues was responsible for their folded conformations.

The group of Toth used SAA **72** (Figure 21) to “glycosylate” Leu- and Met-enkephalins via amide bond linkage to the C-terminal Leu- or Met respectively (Figure 32).^[157]

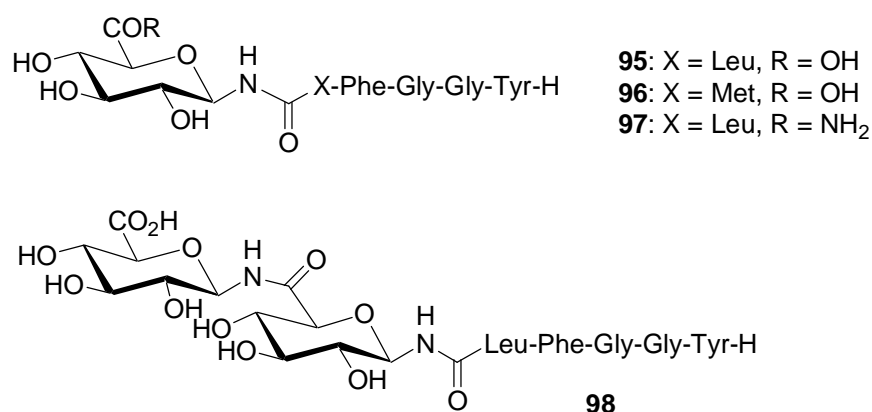


Figure 32: SAA “glycosylated” enkephalins.^[157]

They constructed the peptides **95-98** on solid phase, using Fmoc-strategy and HBTU/HOBt/DIEA as coupling reagents. The peracetylated SAA **72** (Figure 21) azide precursor was reduced on resin by treatment with a mixture of triethylamine and propane-1,3-dithiol to generate the free amine *in situ*. They thereby used the azide as a

amine protecting group instead of the Fmoc-protected SAA **72**. Pharmacological evaluation, using a GPI and mouse vas deferens (MVD) assay revealed, that **95** was 3 times more potent in the GPI assay and 40 times more potent in the MVD assay than Leu-enkephalinamide at inhibiting electrically stimulated muscle contractions.

2.7.3 Protein:Farnesyltransferase

Inhibition of Protein:Farnesyl Transferase (PFT) should be effective to combat colon and pancreatic carcinomas.^[173] Ras protein association with the plasma membrane is initiated by post-translational farnesylation of the cysteine unit of the CAAX box (C, cysteine; A, any aliphatic amino acid; X, serine or methionine) in the pre-Ras protein by PFT, and that is essential for Ras function.^[174] Continuously switched on phosphorylation cascade is caused by the activated GTP-bound state, in which oncogenic Ras proteins are locked. Van Boom et al. used SAA **77** and SAA **99** (Figure 33) as dipeptide isoster to replace AA. The resulting compounds **100** and **101** were both less active than for instance CAAX based inhibitors containing 4-aminobenzoic acid as AA. However both compounds show a distinct inhibitory effect – the “2,6-*cis*” isomer, the one containing SAA **77** is about twice as active as the “2,6-*trans*” isomer, containing SAA **99** (Figure 33).^[154]

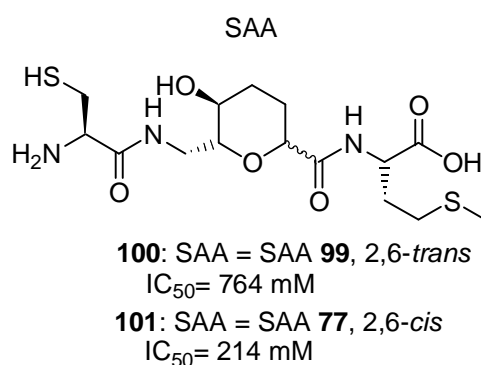


Figure 33: Structures and IC₅₀ values of PFT inhibitors by van Boom et al.^[154]

2.7.4 Integrin-Ligands

Integrins are located at the cell surface of a number of different cell types. Several play a major role in cell-matrix interaction as well as in angiogenesis, which is important for tumorigenesis. This invoked a pharmaceutical interest in $\alpha_v\beta_3$ -antagonists, to block tumor induced neo-angiogenesis.^[160, 175-179] The recognition sequence of many integrin ligands has been shown to consist of the three amino acids arginine (R), glycine (G), and aspartic acid (D), the “RGD”-motif. In our group SAAs have been used in cyclic RGD analogues as turn mimetics,^[117] as well as “glycosylating agent” to improve the pharmacokinetic properties of the compounds^[117, 155] and for tumor imaging to introduce the radio-nuclides.^[156] In the earliest attempts to modify cyclic RGD-peptides with carbohydrates impaired the biological activity of the RGD-compounds.^[180, 181] In more recent work^[117] the cyclic pentapeptide *cyclo*(-Arg-Gly-Asp-D-Phe-Val-) **102**, which binds selectively $\alpha_v\beta_3$ -integrins, was chosen as a lead structure.^[160, 175-179] In **102** the backbone conformation of the residues D-Phe-Val resembles a β II'-turn, thus forcing the RGD-sequence, which acts as pharmacophore, into a kinked, $\alpha_v\beta_3$ -selective conformation. Fully benzylated Gum **43**, (both the α - and the β -anomer) has been shown to induce the type of turn necessary for the biological activity,^[15, 18, 21] and also had the aromatic functionality required for enhanced activity. Therefore we used both anomers to replace D-Phe-Val in **102** to give **103** and **104**, which exhibit a relatively high $\alpha_v\beta_3$ activity of $IC_{50}=150$ nM (**103**) and 25 nM (**104**). However **104** showed also a high activity against the $\alpha_{IIb}\beta_3$ -receptor ($IC_{50}=13.4$ nM). The loss of selectivity of **104** compared to that of the α -SAA-peptide **103** can be explained by the higher flexibility of β -SAA-peptide **104**. Because of that flexibility a kinked as well as a stretched conformation can be realized in solution. The compound is therefore able to re-adjust its conformation, matching the steric demands of both the $\alpha_{IIb}\beta_3$ - and $\alpha_v\beta_3$ -receptor pockets: high activity with a loss of selectivity is the consequence (Figure 34). This is confirmed by their NMR-based structural analysis and subsequent MD-simulations.

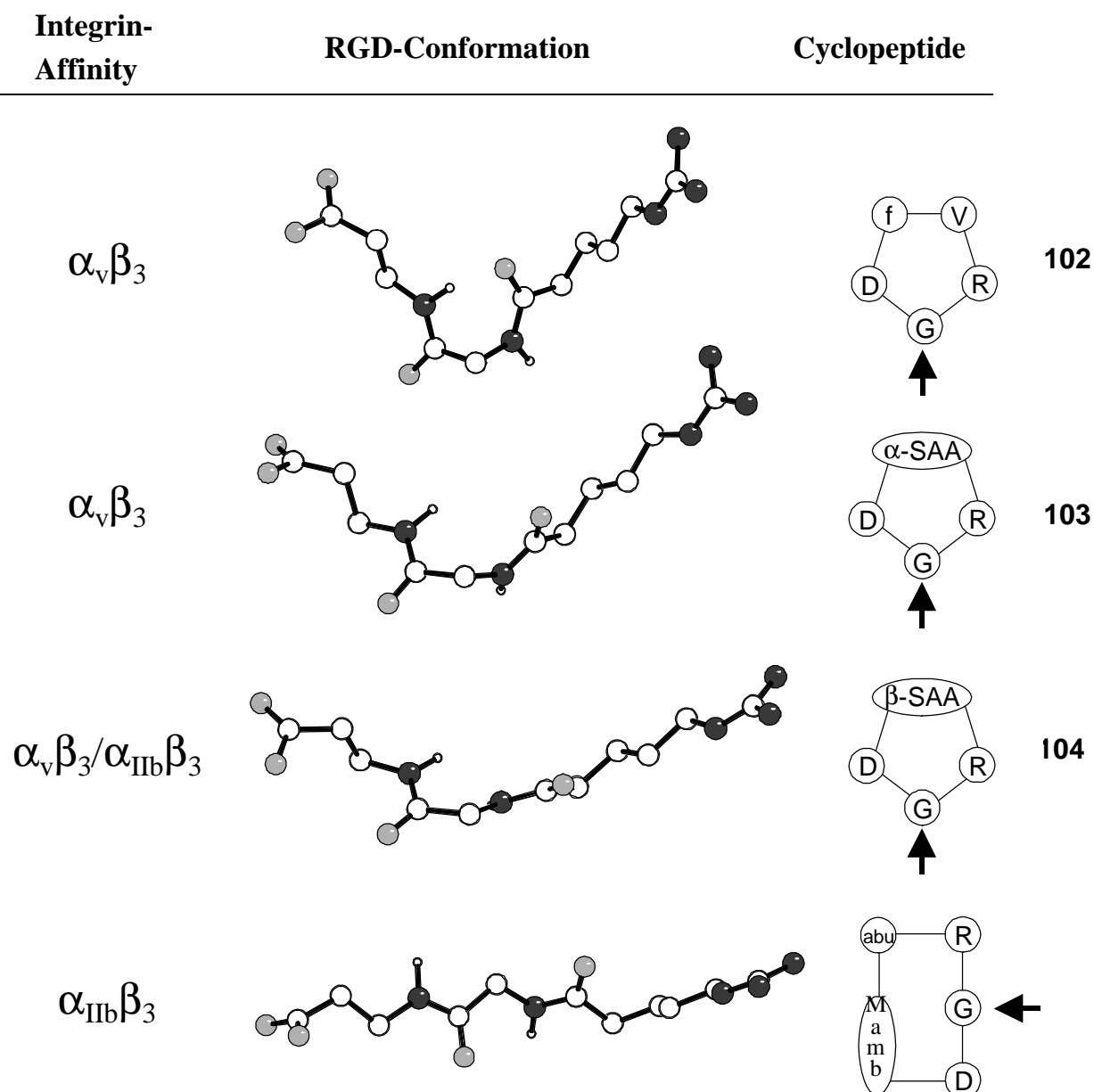


Figure 34: The RGD-conformations of the **a**-(103) and **b**-compounds (104) are compared to typical representatives of $\alpha_v\beta_3$ - and $\alpha_{IIb}\beta_3$ -antagonist structures, to the lead peptide cyclo(-RGDfV-) and the compound cyclo(-D-Abu-NMeArg-Gly-Asp-Mamb-) (Abu = A-aminobutyric acid, Mamb=meta-(aminomethyl)benzoic acid).^[182] View along the pharmacophoric RGD-moiety is directed parallel to the ring plane of the cyclic peptide, as indicated by black arrows.

To improve pharmacokinetic properties Val was substituted by Lys, which was glycosylated with different SAAs via an amide bond.^[117, 155, 156] Activity and selectivity was sometimes even enhanced. Furthermore via the amine function of the SAAs

^{18}F -labeling is possible.^[156, 183] In *in vivo* studies using $\alpha_v\beta_3$ -positive and -negative murine and xenotransplanted human tumors receptor-specific binding of the radio-labeled **105** yielded high tumor:background ratios. First imaging results, using a small animal positron emission tomograph suggest **105** is suitable for noninvasive determination of the $\alpha_v\beta_3$ integrin status and therapy monitoring.

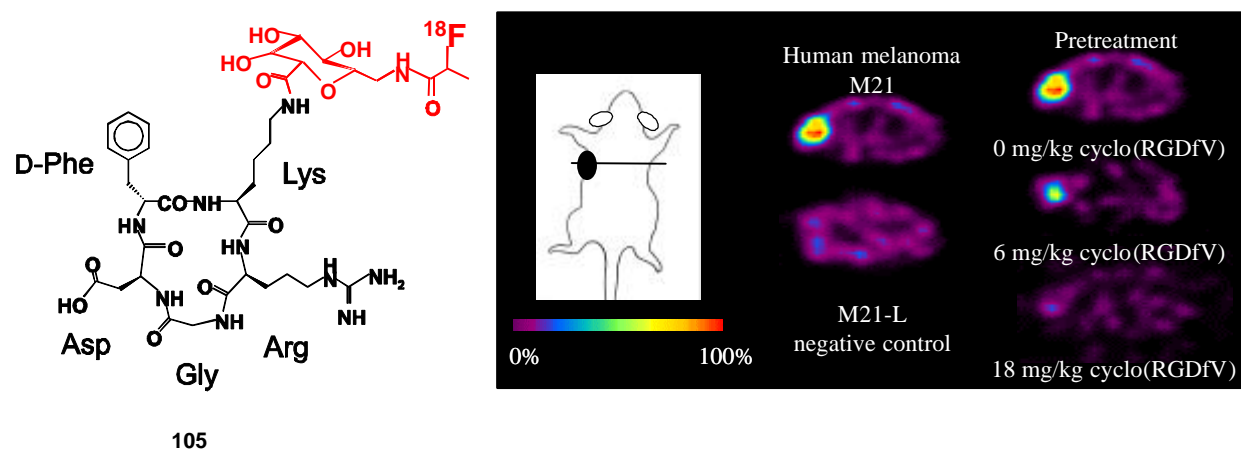
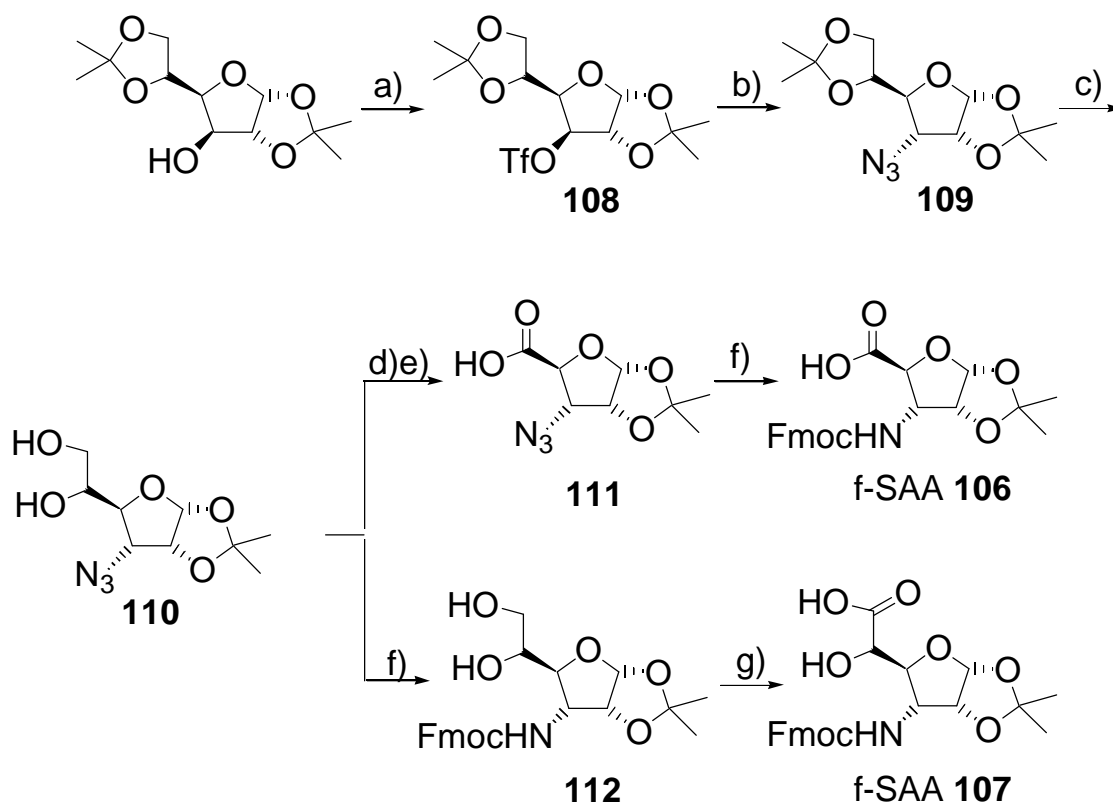


Figure 35: Structure of **105** and transaxial small animal PET images of nude mice bearing human melanoma xenografts, treated with **105**.

3 Results and Discussion

3.1 Synthesis of Two New Furanoid SAAs^[22, 118-121, 184, 185]

In contrast to most other SAAs so far described, synthesis of f-SAA **106** and f-SAA **107** is simple and direct (Scheme 5). Both were synthesized via the azides **109** and **110**.



Scheme 5: Synthesis of Fmoc-protected f-SAA **106** and f-SAA **107**: a) Tf_2O , py, -10°C , CH_2Cl_2 , 98 %; b) NaN_3 , Bu_4NCl (cat), 50°C , DMF, 70 %; c) conc. HOAc, 3h, 65°C , 94 %; d) NaIO_4 , 5h, 10°C , MeOH; e) KMnO_4 , 50% HOAc, rt, 89 % over two steps; f) H_2 , Pd/C, FmocCl, NaHCO_3 , pH 8-9, MeOH, THF, rt, 76-90 %; g) NaOCl, TEMPO (cat), KBr, CH_2Cl_2 , sat. aq NaHCO_3 , Bu_4NCl , 62%.

The synthesis of the azide precursor **109**, which has been reported before,^[1, 186-190] has been optimized. However, protected or unprotected f-SAA **106** has not so far been reported in the literature. The key step of the synthesis of f-SAA **106** is the azidolysis of the triflate activated diacetone glucose **108** (Scheme 5). Elimination occurs as a major side-reaction (Table 2).^[188-190]

Table 2: Reaction conditions, reagents and yields from the literature for the conversion of **108** to **109**.

Solvent	Reagents	Conditions	Yield	Author (et al.)/ Ref.
DMF	NaN ₃	50°C, 3.5 h	48 %	L. Daley ^[188]
HMPT	NaN ₃		60 %	J. M. G. Fernández ^[190]
DMF	guanidinium-azide	25°C, 6 h	61 %	H. H. Baer ^[189]
DMF	NaN ₃ , cat. Bu ₄ NCl	50°C, 5 h	70 %	this work ^[118-121]
THF	Me ₃ SiN ₃ , Bu ₄ NF	50°C, Ar, 12 h	exclusive elimination	this work ^[119]

This may be attributed to the poor solubility of azides in organic solvents. Considerably higher yields of 70 % were achieved and expensive^[189] or toxic^[190] reagents were avoided, by the simple addition of catalytic amounts of the phase-transfer-catalyst Bu₄NCl. The Bu₄NCl renders the NaN₃ significantly more soluble. Thus under inversion of configuration of C³, at 50°C in DMF, the triflate-ester **108** is converted to the azide **109** in 70 % yield. Efforts to further enhance substitution yields and suppress elimination more sufficiently by using the “naked” azide-anion generated *in situ* from trimethylsilylazide and t-Bu₄NF failed: Elimination took place almost exclusively - **109** could not be detected.

The exocyclic hydroxyl groups of **109** were quantitatively and selectively deprotected to **110** using concentrated acetic acid.^[186] To obtain Fmoc-protected f-SAA **106** the diol **110** is oxidatively cleaved using sodium periodate, followed by potassium permanganate oxidation to yield the acid **111**.^[186] In an one-pot reaction the azide **111** was reduced and simultaneously Fmoc-protected to yield about 70 % of the Fmoc-protected f-SAA **106**, suitable for solid phase synthesis. Because the acetonide

is fused to a second five-membered ring, it is stable against conventional acids like pure trifluoroacetic acid or 1N hydrochloric acid. The overall yield of f-SAA **106** starting from diacetone glucose was 44%.

For the preparation of f-SAA **107** the azide **110** is first reduced and Fmoc-protected in a similar one-pot reaction as for the conversion of the acid **111** to Fmoc-protected f-SAA **106**, followed by selective oxidation of the primary alcohol with 2,2,6,6-tetramethylpiperidin-1-oxyl (TEMPO), sodium hypochlorite and potassium bromide. To prevent decarboxylation during TEMPO oxidation, it is crucial to keep the pH between 8.5 and 9.5, and the temperature below 0 °C.

3.2 Foldamers^[22, 118, 119, 184]

Carbohydrates as well as peptides and proteins are essential biopolymers of life. They are involved in complex biological processes such as catalysis and highly selective molecular recognition. In order to perform those functions the correct folding of the biopolymers creating the active site is crucial, since any kind of interaction is observed only, if the reactive groups are positioned in the correct spatial orientation to each other. Thus the development of small, easy-to-functionalize building blocks and oligomers with backbones of discrete and predictable folding patterns (“foldamers”)^[137] is required in order to design and develop molecules with useful biological functions. Chimeras of the three big classes of biopolymers, that is, nucleic acids, proteins and carbohydrates, have attracted great interest as both functional, and structural analogues in recent years, also because of their potential application in drug design. However, sugar amino acids (SAAs) and their oligomers, which bridge carbohydrates and proteins, have only recently been investigated (See chapter 2.6.2).^[3, 5, 14-21, 56]

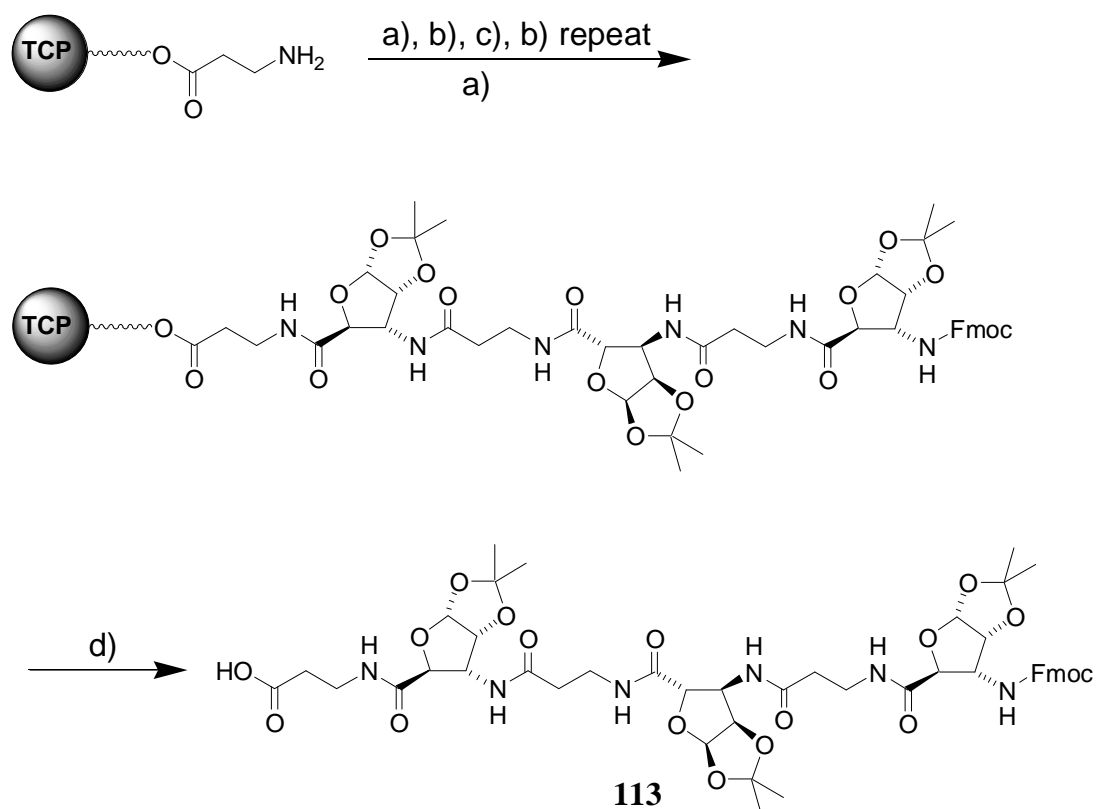
The new furanoid β - and γ -SAA building blocks f-SAA **106** and f-SAA **107** will be presented as analogues to β - and γ -peptides, as structural templates aiming at new structures for peptidomimetic drug design, and as potential foldamers.^[184, 191] The linear mixed oligomer Fmoc-[f-SAA**106**- β -hGly]₃-OH **113** and the cyclic

mixed oligomer $\text{cyclo}[-\text{f-SAA106}-\beta\text{-hGly-}]_3$ **114** consist of the f-SAA **106** alternating with $\beta\text{-hGly}^f$ (β -alanine), thus forming hybrids between SAAs and β -peptides. The linear mixed γ -hexapeptide **115** is built up of alternating f-SAA **107** and γ -amino butyric acid (GABA) units. $\beta\text{-hGly}$ and GABA were used as amino acid counterparts, because they represent, likewise to f-SAA **106** and f-SAA **107**, β - and γ -amino acids respectively. They are completely unsubstituted, and do not form secondary structures. Thus secondary structure is induced exclusively from the incorporated SAA.

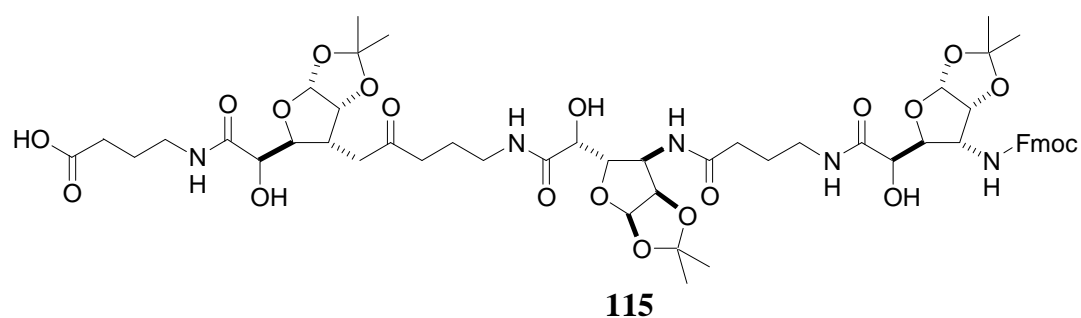
3.2.1 Solid Phase Synthesis of the Linear Mixed SAA-AA-Oligomers **113** and **115**

The mixed SAA oligomers **113** and **115** were synthesized using Fmoc strategy as shown in Scheme 6. The f-SAAs **106** and **107** were alternately coupled with β -homoglycine or GABA respectively to form oligomers **113** and **115**. Tritylchloropolystyrene (TCP) resin was employed as solid support. Two equivalents of the f-SAA derivative, whereas three equivalents of β -homo-glycine or GABA were used. Stoichiometric quantities, that is 2 or 3 equivalents of [O-(7-azabenzotriazol-1-yl)-1,1,3,3-tetramethyluronium hexafluorophosphate] (HATU) and 20 or 30 equivalents of 2,4,6-collidine as base were used as coupling agent.^[170, 192, 193] After cleavage from the resin with hexafluoro isopropanol (20 % in dichloromethane, 3*10 min),^[194] rp-HPLC purification yielded 71.3 mg of the linear oligomer **113** (41 % yield) and 10 mg (4.7 % yield) of **115** in over 99 % HPLC-purity.

^f The notation $\beta\text{-HXaa}$ for a homolog of the α -amino acid Xaa was introduced by Ondetti and co-workers^[147] and has been used and refined by Seebach and co-workers to $\beta^2\text{-}$ and $\beta^3\text{-HXaa}$, where the numbers indicate the position of the side chains in the β -amino acids.^[148]



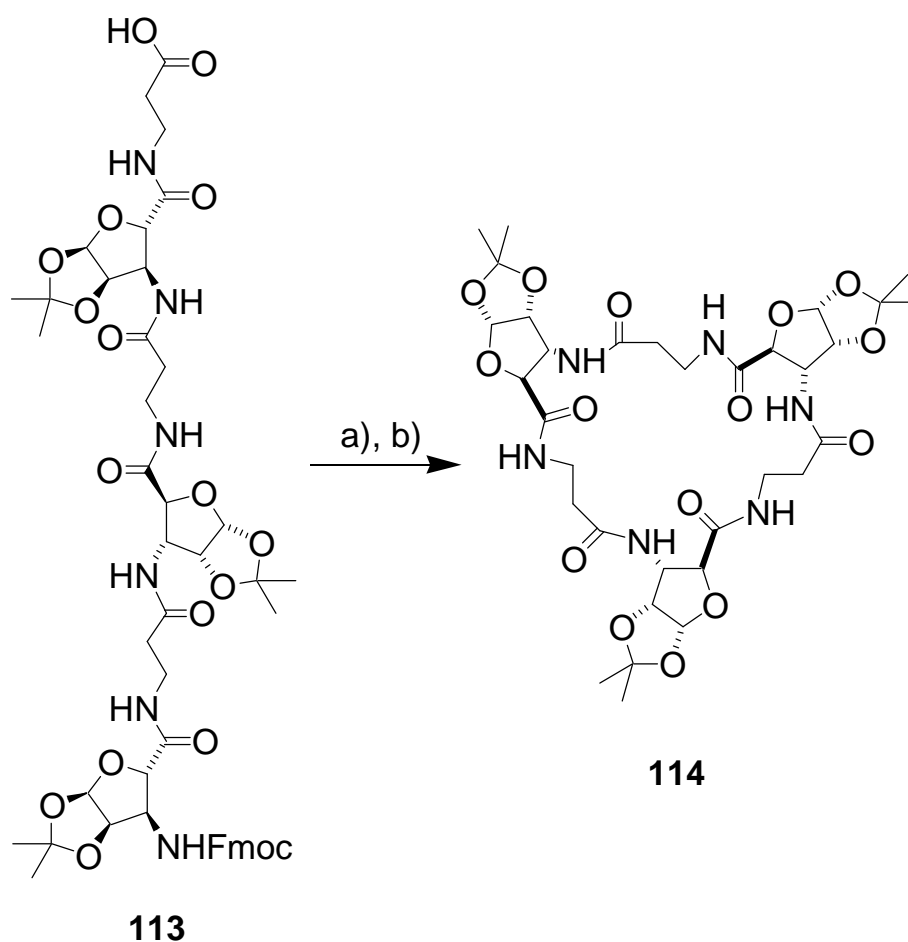
analogous synthesis of oligomer **115**:



Scheme 6: Synthesis of the linear oligomer **113**: a) HATU (2 equiv), 2,4,6-collidine (20 equiv), **1** (2 equiv), rt, NMP; b) i) washing: NMP (5 × 3 min), ii) Fmoc deprotection: 20 % piperidine (pip) in DMF (2 × 10 min), iii) washing: NMP (5 × 3 min); c) HATU (3 equiv), 2,4,6-collidine (30 equiv), β -homo-glycine (3 equiv), rt, NMP; d) i) washing: NMP (3 × 3 min), CH₂Cl₂ (1 × 3 min), ii) vacuo overnight, iii) cleavage: 20 % HFIP in CH₂Cl₂ (3 × 10 min).

3.2.2 Synthesis of the Cyclic Mixed [f-SAA106-b-hGly]₃ Oligomer **114** in Solution

After Fmoc-deprotection **113** was cyclized using 1 equivalent of HATU and 10 equivalents of 2,4,6-collidine at high dilution (0.4 mM), after 24 h an additional 0.1 equivalents of HATU and 1 equivalent of 2,4,6-collidine were added to afford **114** in quantitative yield (Scheme 7) in a purity >95 % after preparative HPLC.



Scheme 7: Cyclisation of the Fmoc-protected linear **113** to the cyclic **114**: a) Fmoc deprotection: 20 % pip in DMF (2 × 10 min), *rp*-HPLC purification; b) 0.4 mM in DMF, HATU (1.1 equiv, added in intervals), 2,4,6-collidine (11 equiv), 25 h, *rp*-HPLC purification, HPLC purity >95 %.

3.2.3 Structural Analysis

3.2.3.1 CD Spectroscopy

CD spectroscopy has been used successfully to deduce the secondary structure of peptides and proteins consisting of α -amino acids in solution. Recently Gellman's and Seebach's groups expanded the usage of CD spectroscopy to prove secondary structures of β - and γ -peptides.^[136, 138, 141, 143, 150, 195-200]

CD data for linear **113** in MeCN and MeCN-water solutions at various temperatures (Figures 36 a-d) reveal a distinctive secondary structure of the linear oligomer **113**. In order to allow comparison of the different CD curves of the mixed oligomers **113-115**, and the monomeric f-SAAs **106** and **107**, each curve was divided by the number of amide bonds present.

Comparison of the CD curves of Fmoc-protected f-SAA **106** with the curves of the linear mixed oligomer **113** (Figure 36a) shows, that the major part of the observed molar ellipticity T per residue is a result of cooperative effects due to the orientation of the backbone amide chromophores caused by a secondary structure and not a result of a single chromophore within the f-SAA **106** residues. The CD signature of **113** (Figure 36a) comprises a strong minimum at about 188 nm, a zero crossing at about 193 nm, and a strong maximum at about 202-203 nm and a weak minimum at about 239 nm.

As expected for secondary structural effects the maxima of the CD curves decrease with increasing temperature (Figure 36b).

A random structure would show the same average spectrum at all different temperatures. When changing the solvent from the relatively unpolar solvent MeCN to a one to one mixture of MeCN and water, the molar ellipticity for **113** decreases to almost half of the value of pure MeCN (Figure 36c). This may be due to the fact that the secondary structure the curve corresponds to is less populated in more polar solvents. As the CD signature of **113** in MeCN and MeCN-water solutions at temperatures between 20 and 75 °C is independent from concentration between 0.5 mM and 0.125 mM, it seems unlikely that aggregation occurs under the chosen conditions.

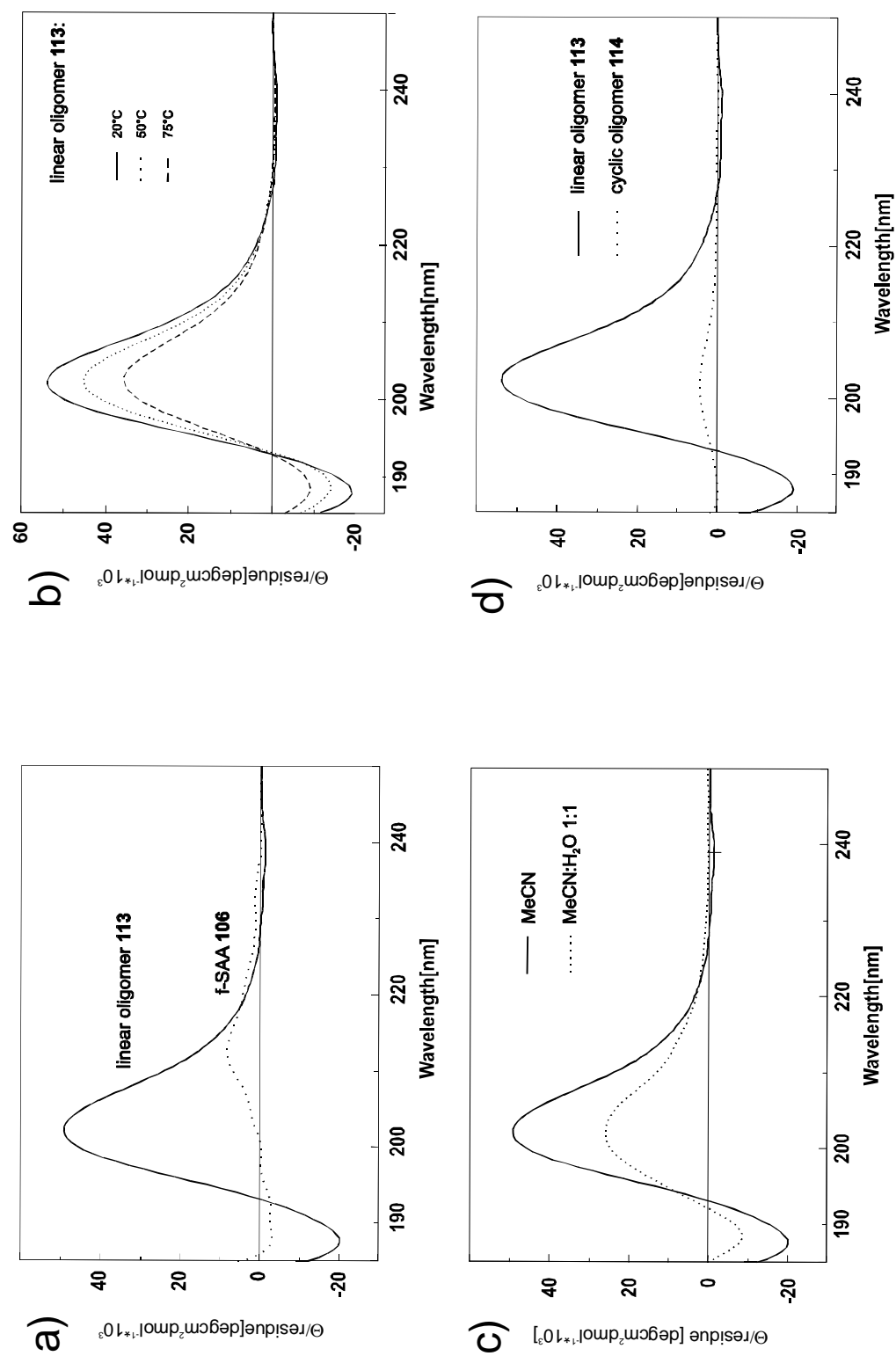


Figure 36: a) CD spectra (molar ellipticity Θ per residue in $\text{deg cm}^2 \text{dmol}^{-1} \cdot 10^3$) of the linear Fmoc-[f-SAAI106- β -hGly]₃-OH 113 and of Fmoc-protected f-SAA 106 in CH_3CN at 20°C at 0.125 mM (113), and 0.5 mM (106). b) CD data for the linear Fmoc-[f-SAAI106- β -hGly]₃-OH 113 at 0.125 mM in CH_3CN at 20, 50 and 75 °C. c) CD data for the linear Fmoc-[f-SAAI106- β -hGly]₃-OH 113 at 0.125 mM in CH_3CN and CH_3CN -water. d) CD spectra of the linear Fmoc-[SAAI106- β -hGly]₃-OH 113 and its cyclic analogue cyclo[f-SAAI106- β -hGly]₃ 114 at 0.125 mM and 20 °C in CH_3CN .

The CD signature of **113** (strong minimum at 188 nm, a zero crossing at about 193 nm, strong maximum at 202-203 nm, weak minimum at 239 nm) differs from the so far known CD patterns of β -peptides, which are associated with β -peptide structures. The CD pattern of the 12/10/12-helix shows a strong maximum at 205 nm, while the CD pattern of the 2.5_1 - or 12-helix has a maximum at about 204 nm, zero crossing at about 214 nm and a minimum at 221 nm. The 3_1 - or 14-helix finally exhibits a maximum at 200 nm and a minimum at 215 nm. However the influence of the orientation of the different chromophores to the CD pattern is not known and rationalized. Especially in the mixed 12/10/12-helix the contribution of the different turns to the overall CD pattern is not known. Furthermore, it is not possible to differentiate between the contribution of the f-SAA **106** residues' chiral centers and the contribution of the amide chromophores to the overall molar ellipticity of the linear oligomer **113**. Thus from the CD spectra of **113** only the presence of a stable secondary structure can be concluded. None of the known β -peptide helices can be excluded.

The typical CD signature of **113** is lost upon cyclisation to **114** (Figure 36d). This implies a drastic change of the orientation of the backbone amide chromophores upon cyclisation. However, the maximum is still at about 202 nm and the minimum at about 188 nm.

Due to low solubility of **115** in MeCN no CD spectra were recorded in this solvent. CD spectra of **115** in MeOH did not provide any useful structural information. The spectra were not very intense, and almost temperature independent. This suggests that there exists no stable secondary structure of **115** in MeOH.

3.2.3.2 NMR Analysis and MD-Calculations^g

Two-dimensional NMR data was obtained for **113** in MeCN and DMSO at 300 K. All ¹H resonances of each of the residue's spin systems were assigned by means of total correlation spectroscopy (TOCSY)^[201] and correlation spectroscopy (COSY).^[202] The backbone resonances were assigned using sequential C_β, C', H_α and H^N chemical shift information derived from HMQC^[203] and HMBC^[204] experiments as outlined in the experimental section. All the carbon signals were assigned, with the exception of the quaternary Fmoc-carbons, the quaternary carbons of the acetonide protecting groups of the f-SAA **106** residues, and the terminal carbon of the carboxylate function. Stereospecific assignment, utilizing NOESY^[205] cross-peak patterns, was possible for all the prochiral H_α and H_β protons of the β-homoglycine residues and for the prochiral methyl groups of all f-SAA **106** residues, with the exception of the terminal H_α and H_β resonances of β-hGly 6.

The secondary structure of **113** in MeCN is defined by 24 inter-residue NOE contacts comprised of a total set of 76 NOE restraints deduced from a NOESY experiment (see experimental section).

A first restrained conformational search, based on those 76 NOE cross peaks, was performed by utilizing standard simulated annealing protocols with the X-PLOR package,^[206] yielding an ensemble of 10 structures with good convergence. The structure which best fulfilled the experimental restraints was then used as a starting structure for a 150 picosecond simulated dynamics run. The MD calculation was carried out with the program Discover,^[207] using the CVFF forcefield, for further refinement. The refinement was performed in an explicit, all-atom MeCN solvent box developed especially for this purpose by Georg Voll in our group. This resulted in the 12/10/12 helical structure of **113**, depicted in Figure 37. The averaged structure was

^g The assignment of the MeCN spectra of **113** and subsequent distance geometry calculations were carried out by Vincent Truffault. The MD structural refinement was done by Georg Voll. All NMR spectra were recorded by myself on 500 MHz and 600 MHz spectrometers in MeCN, DMSO and pyridine. The assignment and structural calculations for the oligomers **113-115** in DMSO were as well performed by myself.

finally used as a starting structure for a further unrestrained dynamics simulation, and remained stable in the CVFF forcefield.

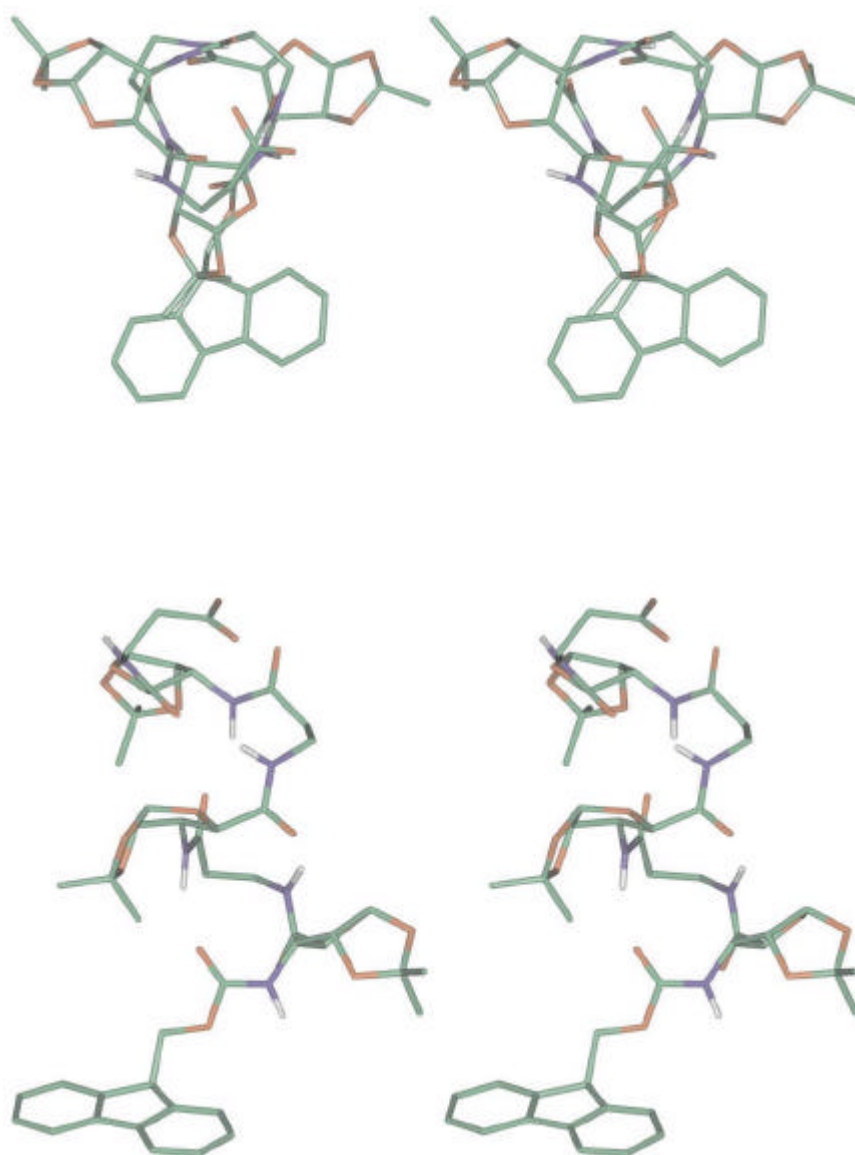


Figure 37: Stereo view of oligomer **113**'s average structure (deduced by a 150 picosecond restrained molecular dynamics simulation in an explicit, all-atom MeCN solvent box). Top view and side view of the formed right handed 12/10/12-helix of **113**, consisting of a central 10-membered and two terminal 12-membered H-bonded rings, and with C=O and N-H bonds pointing alternatively up and down along the axis of the helix are shown. All four H-bonds formed are depicted.

The deduced conformation is right-handed helical, with the helix consisting of a central 10-membered and two terminal 12-membered H-bonded rings, and with C=O and N-H bonds pointing alternatively up and down along the axis of the helix. Four hydrogen bonds are formed, which are shown schematically in Figure 38.

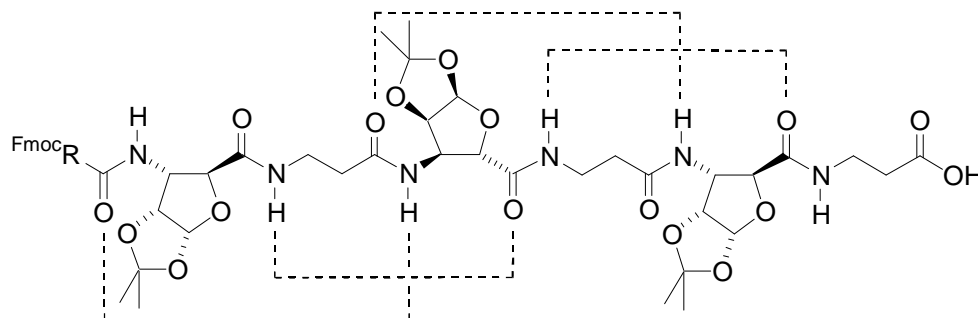


Figure 38: Schematic drawing of oligomer **113** with the hydrogen bonds formed in its MeCN solution structure of a 12/10/12 helix.

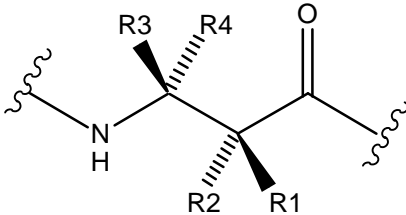
We have carefully checked for evidence of all other possible helix types, which β -peptides may adopt as predicted by quantum mechanical calculations.^[208-210] All distinctive cross peaks for the other possible helix types 10/10/10, 12/12/12, and 14/14/14, as well as for the most likely 10/12/10 helix (the counterpart of the observed 12/10/12 helix), were missing in the NOESY spectrum. All other characteristic distances, which would lead to strong signals for the mentioned helices, are represented by only weak signals in the spectrum. We therefore conclude that **113** assumes plain 12/10/12 helical conformation in MeCN, in competition with a slightly unfolded helix (see experimental section).

This is the first occasion of this type of helix found for SAA-homooligomers or short SAA- β -amino acid conjugates. So far, a similar helix has only been found by Seebach and co-workers for pure β -peptides.^[150] The substitution pattern of these β -peptides, which have been shown to form this “mixed 12/10/12 helix”, is very different from that of oligomer **113**. Oligomer **113** (when considered as a β -peptide) consists of alternating (S,S)-disubstituted β -(Sugar) amino acids^h and the

^h Here, only the substitution along the resulting peptidic backbone is considered

unsubstituted β -hGlys, denoted $[\text{SS-U}]_3$, according to the nomenclature of Hofmann and Günther^[209] (depicted in Table 3). Seebach's β -peptide however shows the very different substitution pattern of $[\text{B-A}]_3$, where the β -amino acid residues are alternately (S)-mono-substituted in the α - or in the β -position.

Table 3: Nomenclature of Substitution Patterns of **b**-Peptides.



R_1	R_2	R_3	R_4	Seebach ⁱ	Symbol
H	H	H	H	$-\beta\text{-hGly}-$	$-\text{U}-$
$R \neq \text{H}$	H	H	H	$-(\text{S})\beta^2\text{-hX}_{\text{aa}}-$	$-\text{A}-$
H	H	$R \neq \text{H}$	H	$-(\text{S})\beta^3\text{-hX}_{\text{aa}}-$	$-\text{B}-$
H	$R \neq \text{H}$	$R \neq \text{H}$	H	$-(\text{R,S})\beta^{2,3}\text{-hX}_{\text{aa}}-$	$-\text{RS}-$
$R \neq \text{H}$	H	$R \neq \text{H}$	H	$-(\text{S,S})\beta^{2,3}\text{-hX}_{\text{aa}}-$	$-\text{SS}-$

The quantum-mechanical investigation of β -peptides by Möhle and coworkers^[208] reveals the helix types 10/10/10, 12/12/12, 14/14/14, 10/12/10 and 12/10/12 as stable conformations for various types of β -peptides (either with one or two different amino acids in the repeat unit), with the most stable conformation depending on the substitution pattern of the amino acid. Interestingly, for an alternating $[\text{BA}]$ -substitution pattern, helix type 12/10/12 is predicted to be the most stable type in non-polar solvents. This may be ascribed to the fact that in the 12/10/12-helix, the carbonyl functions alternately point towards the N-terminus and the C-terminus,

ⁱ The notation $\beta\text{-hXaa}$ for a homologue of the α -amino acid Xaa was introduced by Ondetti and co-workers,^[147] and has been used and refined by Seebach and co-workers to β^2 - and β^3 -hXaa, where the numbers indicate the position of the side chains in the β -amino acids.^[148]

resulting in a low overall dipole momentum of the helix. For the [BA]-substitution pattern, the spatial constraints imposed by the β -substituent of the first amino acid in the sequence leads to a lower energy of a 12/10/12 helix in respect to a 10/12/10 helix, which also has a low overall dipole momentum. Furthermore, it has been shown that substitution in β -position has a considerably higher structural influence than substitution in α -position.^[210] Therefore, in a [SS]-substituted β -amino acid, the influence of the β -substituent will dominate over the influence of the α -substituent. On the other hand, an unsubstituted β -amino acid lacks a β -substituent with its dominating structural influence. Thus, the [SS]-substituted f-SAA **106** in **113** rather acts like a [B]-substituted β -amino acid than an [A]-substituted one, whereas the unsubstituted β -hGly in **113** behaves like an [A]-substituted β -amino acid. In consequence the oligomer **113**'s substitution pattern of [SS-U]₃ should induce similar secondary structures as the [AB]₃ substitution pattern of Seebach's "mixed" β -peptides. This would explain why oligomer **3** forms the 12/10/12-helical structure in MeCN.

NMR structural analysis of oligomer **113** in DMSO revealed, that no longer a 12/10/12 helix is formed exclusively. This observation is in agreement with the results from the CD-spectra and quantum mechanical calculations, which reveal that helices with a large permanent dipole moment become favored in polar solvents over helices with a small dipole moment (such as the 12/10/12 helix).^[208-210]

Similar to the procedure often used to deduce the sugar ring conformations of DNA or RNAs, the conformation of the f-SAA **106** residues in the linear oligomer **113** in DMSO was deduced (Figure 41), utilizing the information contained in the coupling constants $^3J(\text{H}^1\text{H}^2)$ of 5.3 Hz, $^3J(\text{H}^3\text{H}^4)$ of 10 Hz, and $^3J(\text{H}^N\text{H}^3)$ of 8.9 Hz. For that task the refined Karplus equation of Haasnoot et al. was used (Equation 1).^[211] In their equation the relationship between vicinal NMR proton-proton coupling constants and the pseudorotational properties of the furanoid sugar ring are taken into account. It also allows an accurate correction for the effects of electronegativity and orientation of substituents on $^3J(\text{HH})$.

$${}^3J(\text{H}^{\text{A}}\text{H}^{\text{B}}) = P_1 \cos^2 F_{\text{AB}} + P_2 \cos F_{\text{AB}} + P_3 + \sum_i S_i \{ P_4 + P_5 \cos^2(\varphi_i F_{\text{AB}} + P_6 \varphi_i) \}$$

Equation 1: Haasnoot et al.'s refined Karplus equation for furanoid sugar rings,^[211] which was used to determine the conformation of f-SAA **106** in oligomer **113** in DMSO. P_{1-6} are empirical determined parameters, their value depends on whether a $\text{H}^{\text{A}}\text{C}-\text{CH}^{\text{B}}$ or a $\text{H}^{\text{A}}\text{HC}-\text{CH}^{\text{B}}$ fragment is analyzed; F_{AB} is the proton–proton torsion angle, φ_i is either +1 or –1, depending on the orientation of the substituent S_i , S_i is the difference in the Huggins electronegativity of substituent S_i to hydrogen.

The first three terms describe the dependence of the vicinal coupling in a given H–C–C–H fragment on the proton-proton torsion angle F . The remaining terms account for the dependence of ${}^3J(\text{HH})$ on electronegative substituents, S_i , and (as the orientation of the substituent relative to the coupling protons plays an important role in this effect) these terms are also dependent on F . This term must be applied to all the non-hydrogen substituents on the central carbons of the H–C–C–H fragment under study, hence the summation sign. The magnitude of the correction due to each substituent S_i is correlated with the difference in the Huggins electronegativity between the substituent and hydrogen ($S_i = \chi_i^{\text{subst}} - \chi_{\text{H}}$). The relevant S_i used were: $S_{\text{C}} = 0.4$, $S_{\text{O}} = 1.3$, $S_{\text{N}} = 0.85$. In addition this primary (a) S_i values are influenced by β -substituents. As electronegative β -substituents demonstrate an opposite behavior compared with that of α -substituents (S_i), one can consider the influence of a β -substituent as moderating the electronegativity effect of an α -substituent. This is expressed by a formula where the electronegativity of an α -substituent S_i is defined by equation 2:

$$S_i^{\text{group}} = S_i^{\text{a-substituent}} - P_7 \sum_j S_j^{\text{b-substituent}}$$

Equation 2: Influence of the electronegativity of the group S_i^{group} attached to the fragment H–C–C–H as defined by Haasnoot et al..^[211] The summation is over all the substituents j attached to the α -substituent. S_i^{group} is the difference in electronegativity of the whole substituent group to a hydrogen; $S_i^{\text{a-substituent}}$ and $S_j^{\text{b-substituent}}$ are the difference in electronegativity for the **a**- or each of the **b**-substituents respectively; P_7 is an empirically derived constant by Haasnoot et al..^[211]

ρ_i^{group} is used in Equation 1, when a more refined calculation is desired. Here ρ_i^{group} was used.

The change of the position of a substituent S_i with respect to its geminal proton causes a change in the sign of the angle F in the electronegativity term in Equation 1. The influence of this relative orientation of the substituent S_i , was incorporated into Equation 1 by means of ρ_i . According to the orientation of the substituent S_i , ρ_i becomes +1 or -1 as depicted in Figure 39.

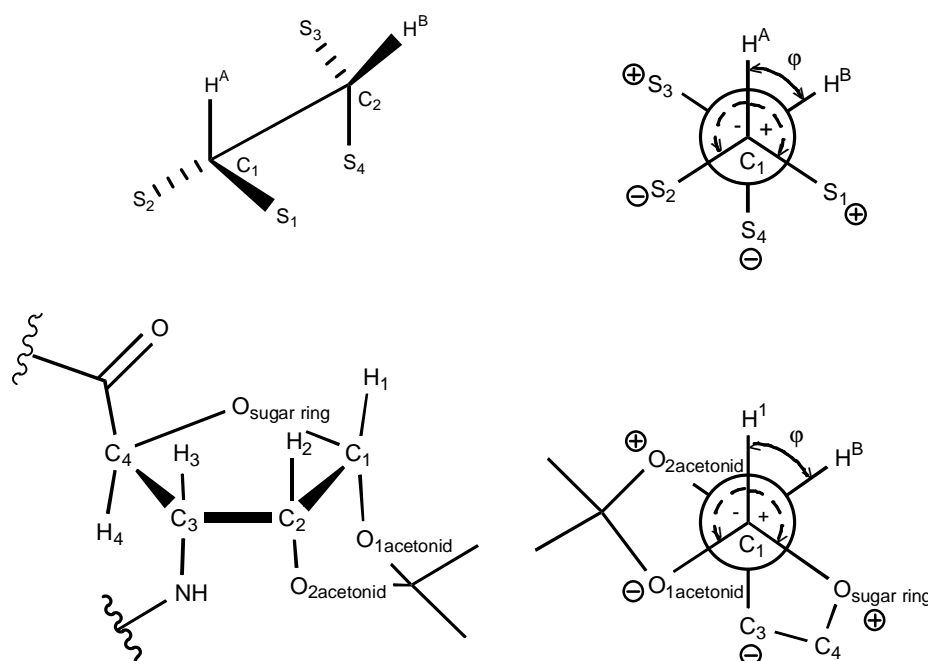


Figure 39: Definition of “positive” ($\rho_i = + 1$) and “negative” ($\rho_i = - 1$) substituents and application to H^1H^2 of *f*-SAA **106**.

Projecting the $H^A-C^1-C^2-H^B$ fragment along the vector C^1-C^2 (Figure 39) the orientation of a substituent S on C^1 is defined as being positive ($\rho_i = + 1$), when the projected valency angle between H^A and S amounts to approximately $+120^\circ$, counting clockwise from H^A . The orientation of the substituent is negative ($\rho_i = - 1$), when this angle amounts to 240° .

Application of the Equations 1 and 2, the definition of ρ_i depicted in Figure 39 and the ρ_i s listed above, resulted in the modified Karplus curves for ${}^3J(H^1H^2)$ and ${}^3J(H^3H^4)$ of *f*-SAA **106** shown in Figure 40.

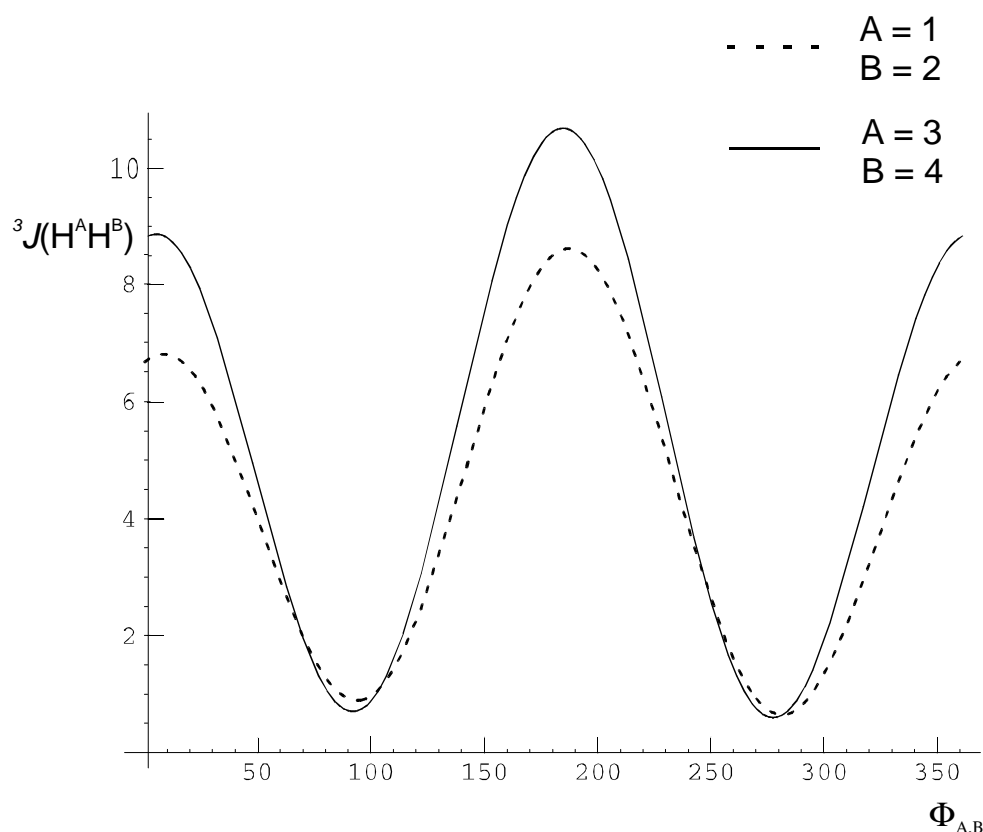


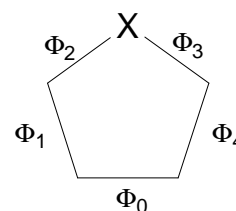
Figure 40: Karplus curves (refined, using Haasnoot et al.'s Equation 1) for the relation ${}^3J(H^1H^2) - F_{1,2}$ depicted (---), and ${}^3J(H^3H^4) - F_{3,4}$ depicted (—) of *f*-SAA 106.

The concept of pseudorotation was introduced by Kilpatrick et al.^[212] in their discussion of the “indefiniteness” of the cyclopentane ring. The starting point for defining the geometry of 5-membered rings is cyclopentane. It has been shown^[213] that the relationship between the five endocyclic torsion angles (F_0 - F_4) can be described by the simple cosine function in Equation 3.

$$F_j = F_m \cos(P + 4jp/5), \quad j = 0-4;$$

F_m = puckering amplitude

P = phase angle of pseudorotation



Equation 3: Relation between the endocyclic proton–proton torsion angle F_j , the puckering amplitude F_m and the phase angle of pseudorotation P , as well as the definition of the different endocyclic torsion angles in heterocyclic 5-membered rings F_j .

The application of the concept of pseudorotation and empirical correlations between the parameters governing the conformation of furanosides fragments in solid state, resulted in Equations 4a-c, interrelating the proton–proton torsion angles $F_{A,B}$ and the pseudorotation parameters F_m and P for α -D-ribose (and several others not listed here).^[214] f-SAA **106** is a derivative of ribofuranoic acid, hence Equations 4a-c are applicable.

$$F_{1,2} = 3.3^\circ + 1.102 F_m \cos(P-144^\circ) \quad (\text{a})$$

$$F_{2,3} = 0.2^\circ + 1.090 F_m \cos P \quad (\text{b})$$

$$F_{3,4} = -124.9^\circ + 1.095 F_m \cos(P+144^\circ) \quad (\text{c})$$

Equation 4: *Relation between the proton–proton torsion angles $F_{A,B}$ and the pseudorotation parameters F_m and P for α -D-ribose.*

When using the concept of pseudorotation, the conformation of the furanoid sugar ring is fully accounted for by the puckering amplitude F_m and the phase angle of pseudorotation P . It therefore was sufficient to determine only the two proton-proton torsion angles $F_{1,2}$ and $F_{3,4}$, in order to deduce the complete ring conformation of f-SAA **106** in oligomer **113** in DMSO shown in Figure 41. For f-SAA **106** in the linear oligomer **113** in DMSO $F_m = 38^\circ$, and $P = 21.8^\circ$ are obtained, when applying the Equations 1-4 in the above described manner. This corresponds to a C^3' -endo conformation, when using DNA/RNA nomenclature.

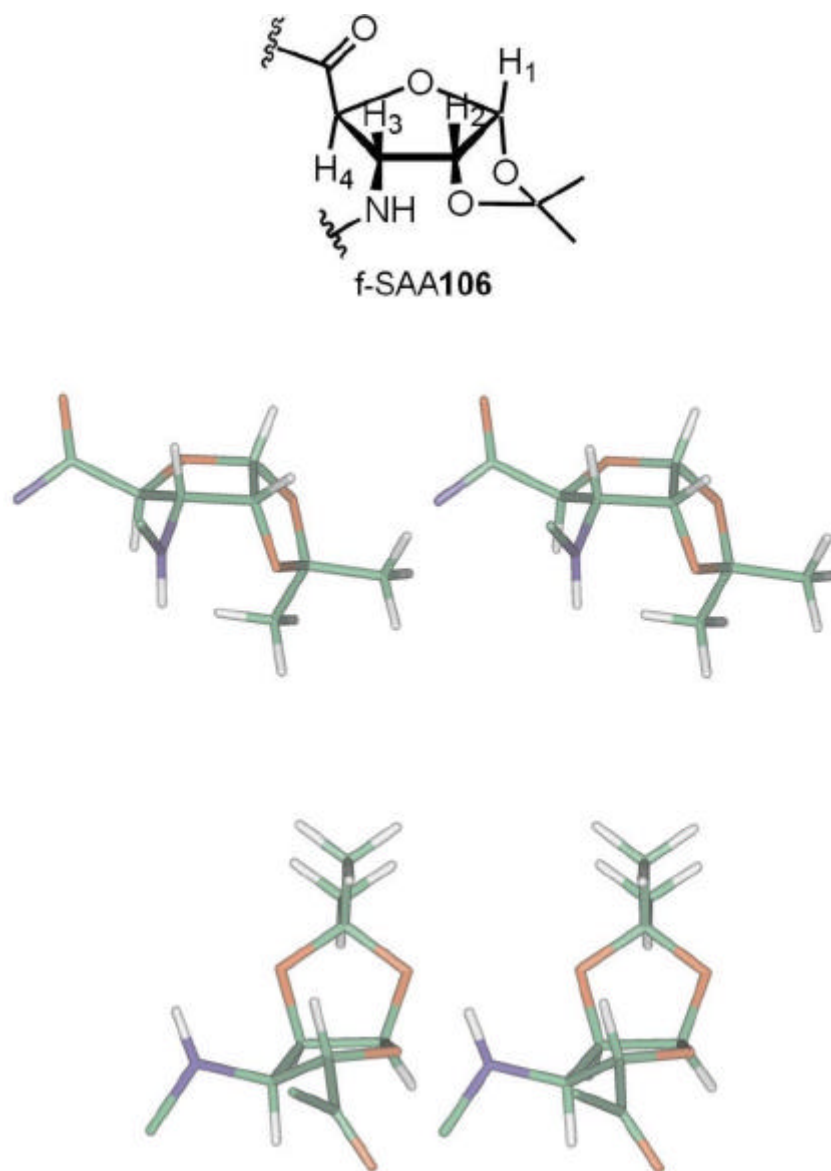


Figure 41: Stereoviews of the conformation of the *f*-SAA 106 residues of the linear oligomer 113 in DMSO. In DNA/RNA nomenclature this corresponds to a C^3' -endo conformation. Pseudorotational parameters deduced: puckering amplitude $F_m = 38^\circ$, phase angle of pseudorotation $P = 21.8^\circ$.

The coupling constants $^3J(H^\beta H^N)$ and $^3J(H^{\beta'} H^N)$ of the β -hGlys were also measured. For the H^β they are about 5.8 Hz, for the $H^{\beta'}$ around 6.7 Hz. This implies a gauche conformation. The chemical shifts of H^β and $H^{\beta'}$ of the same β -hGly differ by about 0.1 ppm. However, for all three β -hGly residues the different H^β 's and $H^{\beta'}$'s have almost identical chemical shifts. The H^N chemical shifts, on the other hand, are very well dispersed (Figure 42).

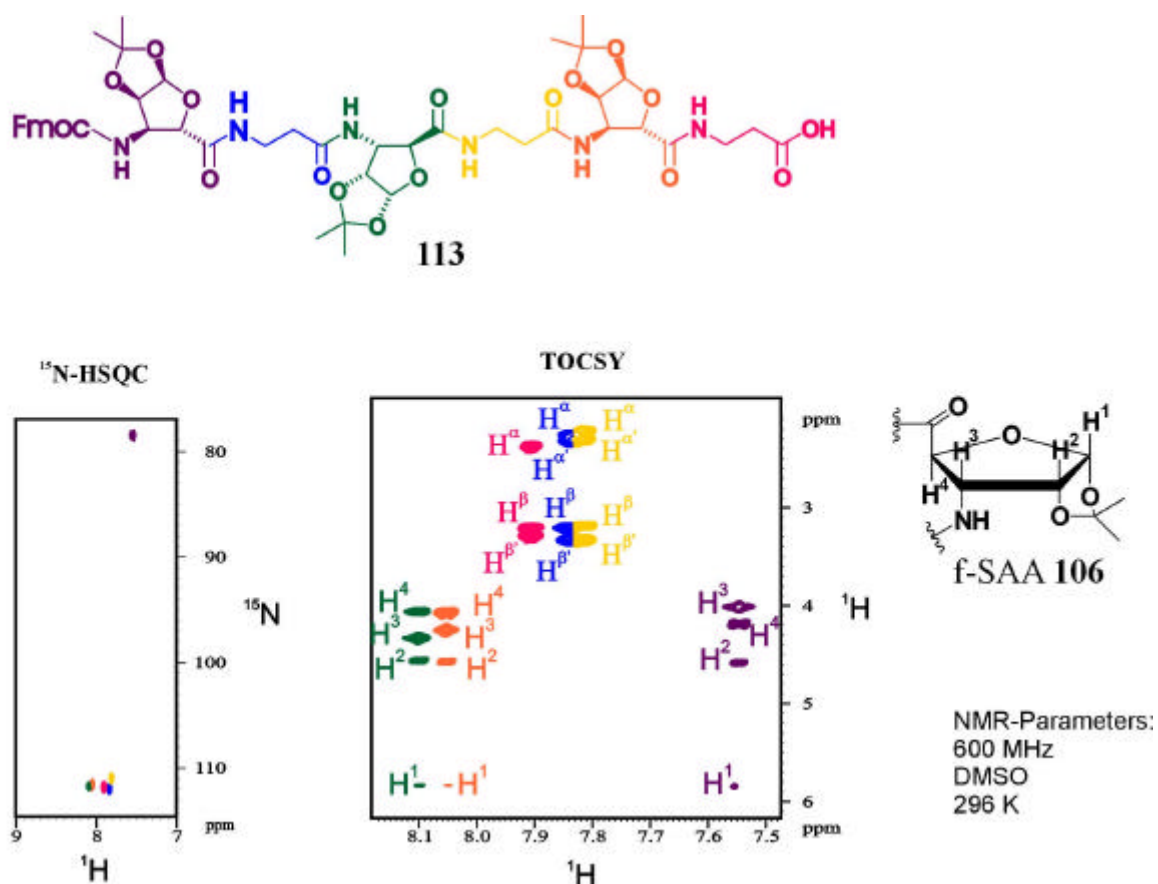


Figure 42: H^N region of the ^{15}N -HSQC and TOCSY spectra of oligomer **113** in DMSO at 296 K.

However, due to large overlaps of the sugar and alkyl protons in the NOESY spectra recorded in DMSO [d_6], the integration of several cross peaks is not possible, thus preventing reliable 3D structure modeling. Nonetheless these results show, that **113** also forms an ordered structure in DMSO, with a periodical structural motif, since all the β-hGlys and f-SAA **106** residues have coupling constants in the same range, and similar chemical shifts.

NMR studies for **115** and **114** at 500 or 600 MHz in DMSO and/or pyridine were performed. Full sequential assignment of **115** and **114** was achieved similar to the above described procedure for **113**. NOESY and ROESY spectra were recorded to obtain 3D structural information. The amide protons of the linear oligomer **115** have different chemical shifts (Figure 43). However due to large overlap of several NOEs no reliable structural calculation is possible.

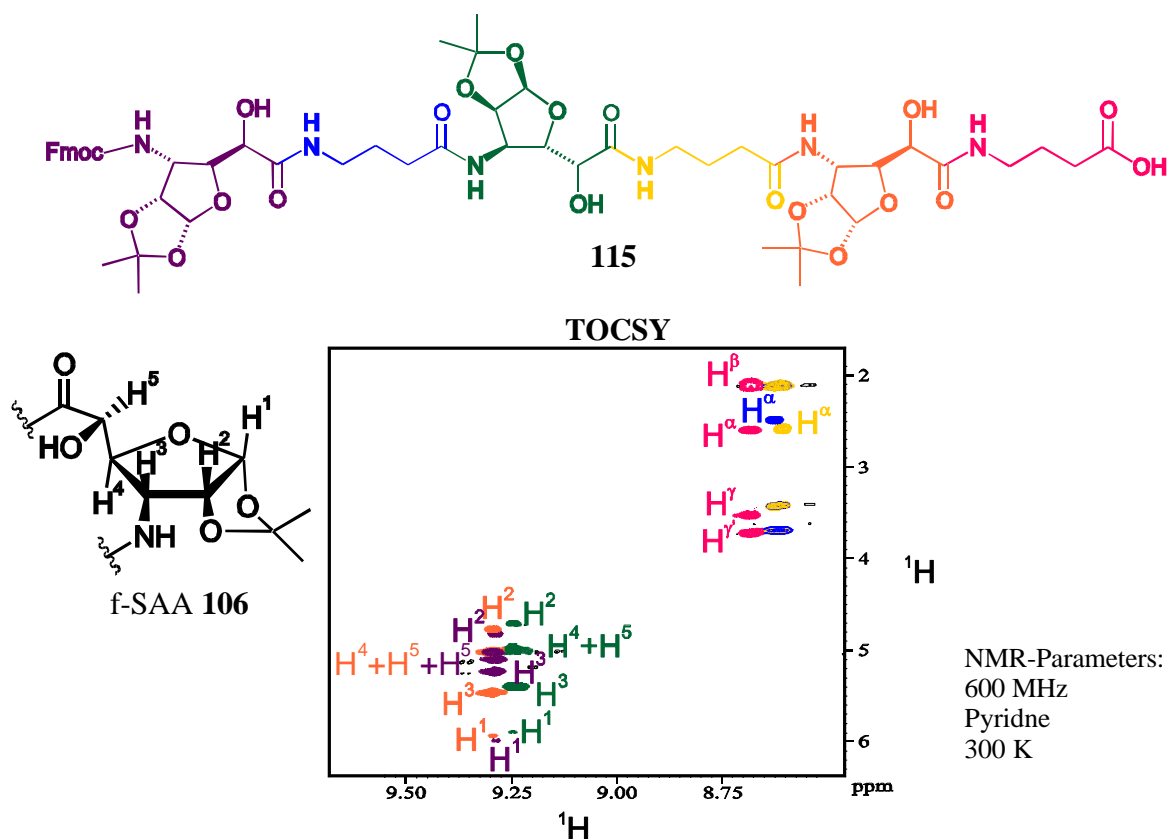


Figure 43: Amide bond region of the TOCSY of **115** measured at 600 MHz, and 300 K in $[D_5]$ pyridine.

The cyclic oligomer **114** exhibits apparent C_3 symmetry on the NMR chemical shift time scale (Figure 44), and mean J-coupling constants of 7 Hz between the H^N 's and the H^3 's of the f-SAA **106** residues (as opposed to the well differentiated residues in the linear oligomer **113** in DMSO).

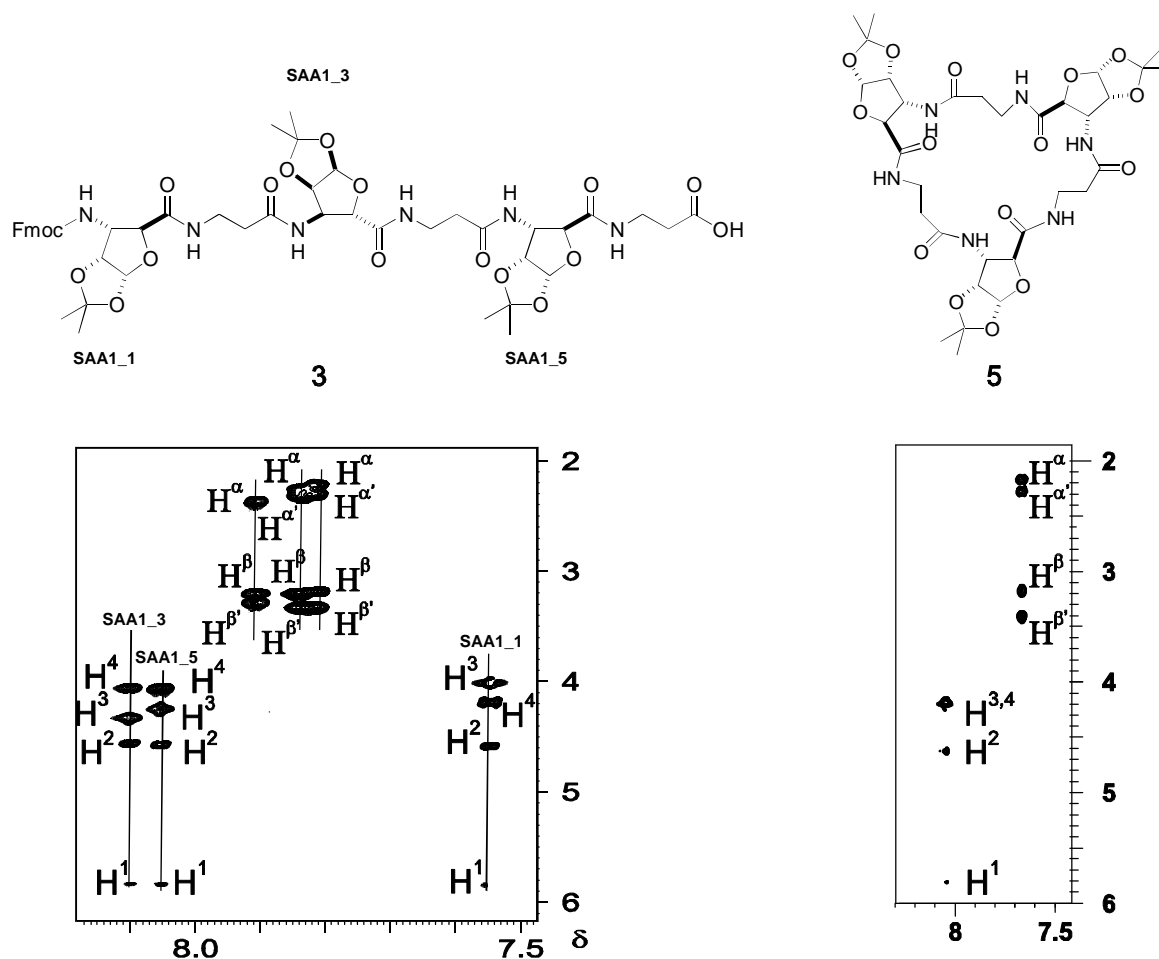


Figure 44: Amide bond region of the TOCSY spectra of the linear **113** and the cyclic **114** measured at 600 MHz, and 296 K in $[d_6]$ DMSO.

3.2.4 Conclusions

The straightforward syntheses in a few steps from diacetone glucose of two new furanoid sugar amino acids is described, making them easily accessible and therefore to useful building blocks for combinatorial syntheses. f-SAA **106** resembles a β -amino acid, while f-SAA **107** resembles a γ -amino acid. Thus, f-SAA **106** was used in conjunction with β -homoglycine for the synthesis of the mixed, linear and cyclic oligomers **113** and **114**. For the synthesis of linear oligomer **115** f-SAA **107** was used with GABA as amino acid counterpart. **113** and **115** were assembled successfully using standard solid-phase peptide synthesis.

The linear Fmoc-[f-SAA**106**- β -hGly]₃-OH **113** exhibited 12/10/12 helical secondary structure in MeCN as proven by NMR studies, and subsequent molecular dynamics calculations. This is remarkable, since **113** contains β -homoglycine, which is known to destabilize helices.^[149] Stable secondary structures were only reported for β -peptides consisting almost exclusively of substituted β -amino acids. It is obvious that the unsubstituted β -homoglycin is much more flexible (compare Gly substitution of L- α -amino acids in α -peptides). Hence, in short oligomeric sequences f-SAA **106** very strongly induces the secondary structural element of a 12/10/12-helix. We can not confirm Seebach's hypothesis, that the driving force of the 12/10/12-helix formation is the hydrophobic interaction between the side chains of the *i* and *i*+3 residues.^[140] In our 12/10/12-helix forming oligomer **113** either *i* or *i*+3 is a β -hGly residue and therefore has no side chains. However, these hydrophobic interactions surely stabilize Seebach's 12/10/12 helical conformations for his "mixed" β -peptides. The 12/10/12 preferred helical conformation of **113** is lost in the polar solvent DMSO. In DMSO **113** also adopts a secondary structure with a periodic structural motif.

The more flexible Fmoc-[f-SAA**107**-GABA]₃-OH **115** shows random coil behaviour.

Another remarkable feature is, that cyclo[-f-SAA**106**- β -hGly-]₃ **114** is well soluble in organic solvents, such as MeCN, DMSO and MeOH. Cyclic β -peptides prepared by Seebach et al. exhibited low solubility in classical, pure organic

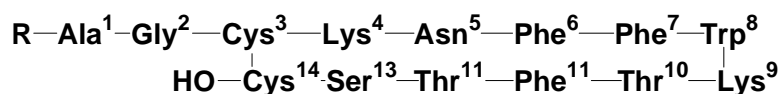
solvents.^[138, 139, 215] Thus, 1D NMR studies were either not possible or [d₈]-THF solutions containing more than 10 equivalents of anhydrous LiCl had to be used.^[215] Cyclic oligomer **114** exhibits a C₃ symmetric conformation on the NMR chemical shift time scale. However, our preliminary NMR results do not yet give evidence of clearly distinct conformation, since the observed NMR signals are averaged, and similar to those of the monomeric subunits.

The new compounds presented here are useful as new structural templates,^[22, 120] and might also be of interest for host-guest chemistry.^[59, 101]

3.3 Somatostatin Analogues Containing f-SAA 106 and f-SAA 107 as Structure-Inducing Templates

3.3.1 Somatostatin – General Introduction

Somatostatin (Figure 45) is a cyclic peptide hormone, which was first isolated from ovine hypothalamus in 1973, while searching for the growth hormone of the pituitary gland.^[216] Due to its central role in the regulation of growth hormone secretion, it is often referred to as somatotropin release-inhibiting factor (SRIF) or growth hormone (GH) release-inhibiting factor.^[217] Native somatostatin occurs in two biologically active forms, somatostatin-14 (SST-14 or SRIF-14) and a 28-residue peptide with an additional 14 amino acids at the N-terminus of SST-14, somatostatin-28 (SST-28 or SRIF-28).^[218]



SST 14: R= H

SST 28: R= HSer-Ala-Asn-Ser-Asn-Pro-Ala-Met-Ala-Pro-Arg-Lys-

Figure 45: Bioactive forms of native somatostatin: somatostatin-14 (SST 14 or SRIF-14) and somatostatin-28 (SST 28 or SRIF-28).

Both of them are derived from the polypeptide precursor prosomatostatin.^[219] Somatostatin is synthesized in neuronal and endocrine cells in various body-tissues.

3.3.1.1 Physiological Activity of Somatostatin

It was shown that somatostatin not only inhibits growth hormone (GH) release, but acts on a variety of physiological functions in various areas of the body.^[220] All its actions are inhibitory in nature. Somatostatin inhibits virtually every endocrine and

exocrine secretion, such as insulin, glucagon, gastrin, secretin and pepsin secretion. It inhibits the gastrointestinal absorption of ions, nutrients and minerals, inhibits cell proliferation and modulates vascular contraction. Motoric, sensory, behavioral, cognitive and autonomic effects as well as intestinal motility are influenced. These pleiotropic effects can be resolved in three cellular processes, that are modulated by somatostatin: neurotransmission, secretion, and cell proliferation (Figure 46).

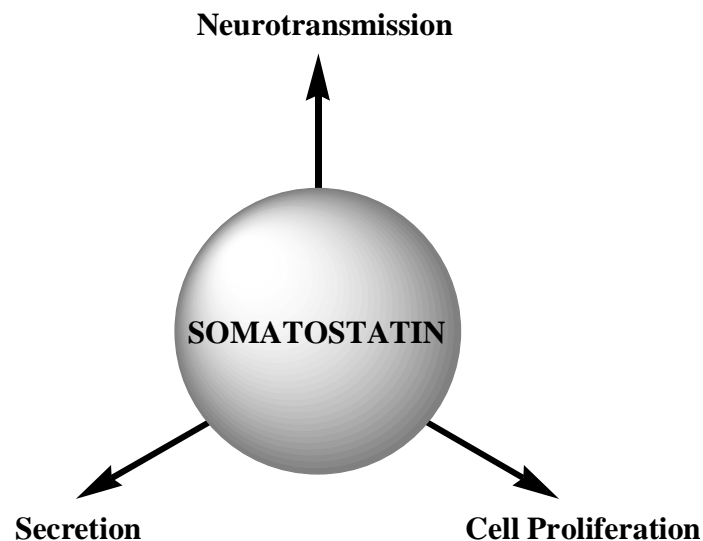


Figure 46: Cellular processes influenced by somatostatin (SST 14 and SST 28).

Because of its wide range of physiological functions, somatostatin may play an important role in the treatment of numerous human diseases, such as diabetes, cancer and in all diseases based on endocrine and gastrointestinal malfunction. This therapeutic potential was recognized years ago. However, the clinical use of somatostatin itself has been hampered, because of its very short half-life in circulation of about one minute and because of its lack of selectivity. So obtaining potent, selective and stable analogues that could be useful clinically proved to be very difficult.

3.3.1.2 Non-peptidic Somatostatin Analogues

The pharmacological limitations of somatostatin analogues, such as their poor oral bioavailability or too short half-life, are the main reasons for the steadily growing interest in a rational design of nonpeptide mimetics of somatostatin.

Hirschmann *et al.* designed peptidomimetics of somatostatin employing a β -D-glucose scaffold **52** (Chapter 2.7.1, Figure 6).^[70, 74] The SAA **43** containing somatostatin analogue (Chapter 2.7.1) is also considered as a nonpeptidic mimetic of somatostatin.

Damour *et al.* synthesized a series of 3-functionalized proline and β -lactam derivatives bearing an aryl group, such as a phenyl or a 3-indolyl, either in position 3 of the proline moiety (**116–120**) or on the 3-methyl chain of the β -lactam skeleton (**121, 122**) (Figure 47).^[221]

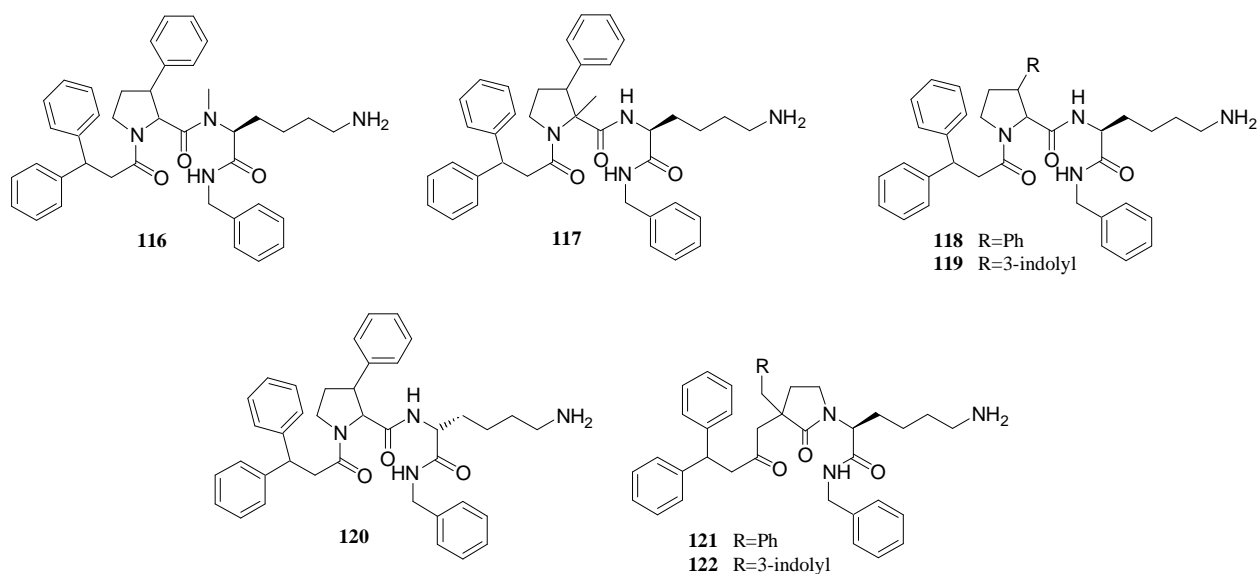


Figure 47: Structures of non-peptidic analogues of SST based on 3-functionalized proline (**116–120**) and β -lactam (**121, 122**).

The enzymatic stability of β -peptides makes them an interesting alternative to natural peptides in medicinal chemistry.^[222] Seebach *et al.* used β -peptides as somatostatin mimetics. Their β -dipeptide **123** shows high selectivity to SSTR 4.^[223, 224]

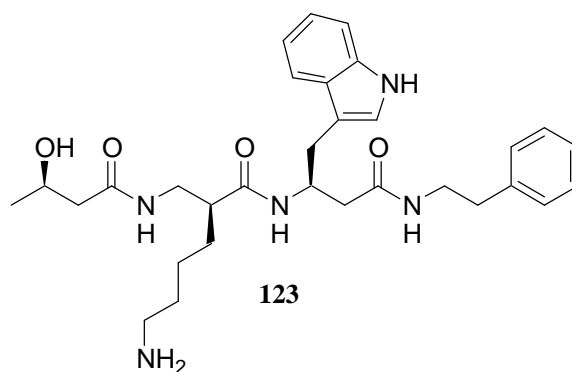


Figure 48: Seebach's *b*-dipeptide **123** somatostatin analogue, selective on SSTR 4 with a K_D of 74 nM.

Until 1998 there were no reports in the literature of the successful development of a selective, competitive somatostatin receptor ligand of nonpeptidic origin. The first potent nonpeptidic agonists to selectively bind at the SSTR 2 receptor (in the nanomolar range) were reported by the Merck group.^[225, 226] They described studies utilizing direct screening, which resulted in the discovery of first lead from which a new class of small nonpeptide analogues of somatostatin was derived. Among them two analogues, **124** and **125** (Figure 49), exhibited low nanomolar binding to human SSTR2, functional potency and high selectivity (> 1000-fold) toward the other receptor subtypes. **125** has even higher affinity for SSTR2 than somatostatin.

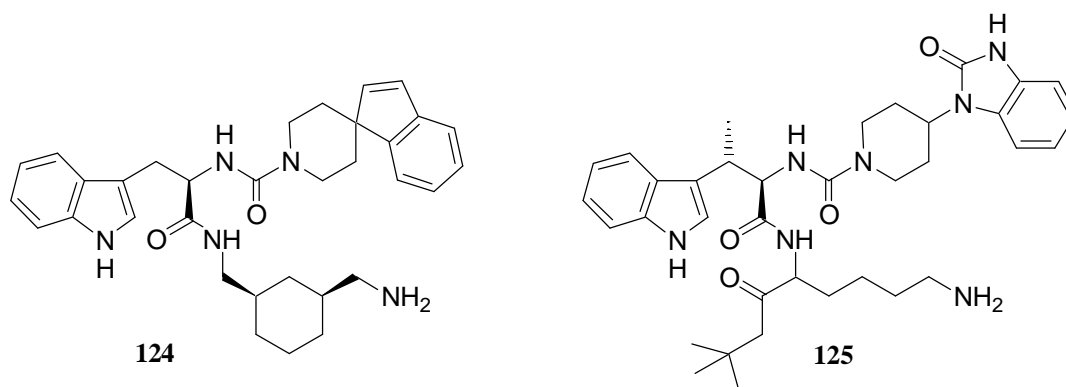


Figure 49: Structure of **124** and **125**.

Ankersen *et al.*^[227] initiated a screening program to identify new nonpeptide chemical entities with affinities for somatostatin receptor subtypes. Because four amino acid residues, Phe⁷, Trp⁸, Lys⁹ and Thr¹⁰, which comprise a β -turn, are thought to be

necessary for biological activity, they based their screening on a scaffold containing two aromatic groups and a basic group. Two aromatic groups, one of them heteroaromatic, were postulated to mimic Trp⁸ and Phe⁷ residues of SRIF. Lys⁹ was mimicked by primary amino groups, as well as by all sorts of nitrogen-containing functional groups. The most potent compound of this series, **126** (Figure 50) binds to the SSTR4 receptor with an affinity of 6 nM and at least a 100-fold selectivity for SSTR4 over the other four somatostatin receptor subtypes. In a functional assay, **126** showed full somatostatin receptor agonism (95% of SRIF) with an EC₅₀ of 2 nM.

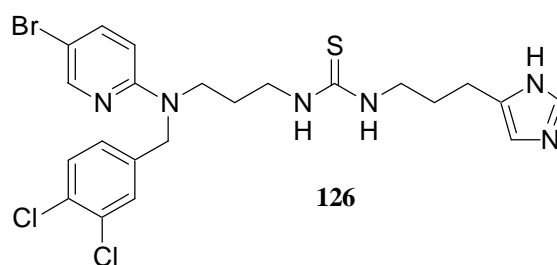


Figure 50: Structure of non-peptidic SST analogue **126**.

The lack of somatostatin analogues, both peptide and nonpeptide, with selectivity for all five receptor subtypes has impeded progress in understanding the functions associated with these receptors. The use of combinatorial chemistry seemed to be the fastest way to identify nonpeptide ligands selective for each of somatostatin receptor subtypes. Recently, the Merck group^[228] used an integrated approach of combinatorial chemistry and high-throughput receptor-binding techniques to rapidly identify subtype-selective compounds. Nonpeptide agonists of each of the five somatostatin receptors were identified in combinatorial libraries constructed on the basis of molecular modeling of the known peptide analogues (Figure 51). These nonpeptide, small-molecule analogues of somatostatin may be useful in the development of orally active chemotherapeutic agents capable of crossing the blood–brain barrier.

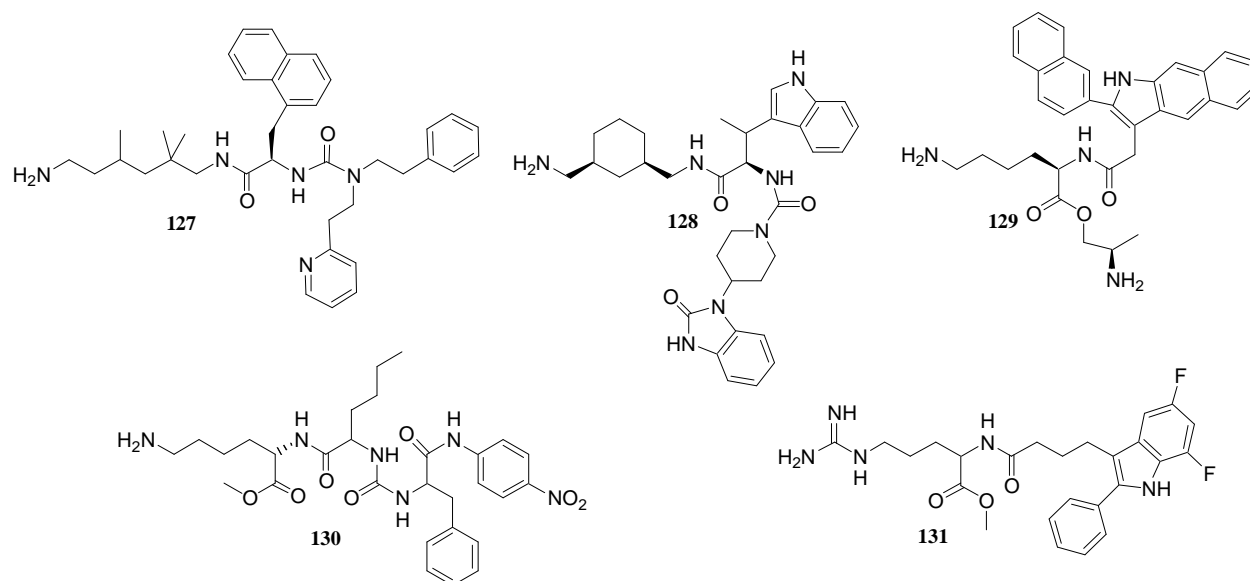


Figure 51: *SSTR* subtype selective nonpeptide agonists **127-131** of the somatostatin receptor identified by use of combinatorial chemistry.

3.3.1.3 Somatostatin Receptors

Somatostatin acts via a family of high-affinity plasma membrane receptors termed SST receptors or SSTR.^[229-232] Beginning in 1992, the structures of the SSTRs were elucidated by molecular cloning.^[233, 234] Five individual subtypes were rapidly identified and shown to consist of a family of heptahelical G protein-coupled receptors (GPCR).^[229, 230, 232, 234-238] Human SST receptors (hSSTR) are encoded by a family of five nonallelic genes located on separate chromosomes. Four of the genes are intronless, the exception being SSTR 2, which gives rise to spliced variants SSTR 2A and SSTR 2B, which differ only in the length of the cytoplasmic C-tail.^[229, 230] There are thus six putative SSTR subtypes of closely related size, each displaying a seven trans-membrane domain (TM) topology. All SSTR-isoforms that have been cloned so far from humans as well as from other species possess a highly conserved sequence motif YANSCANP1/VLY in the VIIth TM, which serves as a signature sequence for this receptor family.^[229, 230] Overall, there is 39-57% sequence identity among the various members of this family, with SSTR 1 and SSTR 4 showing the highest

sequence identity. The individual subtypes display a remarkable degree of structural conservation across species. Thus there is 94-98% sequence identity between the human, rat, and mouse isoforms of SSTR 1.^[220]

The receptors can be further divided into two subfamilies: SSTR 2, 3, and 5 react with octapeptide and hexapeptide SRIF analogues and belong to one subclass; SSTR 1 and 4 react poorly with these compounds and form the second subclass.

SSTRs are located in various densities throughout our body (Figure 52). They are widely expressed in many tissues, frequently as multiple subtypes that coexist in the same cell.

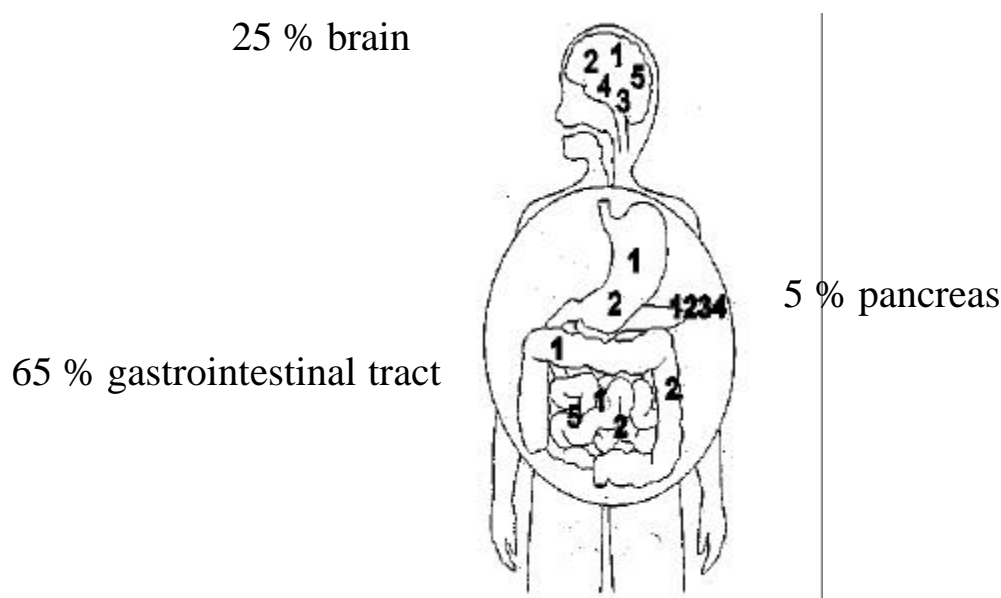


Figure 52: Distribution of somatostatin receptors in our body. The numbers 1-5 refer to the somatostatin receptors SSTR 1-5.

SSTRs are found in the brain, gut, pituitary, endocrine and exocrine pancreas, adrenals, thyroid, kidneys, gastrointestinal tract, and immune cells.^[220, 229, 230, 232, 239-241]

The deduction of the specific functional roles of the different SSTRs is under continuous and extensive investigation. SSTR 2 has been proposed to play a major role in inhibiting growth hormone regulation, glucagon and gastric acid secretion by somatostatin and its analogues.^[230] Receptor SSTR 5 has been found to have a limited role in growth hormone regulation, but instead may have a selective function in controlling insulin secretion.^[230, 242]

3.3.2 Somatostatin Analogues and Cancer

Various isoforms of the SSTRs are overexpressed on a large number of tumor cells, such as AtT-20 pituitary tumor cells, hamster insulinoma and Rin m5F islet tumor cells, AR42J, and MiaPaCa pancreatic tumor cells and in human breast cancer, neuroblastoma, glioma, and leukemic and myeloma cell lines.^[220, 229, 230, 232]

Some researchers claim, that SSTR 2 and 5 mediate the antiproliferative effects of somatostatin and its analogues on tumor growth,^[243-245] other postulate, that SSTR 1, 2, 4 and 5 induce cell cycle arrest, while SSTR 3 triggers apoptosis accompanied by activation of p53 and the pro-apoptotic protein Bax,^[239] again other authors suggest, that only equipotent binding to all five SSTRs, causes the desired high antitumor activity of somatostatin analogues.^[246] Therefore two major classes of somatostatin analogues have been developed: The receptor selective ones and the universal ones.

3.3.2.1 Chemotherapy

For some neoplasms, such as testicular cancer, cytotoxic chemotherapy is very effective. However, one of the major problems of cancer treatment is the development of resistance to chemotherapy.^[247] Furthermore conventional chemotherapeutic drugs, have shown limited efficacy and considerable toxicity in the first place.^[248] The efficacy of cytotoxic chemotherapy in the treatment of many common neoplasms such as those of the lung, breast, prostate, bowel, pancreas, liver, and kidney is limited. Cure of macroscopic metastatic disease is exceedingly rare, and palliation of symptoms of metastatic neoplasms by cytotoxic chemotherapy is problematic, since the toxicity of the treatment often outweighs any improvement in quality of life resulting from the temporary decrease in tumor burden.^[249-252] Because of this situation, a lot of effort is put into the development of novel cytotoxic agents and innovative noncytotoxic approaches.

Amongst the various anti-cancer agents, increasing attention is being paid to somatostatin analogues. The aim is to find somatostatin analogues, which induce cell cycle arrest, but do not retain the hormonal activity of somatostatin.

3.3.2.2 Somatostatin Analogues in Clinical Use

The increasing attention directed to somatostatin analogues, such as octreotide **132**, is largely due to the antineoplastic (that is mainly antiproliferative) activity of these compounds in a variety of experimental models in vitro and in vivo and to the clinical experience with somatostatin analogues in the treatment of conditions like acromegaly and GEP tumors. These analogues have been shown to be well tolerated compared to other antineoplastic therapeutics currently in use.^[248] However thus far, only three octapeptide somatostatin analogues are in clinical studies and/or use. They are octreotide **132** (SMS 201,995, sandostatin), lanreotide **133** (BIM 23,014, somatuline) and vapreotid (RC-160, octastatin) **134** (Table 4).

Besides being used in cancer treatment and palliation, radio labeled somatostatin analogues are employed for the localization of primary and metastatic tumors expressing somatostatin receptors.^[166, 253, 254] The so-called “somatostatin receptor scintigraphy” is indeed the most important clinical diagnostic investigation for patients with suspected neuroendocrine tumors. Targeted radiotherapy, which is in clinical trials, represents the obvious extension of somatostatin scintigraphy.^[255, 256]

3.3.2.3 Apoptosis

In multicellular organisms, homeostasis is maintained through a balance between cell proliferation and cell death. Although much is known about the control of cell proliferation, considerable less is known about the control of cell death. Physiological cell death occurs primarily through an evolutionarily conserved programmed form of cell suicide termed apoptosis (greek: *apo* = off, from; *ptosis* = falling). The basic machinery to carry out apoptosis appears to be present in essentially

all mammalian cells at all times, but the activation of the suicide program is regulated by a wide range of regulatory stimuli that originate from both the intracellular and the extracellular milieu.^[257-262] Malfunction of apoptosis leads to severe diseases, such as cancer, viral infections and Alzheimer's disease. Treatments designed to specifically alter the apoptotic threshold may have the potential to change the natural progression of some of these diseases.

Recent research has demonstrated that Kéri's somatostatin analog TT232 (**135**) is capable of inducing apoptosis selectively in certain tumor cell lines, without the hormonal bioactivity of native somatostatin.^[165, 247, 263, 264]

3.3.2.4 Concept, Strategy and Design of SAA Containing Somatostatin Analogues

3.3.2.4.1 Structure Activity Relationship Considerations

Extensive structure activity relationship studies of somatostatin revealed that the essential pharmacophore of somatostatin is Phe⁷-Trp⁸-Lys⁹-Thr¹⁰.^[265, 266] According to those studies Lys⁹ and Trp⁸ are assumed to be absolutely crucial for activity, while moderate substitutions of Phe⁷ and Thr¹⁰ are tolerated. Further structure-activity relationship studies of somatostatin revealed that the structural reduction retaining the cyclic nature of somatostatin led to a β -turn about the native Phe⁷-Trp⁸-Lys⁹-Thr¹⁰-sequence of somatostatin.^[159, 167, 267-273] Hence, replacement of Trp⁸ with D-Trp stabilizes the β -turn of the postulated active conformation of somatostatin. Activity is thus increased, while at the same time enzymatic stability is enhanced.^[274, 275] D-Trp⁸ SST-14^[274] **136** (Table 4) was the first analogue with significantly higher potency than somatostatin itself. Ever after D-Trp⁸ substitution has been considered critical for the potency of somatostatin analogues. It therefore has been retained in almost all somatostatin analogues synthesized thereafter (Tabel 4).

The "Veber-Hirschmann" peptide cyclo[-Phe-Pro-Phe⁷-D-Trp⁸-Lys⁹-Thr¹⁰-] **50** showed similar activity as somatostatin (Figure 6; chapter 2.7.1).^[158, 276-278] However, its clinical development has been halted due to steatorrhea caused as a side

effect. However replacement of the Phe-Pro bridge with Phe-Ala(NMe) resulted in Seglitid **137**, which is in clinical trials.^[279] In 1994 the incorporation of glucosyluronic acid methylamine (Gum) **43** as a dipeptide isoster replacing the Phe-Pro bridge in the sequence of **50** (See chapter 2.7.1) was introduced by our group.

Table 4: Structure of somatostatin and some of its peptidic analogues.

name	structure	
Somatostatin-14 (SRIF-14, SST-14)	H-Ala ¹ -Gly ² -Cys ³ -Lys ⁴ -Asn ⁵ -Phe ⁶ - Phe⁷-Trp⁸ HO-Cys ¹⁴ -Ser ¹³ -Thr ¹² -Phe ¹¹ -Thr ¹⁰ -Lys ⁹	
Somatostatin-28 (SRIF-28, SST-28)	H-Ser-Ala-Asn-Ser-Asn-Pro-Ala-Met-Ala-Pro Arg-Lys-Ala-Gly-Cys-Lys-Asn-Phe- Phe-Trp HO-Cys-Ser-Thr-Phe- Thr-Lys	
D-Trp⁸ SST-14 ^[265]	H-Ala ¹ -Gly ² -Cys ³ -Lys ⁴ -Asn ⁵ -Phe ⁶ - Phe⁷-DTrp⁸ HO-Cys ¹⁴ -Ser ¹³ -Thr ¹² -Phe ¹¹ -Thr ¹⁰ -Lys ⁹	136
Octreotide ^[269] (Sandostatin, SMS 201-995)	H-DPhe-Cys- Phe-DTrp Thr(ol)-Cys- Thr-Lys	132
Vapreotid (RC-160)	H-DPhe-Cys- Phe-DTrp H ₂ N-Trp-Cys- Val-Lys	134
Seglitid ^[279] (MK678)	(NMe)Ala- Tyr-DTrp Phe- Val-Lys	137
Lanreotid ^[280, 281] (BIM23014)	H-DβNal-Cys- Tyr-DTrp HO-Thr-Cys- Val-Lys	133
Veber-Peptid ^[158, 276-278] (L-363,301)	Pro- Phe-DTrp Phe- Thr-Lys	50
TT-232 ^[165, 247, 263, 282]	H-DPhe-Cys- Tyr-DTrp H ₂ N- Thr-Cys-Lys	135

Hirschmann et al.'s β-D-glucose scaffold derived somatostatin analogue **52** showed moderate activities, which demonstrated (See also 2.7.1, Figure 6)^[70, 74], that the peptide backbone is not a crucial part of the pharmacophore, but serves as a

scaffold to support the side-chains of Phe⁷, Trp⁸, Lys⁹ and Phe¹¹ in the required spatial arrangement. This is also supported by several nonpeptidic, highly receptor selective and active compounds, found in a combinatorial approach using high-throughput screening techniques (See also Chapter 3.3.1.2).^[225-228, 266, 283-285]

3.3.2.4.2 Stability - Cleavage Sites of Native Somatostatin

One of the major drawbacks of the therapeutic use of somatostatin itself is the low half life in the body of about one minute. For native somatostatin SST 14, at least 5 sites of enzymatic cleavage are known (Figure 53).^[286] Trypsin-cleavage between Trp⁸ and Lys⁹, causes complete loss of activity, as well as cleavage between Phe⁶ and Phe⁷ and cleavage between Thr¹⁰ and Phe¹¹. Aminopeptidase attack at the N-terminus is less threatening, since the resulting one or two amino acid shorter peptides retain activity completely.

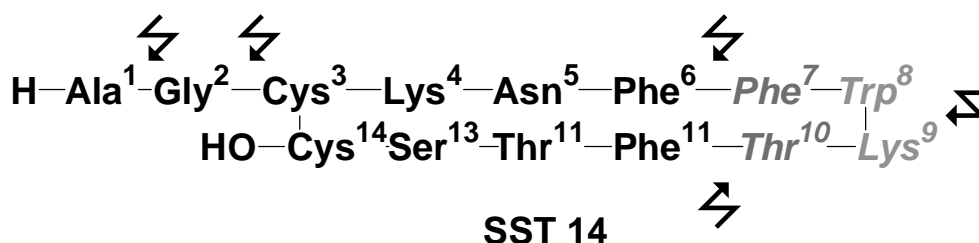


Figure 53: *Enzymatic cleavage sites of Somatostatin 14.*

3.3.2.4.3 Design of Apoptosis Inducing Somatostatin Analogues

The ultimate goal is a drug, which induces apoptosis selectively on tumor cells, without damaging healthy surrounding tissue, and without somatostatin's hormonal activities; a drug, which is orally available, stable in circulation with a long half life.

For that aim several parameters, such as the enzymatic stability and the optimum presentation of the pharmacophore, that is in the right spatial orientation,

have to be optimized. The pharmacophore might be optimized itself, since nature only has 21 natural amino acids to choose from, while chemist can use any unnatural amino acid as well.

To design such a drug, we used TT-232 **135** (Table 4) as a lead structure, since this is the only compound known so far to selectively induce apoptosis on tumor cells, without any of somatostatins hormonal activities. As a second lead structure we used the Veber-Hirschmann-peptide **50** (Table 4).

To optimize the enzymatic stability and to introduce at the same time a spatial constraint, we replaced the Cys-Cys-disulfide bridge of TT-232 (**135**) and the Phe-Pro bridge of the Veberpeptide **50** by the SAAs f-SAA **106** and f-SAA **107** (Figure 54). The SAAs are not recognized by peptidases. Thereby the lethal cleavage sites in native somatostatin (Figure 53) between Phe⁶ and Phe⁷ and between Thr¹⁰ and Phe¹¹ are “blocked”. The resulting compounds should show considerable longer half life in circulation.

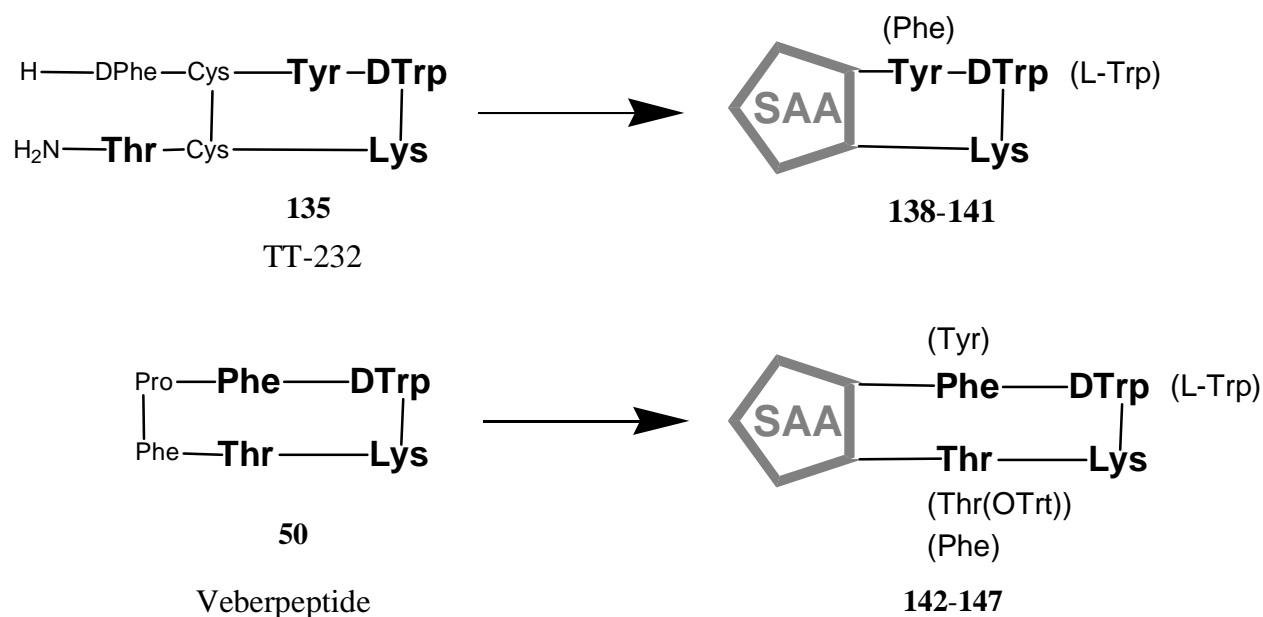


Figure 54: Design of somatostatin analogues; SAA= f-SAA **106**.

f-SAA **106** and **107** were especially designed as structure inducing templates, which are cheaper and faster to synthesize than the previously described SAAs and turn-mimetics.^[18, 21] (Their synthesis is described in chapter 2.3.2.5). At the Phe⁷ position of the natural sequence always Phe and Tyr and in the Thr¹⁰ position Thr,

Thr(OTrt) or Phe were used, since for those two amino acids moderate substitutions are tolerated. The aim of modifying those positions is to gain more selectivity and activity. D- and L-Trp were placed in the Trp⁸ position. This resulted in a family of four TT-232 derived and six Veber-Hirschmann peptide derived compounds.

Antitumor activity tests (Chapter 3.3.2.6) showed only activity for Veber-Hirschmann peptide derived compounds cyclo[–Tyr–D-Trp–Lys–Thr(OTrt)–f-SAA 106–] **142** and cyclo[–Tyr–Trp–Lys–Thr(OTrt)–f-SAA 106–] **143**, with a Thr(OTrt) in the Thr¹⁰ position. Therefore a big aromatic residue in that position seemed to be crucial for antitumor-activity. Based on this results a second larger library was designed (Figure 55).

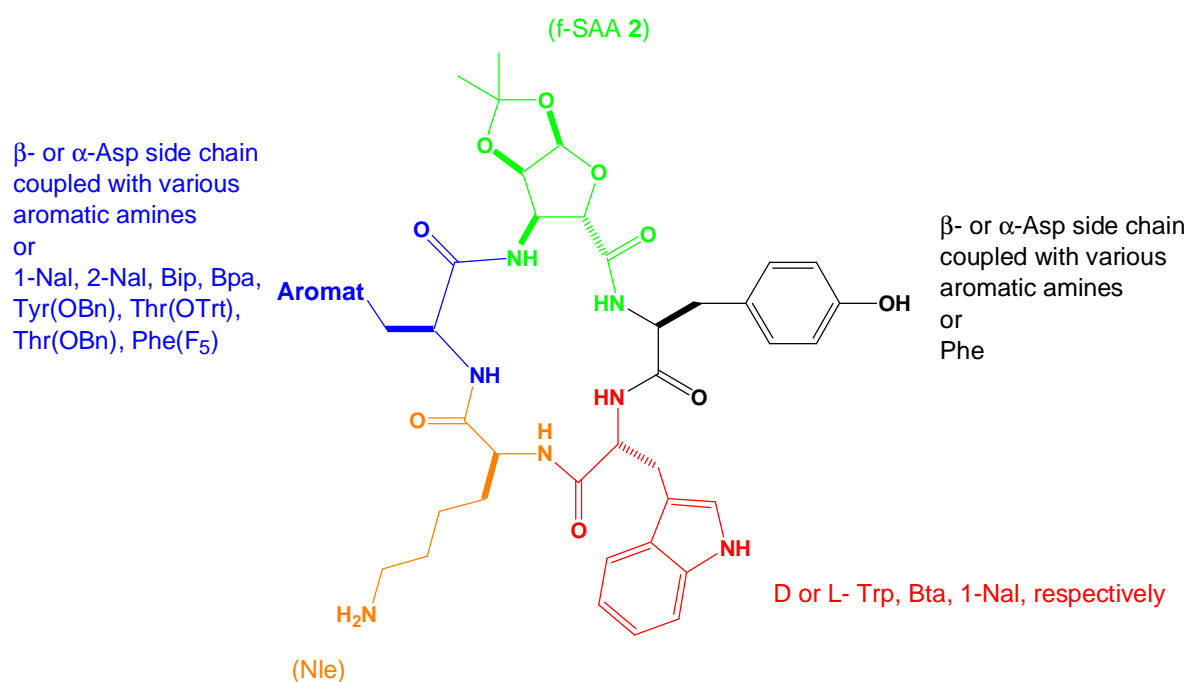


Figure 55: Design of second library, based on cyclo[–Tyr–Trp–Lys–Thr(OTrt)–f-SAA 106–] **142** and cyclo[–Tyr–D-Trp–Lys–Thr(OTrt)–f-Saa 106–] **143**. Color code: Trp⁸ position red, Lys⁹ position orange, Thr¹⁰ position blue, and f-SAA bridge green.

In a first strategy it was planned to introduce a large number of different aromatic side chains in the Thr¹⁰ position, by putting an aspartic acid (either as a α- or a β-amino acid) in that position and then couple it with different aromatic amines on solid phase (Figure 56). This strategy was designed to rapidly introduce a large diversity to the library during the solid phase assembly of the compounds.

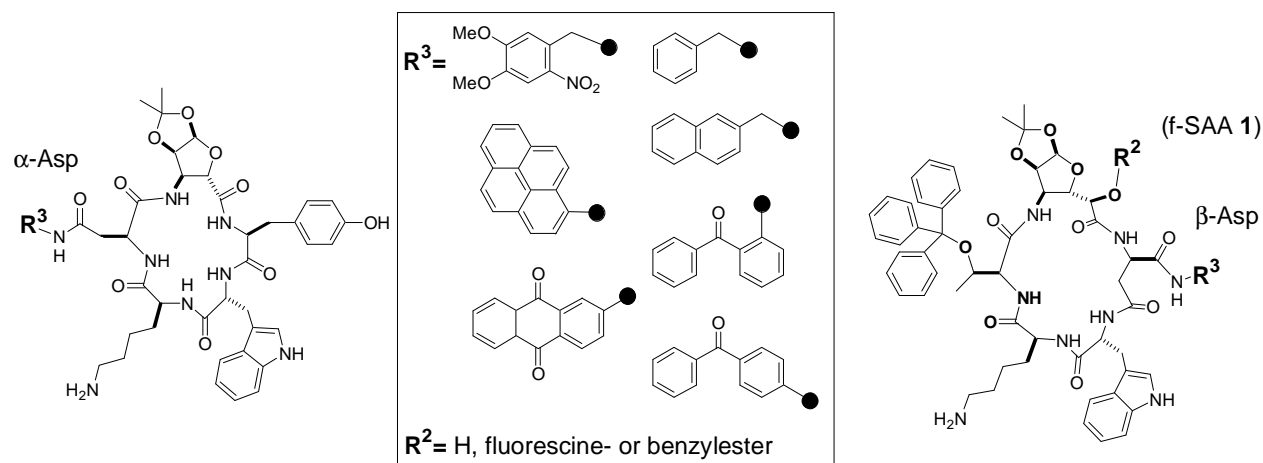


Figure 56: Strategy to rapidly introduce diversity on bead; and amines used.

However, all of the various coupling reagents and conditions applied did not result in satisfactory yields, to make this a rapid, successful and general way to introduce diversity into solid phase libraries (for the different synthetic strategies tried out see Chapter 2.3.2.5 and 4). Therefore the strategy to insert an aromatic residue in the Thr¹⁰ position was changed: Ready made aromatic building blocks were used for the assembly of the compounds. Various unnatural aromatic amino acids such as 1- and 2-naphthylalanine (1-Nal, 2-Nal), biphenylalanine (Bip), benzophenon-alanine (Bpa), pentafluorophenyl-alanine (Phe(F₅)), etc. as well as benzylethers of the natural amino acids Tyr and Thr were integrated into the sequence (Figure 57).

Diversity was also introduced, by replacing the amino acids of the pharmacophore Trp⁸ and Lys⁹ by several unnatural amino acids. Trp⁸ was substituted with 1-Nal, and D- and L-benzothienylalanine (Bta) in the otherwise unmodified **143** sequence. Lys⁹ was replaced by norleucine, to test, if the amino functionality is crucial for activity or if only the alkyl residue is responsible for recognition. Since the incorporation of Bta in the Trp⁸ position improved activity tremendously, several derivatives of D- and L-Bta containing analogues with various aromatic side chains in the Thr¹⁰ position were synthesized as well.

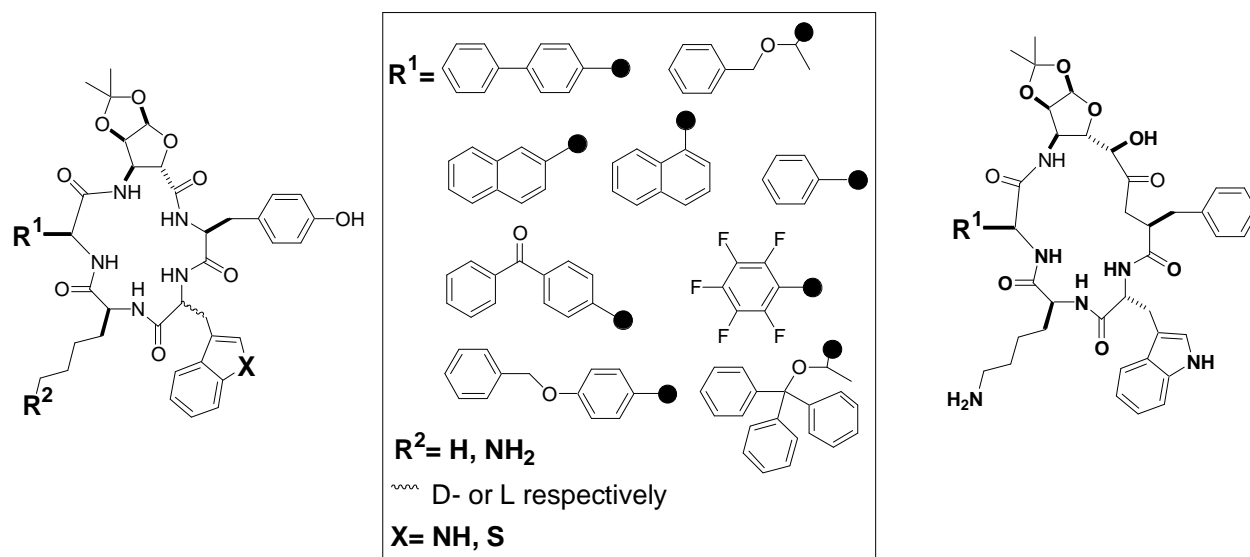


Figure 57: Variations of **143**: variations of the aromatic residue in the Thr¹⁰ position, variations of the f-SAA residue, variations of the Trp⁸ position and variation of Lys⁹. Not all possible combinations were synthesized.

3.3.2.5 Synthesis of SAA Containing Somatostatin Analogues on Solid Phase

The peptides were assembled on solid phase on tritylchloride-polystyrene-(TCP)-resin. Standard Fmoc-protocol was employed, using 2 equivalents of the amino acid (or 1.5 eq. of the f-SAA), 2 equivalents of HATU ([O-(7-azabenzotriazol-1-yl)-1,1,3,3-tetramethyl-uronium hexafluorophosphate]) and 2 equivalents of HOAt (1-Hydroxy-7-azabenzotriazol) as coupling reagents and 2,4,6-collidine (20 eq.) as base.^[170, 192, 193] The first amino acid anchored to the resin was either Fmoc-Tyr-OH, Fmoc-Phe-OH or Fmoc-D-Asp-Dmab (aspartic acid, used as a β -amino acid, the acid side chain is built into the backbone) respectively. Sidechain-unprotected tyrosine and tryptophane were used. This proved to be even beneficially to coupling but especially to cyclization yields, compared to the use of t-Bu-protected tyrosine and Boc-protected tryptophane. Lysine was orthogonally protected with the hydrazine labile ivDde-protecting group (1-(4,4-dimethyl-2,6-dioxo-cyclo-hexylidene)3-methylbutyl-).^[287] After final Fmoc-deprotection the linear peptides were cleaved from the resin with

hexafluoro isopropanol (20 % in dichloromethane, 3*20 min),^[194] before being cyclized using DPPA (DiphenylPhosPhoryl Azide) and NaHCO₃ in DMF (0,1 mM).^[288, 289] Deprotection with 3% hydrazine in DMF led to the crude cyclic peptides. rp-HPLC purification yielded the cyclic compounds **138-161** in over 99 % HPLC-purity and good overall yields between 20 and 41 %.

For the coupling of the deprotected side chain carboxylic function with various amines on bead, a protocol were the coupling reagents and the amine were added in small portions over several hours, proved most effective. Different coupling reagents and conditions were tested, with HATU/HOAt/2,4,6-collidine working the best. However, the yields were always low, especially when coupling aromatic amines (as is to be expected, due to their lower nucleophilicity). Therefore this strategy, proved not an effective way to introduce diversity in combinatorial libraries. Most often the yields were too low, to provided enough material for the biological test. The same is true for esterification on bead of f-SAA **107**.

3.3.2.6 Antitumor Activity of the f-SAA Containing Compounds^j

3.3.2.6.1 Antitumor Activity of the 1st Library on Multidrug-Resistant and Drug-Sensitive Tumorcells

Antitumor activity of the TFA salts of the compounds **138-147** was tested on drug sensitive rat hepatoma carcinoma cell line Clone 2^[290] and multidrug-resistant subclone Clone 2(10x80)T1 for the first library of 10 compounds (Figure 58).^[291] The concentration of compounds **138-147**, which reduced the viability of the treated cells by 50% compared to controls (IC₅₀ values), were determined from at least 2 independent experiments for each compound tested, using the XTT assay.^[292, 293]

^j Tests were performed by our collaborators Gyorgy Kéri and Richard Schwab from the Semmelweis Medicinal University, Budapest, Hungary and Aniko Venetianer from the Hungarian Academy of Sciences, Szeged Temesvari krt., Hungary

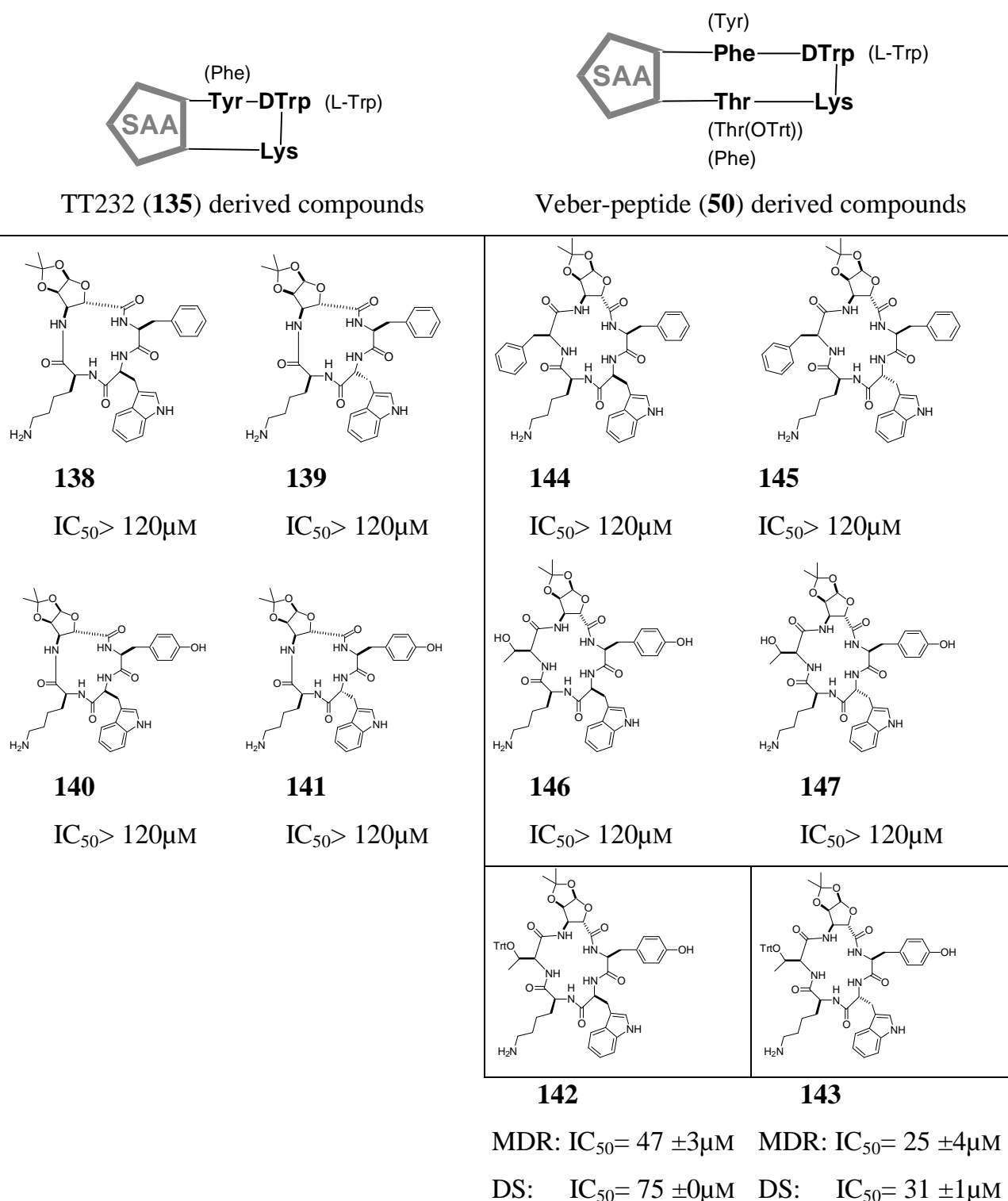


Figure 58: Structures and activities of compounds **138-147**. Cell lines used for IC_{50} -determination: MDR: multidrug resistant hepatoma cell line clone 2(10x80)T1;^[291] DS: drug sensitive hepatoma cell line clone 2;^[290] was internal reference for all tests: MDR: $9 \pm 0.5 \text{ nM}$; DS: $10 \pm 0.7 \text{ nM}$.

Compound **142** showed an IC_{50} of $75\mu\text{M}$ for the drug sensitive, and of $47\mu\text{M}$ for the MDR cell line. Compound **143** containing D-Trp, was even more active with an IC_{50} of $31\mu\text{M}$ for the drug sensitive and of $25\mu\text{M}$ for the drug resistant cell line. **135** was used as internal reference, with IC_{50} values of $10\mu\text{M}$ for the drug sensitive clone and $9\mu\text{M}$ for the MDR one. Compounds **146** and **147**, with Thr in the Thr¹⁰ position, and compounds **144** and **145** with the comparably small aromatic amino acid Phe in the 10 position, show IC_{50} values over $120\mu\text{M}$, while compounds **142** and **143**, with the big aromatic trityl ether in the corresponding position, show high activities.

3.3.2.6.2 Antitumor Activity Tests of the 2nd Library

Compounds **148 - 161** (Figure 59) of the second library were tested on two cell-lines, A431^{[294]k} (an epidermoid cancer) and Panc-1^l (a well differentiated pancreatic adenocarcinoma), both of human origin.

^k Reference for A-431 in the "American Type Culture Collection" is found under <http://phage.atcc.org/cgi-bin/searchengine/longview.cgi?view=ce,663682,CRL-661555&text=a-663431>

^l Reference for Panc-1 in the "American Type Culture Collection" is found under <http://phage.atcc.org/cgi-bin/searchengine/longview.cgi?view=ce,609764,CRL-1469&text=panc-1>

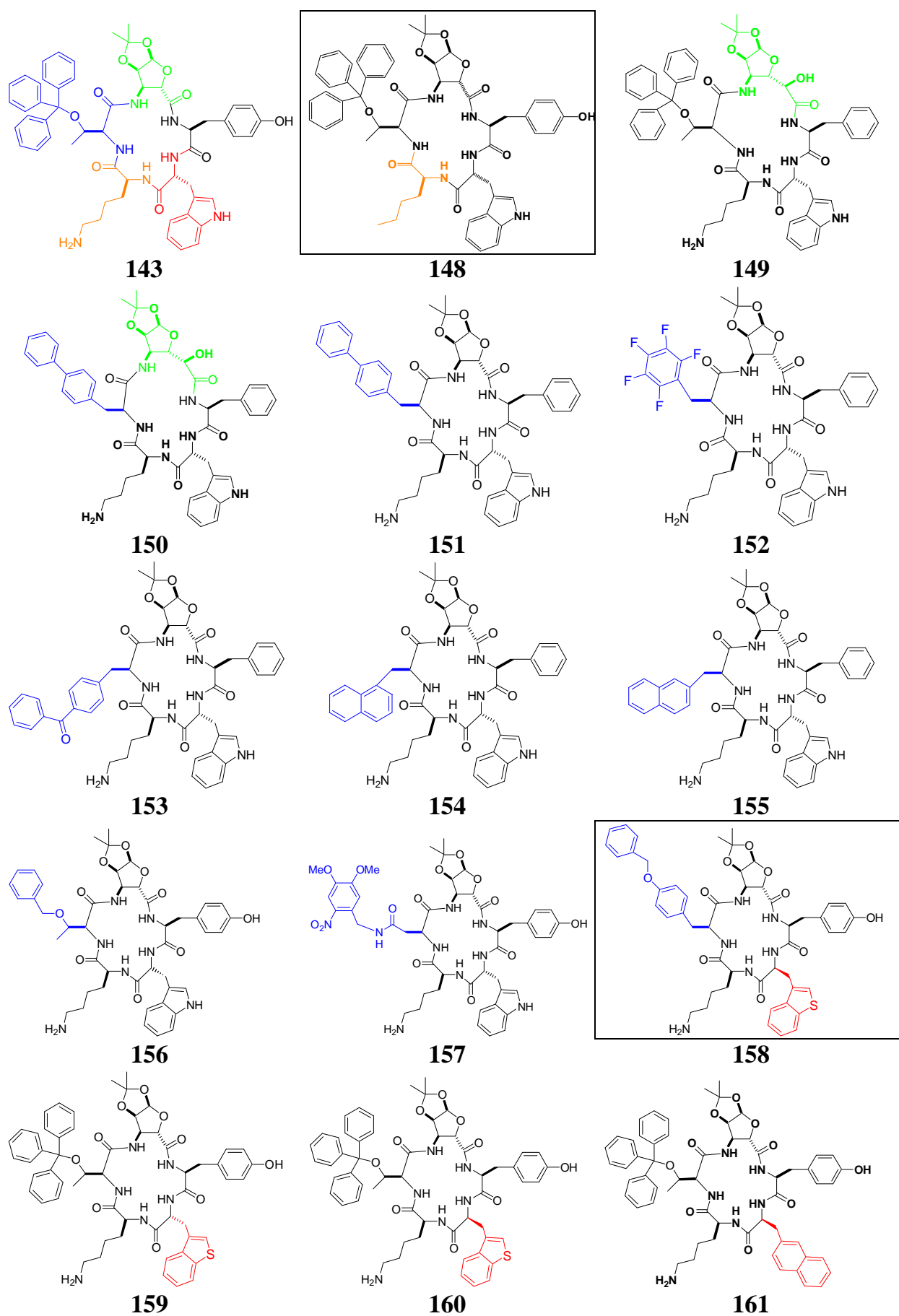


Figure 59: Structures of compounds **148-161** tested on human cancer cell lines *A431^k* (epidermoid cancer) and *Panc-1^l* (pancreatic adenocarcinoma).

Each compound was tested under 4 conditions: 6 h (to exclude necrosis^m) and 48 h to see inhibition of proliferation and apoptosis. High ratio between 48/6 h inhibition shows little necrotic, but pronounced apoptotic activity of the tested compound. The results are summarized in Table 5.

Table 5: Apoptotic activity of compounds **148-161** (Figure 58).

compound	IC ₅₀ [μM] [*]	Necrosis ^{**}
148	= 10	non
149	~ 50	some
150	~ 60	some
151	> 100	yes
152	> 100	yes
153	~ 100	almost non
154	> 100	
155	~ 110	some
156	~ 50	some
157	> 2	
158	= 35	almost non
159	~ 38	non
160	40 ^{Panc-1} 50 ^{A431}	some
161	40 ^{Panc-1} 55 ^{A431}	some

* Cell lines used for IC₅₀ determination: A431^[294] (an epidermoid cancer) and Panc-1 (a well differentiated pancreatic adenocarcinoma), both of human origin. Only when the IC₅₀ values were not the same for both cell lines, different IC₅₀ values are given with the respective corresponding cell line noted in the superscript index.

** The quantity of necrosis detected as number of cell deaths after 6 h of incubation.

Compound **148**, where the Lys⁹ side chain of the parent compound **143** is replaced by norleucine, shows the highest apoptotic activity of all compounds tested so far. With its IC₅₀ value of 10 μM for the pancreatic cancer cell line panc-1 and for the epidermoid cancer cell line A431, it presumably is considerable more active than **143** and TT232 **135**. It shows no unspecific cytotoxic activity (no necrosis), which is

^m *nekrosis*: Late Latin (originating from Greek *nekrOsis*): *nekros* dead body)

necrosis: non-specific, non-selective cell death, caused by outer stress

crucial for its potential use as an anti-tumor drug. These results show that lysine in the Lys⁹ position is by no means essential for inducing apoptosis in cancer cells. The removal of the charged amine in the side chain even results in higher apoptotic and antiproliferative activity on cancer cells. Substitution of Trp⁸, the other amino acid, which has so far been considered as a crucial part of the pharmacophore, resulted in compounds **158-161**. All of these compounds show similar activities (all IC₅₀s ~ 40 μM) as the parent compound **143**. Variation of the aromatic side chain in the Thr¹⁰ position, demonstrated, that this position is very sensitive to structural variations. The “wrong” aromatic side chain either causes complete loss of antiproliferative and apoptotic activity or might cause unspecific cytotoxicity (that is induce necrosis). Substitution of the Thr(OTrt) side chain of **143** with the side chain of biphenyl alanine (Bip) (compound **151**) for instance, caused a necrotic IC₅₀ of about 50 μM in the epidermoid cancer cell line A431. However, substitution of the Thr(OTrt) with the – under physiological conditions much more stable – benzylated tyrosine (compare **158** and **160**) enhanced the apoptotic and antiproliferative activity slightly. **158**'s apoptotic and antiproliferative IC₅₀ value of 35 μM (for both A431 and Panc-1) is about the same as that of **143** and is in the same order as that of TT232 **135**.

3.3.2.7 Conclusions and Outlook

The studies presented here demonstrate that a big aromatic residue in the Thr¹⁰ position seems to be imperative for high antiproliferative and apoptotic activity. Compounds **142** and **143** with IC₅₀ values in the low μM range are very promising leads for potential chemotherapeutic drugs against multidrug-resistant hepatoma carcinoma. The results obtained from preliminary tests using epidermoid and pancreatic human tumor cell lines suggest, that removal of the charged amine functionality, that is replacement of Lys⁹ with Nle as in **148**, enhances apoptotic and antiproliferative activity considerably. **148** is presumably more active than TT232 **135**, the only other compound known to show apoptotic and antiproliferative activity against carcinoma cell lines. Replacement of the Trp⁸ with D-Bta (D-Benzothierylalanin) resulting in compound **159**, with L-Bta resulting in compound **160** or with 2-naphtyl alanine (2-Nal) resulting in compound **161** leads to equal or slightly enhanced antiproliferative and apoptotic activity. Therefore the paradigm, that the sequence Lys⁹-Trp⁸ is the essential pharmacophore for antitumor activity, is not true.

158 is a very interesting drug candidate against epidermoid, pancreatic and most probably several other tumors. Its IC₅₀ is in the same low μM range as that of **143** and TT232 **135**. The replacement of Thr(OTrt) of the **143** parent compound with Tyr(OBn), and the introduction of the unnatural amino acid Bta in the Trp⁸ position should make it considerable more stable under physiological conditions than **143**. However, it might still be optimized by substituting Lys⁹ with Nle. This would even make the synthesis easier and cheaper, since no longer an orthogonal protecting group of the amine side chain is needed.

The nonproteinogenic properties of SAAs should make the compounds physiologically more stable, as does the introduction of Nle (since the peptidase trypsin recognizes the peptide-sequence Trp-Lys), and Bta or 2-Nal and other non-natural amino acids.

Preliminary studies suggest that our f-SAA **106** containing compounds selectively exert their apoptotic and antiproliferative activity against cancer cells. We know, that the apoptosis induced by the compounds **142** and **143** is mediated via a so

called tumor markerⁿ. Therefore only tumor cells should receive the apoptotic signals induced by our compounds and thereby programmed suicidal cell death is triggered exclusively for them.

In vivo studies in several animal models as well as studies to determine the toxicological profile of the compounds **143**, **148**, and **158** are planned.

ⁿ Tumor markers are biomolecules exclusively present in tumor cells and sometimes in embryonic cells.

3.3.3 Neurogenic Inflammation – Inflammatory Diseases

A lot of the diseases common in the well developed countries are based on inflammatory processes. In all those processes neurogenic inflammation plays an important part.

3.3.3.1 General Introduction

In all inflammatory processes occurring in the body neurogenic components, such as certain neuropeptides are involved. Neurogenic inflammation consists of a vicious cycle: The inflammation replicates itself, generating chronic inflammation and pain. Neuropeptides released due to inflammation cause yet again inflammation. The exact mechanism of those inflammatory processes is not yet fully understood. However we do know, that neurogenic inflammation is a major cause of many diseases. These include allergic inflammations of mucous membranes and airways, such as asthma, bronchitis, rhinitis and hay fever as well as arthritis, allergic conjunctivitis, urticaria,^o inflammations of the gastrointestinal system, such as colitis and inflammatory diseases of the skin, such as psoriasis.^p This list is far from exhaustive.

To date there is no drug on the market, that reliably inhibits neurogenic inflammation,^[295] thereby providing a possibility of an efficient treatment of the pathological pictures of the above listed diseases. This results in the misery of chronic pain, which extremely effects the quality of life of these patients. Classic non-steroidal anti-inflammatory drugs like for instance salicylate, amidopyridine, phenylbutazone, flufenamic acid or indomethacin do not inhibit neurogenic inflammation at all.

^o *Urtica*: latin for stinging-nettel; *urticaria*: an allergic disorder marked by raised edematous patches of skin or mucous membrane and usually intense itching and caused by contact with a specific precipitating factor (as a food, drug, or inhalant) either externally or internally

^p from Greek *psOrian* to have the itch, *Psoriasis*: a chronic skin disease characterized by circumscribed red patches covered with white scales

Steroids do inhibit neurogenic inflammation, but only in very high doses, that cause considerable toxic side effects. Opiates alone proved to be effective. However, they cannot be used due to their tremendous side effects.^[296, 297]

Pretreatment with somatostatin prevented experimentally induced neurogenic inflammation. Nonetheless, it is of no therapeutic use due to its extremely short half life ($t_{1/2} < 1$ min) in the body and its lack of selectivity.

It has been shown that somatostatin can be found in the peripheral endings of capsaicin-sensitive primary afferent neurons (CSPAN) and is liberated upon stimulation. Capsaicin (8-methyl-N-vanillyl-6-nonene amide), the pungent substance of red pepper, selectively stimulates or, in high doses, degenerates a subgroup of primary afferent neurons (small dark nerve cells). Because of this property, this subpopulation of neurons is called “capsaicin-sensitive primary afferent neurons” (CSPAN) (Figure 60).^[298-300] CSPAN form about one half of the nerve cell population of sensory ganglions. This group includes the C-polymodal nociceptors^q amounting to about 60 to 70% of C-afferentation of the skin as well as the perivascular chemoceptive interoceptors^r of the mucous membranes (conjunctiva, airways, urogenital system, etc.) and visceral organs (heart, kidney, stomach etc.), which can be excited by chemical painstimuli (bradykinin,^s acids, capsaicin). A common property of these nociceptive afferents is that when stimulated, they release tachykinins (TKs)^t (substance P (SP), neurokinin A), calcitonin gene-related peptide (CGRP)^[300] and

^q *nocere*: Latin for to harm;

Nociceptors are peripheral high threshold receptors for pain. All of them are free nerve endings. There are several distinct types of nociceptors:

- mechano-nociceptors - generally stimulus specific (intense pressure, pinching); mediate fast/first pain, via AS (small diameter, myelinated) afferent fibres.
- polymodal nociceptors - respond to many different forms of noxious stimuli: chemicals, intense heat, etc.; mediate slow/second pain, via C (small diameter, unmyelinated) afferent fibres
- 'Silent' nociceptors - respond only after tissue damage (or sensitization)

^r *interoceptors*: receptors for stimuli from within the body itself.

(*exteroceptors*: receptors for stimuli outside the body)

^s a kinin (*kinin*: polypeptide hormones that are formed locally in the tissues and cause dilation of blood vessels and contraction of smooth muscle), which is a linear nonapeptide and is formed locally in injured tissue, acts in vasodilation (widening of the lumen of blood vessels) of small arterioles. It is considered to play a part in inflammatory processes.

^t A family of biologically active peptides sharing a common conserved C-terminal sequence, -Phe-X-Gly-Leu-Met-NH₂, where X is either an aromatic or a branched aliphatic amino acid

somatostatin from their peripheral endings. (Substance P is a neuropeptide of the sequence H-Arg-Pro-Lys-Pro-Gln-Gln-Phe-Phe-Gly-Leu-Met-NH₂. SP is widely distributed in the brain, spinal cord, and peripheral nervous system, and acts across nerve synapses to produce prolonged postsynaptic excitation.)

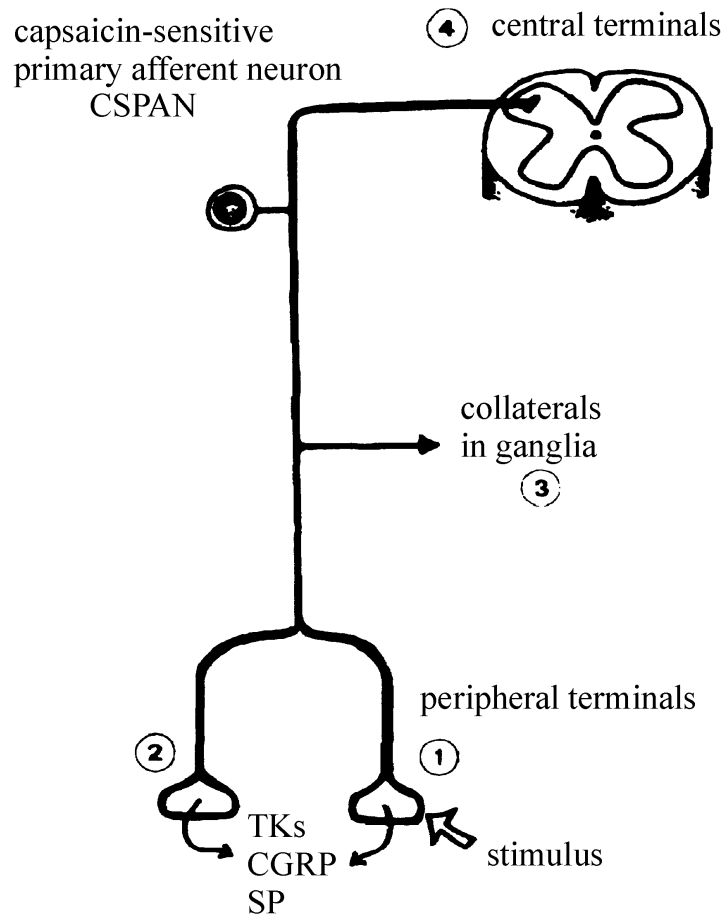


Figure 60: Schematic drawing of the functional anatomy of the capsaicin-sensitive primary afferent neuron (CSPAN). Sensory neuropeptides (TKs - substance P (SP) and neurokinin A - and CGRP) are synthesized in the perikaryon and transported to both peripheral (1, 2, 3) and central terminals (4) of the CSPANs. Environmental stimuli (mechanical, chemical, thermal) induce the release of sensory neuropeptides (like SP, NKA, and CGRP) from the same nerve terminal at which they activate afferent discharge.

During inflammation or tissue damage an overall up-regulation of the synthesis of sensory neuropeptides by the dorsal root ganglion (DRG)^u neurons and increased release from central endings is caused (Figure 61). Increased afferent activity by peripheral stimuli and increased nerve growth factor (NGF) production by target tissues are mechanisms inducing changes in the expression of sensory neuropeptides by CSPANs. There is also evidence for increased transport of sensory neuropeptides. Decreased immunostaining for sensory neuropeptides in peripheral tissues is observed. This is due to tissue damage as well as due to increased release of sensory neuropeptides contributing to initiation and maintenance of the inflammatory process (neurogenic inflammation).

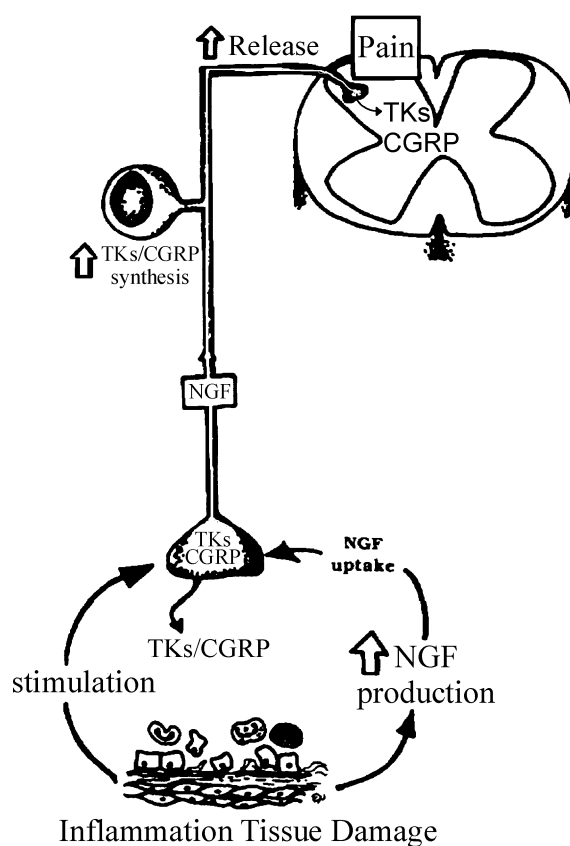


Figure 61: Changes occurring in CSPANs during inflammation/ tissue damage.

^u *dorsal root*: the one of the two roots of a spinal nerve that passes dorsally to the spinal cord and consists of sensory fibres

ganglion: a mass of nerve tissue containing nerve cells external to the brain or spinal cord

The TKs (especially substance P) induce plasma extravasation^v and neurogenic inflammation, whereas CGRP gives mainly rise to vasodilation^w of the arterioles and enhancement of microcirculation.

Thus, the capsaicin-sensitive peptidergic sensory nerve endings and terminal varicosities^x equally provide both a nociceptive afferent function as well as an efferent function eliciting a local tissue response. They play an important role in the signaling of neuropathic or inflammatory as well as hot stimulus- or irritant-induced pains.^[301]

To conclude: CSPANs synthesize and utilize neuropeptides and tachykinins such as substance P (SP) as transmitters. We know that SP plays an important role in the neurogenic inflammatory process, but the exact mechanism is not yet completely understood. However, we do know, that the inhibition of mechanical, chemical and thermal induced SP and CGRP release, prevents the inflammatory process and pain otherwise caused.

3.3.3.2 Biological Test on Anti-inflammatory Activity of Compounds 142-145^y

Since pretreatment with somatostatin prevented experimentally induced neurogenic inflammation, we tested the above described and synthesized somatostatin analogues **142-145** (c.f. chapter 3.3.2.5) from the first library on their potential to prevent and to cure neurogenic inflammation. We do know, as described above, that the inhibition of mechanical, chemical and thermal induced substance P (SP) and CGRP release, prevents the inflammatory process and pain otherwise caused. We therefore screened for the ability of our compounds to inhibit the release of substance P and CGRP *in vitro*. The release of sensory peptides from the tissue of rat tracheas in an organ bath was induced by electric (40 V, 0,1 ms, 10 Hz, 120s) and chemical (10^{-7} M of capsaicin) stimulation, in the presence and in the absence of the tested

^v *extravasation*: escape of a fluid from a (blood) vessel into surrounding tissue

^w *vasodilation*: widening of the lumen of blood vessels

^x *varicosity*: part of the ending of neurons

^y Tests were performed by our collaborators Gyorgy Kéri and Jozsef Nemeth from the Department of Medicinal Chemistry, Semmelweis Medicinal University, Budapest, Hungary

compound. The concentration of SP, CGRP and somatostatin were determined by using a specific radioimmunoassay developed by Kéri and co-workers.^[302, 303] For compounds **144** and **145** no substance P release inhibition could be detected in our test set up. However, compound **142** inhibited substance P release with 37.02 % (**significance^z), compound **143** with 19.1 % (*significance). The anti-neurogenic inflammation activity of **142** and **143** is in the same range as the activity of TT232 **135**. Non of the analogues of TT232 **135** tested (or any other compound ever tested) had remotely the same activity as **142** or **143**.

3.3.3.3 Conclusions

Whilst acute pain has undoubted survival value, the misery of chronic pain caused by neurogenic inflammation and may be e.g. associated with arthritis or terminal cancer, is less easy to comprehend. The compounds **142** and **143** are very interesting lead compounds for drugs against asthma, arthritis, allergic inflammations, hay fever, conjunctivitis and all other, often chronic, diseases, where inflammation processes are involved. The analogues **142** and **143** diminish inflammations of both neurogenic and non-neurogenic origin with simultaneous exertion of an analgetic effect. They should be considerable more stable than somatostatin or TT232 **135** the only other compound known to induce an equally strong anti-inflammatory effect by substance P release inhibition. There is evidence that **142** and **143** induces no endocrine effects, which would appear as severe side effects during the anti-inflammatory or analgetic treatment, and seems to be more effective with considerable less side effects than any drug on the market against inflammatory processes (such as cortisone).

Interestingly the good antitumor analogues are also the best inhibitors of neurogenic inflammation. We therefore will test the promising lead compounds **148** and **158** for the anti-cancer indication from the second library, also on their ability to inhibit substance P release and thereby neurogenic inflammation. Compound **158** would be especially interesting, since it is chemically more stable than the trityl ether containing compounds, and its activity should be in the same order.

^z ***significance*: the error is bellow 0.001; **significance*: the error is bellow 0.05

4 Summary

A straightforward synthesis of the two new furanoid sugar amino acids f-SAA **106** and f-SAA **107** in high yields in a few steps from glucose was developed. The described new synthetic pathway allows an easy access to f-SAA **106** and f-SAA **107**, making them useful building blocks and structural templates for drug design and combinatorial syntheses. Their synthesis starts from readily available diacetone glucose, and is faster, easier to scale up and cheaper, than the syntheses of other SAAs so far known.

f-SAA **106**'s and f-SAA **107**'s structural properties have been studied. Linear and cyclic mixed oligomers of f-SAA **106** and f-SAA **107** were synthesized and solution structures extensively investigated by circular dichroism (CD) and 2D-NMR spectroscopy. The linear oligomer Fmoc-[f-SAA**106**- β -hGly]₃-OH **113** exhibited 12/10/12 helical secondary structure in MeCN as proven by NMR, and subsequent molecular dynamics calculations. It is very remarkable that **113** forms a stable secondary structure, since stable secondary structures were only reported for β -peptides consisting almost exclusively of α - or β -substituted β -amino acids. The unsubstituted β -homoglycin is obviously much more flexible than substituted β -amino acids. f-SAA **106** therefore very strongly induces turn elements in short oligomeric sequences.

Furthermore the insights gained on the structure inducing properties of the f-SAAs **106** and **107**, were applied to biologically active systems. A first library of 12 somatostatin analogues was designed under consideration of structure activity relationships. After biological testing (antiproliferation and selective induction of apoptosis on tumor cells) the identified lead structures were further optimized, in a second, larger library. From those libraries several promising drug candidates against both cancer and inflammatory diseases could be extracted. 10 analogues have IC₅₀ values in the low μ M-range. **142**, **143**, **148** and **158** possess antiproliferative and apoptotic activity against several different multidrug-resistant and/or drug-sensitive carcinoma cell lines. Some of these compounds are more active than TT232 **135**, the only other compound

known to show apoptotic and antiproliferative activity against multi drugresistant carcinoma cell lines. Preliminary studies suggest that our compounds selectively exert their apoptotic and antiproliferative activity against cancer cells.

The compounds **142** and **143** are also interesting lead compounds for drugs against asthma, arthritis, allergic inflammations, hay fever, conjunctivitis and all the other, often chronic, diseases, where inflammation processes are involved. The analogues **142** and **143** diminish inflammations of both neurogenic and non-neurogenic origin with simultaneous exertion of an analgetic effect. There is evidence that **142** and **143** induces no endocrine effects, which would appear as severe side effects during the anti-inflammatory or analgetic treatment, and seems to be more effective with considerable less side effects than any drug on the market against inflammatory processes (such as cortisone).

The nonproteinogenic properties of f-SAAs **106** and **107** should make the compounds physiologically more stable than the purely peptidic TT232 (**135**), the only other compound known to comparably induce either apoptosis on multidrug resistant tumor cells or to prohibit inflammation by substance P release inhibition.

5 Experimental Section

General: Solvents for moisture sensitive reactions were distilled and dried according to standard procedures. All other solvents were distilled before use. Pd/C was donated by Degussa, Frankfurt/M., Germany. Flash column chromatography (FC) was performed with solvents indicated on silica gel 60, 230 - 400 mesh (Merck KGaA, Darmstadt). For solid-phase synthesis TCP resin (tritylchloropolystyrene-resin) from PepChem Goldammer & Clausen, H- β -hGly-2-CITrt resin and Fmoc- β -hGly-OH from Novabiochem, HATU from Perseptive Biosystems and Fmoc-GABA-OH (Fmoc-4-aminobutyric acid) from Neosystems were used. All reactions were monitored by thin-layer chromatography with 0.25-mm precoated silica gel 60 F₂₅₄ aluminium plates (Merck KGaA, Darmstadt). Melting points were obtained on a Büchi-Tottoli apparatus and are uncorrected. RP-HPLC analysis and semiscale preparations were carried out on a Waters (high pressure pump 510, multi-wavelength detector 490E, chromatography workstation Maxima 820), a Beckman (high pressure pump 110B, gradient mixer, controller 420, UV detector Uvicord from Knauer), or an Amersham Pharmacia Biotech (Äkta Basic 10/100, autosampler A-900) facility. RP-HPLC preparative separations were carried out on a Beckman System Gold (high pressure pump module 126, UV detector 166). C₁₈-columns were used. As solvents, solvent A: H₂O + 0.1% CF₃COOH, and B: CH₃CN + 0.1% CF₃COOH with UV detection at 220 and 254 nm, were used. ¹H, and ¹³C, and 2D NMR spectra were recorded on either Bruker - AC 250, Bruker DMX-500 or Bruker DMX-600 spectrometers. Proton chemical shifts are reported in ppm relative to residual CHCl₃ (δ = 7.24), DMSO (δ = 2.49) or pyridine (d=7.19, 7.55, 8.71). Multiplicities are given (obtained from 1D spectra) as s (singlet), d (doublet), t (triplet), q (quartet), m (multiplet), br (broad). ¹³C chemical shifts are reported relative to CDCl₃ (δ = 77.0), [D₆] DMSO- (δ = 39.5) and [D₅] pyridine (d= 123.5, 135.5, 149.9). Data was processed on a Bruker X32 workstation using the UxNMR-software. Assignment of proton and carbon signals was achieved by HMQC,^[203] COSY,^[202] TOCSY^[201] and HMBC^[204] experiments. Coupling constants were determined whenever possible from the corresponding 1D-spectrum, and in some cases from different COSY experiments. HPLC-ESI mass

spectra were recorded on a Finnigan NCQ-ESI with HPLC conjunction LCQ (HPLC-system Hewlett Packard HP 1100, Nucleosil 100 5C₁₈). IR spectra were recorded on a Perkin-Elmer 257 spectrophotometer. High-resolution mass spectra were performed by the Department of Chemistry of the Ludwigs Maximilians University of Munich on Finnigan MAT 95Q, using fast ion bombardment with Cs⁺ ions and *m*-nitrobenzylalcohol (matrix).

General procedure for reduction and simultaneous Fmoc protection of azides

(GP 1): A stirred solution of the azide in MeOH/H₂O 2:1 (0.15 M) is adjusted to pH 8 with saturated NaHCO₃ solution. A solution of Fmoc-Cl (1.1 equiv) in THF (0.16 M) is added to this solution, followed by the addition of the catalyst Pd/C (Degussa E 101 w/w 10 %, wet 49.7 % H₂O, 1g cat per g azide). The suspension is flushed several times with H₂. The reaction is generally completed after 18-24 h (TLC control). Solvents are removed under reduced pressure. The residue is suspended in water, and the pH is adjusted to 8-9 with saturated NaHCO₃ solution, and the aqueous phase is extracted with AcOEt (3x). The combined organic phases are washed with NaHCO₃. The aqueous phase is adjusted to pH 1 with 1N HCl and extracted with AcOEt (3x). The organic phase is washed with sat. aqueous NaCl solution, dried (MgSO₄) and concentrated under reduced pressure.

General procedure for anchoring of the first Fmoc-protected amino acid on

TCP resin (GP 2): The unloaded dry TCP resin in a syringe (exact weight known), completed with a frit, was swelled in NMP (30 min). The resin was filtered off, before a solution (~ 0.125 M) of 1.2 equiv of Fmoc-protected amino acid (with respect of the theoretical capacity of the TCP resin) and 2.5 equiv DIPEA (with respect to the quantity of Fmoc-protected amino acid used) in DCM (abs.) was added. After shaking for 1h at rt the capping solution (20% DIPEA in MeOH) is added. After 15 min the resin is filtered off, and the resin is washed with DCM (3 × 3 min), DMF (3 × 3 min),

and MeOH (3 × 3 min), and dried overnight under vacuo. Subsequently the exact weight of the dried resin was determined, and the loading of the resin was calculated:

$$c[\text{mol/g}] = (m_{\text{total}} - m_{\text{resin}}) / \{MG_{\text{Xaa}} - 36.461\} \times m_{\text{total}}$$

c loading

m_{resin} mass of resin before loading

m_{total} mass of loaded resin

MG_{Xaa} molar weight of the Fmoc-protected amino acid (Xaa)

General procedure for solid-phase peptide synthesis (GP 3)

General procedure for the solid phase synthesis of the oligomers 3 and 4 (GP 3a):

The Fmoc-protecting group of the amino acid attached to the resin is removed by treating the resin with a 20% piperidine solution in DMF (2 × 10 min). The resin is filtered off and washed with NMP (5 × 3 min), before a solution of the next Fmoc-protected amino acid (2 equiv Fmoc-SAA-OH, but 3 equiv Fmoc-β-hGly-OH or Fmoc-GABA-OH), HATU^[192, 193] (2 equiv for SAA coupling, 3 equiv for other amino acids), and 2,4,6-collidine (20 equiv/30 equiv) in NMP is added. After 3-48 h reaction is complete (monitoring by ESI-HPLC-MS). The resin is washed with NMP (5 × 3 min), prior to the subsequent Fmoc-deprotection and coupling steps. After coupling of the last amino acid, the resin is washed with NMP (3 × 3 min), CH₂Cl₂ (1 × 3 min), and dried overnight under vacuo. The oligomers are cleaved from the dry resin using 20% HFIP solution in CH₂Cl₂ (3 × 10 min). The crude peptides were purified via RP-HPLC.

General Procedure for solid phase peptide synthesis (GP 3b):

The preloaded resin was swelled for 30 min in NMP. The Fmoc-protecting group of the amino acid attached to the resin is removed by treating the resin with a 20% piperidine solution in DMF (3 × 10 min). The resin is filtered off and washed with NMP (5 × 3 min), before a solution of the next Fmoc-protected amino acid (3 equiv),

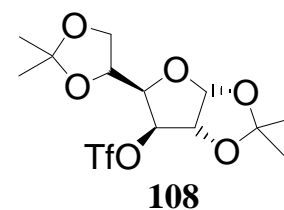
or of the Fmoc-protected f-SAA (1.5 equiv), HATU and HOAt^[192, 193] (1.5 equiv each for SAA coupling, 3 equiv each for other amino acids), and 2,4,6-collidine (15 equiv/30 equiv) in NMP (for coupling with Fmoc-protected f-SAA **106** DMF, was used as solvent) is added. After 2-3 h reaction is complete (monitoring by ESI-HPLC-MS). The resin is washed with NMP (5 × 3 min), prior to the subsequent Fmoc-deprotection and coupling steps. After coupling of the last amino acid, and subsequent Fmoc-deprotection, the resin is washed with NMP (3 × 3 min), CH₂Cl₂ (1 × 3 min), and dried overnight *in vacuo*. The compounds are cleaved from the dry resin using 20 % HFIP solution in CH₂Cl₂ (3 × 10 min).^[194] The crude peptides were purified via RP-HPLC. In all cases peptide (HPLC) purity was > 99 %.

General procedure for cyclization with DPPA/NaHCO₃ (GP 4):

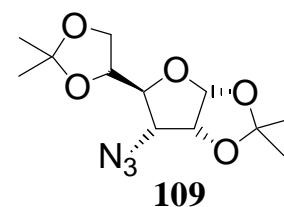
The Fmoc-deprotected linear peptide is dissolved in DMF (0.1 mM), and DPPA (3 equiv) and NaHCO₃ (11 equiv) are added.^[288, 289] After 12 h reaction is usually complete. After side chain deprotection (c. f. **GP 5**) the cyclic peptides were precipitated with Et₂O and purified via RP-HPLC, and finally lyophilized from water or dioxane.

General procedure for ivDde deprotection (GP 5):

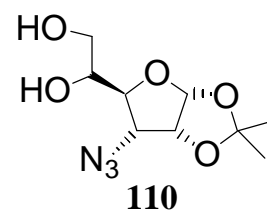
The peptide is dissolved in 3 % hydrazine/DMF solution, stirred for 10-15 min, and the solvent is evaporated. This procedure is repeated 3 times.



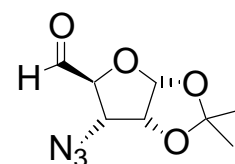
1,2:5,6-Di-O-isopropylidene-3-O-triflyl- α -D-glucofuranose (108): Triflic anhydride (54.2 g, 0.19209 mol) was slowly added to a stirred solution of diacetoneglucose (25 g, 0.96 mol), and pyridine (30.39 g, 0.384 mol) in CH_2Cl_2 (1 L) in a three-necked flask at -10°C (acetone-ice bath).^[304, 305] Pyridinium triflate salt precipitated, and the solution turned brown. The reaction was complete after 1.5 h (TLC control: AcOEt/hexane 2:1). The reaction mixture was poured onto ice water (1 L). The aq phase was extracted with CH_2Cl_2 (4 \times). The organic phases were dried (MgSO_4), and repeatedly coevaporated with toluene to remove pyridine. The brown residue was extracted with hexane (3 \times). Evaporation of hexane yielded the desired product as white crystals (36.88 g, 98 %). $R_f = 0.61$ (AcOEt/hexane 2:1); m.p. and ^1H NMR were in agreement with ref.^[305]



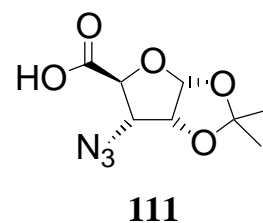
3-Azido-3-deoxy-1,2:5,6-di-O-isopropylidene- α -D-allofuranose (109): A solution of **108** (37.1 g, 0.0945 mol) in DMF (200 mL) was added slowly to a solution of NaN_3 (12.3 g, 0.189 mol), Bu_4NCl (catalytic, ~ 0.1 g) in DMF (1.5 L) at 50°C . The reaction was complete after 5 h of stirring at 50°C (TLC control: AcOEt/hexane 2:1). DMF was removed under reduced pressure, and the residue was dissolved in AcOEt. The organic phase was washed with H_2O (2 \times). The aqueous phase was re-extracted with AcOEt (2 \times) until TLC showed no traces of **109**. The combined organic phases were dried (MgSO_4) and evaporated to yield a syrup of crude **109** and elimination by-product. (^1H NMR gave a ratio of **109**:elimin. of 7:3). The crude product **109** was purified by FC (AcOEt/hexane 1:3) to yield **109** (18.2 g, 70 %) as a colorless liquid. $R_f = 0.55$ (AcOEt/hexane 1:3); ^1H NMR of both **109** and of the elimination product were in agreement with ref.^[189].



3-Azido-3-deoxy-1,2-O-isopropylidene-a-D-allofuranose (110): For oxidation,^[186] **109** (16 g, 0.056 mol) was dissolved in AcOH (77%, 38 mL) and stirred under reflux for 3 h. After evaporation of the organic solvent, crude **109** was purified by FC (AcOEt/hexane 2:1) to give **109** as white crystals (12.9 g, 94 %). M.p. and ¹H NMR were in agreement with ref. ^[306].

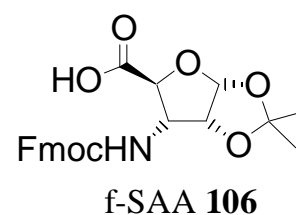


3-Azido-3-deoxy-1,2-O-isopropylidene-a-D-ribofuranose aldehyde: NaIO₄ (8.4 g, 0.036 mmol) was added gradually to a cooled solution (10°C) of **110** (8 g 0.0327 mol) in MeOH (60 mL) and H₂O (100 mL).^[186] The mixture was stirred for 5 h. The inorganic salts were precipitated by the addition of MeOH (150 mL), filtered off, and washed several times with MeOH. The combined organic phases were removed under vacuum to yield the aldehyde as a light yellow syrup. The crude aldehyde was used without further purification for the oxidation to **111**. ¹H NMR (250 MHz, CDCl₃/MeOD, 298 K): d=1.35 (s, CH₃), 1.55 (s, CH₃), 3.65 (dd, *J*_{3,4}=4.72, *J*_{2,3}=4.37 Hz, H³), 4.1 (d, *J*=4.7 Hz, H⁴), 4.7 (dd, *J*_{1,2}=3.7, *J*_{2,3}=4.5 Hz, H²), 5.9 (d, *J*_{1,2}=3.8 Hz, H¹), 9.7 (br. s, H⁵).

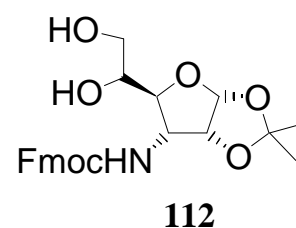


3-Azido-3-deoxy-1,2-O-isopropylidene-a-D-ribofuranic acid (111): KMnO₄ (6.7 g, 42 mmol) was added slowly to a stirred solution of the above described aldehyde in HOAc (50 %, 150 mL) resulting in a purple solution ^[186]. After 12 h reaction was

complete. The solution was adjusted to pH 1 with conc. HCl, excess KMnO_4 was removed with Na_2SO_3 . The solution was extracted with CHCl_3 (3x). The organic phase was dried (MgSO_4) and concentrated under reduced pressure. Recrystallization from AcOEt/hexane afforded **111** (4.29 g, 1.87 mmol, 89 % over two steps) as white crystals.

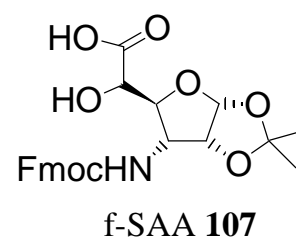


3-Amino-3-deoxy-N-9-fluorenylmethoxycarbonyl-1,2-isopropylidene- α -D-ribofuranic acid (f-SAA 106): According to **GP 1**, azide **9** (1 g, 4.36 mmol) was reduced to the amine and simultaneously Fmoc-protected to yield f-SAA **106** (1.4 g, 3.29 mmol, 76 %) as a colorless syrup which later crystallized. ^1H NMR (500 MHz, $[\text{D}_6]$ DMSO, 300 K): δ =1.26 (s, 3H, CH_3), 1.46 (s, 3H, CH_3), 4.07 (m, H^3), 4.22 (m, 1H, Fmoc-CH), 4.25 (m, 1H, H^4), 4.30 (m, 2H, $\text{CH}_2^{\text{Fmoc}}$), 4.60 (t, $J=4.0$, 1H, H^2), 5.84 (d, $J=3.4$, 1H, H^1), 7.32 (m, arom H), 7.40 (m, arom H), 7.63 (m, H^{N}), 7.72 (m, arom H), 7.87 (d, $J=7.3$ Hz, 2H, arom H); ^{13}C NMR (125MHz, $[\text{D}_6]$ DMSO, 300 K): δ =26.06 (CH_3), 26.29 (CH_3), 46.30 (CH^{Fmoc}), 56.25 (C^3), 65.61 ($\text{CH}_2^{\text{Fmoc}}$), 75.36 (C^4), 78.01 (C^2), 104.17 (C^1), 111.63 ($\text{C}^{\text{isoprop.}}$), 119.75 (C^{arom}), 124.89 (C^{arom}), 127.17 (C^{arom}), 143.32 (C^5); FAB-HRMS calcd for $\text{C}_{23}\text{H}_{23}\text{NO}_7\text{Na}$ $[M+\text{Na}]^+$ 448.1372, found 448.1366;



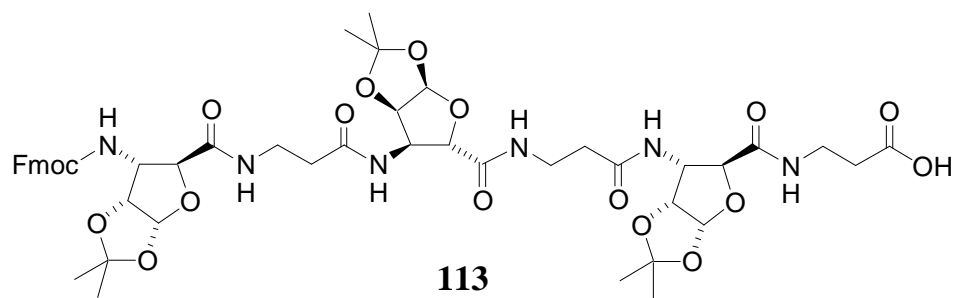
3-Amino-3-deoxy-N-9-fluorenylmethoxycarbonyl-1,2-isopropylidene- α -D-allofuranose (112): According to **GP 1**, azide **110** (2 g, 8.31 mmol) was reduced to the amine and Fmoc-protected. FC (AcOEt/hexane 1:1 \rightarrow 1) afforded **112** (3.3 g, 7.48 mmol, 92 %) as a white powder. ^1H NMR (500 MHz, CDCl_3 , 300 K): δ =1.35 (s, 3H, CH_3), 1.55 (s, 3H, CH_3), 2.12 (s, 0.8H, OH), 3.60-4.65 (m, 13H, H^2 , H^3 , H^4 , H^5 ,

H⁶, H^{6'}, CH₂^{Fmoc}, CH^{Fmoc}, H₂O), 5.47 (br. s, 1H, H^N), 5.80 (br. s, 1H, H¹), 7.32 (m, 2H, H^{arom}), 7.40(m, 2H, H^{arom}), 7.57(m, 2H, H^{arom}), 7.76 (d, *J*=6.7 Hz, 2H, H^{arom}); ¹³C NMR (125MHz, CDCl₃, 300 K): d=26.46 (CH₃), 26.61 (CH₃), 47.12 (CH^{Fmoc}), 55.74 (C³), 63.73 (C⁴), 67.47 (C⁵), 79.25 (C²), 80.41 (CH₂^{Fmoc}) 103.77 (C¹), 112.85 (C^{isoprop.}), 120.05 (C^{arom}), 124.90 (C^{arom}), 127.80 (C^{arom}), 141.32, 143.53, 143.57 (C^{arom}, C⁶); ESI-MS: calcd. for C₂₄H₂₇NO₇Na 464.1685, found 464.1; *t*_R=14.41 (HPLC-MS, 30-90%B in 20min).



3-Amino-3-deoxy-N-9-fluorenylmethoxycarbonyl-1,2-isopropylidene-

α-D-allofuranic acid (f-SAA 107): The diol **112** and TEMPO (1 mg, 0.064 mmol, 0.011 equiv) was suspended in CH₂Cl₂ (1.8 mL) at 0°C, a solution of KBr (14.5 mg, 0.064 mmol, 0.11 equiv) and *t*Bu₄NCl (8.9 mg) in sat. aq NaHCO₃ (1.2 mL) was added slowly. To this a mixture of NaOCl (13%, 1.5 mL), sat. aq NaCl (1.32 mL) and sat. aq NaHCO₃ (0.7 mL) was added dropwise over a period of 30 min. The reaction mixture was stirred overnight, diluted with AcOEt (2 mL). The organic phase was extracted twice with brine. The aq phase was adjusted to pH 2 with diluted HCl (1 N) and extracted with AcOEt. Removal of the combined organic phases under reduced pressure afforded f-SAA **107** as a colorless syrup (0.17 g, 62%). ¹H NMR (500 MHz, [D₆] DMSO, 300 K): d=1.25 (s, 3H, CH₃), 1.47 (s, 3H, CH₃), 4.05-4.30 (m, 6H, H³, H⁴, H⁵, CH₂^{Fmoc}, CH^{Fmoc}), 4.55 (br. s, 1H, H²), 5.73 (br. s, 1H, H¹), 7.30-7.90 (m, 9H, H^{arom}, H^N); ¹³C NMR (125 MHz, [D₆] DMSO, 300 K): d=23.97 (CH₃), 24.39 (CH₃), 45.19 (CH^{Fmoc}), 51.88 (C³), 63.70 (C⁴), 67.18 (C⁵), 75.30 (C²), 76.98 (CH₂^{Fmoc}), 101.73 (C¹), 111.35 (C^{isoprop.}), 117.20 (C^{arom}), 122.39 (C^{arom}), 124.14 (C^{arom}), 124.51 (C^{arom}), 143.80 (C⁶); FAB-HRMS calcd for C₂₄H₂₅NO₈Na [*M*+Na]⁺ 478.1478, found 478.14167; *t*_R=15.71 (HPLC-MS, 10-90%B in 20min).



Fmoc-[f-SAA106-β-hGly]₃-OH (113): In a syringe (10 mL), completed with a frit, preloaded H-β-hGly-2-ClTrt resin (399.5 mg, 0.44 mmol g⁻¹, 0.17578 mmol) was swelled for 45 min in NMP. According to **GP 3a**, Fmoc-protected f-SAA **106** (0.1494 g, 0.35156 mmol, 2 equiv) and Fmoc-β-hGly (0.1642 g, 0.5273 mmol, 3 equiv) were coupled alternately to the hexamer. Cleavage yielded the crude **113** as a redish syrup, which was purified by RP-HPLC (40.5-54%B in 30 min) to yield **113** (71.3 mg, 41 %) as a white, fluffy solid. ¹H NMR (600 MHz, [D₆] DMSO, 296 K): δ=1.223 (f-SAA106, CH₃), 1.242 (f-SAA106, CH₃), 1.264 (f-SAA106, CH₃), 1.279 (f-SAA106, CH₃), 1.386 (f-SAA106 3, CH₃), 1.413 (f-SAA106, CH₃), 2.220 (β-hGly 4, H^a), 2.263 (β-hGly 2, H^a), 2.304 (β-hGly 4, H^a), 2.318 (β-hGly 2, H^a), 2.378 (β-hGly 6, H^a), 3.192 (β-hGly 4, ³J(H^N/H^β)=6.1, H^β), 3.203 (β-hGly 2, ³J(H^N/H^β)=5.8, H^β), 3.204 (β-hGly 6, ³J(H^N/H^β)=5.7, H^β), 3.298 (β-hGly 6, ³J(H^N/H^{β'})=6.7, H^{β'}), 3.328 (β-hGly 4, ³J(H^N/H^{β'})=6.4, H^{β'}), 3.330 (β-hGly 2, ³J(H^N/H^{β'})=6.8, H^{β'}), 4.020 (f-SAA106 1, ³J(H³/H⁴)=10.0, ³J(H^N/H³)=8.9, H³), 4.066 (f-SAA106 3, ³J(H³/H⁴)=10.4, H⁴), 4.071 (f-SAA106 5, ³J(H³/H⁴)=10.0, H⁴), 4.200 (f-SAA106 1, ³J(H³/H⁴)=10.0, H⁴), 4.219 (CH^{Fmoc}), 4.256 (f-SAA106 5, ³J(H³/H⁴)=10.0, ³J(H^N/H³)=8.8, H³), 4.296 (CH₂^{Fmoc}), 4.335 (f-SAA106 3, ³J(H³/H⁴)=10.4, ³J(H^N/H³)=9.1, H³), 4.583 (f-SAA106 1, ³J(H¹/H²)=5.3, H²), 4.565 (f-SAA106 3, ³J(H¹/H²)=5.3, H²), 4.576 (f-SAA106 5, ³J(H¹/H²)=5.3, H²), 5.85 (f-SAA106, ³J(H¹/H²)=5.3, H¹), 7.317 (Fmoc), 7.401 (Fmoc), 7.549 (f-SAA106 1, ³J(H^N/H³)=8.9, H^N), 7.731 (Fmoc), 7.813 (β-hGly 4, ³J(H^N/H^β)=6.1, ³J(H^N/H^{β'})=6.4, H^N), 7.837 (β-hGly 2, ³J(H^N/H^β)=5.8, ³J(H^N/H^{β'})=6.8, H^N), 7.885 (Fmoc), 7.905 (β-hGly 6, ³J(H^N/H^β)=5.7, ³J(H^N/H^{β'})=6.7, H^N), 8.050 (f-SAA106 5, ³J(H^N/H³)=8.8, H^N), 8.098 (f-SAA106 3, ³J(H^N/H³)=9.1, H^N), 12.212 (β-hGly 6, COOH); Temperature coefficients [-Δδ/ΔT]: ¹H NMR (500 MHz, [D₃] CD₃CN, 295 - 320 K, ΔT= 5 K) f-SAA106 1 H^N: 4.92; β-hGly 2 H^N: 2.48; f-SAA106 3 H^N: 7.90; β-hGly 4 H^N: 4.17;

f-SAA106 5 H^N: 9.25; β-hGly 6 H^N: 1.95; ¹³C NMR (150 MHz, [D₆] DMSO, 296 K): d=22.179 (f-SAA106, CH₃), 23.012 (f-SAA106 3, CH₃), 26.207 (f-SAA106, CH₃), 26.393 (f-SAA106, CH₃), 28.708 (f-SAA106, CH₃), 29.588 (f-SAA106, CH₃), 33.266 (β-hGly 6, C^a), 34.6 (β-hGly, C^b), 34.7 (β-hGly 2+4, C^a), 35.2 (β-hGly, C^b), 46.383 (Fmoc, CH), 54.388 (f-SAA106 5, C³), 54.560 (f-SAA106 3, C³), 56.726 (f-SAA106 1, C³), 65.662 (Fmoc, CH₂), 76.360 (f-SAA106 1, C⁴), 76.660 (f-SAA106 3+5, C⁴), 78.575 (f-SAA106, C²), 104.103 (f-SAA106, C¹), 119.871 (Fmoc, CH^{arom}), 125.04 (Fmoc, CH^{arom}), 126.967 (Fmoc, CH^{arom}), 127.226 (Fmoc, CH^{arom}) 155.429 (Fmoc, NCOO), 168.149 (f-SAA106 1, C⁵), 168.297 (f-SAA106 5, C⁵), 168.515 (f-SAA106 3, C⁵), 170.431 (β-hGly 4, CO), 170.590 (β-hGly 2, CO); ¹⁵N NMR (60 MHz, [D₆] DMSO, 296 K): d=78.46 (f-SAA106 1, NH), 110.86 (β-hGly 4, NH), 111.53 (f-SAA106 5, NH), 111.84 (β-hGly 6, NH), 111.86 (f-SAA106 3, NH), 111.88 (β-hGly 2, NH); *t*_R=13.65 (HPLC-ESI-MS, 30-90%B in 20min); ESI-MS: 1053.2 [M-H+2Na]⁺, 1047.2 [M+K]⁺, 1031.3 [M+Na]⁺, 1009.1 [M+H]⁺; FAB-HRMS calcd for C₄₈H₆₀N₆O₁₈Na [M+Na]⁺ 1031.3861, found 1031.3852

NMR and structure determination of 113: All NMR spectra were acquired at 300 K in MeCN on a Bruker DMX500 spectrometer, processed and analyzed using the X-WINNMR [‘X-WINNMR V3.0’, Bruker, Karlsruhe] and AURELIA [‘AURELIA V2.8.11’, Bruker, Karlsruhe] software, respectively. As described previously, sequential assignment was done using information on the intra-residual and sequential C^b, C’, H^a and H^N chemical shifts taken from COSY,^[202] TOCSY,^[201] HMQC^[203] and HMBC^[204] experiments. The COSY, HMQC and HMBC were all recorded with 8192 (t₂) * 512 (t₁) complex points using 8, 16 and 64 scans per increment, respectively. A mixing time of 75 ms and a data size of 2048 * 512 in t₂ and t₁, respectively, were used for the TOCSY experiment. NOESY^[205] experiments using four mixing times (100, 200, 400, 600 ms) were measured and distance data were derived from the NOESY spectra (8192 (t₂) * 512 (t₁) complex points and 16 scans per increment). A mixing time of 400 ms was necessary to achieve adequate cross-peak intensities. At this mixing time, most of the NOE build up curves were still in the linear region. However, some of the integrated 76 NOESY cross-peaks were adjusted manually to account for spin diffusion. On the derived distances, a tolerance of ± 10 % was applied to obtain upper and lower bound distance restraints

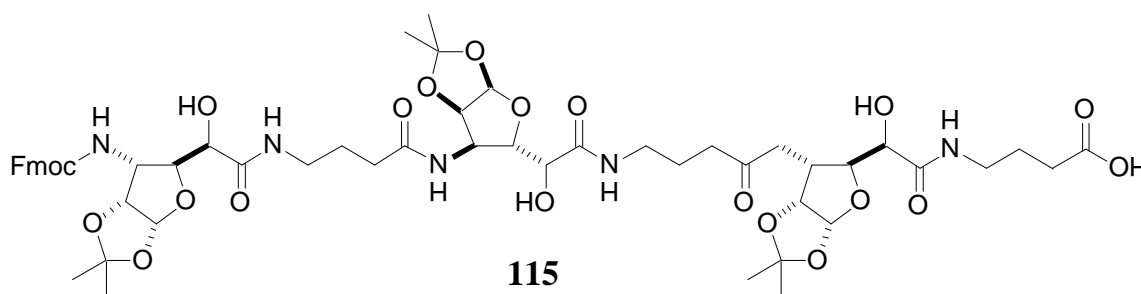
for structural calculations. Allowances for the use of pseudo-atoms were added only for the terminal H^α and H^β spin groups of β-hGly 6, which could not be stereospecifically assigned. A first restrained conformational search was performed with the X-PLOR package,^[206] using standard simulated annealing protocols, yielding an ensemble of 10 structures with good convergence. This ensemble already clearly showed a 12/10/12-helical conformation. The structure which best fulfilled the experimental restraints was then used as a starting structure for a 150 picosecond simulated dynamics run in the CVFF forcefield, using Discover, version 2.98.^[207] Since to our knowledge no explicit, all-atom acetonitrile solvent box is available for this program package, we equilibrated a solvent box of 31.3 x 31.9 x 31.5 Å³, containing 360 CH₃CN molecules, for this purpose. The dynamics run was then performed in a solvent box of 47 x 47 x 47 Å³, containing 1039 CH₃CN molecules, and using the equilibrated box as a template. During simulation time, 1500 frames were collected in the trajectory. Restraint violations all remained below 0.1 Å, except for one contact. Averaging of the heavy atom coordinates over the 150 picosecond trajectory, and subsequent 300 steps of steepest descent minimization yielded the structure of **113**, as described in the main section. Trajectory population statistics for the hydrogen bonds are shown in Table 6.

Table 6: *Trajectory population statistics for hydrogen bonds*

Acceptor–Donor-Pair	Averg. dist. N-O [Å]	Averg. dist. H-O [Å]	Averg. angle N-H-O [°]	Population [%]
Fmoc CO – f-SAA106 3 HN	3.77	2.94	142.5	52.2
f-SAA106 3 CO – β-hGly2 HN	3.70	2.86	142.6	41.0
β-hGly2 CO – f-SAA106 5 HN	3.30	2.34	158.0	85.5
f-SAA106 5 CO – β-hGly4 HN	3.52	2.62	149.9	65.5

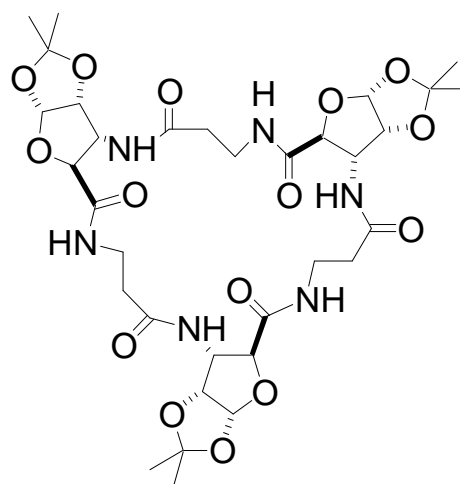
To test the stability of the average minimized structure under unrestrained conditions, it was used as the starting structure for a further free dynamics simulation of

150 picoseconds duration in explicit solvent (CH_3CN Box, dimensions $43 \times 43 \times 43 \text{ \AA}^3$, 779 CH_3CN molecules). During this simulation, 5 restraints were violated by more than 0.1 \AA . The violated NOEs indicate an occasional, partial unwinding of the helix, which can be explained by the fact that acetonitrile is not a completely unpolar solvent.



Fmoc-[f-SAA107-GABA]₃-OH (115): In a syringe (10 mL), completed with a frit, TCP resin (1.0550 g, $\sim 0.95 \text{ mmol g}^{-1}$) was swelled in NMP (30 min). After filtering off the resin, a solution of Fmoc-GABA (0.3274 g, 1.002 mmol, 1 equiv) and $(i\text{Pr})_2\text{EtN}$ (0.51 mL, 3.004 mmol, 3 equiv) in CH_2Cl_2 (7.5 mL) was added. After 2h the resin was filtered off, washed with CH_2Cl_2 ($3 \times 3 \text{ min}$), DMF ($3 \times 3 \text{ min}$) and MeOH ($3 \times 3 \text{ min}$), before dried under reduced pressure overnight. The resin's loading was $0.591 \text{ mmol g}^{-1}$, according to gravimetric measurements. In a syringe (10 mL) the GABA loaded resin (0.3164 g , $0.591 \text{ mmol g}^{-1}$, 0.187 mmol) was swelled for 30 min in NMP. According to **GP 3a** Fmoc-protected f-SAA **107** (0.1703 g , 0.3798 mmol , 2 equiv) and Fmoc-GABA (0.1825 g , 0.5610 mmol , 3 equiv) were coupled alternately. Purification by RP-HPLC (36-50 % B in 30 min) yielded **115** (10 mg, 4.7 %). ^1H NMR (600 MHz, $[\text{D}_5]$ pyridine, 300 K): δ =1.181 (f-SAA107 3, CH_3), 1.195 (f-SAA107 3, CH_3), 1.199 (f-SAA107 5, CH_3), 1.218 (f-SAA107 5, CH_3), 1.243 (f-SAA107 1, CH_3), 1.301 (f-SAA107 1, CH_3), 2.097 (GABA 6, H^b), 2.113 (GABA 4, H^b), 2.127 (GABA 2, H^b), 2.499 (GABA 2, H^a), 2.592 (GABA 4, H^a), 2.607 (GABA 6, H^a), 3.414 (GABA 4, H^c), 3.431 (GABA 2, H^c), 3.525 (GABA 6, H^c), 3.686 (GABA 2+4, H^c), 3.728 (GABA 6, H^c), 4.035 (Fmoc, CH), 4.272 (Fmoc, CH_2), 4.715 (f-SAA107 3, H^2), 4.774 (f-SAA107 5, H^2), 4.833 (f-SAA107 1, H^2), 4.992 (f-SAA107 1, H^5), 4.998 (f-SAA107 3, H^4), 4.999 (f-SAA107 3, H^5), 5.018 (f-SAA107 5, H^5), 5.031 (f-SAA107 5, H^4), 5.100 (d, $J=10.1$, f-SAA107 1, H^4), 5.233

(f-SAA107 1, H³), 5.391 (f-SAA107 3, H³), 5.47 (f-SAA107 5, H³), 5.897 (d, $J=2.6$ Hz, f-SAA107 3, H¹), 5.938 (d, $J=2.5$, f-SAA107 5, H¹), 5.985 (br. s, f-SAA107 1, H¹), 7.223 (m, Fmoc, H^{arom}), 7.359 (m, Fmoc, H^{arom}), 7.658 (m, Fmoc, H^{arom}), 7.806 (t, $J=5.9$, Fmoc, H^{arom}), 8.611 (GABA 4, H^N), 8.633 (GABA 2, H^N), 8.69 (GABA 6, H^N), 9.255 (d, $J=9.4$, f-SAA107 3, H^N), 9.289 ($J=9.5$, f-SAA107 1, H^N), 9.303 ($J=9.6$ Hz, f-SAA107 5, H^N); ¹³C NMR (150MHz, [D5] pyridine, 300 K): d=22.94 (f-SAA107 5, CH₃), 23.6 (f-SAA107 1, CH₃), 25.7 (GABA, C^b), 26.14 (f-SAA107 5, CH₃), 30.13 (f-SAA107 1, CH₃), 31.78 (f-SAA107 3, CH₃), 31.91 (GABA 6, C^a), 33.3 (GABA 2, C^a), 33.35 (GABA 4, C^a), 38.49 (GABA 4, C²), 38.7 (GABA 2, C²), 39.15 (GABA 6, C²), 47.196 (Fmoc, CH₂), 50.15 (f-SAA107 3, C³), 50.3 (f-SAA107 5, C³), 52.5 (f-SAA107 1, C³), 61.139 (Fmoc, CH), 70.4 (f-SAA107, C⁵), 80 (f-SAA107 1+5, C²), 80.1 (f-SAA107 3, C²), 81 (f-SAA107, C⁴), 104.3 (f-SAA107 3+5, C¹), 104.4 (f-SAA107 1, C¹), 111 (f-SAA107, C^{isoprop.}), 119.917 (Fmoc, C^{arom}), 125.410 (Fmoc, C^{arom}), 127.063 (Fmoc, C^{arom}), 127.647 (Fmoc, C^{arom}), 171.3 (f-SAA107, CO), 173 (GABA 2, CO), 173.2 (GABA 4+6, CO); t_R=17.06 min(30-60%B in 30min); ESI-MS: 1185 [M-H+2Na]⁺, [M-H+2K]⁺, 1179.2 [M+K]⁺, 1163.4 [M+Na]⁺, 1141.1 [M+H]⁺, 1083.1, 1025.1, 967.1, 179.1; HRMS: m/z calcd for C₅₄H₇₃N₆O₂₁ (M+H): 1141.4829.

**114**

cyclo[-f-SAA106-β-hGly-]₃ (114): **113** (8.9 mg) was dissolved in 20 % piperidine in DMF (300 μL). After 30 min deprotection was complete. Purification by RP-HPLC (20-80 % B in 30 min) afforded deprotected **113** as a white fluffy powder (6.5 mg, quantitative). Deprotected **113** (3.9 mg, 4.96×10^{-3} mMol) was dissolved in DMF

(11 mL), a solution of HATU^[192, 193] (1 mL of a solution of 18.8 mg HATU in 10 mL DMF) and 2,4,6-collidine (6.5 μ L) was added. After 24 h reaction was not complete. Additional HATU solution (100 μ L of a solution of 18.8 mg HATU in 10 mL DMF) and 2,4,6-collidine (1 μ L) were added. After further 2 h the reaction was complete (HPLC control). Purification by RP-HPLC (20-80 % B in 30 min) afforded **5** as a white fluffy solid (3.8 mg, quant.). ¹H NMR (500 MHz, [D₆] DMSO, 300 K): δ =1.29 (s, 9H, 3 \times CH₃), 1.46 (s, 9H, 3 \times CH₃), 2.18 (m, 3H, 3 \times H^a), 2.29 (m, 3H, 3 \times H^a), 3.19 (m, 3H, 3 \times H^b), 3.42 (m, 3H, 3 \times H^b), 4.20 (m, 6H, 3 \times H³+3 \times H⁴), 4.64 (dd, J_{H2-H1} = 3.26, J_{H2-H3} = 4.24, 3H, 3 \times H²), 5.82 (d, J =3.3, 3H, 3 \times H¹), 7.67 (t, J =6.0, 3 \times β -hGly-H^N), 8.03 (d, J =7.0 Hz, 3 \times f-SAA1-H^N) ; ¹³C NMR (125 MHz, [D₆] DMSO, 300 K, HMQC-experiment): δ =26.23 (CH₃), 26.46 (CH₃), 35.13 (C^b), 35.37 (C^a), 54.83 (C³), 76.63 (C⁴), 78.98 (C²), 104.05 (C¹); t_R = 20 min (15-85%B in 30min); ESI-MS: 921.3 [M+TFA+K]⁺, 905.3 [M+TFA+Na]⁺, 807.4 [M+K]⁺, 791.5 [M+Na]⁺, 769.3 [M+H]⁺.

Synthesis of the first library of somatostatin analogues 138-141 and 142-147:

Loading of the TCP resin with Fmoc-Phe-OH:

For the syntheses of

cyclo[–Phe–Trp–Lys–f-SAA106–] **138**,

cyclo[–Phe–DTrp–Lys–f-SAA106–] **139**,

cyclo[–Phe–Trp–Lys–Phe–f-SAA106–] **144**,

cyclo[–Phe–DTrp–Lys–Phe–f-SAA106–] **145**:

According to GP 2, TCP resin (2.008 g) was loaded with Fmoc-Phe-OH (933.6 mg, 2.4098 mmol) and DIPEA (1.05 mL, 6.025 mmol) in 16 mL DCM. The loading was $c = 0.677$ mol/g resin.

Loading of the TCP resin with Fmoc-Tyr-OH:

For the syntheses of

cyclo[–Tyr–Trp–Lys–f-SAA106–] **140**,

cyclo[–Tyr–DTrp–Lys–f-SAA106–] **141**,

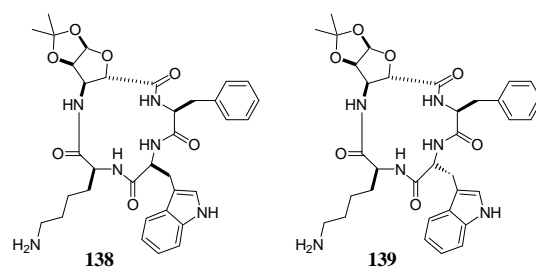
cyclo[–Tyr–Trp–Lys–Thr(OTrt)–f-SAA106–] **142**,

cyclo[–Tyr–DTrp–Lys–Thr(*O*Trt)–f-SAA106–] **143**,

cyclo[–Tyr–Trp–Lys–Thr–f-SAA106–] **146**,

cyclo[–Tyr–DTrp–Lys–Thr–f-SAA106–] **147**:

Similar to GP 2 (instead of DIPEA 2,4,6-collidine was used as base), TCP resin (1.300 g) was loaded with Fmoc-Tyr-OH (629 mg, 1.56 mmol) and 2,4,6-collidine (2.77 mL) in 10 mL DCM. The loading was $c = 0.477$ mmol/g resin.



Synthesis of 138 and 139: According to GP 3b, **138** and **139** were synthesized parallel in the same syringe ((2 mL), 137 mg of the Fmoc-Phe-OH loaded TCP resin). Coupling was verified by a sample cleavage of the depeptide Fmoc-f-SAA 106–Phe-OH: ESI-MS: 1205.6 [2M-H+Na+K]⁺; 1167.2 [2M+Na]⁺; 1144.9 [2M+H]⁺; 611.4 [M+K]⁺; 595.4 [M+Na]⁺; 573.3 [M+H]⁺; $t_R=25.04$ min (anal. HPLC, 20-80%B in 30 min). The first coupling was done with Fmoc-protected f-SAA **106** (60.8 mg), HOAt (18.9 mg), HATU (53 mg) and 2,4,6-collidine (184 μ L). Subsequently Fmoc-Lys(ivDde)-OH (133 mg) (HOAt (31.6 mg), HATU (88.2 mg), 2,4,6-collidine (307 μ L)) was coupled. The resin was split into two equal parts – one for the synthesis of **138**, one for the synthesis of **139**. Coupling with Fmoc-L-Trp-OH, or Fmoc-D-Trp-OH (59.4 mg of L-, or D-Trp respectively) (HOAt (18.9 mg), HATU (52.9 mg), 2,4,6-collidine (184 μ L)) respectively, and subsequent washing Fmoc-deprotection and cleavage steps (GP 3b) yielded the linear, ivDde-protected precursors of compounds **138** and **139**, characterized by HPLC-MS:

H₂N-Trp–Lys(ivDde)–f-SAA 106–Phe-OH (precursor to **138**): 909.5 [M+K]⁺; 893.5 [M+Na]⁺; 871.5 [M+H]⁺. 813.5; [M-acetone +H]⁺; $t_R=11.41$ min (HPLC-MS, 30-90%B in 15min), $t_R=14.41$ min (anal. HPLC, 30-90%B in 15min).

H₂N-DTrp-Lys(ivDde)-f-SAA 106-Phe-OH (precursor to **139**): 915.5 [M-H+2Na]⁺; 909.5 [M+K]⁺; 893.5 [M+Na]⁺; 871.5 [M+H]⁺. 813.5; [M-acetone+H]⁺; *t_R*=11.31 min (HPLC-MS, 30-90%B in 15min).

The precursors to **138** and **139** were cyclized according to GP 4 (DPPA (37.9 μL), NaHCO₃ (25 mg), DMF (12 mL)) to yield the protected cyclic precursors:

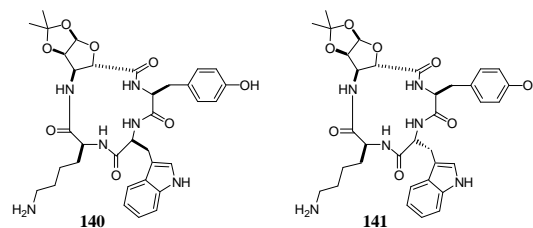
cyclo[-Trp-Lys(ivDde)-f-SAA 106-Phe-] (precursor of **138**): ESI-MS: 1729.0 [2M+Na]⁺; 890.6 [M+K]⁺; 875.7 [M+Na]⁺; 853.6 [M+H]⁺; 795.6 [M-acetone+H]⁺; *t_R*=19.19 min (anal. HPLC, 30-90%B).

cyclo[-D-Trp-Lys(ivDde)-f-SAA 106-Phe-] (precursor of **139**): ESI-MS: 1743.1 [2M+K]⁺; 1729.0 [2M+Na]⁺; 1705.6 [2M+H]⁺; 897.6 [M-H+2Na]⁺; 891.7 [M+K]⁺; 875.7 [M+Na]⁺; 853.6 [M+H]⁺; 795.6 [M-acetone+H]⁺; *t_R*=21.32 min (anal. HPLC, 10-60%B).

ivDde-deprotection according to GP 5, purification via rp-HPLC (semipreparative; gradient: 35-55% B in 30 min (**138**), and 20-60%B in 30 min (**139**), respectively; (B=90% MeCN, 10% H₂O, + 0.1%TFA)), and subsequently lyophilization yielded the compounds **138** (10 mg, 33 %) and **139** (10.7 mg, 36 %) as white, fluffy powder.

138: ESI-MS: 1445.1 [2M+TFA+K]⁺; 1331.3 [2M+K]⁺; 1315.2 [2M+Na]⁺; 1293.2 [2M+H]⁺; 799.1 [M+TFA+K]⁺; 783.1 [M+TFA+Na]⁺; 685.2 [M+K]⁺; 669.4 [M+Na]⁺; 647.2 [M+H]⁺; 589.2 [M-acetone+H]⁺; *t_R*=4.78 min (HPLC-MS, 30-70%B in 15min; B=MeCN+0.1%TFA).

139: ESI-MS: 1445.2 [2M+TFA+K]⁺; 1331.4 [2M+K]⁺; 1315.3 [2M+Na]⁺; 1293.3 [2M+H]⁺; 799.1 [M+TFA+K]⁺; 669.3 [M+Na]⁺; 647.2 [M+H]⁺; 589.3 [M-acetone+H]⁺; *t_R*=5.74 min (HPLC-MS, 30-70%B in 15min; B=MeCN+0.1%TFA).



Synthesis of 140 and 141: According to GP 3b, **140** and **141** were synthesized parallel in the same syringe (2 mL), 190 mg of the Fmoc-Tyr-OH loaded TCP resin). The first coupling was done with Fmoc-protected f-SAA **106** (58 mg), HOAt (18.5 mg), HATU (52 mg) and 2,4,6-collidine (180 μ L). Coupling was verified by a sample cleavage: Some beads were fished out, and the dipeptide Fmoc-f-SAA 106–Tyr-OH cleaved from those beads in an Eppendorf cap according to GP 3b. Characterization: ESI-MS: 1237.6 [2M-H+Na+K]⁺; 1221.4 [2M-H+2Na]⁺; 1215.4 [2M+K]⁺; 1199.2 [2M+Na]⁺; 921.6 [(3M+2K)/2]²⁺; 913.7 [(3M+Na+K)/2]²⁺; 633.4 [M-H+2Na]⁺; 627.4 [M+K]⁺; 611.4 [M+Na]⁺; 589.3 [M+H]⁺; t_R = 21.68 min (anal. HPLC, 20-80%B in 30 min). According to GP 3b Fmoc-Lys(ivDde)-OH (130 mg) (HOAt (31 mg), HATU (86 mg), 2,4,6-collidine (300 μ L)) was coupled. The resin was split into two equal parts – one for the synthesis of **140**, one for the synthesis of **141**. Coupling with Fmoc-L-Trp-OH, or Fmoc-D-Trp-OH (58 mg of L-, or D-Trp respectively) (HOAt (18.5 mg), HATU (52 mg), 2,4,6-collidine (180 μ L)) respectively, and subsequent washing Fmoc-deprotection and cleavage steps (GP 3b) yielded the linear, ivDde-protected precursors of compounds **140** and **141**. The precursors to **140** and **141** were cyclized according to GP 4 (DPPA (38 μ L), NaHCO₃ (25 mg), DMF (12 mL)) to yield the protected cyclic precursors:

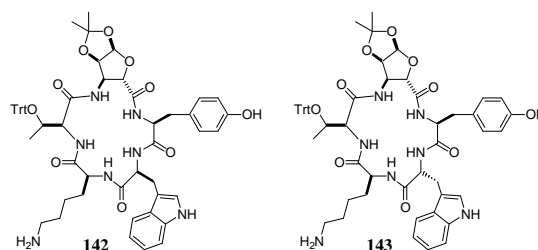
cyclo[–Trp–Lys(ivDde)–f-SAA 106–Tyr–] (precursor of **140**): ESI-MS: 1759.9 [2M+Na]⁺; 906.7 [M+K]⁺; 891.6 [M+Na]⁺; 869.6 [M+H]⁺; 811.6 [M-acetone+H]⁺; t_R = 11.89 min (anal. HPLC, 30-90%B, 30 min).

cyclo[–D-Trp–Lys(ivDde)–f-SAA 106–Tyr–] (precursor of **141**): ESI-MS: 906.7 [M+K]⁺; 891.6 [M+Na]⁺; 869.6 [M+H]⁺; 811.6 [M-acetone+H]⁺; t_R = 11.74 min (anal. HPLC, 30-90%B, 30 min).

ivDde-deprotection according to GP 5, purification via rp-HPLC (semipreparative; gradient: 20-60% B in 30 min (**140**), and 25-60%B in 30 min (**141**), respectively; (B=90% MeCN, 10% H₂O, + 0.1% TFA)), and subsequently lyophilization yielded the compounds **140** and **141** as white, fluffy powder.

140: ESI-MS: 799.2 [M+TFA+Na]⁺; 685.4 [M+Na]⁺; 663.2 [M+H]⁺; 605.3 [M-acetone+H]⁺; $t_R=15.46$ min (anal. HPLC, 20-60%B in 15min; B=MeCN+0.1%TFA).

141: ESI-MS: 1363.3 [2M+K]⁺; 1347.1 [2M+Na]⁺; 1325.2 [2M+H]⁺; 685.4 [M+Na]⁺; 663.3 [M+H]⁺; 605.3 [M-acetone+H]⁺; $t_R=20.19$ min (anal. HPLC, 10-60%B in 15min; B=MeCN+0.1%TFA).



Synthesis of 142 and 143: According to GP 3b, **142** and **143** were synthesized parallel in the same syringe (2 mL, 165 mg of the Fmoc-Tyr-OH loaded TCP resin). The first coupling was done with Fmoc-protected f-SAA **106** (50.5 mg), HOAt (16 mg), HATU (45 mg) and 2,4,6-collidine (156 μ L). Coupling was verified by a sample cleavage: Some beads were fished out, and the dipeptide Fmoc-f-SAA 106-Tyr-OH cleaved from those beads in an Eppendorf cap according to GP 3b. ESI-MS of that sample cleavage: 1237.6 [2M-H+Na+K]⁺; 1221.4 [2M-H+2Na]⁺; 1215.4 [2M +K]⁺; 1199.2 [2M+Na]⁺; 633.4 [M-H+2Na]⁺; 627.4 [M+K]⁺; 611.4 [M+Na]⁺; 589.3 [M+H]⁺. According to GP 3b Fmoc-Thr(OTrt)-OH (115 mg) (HOAt (27 mg), HATU (75 mg), 2,4,6-collidine (260 μ L)), and Fmoc-Lys(ivDde)-OH (112.9 mg) (HOAt (27 mg), HATU (74.7 mg), 2,4,6-collidine (260 μ L)) were coupled consecutively. The resin was split into two equal parts – one for the synthesis of **142**, one for the synthesis of **143**. Coupling with Fmoc-L-Trp-OH, or Fmoc-D-Trp-OH (50 mg of L-, or D-Trp respectively) (HOAt (16 mg), HATU (45 mg), 2,4,6-collidine (156 μ L)) respectively, and subsequent washing Fmoc-deprotection and cleavage steps (GP 3b) yielded the

linear, ivDde-protected precursors of compounds **142** and **143**, characterized by HPLC-MS:

H-Trp-Lys(ivDde)-Thr(OTrt)-f-SAA 106-Tyr-OH (precursor of **142**):
ESI-MS: 1306.4 [M-H+2K]⁺; 1290.5 [M-H+Na+K]⁺; 1274.6 [M-H+2Na]⁺; 1268.6 [M+K]⁺; 1252.6 [M+Na]⁺; 1230.4 [M+H]⁺; 988.5 [M-Trt+H]⁺; 930.5 [M-Trt-acetone+H]⁺; 243 [Trt]⁺; *t*_R=12.90 min (HPLC-MS, 40-90%B in 15min).

H-D-Trp-Lys(ivDde)-Thr(OTrt)-f-SAA 106-Tyr-OH (precursor of **143**):
ESI-MS: 1306.4 [M-H+2K]⁺; 1290.5 [M-H+Na+K]⁺; 1274.6 [M-H+2Na]⁺; 1268,6 [M+K]⁺; 1252.6 [M+Na]⁺; 1230.4 [M+H]⁺; 988.5 [M-Trt+H]⁺; 930.5 [M-Trt-acetone+H]⁺; 243 [Trt]⁺; *t*_R=12.97 min (HPLC-MS, 40-90%B in 15min).

The precursors to **142** and **143** were cyclized according to GP 4 (DPPA (37.9 μL), NaHCO₃ (25 mg), DMF (12 mL)) to yield the protected cyclic precursors:

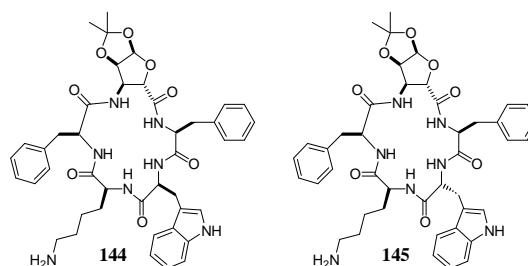
cyclo[-Trp-Lys(ivDde)-Thr(OTrt)-f-SAA 106-Tyr-] (precursor of **142**):
ESI-MS: 1256.7 [M-H+2Na]⁺; 1250.7 [M +K]⁺; 1234.7 [M +Na]⁺; 1219.0 [M +Li]⁺; 970.5 [M-Trt+H]⁺; 912.6 [M-Trt-acetone+H]⁺; 243 [Trt]⁺; *t*_R=22.13 min (HPLC-MS, 30-70%B in 15min).

cyclo[-D-Trp-Lys(ivDde)-Thr(OTrt)-f-SAA 106-Tyr-] (precursor of **143**):
ESI-MS: 1256.7 [M-H+2Na]⁺; 1250.7 [M +K]⁺; 1234.8 [M +Na]⁺; 1218.8 [M +Li]⁺; 970.6 [M-Trt+H]⁺; 912.7 [M-Trt-acetone+H]⁺; 243 [Trt]⁺; *t*_R=22.28 min (HPLC-MS, 30-70%B in 15min).

ivDde-deprotection according to GP 5, purification via rp-HPLC (semipreparative; gradient: 40-65%B in 30 min (**142**), and 50-65%B in 30 min (**143**), respectively; (B=90% MeCN, 10% H₂O, + 0.1% TFA)), and subsequently lyophilization yielded the compounds **142** (8.2 mg, 20 %) and **143** (14 mg, 35 %) as white, fluffy powder.

142: ESI-MS: 1044.5 [M+K]⁺; 1028.5 [M+Na]⁺; 1006.2 [M+H]⁺; 764.4 [M-Trt+H]⁺; 706.4 [M-Trt-acetone+H]⁺; 243.2 [Trt]⁺; *t*_R=13.94 min (HPLC-MS, 30-70%B in 15min; B=MeCN+0.1% TFA).

143: ESI-MS: 1044.5 [M+K]⁺; 1028.6 [M+Na]⁺; 1012.6 [M+Li]⁺; 764.4 [M-Trt+H]⁺; 706.4 [M-Trt-acetone+H]⁺; 243 [Trt]⁺; t_R =14.35 min (HPLC-MS, 30-70%B in 15min; B=MeCN +0.1% TFA).



Synthesis of 144 and 145: According to GP 3b, **144** and **145** were synthesized parallel in the same syringe (2 mL, 371.9 mg of the Fmoc-Phe-OH loaded TCP resin). The first coupling was done with Fmoc-protected f-SAA **106** (160.7 mg), HOAt (51 mg), HATU (144 mg) and 2,4,6-collidine (500 μ L). Coupling was verified by a sample cleavage: Some beads were fished out, and the dipeptide Fmoc-f-SAA 106–Phe-OH cleaved from those beads in an Eppendorf cap according to GP 3b. ESI-MS of that sample cleavage: 1739.1 [3M+Na]⁺; 1716.9 [3M+H]⁺; 1205.5 [2M-H+Na+K]⁺; 1183.4[2M+K]⁺; 1167.4 [2M+Na]⁺; 1145.0 [2M+H]⁺; 897.5 [(3M+2K)/2]²⁺; 889.7 [(3M+Na+K)/2]²⁺; 617.4 [M-H+2Na]⁺; 611.3 [M+K]⁺; 595.3 [M+Na]⁺; 573.2 [M+H]⁺. According to GP 3b Fmoc-Phe-OH (244 mg) (HOAt (85.7 mg), HATU (239 mg), 2,4,6-collidine (835 μ L)), and Fmoc-Lys(ivDde)-OH (362 mg) (HOAt (85.6 mg), HATU (239 mg), 2,4,6-collidine (835 μ L)) were coupled consecutively. The resin was split into two equal parts – one for the synthesis of **144**, one for the synthesis of **145**. Coupling with Fmoc-L-Trp-OH, or Fmoc-D-Trp-OH (161 mg of L-, or D-Trp respectively) (HOAt (51 mg), HATU (144 mg), 2,4,6-collidine (501 μ L)) respectively, and subsequent washing Fmoc-deprotection and cleavage steps (GP 3b) yielded the linear, ivDde-protected precursors of compounds **144** and **145**, characterized by HPLC-MS:

H–Trp–Lys(ivDde)–Phe–f-SAA 106–Phe–OH (precursor of **144**): ESI-MS: 1062.6 [M-H+2Na]⁺; 1056.6 [M+K]⁺; 1040.6 [M+Na]⁺; 1018.6 [M+H]⁺; 960.6

$[M\text{-acetone}+H]^+$; $t_R=16.53$ min (anal. HPLC, 30-90%B in 30 min), $t_R=9.49$ min (HPLC-MS, 40-90%B in 15 min).

H-D-Trp-Lys(ivDde)-Phe-f-SAA 106-Phe-OH (precursor of **145**): ESI-MS: 1062.6 $[M-H+2Na]^+$; 1056.6 $[M+K]^+$; 1040.6 $[M+Na]^+$; 1018.6 $[M+H]^+$; 960.6 $[M\text{-acetone}+H]^+$; $t_R=9.17$ min (HPLC-MS, 40-90%B in 15 min).

The precursors to **144** and **145** were cyclized according to GP 4 (DPPA (112 μ L), $NaHCO_3$ (73 mg), DMF (35 mL) respectively) to yield the protected cyclic precursors:

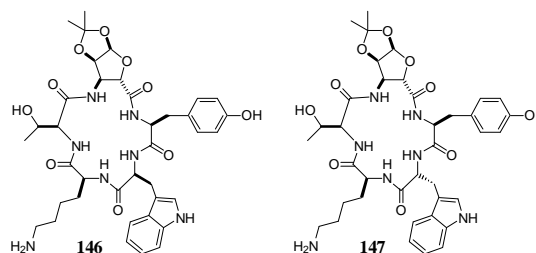
cyclo[-Trp-Lys(ivDde)-Phe-f-SAA 106-Phe-] (precursor of **144**): ESI-MS: 1038.6 $[M+K]^+$; 1022.6 $[M+Na]^+$; 1006.8 $[M+Li]^+$; 1000.6 $[M+H]^+$; 942.6 $[M\text{-acetone}+H]^+$; $t_R=19.99$ min (HPLC-MS, 30-70%B in 15 min).

cyclo[-D-Trp-Lys(ivDde)-Phe-f-SAA 106-Phe-] (precursor of **145**): ESI-MS: 1039.6 $[M+K]^+$; 1022.6 $[M+Na]^+$; 1006.6 $[M+H]^+$; 942.6 $[M\text{-acetone}+H]^+$; $t_R=20.43$ min (HPLC-MS, 30-70%B in 15 min).

ivDde-deprotection according to GP 5, purification via rp-HPLC (semipreparative; gradient: 30-65%B in 30 min (**144**), and 30-45%B in 30 min (**145**), respectively; (B=90% MeCN, 10% H_2O , + 0.1% TFA)), and subsequently lyophilization yielded the compounds **144** (41.3 mg, 41 %) and **145** (35.5 mg, 36 %) as white, fluffy powder.

144: ESI-MS: 1739.4 $[2M+TFA+K]^+$; 1625.4 $[2M+K]^+$; 1609.3 $[2M+Na]^+$; 1587.3 $[2M+H]^+$; 946.2 $[M+TFA+K]^+$; 930.2 $[M+TFA+Na]^+$; 832.4 $[M+K]^+$; 816.4 $[M+Na]^+$; 794.3 $[M+H]^+$; 736.3 $[M\text{-acetone}+H]^+$; $t_R=13.76$ min (anal. HPLC, 30-70%B in 30 min; B=MeCN +0.1% TFA).

145: 1739.2 $[2M+TFA+K]^+$; 1625.3 $[2M+K]^+$; 1609.2 $[2M+Na]^+$; 1587.2 $[2M+H]^+$; 946.2 $[M+TFA+K]^+$; 930.2 $[M+TFA+Na]^+$; 832.4 $[M+K]^+$; 816.4 $[M+Na]^+$; 794.3 $[M+H]^+$; 736.4 $[M\text{-acetone}+H]^+$; $t_R=10.47$ min (HPLC-MS, 30-70%B in 15 min; B=MeCN +0.1% TFA).

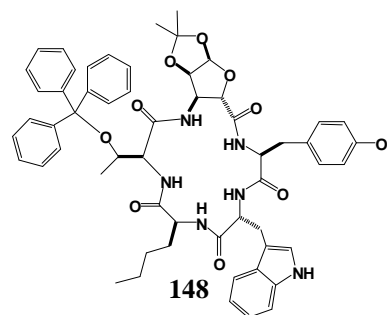


Synthesis of 146 and 147: Syntheses analogous to the synthesis of compounds **142** and **143**, except, that the crude cyclic peptides were stirred in TFA-MeCN solution for five minutes.

Characterization:

146: 764 [M+H]⁺; 706.4 [M-acetone+H]⁺.

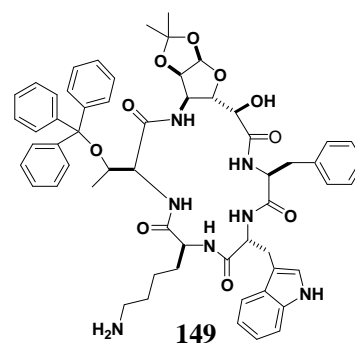
147: 764 [M+H]⁺; 706.4 [M-acetone+H]⁺.



Synthesis of 148: *cyclo*[-D-Trp-Nle-Thr(OTrt)-f-SAA 106-Tyr-]

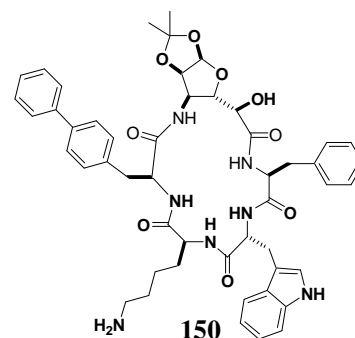
148 was synthesized according to GP 3b (2 mL, 66.8 mg of the Fmoc-Tyr-OH loaded TCP resin). Coupling of the Fmoc-protected f-SAA **106** was verified by a sample cleavage: Some beads were fished out, and the dipeptide Fmoc-f-SAA 106-Tyr-OH cleaved from those beads in an Eppendorf cap according to GP 3b. ESI-MS of that sample cleavage: 1803.0 [3M+K]⁺; 1786.9 [3M+Na]⁺; 1237.3 [2M-H+Na+K]⁺; 1221.4 [2M-H+2Na]⁺; 1215.3 [2M+K]⁺; 1199.1 [2M+Na]⁺; 633.4 [M-H+2Na]⁺; 627.4 [M+K]⁺; 611.3 [M+Na]⁺; 589.1 [M+H]⁺. Coupling of the Fmoc-Thr(OTrt)-OH, was verified by a sample cleavage: Some beads were fished out, and the tripeptide Fmoc-Thr(OTrt)-f-SAA 106-Tyr-OH cleaved from those beads in an Eppendorf cap according to GP 3b. ESI-MS of that sample cleavage: 1885.3 [2M+Na]⁺; 1863.0 [2M+H]⁺; 976.4 [M-H+2Na]⁺; 970.4 [M+K]⁺; 954.4 [M+Na]⁺; 932.4 [M+H]⁺; 243.2 [Trt]⁺. According to GP 3b Fmoc-Nle-OH, and Fmoc-D-Trp-OH were coupled consecutively. Subsequent cleavage from the resin (GP 3b), cyclization according to GP 4, and purification via RP-HPLC (semipreparative; gradient: 50-100%B in 30

min), yielded the **148** as a white fluffy powder: ESI-MS: 1998.7[2M+Li]⁺; 1143.4 [M-H+TFA+K]⁺; 1127.5 [M-H+TFA+Na]⁺; 1029.5 [M+K]⁺; 1013.5 [M+Na]⁺; 997.7 [M+Li]⁺; 990.6 [M+H]⁺; 771.7 [M-Trt+Na]⁺; 749.4 [M-Trt+H]⁺; 691.4 [M-Trt-acetone+H]⁺; 243.2 [Trt]⁺. *t*_R=21.05 min (HPLC-MS, 30-70%B in 15 min).



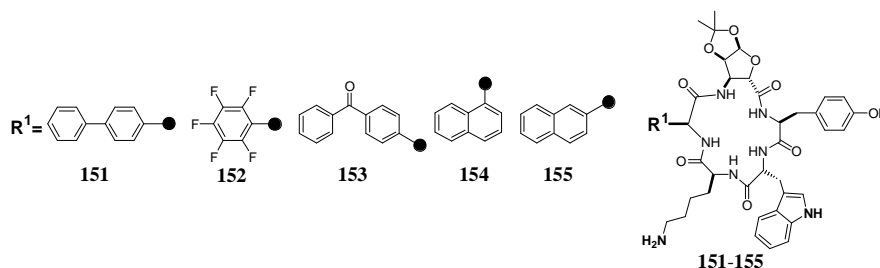
Synthesis of 149: *cyclo*[-D-Trp-Lys-Thr(OTrt)-f-SAA 107-Phe-]

149 was synthesized according to GP 3b (2 mL, 52.4 mg of the Fmoc-Phe-OH loaded TCP resin). Coupling of the Fmoc-protected f-SAA **107** was verified by a sample cleavage: Some beads were fished out, and the dipeptide Fmoc-f-SAA 107-Phe-OH cleaved from those beads in an Eppendorf cap according to GP 3b. ESI-MS of that sample cleavage: 1829.8 [3M+Na]⁺; 1227.2 [2M+Na]⁺; 1205.0 [2M+H]⁺; 663.4 [M-H+Na+K]⁺; 647.4 [M-H+2Na]⁺; 641.3 [M+K]⁺; 625.4 [M+Na]⁺; 603.2 [M+H]⁺; 551.3 [M-acetone+Li]⁺; 545.1 [M-acetone+H]⁺. According to GP 3b Fmoc-Thr(OTrt)-OH, Fmoc-Lys(ivDde)-OH, and Fmoc-D-Trp-OH were coupled consecutively. Subsequent cleavage from the resin (GP 3b), cyclization according to GP 4, the ivDde cyclic precursor *cyclo*[-D-Trp-Lys(ivDde)-Thr(OTrt)-f-SAA 107-Phe-]: ESI-MS: 1264.8 [M+K]⁺; 1248.9 [M+Na]⁺; 1226.5 [M+H]⁺; 1006.8 [M-Trt+Na]⁺; 984.6 [M-Trt+H]⁺; 926.7 [M-Trt-acetone+H]⁺; 243.2 [Trt]⁺. Subsequent ivDde deprotection according to GP 5, and purification via RP-HPLC (semipreparative; gradient: 50-65%B in 30 min), yielded the **149** as a white fluffy powder: ESI-MS: 1058.3 [M+K]⁺; 1042.5 [M+Na]⁺; 1020.2 [M+H]⁺; 800.6 [M-Trt+Na]⁺; 778.4 [M-Trt+H]⁺; 720.4 [M-Trt-acetone+H]⁺; 243.2 [Trt]⁺. *t*_R=15.18 min (HPLC-MS, 30-70%B in 15 min).



Synthesis of 150: *cyclo*[-D-Trp-Lys-Thr(OTrt)-f-SAA 107-Phe-]

150 was synthesized according to GP 3b (2 mL, 52.4 mg of the Fmoc-Phe-OH loaded TCP resin). Coupling of the Fmoc-protected f-SAA **107** was verified by a sample cleavage: Some beads were fished out, and the dipeptide Fmoc-f-SAA 107-Phe-OH cleaved from those beads in an Eppendorf cap according to GP 3b. ESI-MS of that sample cleavage: 1829.8 [3M+Na]⁺; 1227.2 [2M+Na]⁺; 1205.0 [2M+H]⁺; 663.4 [M-H+Na+K]⁺; 647.4 [M-H+2Na]⁺; 641.3 [M+K]⁺; 625.4 [M+Na]⁺; 603.2 [M+H]⁺; 551.3 [M-acetone+Li]⁺; 545.1 [M-acetone+H]⁺. According to GP 3b Fmoc-Bip-OH, Fmoc-Lys(ivDde)-OH, and Fmoc-D-Trp-OH were coupled consecutively. Subsequent cleavage from the resin (GP 3b), cyclization according to GP 4, ivDde-deprotection and purification via RP-HPLC (semipreparative; gradient: 50-65%B in 30 min), yielded **150** as a white fluffy powder: ESI-MS: 938.9 [M+K]⁺; 922.9 [M+Na]⁺; 900.7 [M+H]⁺; 842.7 [M-acetone+H]⁺. $t_R=13.10$ min (HPLC-MS, 30-70%B in 15 min).



Parallel Syntheses of compounds 151-155:

cyclo[-D-Trp-Lys-Bip-f-SAA 106-Phe-] (**151**);

cyclo[-D-Trp-Lys-Phe(F₅)-f-SAA 106-Phe-] (**152**);

cyclo[-D-Trp-Lys-Bpa-f-SAA 106-Phe-] (**153**);

cyclo[-D-Trp-Lys-1-Nal-f-SAA 106-Phe-] (**154**);

cyclo[-D-Trp-Lys-2-Nal-f-SAA 106-Phe-] (**155**).

According to GP 2, TCP resin (2.008 g) was loaded with Fmoc-Phe-OH (933.6 mg, 2.4098 mmol) and DIPEA (1.05 mL, 6.025 mmol) in 16 mL DCM. The loading was $c = 0.677$ mol/g resin.

Each of the compounds **151-155** was prepared in a separate syringe (2 mL, 52.4 mg of the Fmoc-Phe-OH loaded TCP resin each), completed with a frit. The linear precursors of the compounds **151-155** were prepared according to GP 3b. However, if the same amino acid was to be coupled, only one coupling solution was prepared for all of the compounds. This solution was then divided into equal parts, and added to the different syringes. First coupling is performed with Fmoc-protected f-SAA **106** (113.5 mg, 1.5 equiv; HOAt (36.3 mg, 1.5 equiv); HATU (101.3 mg, 1.5 equiv); 2,4,6-collidine (353 μ L, 15 equiv); dissolved in 1 mL DMF; 270.7 μ L coupling solution per syringe). Exemplarily, some beads from the syringe for synthesis of **151** were fished out, the dipeptide Fmoc-f-SAA 106–Phe-OH cleaved according to GP 3b, and characterized by ESI-MS and HPLC: 1738.7 [3M+Na]⁺; 1716.8 [3M+H]⁺; 1205.4 [2M-H+Na+K]⁺; 1167.1 [2M+Na]⁺; 1144.9 [2M+H]⁺; 611.3 [M+K]⁺; 595.3 [M+Na]⁺; 573.2 [M+H]⁺; $t_R=25.04$ min (anal. HPLC, 20-80%B in 30 min). For the second coupling, a different unnatural amino acid was coupled for all of the different compounds **151-155**, and therefore a different coupling solution was prepared for each of them: Each of the coupling solutions consisted of HATU (27 mg), HOAt (10 mg), 2,4,6-collidine (94 μ L), and respectively one of the unnatural amino acids Fmoc-Bip-OH (**151**, 33.0 mg), Fmoc-Phe(F₅)-OH (**152**, 33.9 mg), Fmoc-Bpa-OH (**153**, 35.0 mg), Fmoc-1-Nal-OH (**154**, 31.0 mg), Fmoc-2-Nal-OH (**155**, 31.0 mg), in 300 μ L NMP. Consecutive coupling of Fmoc-Lys(ivDde)-OH (204 mg, 2 equiv; HOAt (47 mg, 2 equiv); HATU (135 mg, 2 equiv); 2,4,6-collidine (470 μ L, 20 equiv); dissolved in 1.5 mL DMF; 300 μ L coupling solution per syringe), and Fmoc-D-Trp-OH (151.2 mg, 2 equiv; HOAt (47 mg, 2 equiv); HATU (135 mg, 2 equiv); 2,4,6-collidine (470 μ L, 20 equiv); dissolved in 1.5 mL DMF; 300 μ L coupling solution per syringe), subsequent Fmoc-deprotection and cleavage from the resin yielded the linear precursors of compounds **151-155**. These were cyclized in individual flasks according to GP 4 (DPPA (23 μ L), NaHCO₃ (14.9 mg), DMF (7.1 mL) each) to yield the protected cyclic precursors, exemplary ESI-MS of

cyclo[-D-Trp-Lys(ivDde)-Phe(F₅)-f-SAA 106-Phe-] (precursor of **151**): ESI-MS: 1134.6 [M-H+2Na]⁺; 1128.6 [M+K]⁺; 1112.7 [M+Na]⁺; 1090.6 [M+H]⁺; 1032.6 [M-acetone+H]⁺. ivDde-deprotection according to GP 5, purification via rp-HPLC (semipreparative; gradient: 45-63%B in 30 min (**151**), 30-70%B in 30 min (**152**), 45-65%B in 30 min (**153**, **155**), 47-55%B in 30 min (**154**), respectively; (B=90% MeCN, 10% H₂O, + 0.1%TFA)), and subsequently lyophilization yielded the compounds as white, fluffy powder.

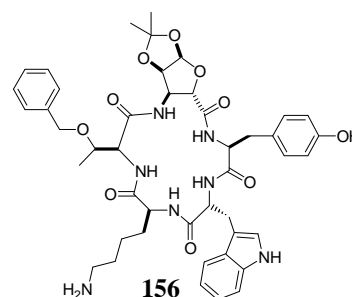
151: ESI-MS: 1028.2 [M+TFA-H+2Na]⁺; 1022.4 [M+TFA+K]⁺; 1006.5 [M+TFA+Na]⁺; 908.4 [M+K]⁺; 892.6 [M+Na]⁺; 870.4 [M+H]⁺; 812.5 [M-acetone+H]⁺; *t_R*=13.05 min (HPLC-MS. 30-70%B in 15min; B=MeCN +0.1%TFA).

152: ESI-MS: 1806.4 [2M(1*¹³C)+K]⁺; 1805.4 [2M+K]⁺; 1790.3 [2M(1*¹³C)+Na]⁺; 1789.3 [2M+Na]⁺; 1768.2 [2M(1*¹³C)+H]⁺; 1767.2 [2M+H]⁺; 922.3 [M+K]⁺; 906.4[M+Na]⁺; 884.3 [M+H]⁺; 826.4 [M-acetone+H]⁺; *t_R*=11.65 min (HPLC-MS, 30-70%B in 15min; B=MeCN +0.1%TFA).

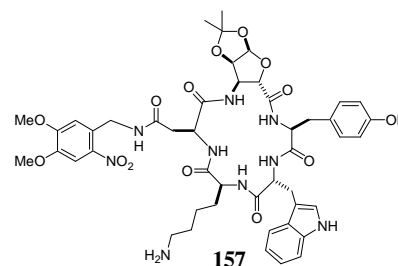
153: ESI-MS: 1056.1 [M+TFA-H+2Na]⁺; 1050.3 [M+TFA+K]⁺; 1034.4 [M+TFA+Na]⁺; 936.5 [M+K]⁺; 920.6 [M+Na]⁺; 898.4 [M+H]⁺; 840.5 [M-acetone+H]⁺. *t_R*=12.19 min (HPLC-MS, 30-70%B in 15min; B=MeCN +0.1%TFA).

154: ESI-MS: 1839.6 [2M+TFA+K]⁺; 1709.6 [2M+Na]⁺; 1687.6 [2M+H]⁺; 1002.1 [M+TFA-H+2Na]⁺; 996.4 [M+TFA+K]⁺; 980.4 [M+TFA+Na]⁺; 882.5 [M+K]⁺; 866.6 [M+Na]⁺; 844.4 [M+H]⁺; 786.5 [M-acetone+H]⁺.

155: ESI-MS: 1840.7 [2M(1*¹³C)+TFA+K]⁺; 1710.6 [2M(1*¹³C)+Na]⁺; 1687.5 [2M+H]⁺; 1002.1 [M+TFA-H+2Na]⁺; 996.4 [M+TFA+K]⁺; 980.3 [M+TFA+Na]⁺; 882.5 [M+K]⁺; 866.6 [M+Na]⁺; 844.4 [M+H]⁺; 786.5 [M-acetone+H]⁺. *t_R*=3.75 min (HPLC-MS, 30-70%B in 15min; B=MeCN +0.1%TFA).

**Synthesis of 156:** *cyclo*[-D-Trp-Lys-Thr(OBzl)-f-SAA 106-Tyr-]

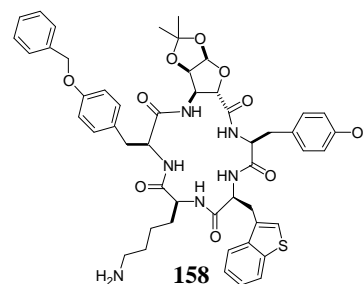
156 was synthesized (2 mL, 66.8 mg of the Fmoc-Tyr-OH loaded TCP resin), according to GP 3b. Coupling of the Fmoc-protected f-SAA **106** was verified by a sample cleavage: Some beads were fished out, and the dipeptide Fmoc-f-SAA 106-Tyr-OH cleaved from those beads in an Eppendorf cap according to GP 3b. ESI-MS of that sample cleavage: 1803.0 [3M+K]⁺; 1786.9 [3M+Na]⁺; 1237.3 [2M-H+Na+K]⁺; 1221.4 [2M-H+2Na]⁺; 1215.3 [2M+K]⁺; 1199.1 [2M+Na]⁺; 633.4 [M-H+2Na]⁺; 627.4 [M+K]⁺; 611.3 [M+Na]⁺; 589.1 [M+H]⁺. According to GP 3b Fmoc-Thr(OBzl)-OH, Fmoc-Lys(ivDde)-OH, and Fmoc-D-Trp-OH were coupled consecutively. Subsequent cleavage from the resin (GP 3b), cyclization according to GP 4, ivDde deprotection according to GP 5, and purification via RP-HPLC (semipreparative; gradient: 35-50%B in 30 min), yielded the **156** as a white fluffy powder: ESI-MS: 892.2 [M+K]⁺; 876.5 [M+Na]⁺; 860.9 [M+Li]⁺; 854.4 [M+H]⁺; 796.3 [M-acetone+H]⁺; *t*_R=8.82 min (HPLC-MS, 30-90%B in 15 min).

**Synthesis of 157:**

157 was synthesized (2 mL, 66.8 mg of the Fmoc-Tyr-OH loaded TCP resin), according to GP 3b. Coupling of the Fmoc-protected f-SAA **106** was verified by a sample cleavage: Some beads were fished out, and the dipeptide Fmoc-f-SAA 106-Tyr-OH cleaved from those beads in an Eppendorf cap according to GP 3b. ESI-MS of

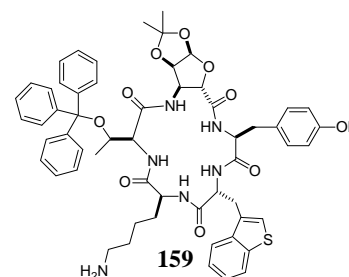
that sample cleavage: 1803.0 [3M+K]⁺; 1786.9 [3M+Na]⁺; 1237.3 [2M-H+Na+K]⁺; 1221.4 [2M-H+2Na]⁺; 1215.3 [2M+K]⁺; 1199.1 [2M+Na]⁺; 633.4 [M-H+2Na]⁺; 627.4 [M+K]⁺; 611.3 [M+Na]⁺; 589.1 [M+H]⁺. Fmoc-Asp(ODmab)-OH was coupled (GP 3b). After washing, the resin was treated with 2% H₂N-NH₂ in DMF (2 × 10 min), for ODmab-deprotection of the carboxylic side chain. Coupling and deprotection (without Fmoc-deprotection !) was verified by a sample cleavage ESI-MS: 1483.4 [2M-H+2K]⁺; 1467.4 [2M-H+Na+K]⁺; 1451.2 [2M-H+2Na]⁺; 1445.3 [2M+K]⁺; 1429.3 [2M+Na]⁺; 764.2 [M-H+Na+K]⁺; 748.2 [M-H+2Na]⁺; 742.2 [M+K]⁺; 726.3 [M+Na]⁺; 704.2 [M+H]⁺; 646.2 [M-acetone+H]⁺; *t*_R=15.76 min (HPLC-MS, 10-90%B in 15min; B=MeCN +0.1%TFA).

For the subsequent coupling of 2-nitro-3,4-dimethoxy-benzylamine several coupling reagents and conditions, were tried out such as: conditions of GP 3b; PyBop (5 equiv), NMM (5 equiv) and amine (5 equiv) in NMP,^[307] and pre-activation (3-4 h) with pyridine (1 equiv), and cyanarylfluoride (1 equiv) in DCM, followed by coupling with the amine (5 equiv) and 2,4,6-collidine (50 equiv) in NMP. Best coupling yields were obtained, when the acid on the resin was pre-activated with HATU/HOAt (0.6 equiv each, 30 equiv 2,4,6-collidine in DMF (0.5 mM)), after 30 min this solution was filtered, and the amine was dissolved in that same solution, and added again to the resin. After 2h coupling time, the resin was filtered off, washed, and the remaining carboxylic side chains again pre-activated with HATU/HOAt. This coupling cycle was repeated 3 times, before coupling according to GP 3b was continued. Fmoc-Lys(ivDde)-OH, and Fmoc-D-Trp-OH were coupled consecutively. Subsequent cleavage from the resin (GP 3b), cyclization according to GP 4, ivDde deprotection according to GP 5, and purification via RP-HPLC (semipreparative; gradient: 30-65%B in 30 min), yielded the **157** as a white fluffy powder: ESI-MS: 995.0 [M+Na]⁺; 978.6 [M+Li]⁺; 972.8 [M+H]⁺; 951.9 [M-acetone+K]⁺; 914.9 [M-acetone+H]⁺; *t*_R=5.0 min (HPLC-MS, 30-70%B in 15 min).



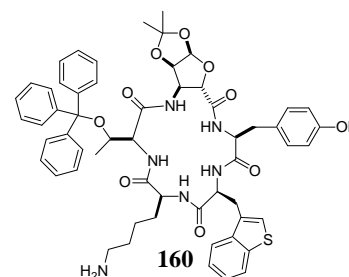
Synthesis of **158**:

158 was synthesized (2 mL, 66.8 mg of the Fmoc-Tyr-OH loaded TCP resin), according to GP 3b. Coupling of the Fmoc-protected f-SAA **106** was verified by a sample cleavage: Some beads were fished out, and the dipeptide Fmoc-f-SAA 106–Tyr-OH cleaved from those beads in an Eppendorf cap according to GP 3b. ESI-MS of that sample cleavage: 1803.0 [3M+K]⁺; 1786.9 [3M+Na]⁺; 1237.3 [2M-H+Na+K]⁺; 1221.4 [2M-H+2Na]⁺; 1215.3 [2M+K]⁺; 1199.1 [2M+Na]⁺; 633.4 [M-H+2Na]⁺; 627.4 [M+K]⁺; 611.3 [M+Na]⁺; 589.1 [M+H]⁺. Subsequent coupling of Fmoc-Tyr(OBzl)-OH (GP 3b) was verified by a sample cleavage ESI-MS: 1742.9 [2M-H+Na+K]⁺; 1727.3 [2M-H+2Na]⁺; 1722.2 [2M(1*¹³C)+K]⁺; 1706.3 [2M(1*¹³C)+Na]⁺; 1705.3 [2M+Na]⁺; 1683.2 [2M+H]⁺; 902.4 [M-H+Na+K]⁺; 886.4 [M-H+2Na]⁺; 880.4 [M+K]⁺; 864.5 [M+Na]⁺; 842.3 [M+H]⁺; 784.4 [M-acetone+H]⁺. According to GP 3b Fmoc-Lys(ivDde)-OH, and Fmoc-D-Trp-OH were coupled consecutively. Subsequent cleavage from the resin (GP 3b), and cyclization according to GP 4, yielded the cyclic precursor *cyclo*[–D-Trp–Lys(ivDde)–Tyr(OBzl)–f-SAA 106–Tyr–]: ESI-MS: 1177.8 [M+K]⁺; 1161.7 [M+Na]⁺; 1139.7 [M+H]⁺; 1081.7 [M-acetone+H]⁺. ivDde deprotection according to GP 5, and purification via RP-HPLC (semipreparative; gradient: 40-65%B in 30 min), yielded the **158** as a white fluffy powder: ESI-MS: 1926.5 [2M(1*¹³C)-H+Na+K]⁺; 1903.9 [2M+K]⁺; 1888.9 [2M(1*¹³C)+Na]⁺; 1866.9 [2M(1*¹³C)+H]⁺; 971.8 [M+K]⁺; 955.7 [M+Na]⁺; 933.6 [M+H]⁺; 883.7 [M-acetone+Li]⁺; 875.7 [M-acetone+H]⁺. *t*_R=11.43 min (HPLC-MS, 30-90%B in 15 min).



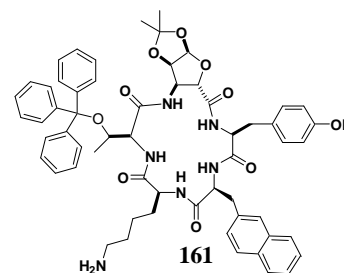
Synthesis of **159**:

159 was synthesized (2 mL, 66.8 mg of the Fmoc-Tyr-OH loaded TCP resin), according to GP 3b. Coupling of the Fmoc-protected f-SAA **106** was verified by a sample cleavage: Some beads were fished out, and the dipeptide Fmoc-f-SAA 106–Tyr-OH cleaved from those beads in an Eppendorf cap according to GP 3b. ESI-MS of that sample cleavage: 1803.0 [3M+K]⁺; 1786.9 [3M+Na]⁺; 1237.3 [2M-H+Na+K]⁺; 1221.4 [2M-H+2Na]⁺; 1215.3 [2M+K]⁺; 1199.1 [2M+Na]⁺; 633.4 [M-H+2Na]⁺; 627.4 [M+K]⁺; 611.3 [M+Na]⁺; 589.1 [M+H]⁺. Subsequent coupling of Fmoc-Thr(OTrt)-OH (GP 3b) was verified by a sample cleavage ESI-MS: 1885.3 [2M+K]⁺; 992.6 [M-H+Na+K]⁺; 976.4 [M-H+2Na]⁺; 970.4 [M+K]⁺; 954.4 [M+Na]⁺; 932.6 [M+H]⁺; 734.3 [M-Trt-H+2Na]⁺; 726.0 [M-Trt+K]⁺; 712.4 [M-Trt+Na]⁺; 690.3 [M-Trt+H]⁺; 678.7 [M-Trt-acetone+K]⁺; 663.5 [M-Trt-acetone+Na]⁺; 632.3 [M-Trt-acetone+H]⁺; 243.2 [Trt]⁺. According to GP 3b Fmoc-Lys(ivDde)-OH, and Fmoc-D-Bta-OH were coupled consecutively. Subsequent cleavage from the resin (GP 3b), and cyclization according to GP 4, yielded the cyclic precursor *cyclo*[–D-Bta–Lys(ivDde)–Thr(OTrt)–f-SAA 106–Tyr–]: ESI-MS: 1269.0 [M(1*¹³C)+K]⁺; 1251.8 [M+Na]⁺; 1230.6 [M(1*¹³C)+H]⁺; 1009.8 [M-Trt+Na]⁺; 987.6 [M-Trt+H]⁺; 243.2 [Trt]⁺. ivDde deprotection according to GP 5, and purification via RP-HPLC (semipreparative; gradient: 40-65%B in 30 min), yielded the **159** as a white fluffy powder: ESI-MS: 1061.6 [M+K]⁺; 1045.6 [M+Na]⁺; 1029.8 [M+Li]⁺; 1023.5 [M+H]⁺; 842.6 [M-Trt-H+Na+K]⁺; 828.5 [M-Trt-H+2Na]⁺; 781.5 [M-Trt+H]⁺; 723.5 [M-Trt-acetone+H]⁺; 243.2 [Trt]⁺. *t*_R=12.29 min (HPLC-MS, 30-90%B in 15 min).



Synthesis of **160**:

160 was synthesized (2 mL, 66.8 mg of the Fmoc-Tyr-OH loaded TCP resin), according to GP 3b. Coupling of the Fmoc-protected f-SAA **106** was verified by a sample cleavage: Some beads were fished out, and the dipeptide Fmoc-f-SAA 106–Tyr-OH cleaved from those beads in an Eppendorf cap according to GP 3b. ESI-MS of that sample cleavage: 1803.0 [3M+K]⁺; 1786.9 [3M+Na]⁺; 1237.3 [2M-H+Na+K]⁺; 1221.4 [2M-H+2Na]⁺; 1215.3 [2M+K]⁺; 1199.1 [2M+Na]⁺; 633.4 [M-H+2Na]⁺; 627.4 [M+K]⁺; 611.3 [M+Na]⁺; 589.1 [M+H]⁺. Subsequent coupling of Fmoc-Thr(OTrt)-OH (GP 3b) was verified by a sample cleavage ESI-MS: 1885.3 [2M+K]⁺; 992.6 [M-H+Na+K]⁺; 976.4 [M-H+2Na]⁺; 970.4 [M+K]⁺; 954.4 [M+Na]⁺; 932.6 [M+H]⁺; 734.3 [M-Trt-H+2Na]⁺; 726.0 [M-Trt+K]⁺; 712.4 [M-Trt+Na]⁺; 690.3 [M-Trt+H]⁺; 678.7 [M-Trt-acetone+K]⁺; 663.5 [M-Trt-acetone+Na]⁺; 632.3 [M-Trt-acetone+H]⁺; 243.2 [Trt]⁺. According to GP 3b Fmoc-Lys(ivDde)-OH, and Fmoc-L-Bta-OH were coupled consecutively. Subsequent cleavage from the resin (GP 3b), and cyclization according to GP 4, yielded the cyclic precursor *cyclo*[–Bta–Lys(ivDde)–Thr(OTrt)–f-SAA 106–Tyr–]: ESI-MS: 1267.8 [M+K]⁺; 1251.8 [M+Na]⁺; 1229.3 [M+H]⁺; 1009.7 [M-Trt+Na]⁺; 987.6 [M-Trt+H]⁺; 929.7 [M-Trt-acetone+H]⁺; 243.2 [Trt]⁺. ivDde deprotection according to GP 5, and purification via RP-HPLC (semipreparative; gradient: 40-65%B in 30 min), yielded the **159** as a white fluffy powder: ESI-MS: 1061.6 [M+K]⁺; 1053.6 [M-H+Li+Na]⁺; 1045.6 [M+Na]⁺; 1029.5 [M+Li]⁺; 1023.5 [M+H]⁺; 842.6 [M-Trt-H+Na+K]⁺; 826.4 [M-Trt-H+2Na]⁺; 781.4 [M-Trt+H]⁺; 723.4 [M-Trt-acetone+H]⁺; 243.2 [Trt]⁺. $t_R=12.29$ min (HPLC-MS, 30-90%B in 15 min).



Synthesis of **161**:

161 was synthesized (2 mL, 66.8 mg of the Fmoc-Tyr-OH loaded TCP resin), according to GP 3b. Coupling of the Fmoc-protected f-SAA **106** was verified by a sample cleavage: Some beads were fished out, and the dipeptide Fmoc-f-SAA 106–Tyr-OH cleaved from those beads in an Eppendorf cap according to GP 3b. ESI-MS of that sample cleavage: 1803.0 [3M+K]⁺; 1786.9 [3M+Na]⁺; 1237.3 [2M-H+Na+K]⁺; 1221.4 [2M-H+2Na]⁺; 1215.3 [2M+K]⁺; 1199.1 [2M+Na]⁺; 633.4 [M-H+2Na]⁺; 627.4 [M+K]⁺; 611.3 [M+Na]⁺; 589.1 [M+H]⁺. Subsequent coupling of Fmoc-Thr(OTrt)-OH (GP 3b) was verified by a sample cleavage ESI-MS: 1885.3 [2M+K]⁺; 992.6 [M-H+Na+K]⁺; 976.4 [M-H+2Na]⁺; 970.4 [M+K]⁺; 954.4 [M+Na]⁺; 932.6 [M+H]⁺; 734.3 [M-Trt-H+2Na]⁺; 726.0 [M-Trt+K]⁺; 712.4 [M-Trt+Na]⁺; 690.3 [M-Trt+H]⁺; 678.7 [M-Trt-acetone+K]⁺; 663.5 [M-Trt-acetone+Na]⁺; 632.3 [M-Trt-acetone+H]⁺; 243.2 [Trt]⁺. According to GP 3b Fmoc-Lys(ivDde)-OH, and Fmoc-2-Nal-OH were coupled consecutively. Subsequent cleavage from the resin (GP 3b), and cyclization according to GP 4, yielded the cyclic precursor *cyclo*[–2-Nal–Lys(ivDde)–Thr(OTrt)–f-SAA 106–Tyr–]: ESI-MS: 1261.7 [M+K]⁺; 1245.6 [M+Na]⁺; 1230.6 [M(1*¹³C)+Li]⁺; 1224.1 [M(1*¹³C)+H]⁺; 1026.6 [M-Trt-H+2Na]⁺; 1018.7 [M-Trt+K]⁺; 1003.6 [M-Trt+Na]⁺; 981.5 [M-Trt+H]⁺; 923.5 [M-Trt-acetone+H]⁺; 243.2 [Trt]⁺. ivDde deprotection according to GP 5, and purification via RP-HPLC (semipreparative; gradient: 40-63%B in 30 min), yielded the **161** as a white fluffy powder: ESI-MS: 1175.3 [M+TFA-H+2Na]⁺; 1169.4 [M+TFA+K]⁺; 1153.3 [M+TFA+Na]⁺; 1056.6 [M(1*¹³C)+K]⁺; 1039.6 [M+Na]⁺; 1017.3 [M+H]⁺; 775.5 [M-Trt+H]⁺; 717.4 [M-Trt-acetone+H]⁺; 243.2 [Trt]⁺. *t*_R=14.46 min (HPLC-MS, 30-70%B in 15 min).

6 References

- [1] J. P. McDevitt, J. Peter T. Lansbury, *J. Am. Chem. Soc.* **1996**, *118*, 3818-3828.
- [2] S. Sabesan, *Tetrahedron Lett.* **1997**, *38*, 3127-3130.
- [3] H. P. Wessel, C. Mitchell, C. M. Lobato, G. Schmid, *Angew. Chem.* **1995**, *107*, 2920-2921.
- [4] K. C. Nicolaou, H. Flörke, M. G. Egan, T. Barth, V. A. Estevez, *Tetrahedron Lett.* **1995**, *36*, 1775-1778.
- [5] Y. Suhara, J. E. K. Hildreth, Y. Ichikawa, *Tetrahedron Lett.* **1996**, *37*, 1575-1578.
- [6] J. C. Estevez, J. W. Burton, R. J. Estevez, H. Ardron, M. R. Wormald, R. A. Dwek, D. Brown, G. W. J. Fleet, *Tetrahedron Asymmetry* **1998**, *9*, 2137-2154.
- [7] D. D. Long, M. D. Smith, D. Marquess, T. D. W. Claridge, G. W. J. Fleet, *Tetrahedron Lett.* **1998**, *39*, 9293-9296.
- [8] O. Schwardt, G. Baisch, R. Öhrlein, *Bioorg. Med. Chem.* **2001**, *9*, 1857-1869.
- [9] G. Baisch, R. Öhrlein, *Bioorg. Med. Chem.* **1998**, *6*, 1673-1682.
- [10] A. Malik, W. Voelter, *Chem. Ztg.* **1989**, *113*, 153-156.
- [11] A. Dondoni, A. Marra, *Chem. Rev.* **2000**, *100*, 4395-4421.
- [12] Fakhar-uz-Zaman, A. Fatima, A. Malik, W. Voelter, *Z. Naturforsch.* **1994**, *49b*, 1434-1438.
- [13] C. D. Apostolopoulos, E. A. Couladouros, M. P. Georgiadis, *Liebigs Ann. Chem.* **1994**, *8*, 781-784.
- [14] E. Graf von Roedern, H. Kessler, *Angew. Chem. Int. Ed.* **1994**, *33*, 667-669.
- [15] E. Graf von Roedern, E. Lohof, G. Hessler, M. Hoffmann, H. Kessler, *J. Am. Chem. Soc.* **1996**, *118*, 10156-10167.
- [16] Y. Suhara, M. Ichikawa, J. E. K. Hildreth, Y. Ichikawa, *Tetrahedron Lett.* **1996**, *37*, 2549-2552.
- [17] L. Szabo, B. L. Smith, K. D. McReynolds, A. L. Parrill, E. R. Morris, J. Gervay, *J. Org. Chem.* **1998**, *63*, 1074-1078.

- [18] E. Lohof, F. Burkhart, M. A. Born, E. Planker, H. Kessler, in *Advances in Amino Acid Mimetics and Peptidomimetics, Vol. 2* (Ed.: A. Abell), JAI Press Inc., Stamford, Connecticut, **1999**, pp. 263-292.
- [19] D. E. A. Brittain, M. P. Watterson, T. D. W. Claridge, M. D. Smith, G. W. J. Fleet, *J. Chem. Soc. Perkin Trans. 1* **2000**, 3655-3665.
- [20] N. L. Hungerford, T. D. W. Claridge, M. P. Watterson, R. T. Aplin, A. Moreno, G. W. J. Fleet, *J. Chem. Soc. Perkin Trans. 1* **2000**, 3666-3679.
- [21] E. Lohof, M. A. Born, H. Kessler, in *Synthesis of Peptides and Peptidomimetics, Vol. E22b* (Eds.: M. Goodman, A. Felix, L. Moroder, C. Toniolo), Georg Thieme Verlag, Stuttgart, **in press**.
- [22] S. A. W. Gruner, E. Locardi, E. Lohof, H. Kessler, *Chem. Rev.* **2002**, special issue on *Glycobiology*, accepted.
- [23] A. R. Williamson, S. Zamenhof, *J. Biol. Chem.* **1963**, 238, 2255-2258.
- [24] K. Heyns, G. Kiessling, W. Lindenberg, H. Paulsen, M. E. Webster, *Chem. Ber.* **1959**, 92, 2435-2438.
- [25] J. P. Waltho, D. H. Williams, E. Selva, P. Ferrari, *J. Chem. Soc. Perkin Trans. 1* **1987**, 9, 2103-2107.
- [26] S. Knapp, *Chem. Rev.* **1995**, 95, 1859-1876.
- [27] S. Knapp, C. Jaramillo, B. Freeman, *J. Org. Chem.* **1994**, 59, 4800-4804.
- [28] C. Coutsogeorgopoulos, A. Bloch, K. A. Watanabe, J. J. Fox, *J. Med. Chem.* **1975**, 18, 771-776.
- [29] J. J. Fox, Y. Kuwada, K. A. Watanabe, *Tetrahedron Lett.* **1968**, 57, 6029-6032.
- [30] M. P. Kotick, R. S. Klein, K. A. Watanabe, J. J. Fox, *Carbohydr. Res.* **1969**, 11, 369-377.
- [31] F. W. Lichtenthaler, T. Morino, H. M. Mezel, *Tetrahedron Lett.* **1975**, 16, 665-668.
- [32] K. A. Watanabe, E. A. Falco, J. J. Fox, *J. Am. Chem. Soc.* **1972**, 94, 3272-3274.
- [33] H. Haruyama, T. Takayama, T. Kinoshita, M. Kondo, M. Nakajima, T. Haneishi, *J. Chem. Soc., Perkin Trans. 1* **1991**, 7, 1637-1640.
- [34] M. Nakajima, K. Itoi, Y. Takamatsu, T. Kinoshita, T. Okazaki, K. Kawakubo, M. Shindo, T. Honma, M. Tohjigamori, T. Haneishi, *J. Antibiot.* **1991**, 44, 293-300.

- [35] D. L. Siehl, M. V. Subramanian, E. W. Walters, S.-F. Lee, R. J. Anderson, a. G. Toschi, *Plant Physiol.* **1996**, *110*, 753-758.
- [36] H. Umezawa, T. Aoyagi, T. Komiyama, H. Morishima, M. Hamada, T. Takeuchi, *J. Antibiot.* **1974**, *27*, 963-969.
- [37] T. W. Brandstetter, C. de la Fuente, Y.-H. Kim, R. I. Cooper, D. J. Watkin, N. G. Oikonomakos, L. N. Johnson, G. W. J. Fleet, *Tetrahedron* **1996**, *52*, 10711-10720.
- [38] J. C. Estevez, M. D. Smith, A. L. Lane, S. Crook, D. J. Watkin, G. S. Besra, P. J. Brennan, R. J. Nash, G. W. J. Fleet, *Tetrahedron Asymm.* **1996**, *7*, 387-390.
- [39] T. W. Brandstetter, M. R. Wormland, R. A. Dwek, T. D. Butters, F. M. Platt, K. E. Tsitsanou, S. E. Zographos, N. G. Oikonomakos, G. W. J. Fleet, *Tetrahedron Asymm.* **1996**, *7*, 157-170.
- [40] J. C. Estevez, M. D. Smith, M. R. Wormland, G. S. Besra, P. J. Brennan, R. J. Nash, G. W. J. Fleet, *Tetrahedron Asymm.* **1996**, *7*, 391-394.
- [41] M. P. Watterson, L. Pickering, M. D. Smith, S. J. Hudson, P. R. Marsh, J. E. Mordaunt, D. J. Watkin, C. J. Newman, G. W. J. Fleet, *Tetrahedron Asymm.* **1999**, *10*, 1855-1859.
- [42] N. L. Hungerford, G. W. J. Fleet, *J. Chem. Soc. Perkin Trans. 1* **2000**, 3680-3685.
- [43] C. J. F. Bichard, T. W. Brandstetter, J. C. Estevez, G. W. J. Fleet, D. J. Hughes, J. R. Wheatley, J. E. Dyson, *J. Chem. Soc. Perkin Trans. 1* **1996**, *17*, 2151-2156.
- [44] J. S. Brimacombe, L. C. N. Tucker, *Carbohydrate Res.* **1966**, *2*, 341-348.
- [45] J. S. Brimacombe, L. C. N. Tucker, *Carbohydrate Res.* **1965**, *1*, 332-333.
- [46] J. R. Wheatley, C. J. F. Bichard, S. J. Mantell, J. C. Son, D. J. Hughes, G. W. J. Fleet, D. Brown, *J. Chem. Soc., Chem. Commun.* **1993**, *13*, 1065-1067.
- [47] L. Poitout, Y. L. Merrer, J.-C. Depezay, *Tetrahedron Lett.* **1995**, *36*, 6887-6890.
- [48] T. K. Chakraborty, S. Jayaprakash, P. V. Diwan, R. Nagaraj, S. R. B. Jampani, A. C. Kunwar, *J. Am. Chem. Soc.* **1998**, *120*, 12962-12963.
- [49] T. K. Chakraborty, S. Ghosh, S. Jayaprakash, J. A. R. P. Sharma, V. Ravikanth, P. V. Diwan, R. Nagaraj, A. C. Kunwar, *J. Org. Chem.* **2000**, *65*, 6441-6457.

- [50] M. D. Smith, D. D. Long, D. G. Marquess, T. D. W. Claridge, G. W. J. Fleet, *Chem. Commun.* **1998**, 2039-2040.
- [51] M. D. Smith, G. W. J. Fleet, *J. Peptide Sci.* **1999**, 5, 425-441.
- [52] D. D. Long, N. L. Hungerford, M. D. Smith, d. E. A. Brittain, D. G. Marquess, T. d. W. Claridge, G. W. J. Fleet, *Tetrahedron Lett.* **1999**, 40, 2195-2198.
- [53] D. D. Long, S. R. J. E., R. J. Nash, D. G. Marquess, J. D. Lloyd, A. L. Winters, N. Asano, G. W. J. Fleet, *J. Chem. Soc. Perkin Trans. 1* **1999**, 901-908.
- [54] M. D. Smith, D. D. Long, A. Martín, D. G. Marquess, T. D. E. Claridge, G. W. J. Fleet, *Tetrahedron Lett.* **1999**, 40, 2191-2194.
- [55] K. Heyns, H. Paulsen, *Chem. Ber.* **1955**, 108, 188-195.
- [56] T. K. Chakraborty, S. Jayaprakash, S. Ghosh, *Combinatorial Chemistry and High Throughput Screening* **2001**, 4, in press.
- [57] A. Dondoni, M.-C. Scherrmann, A. Marra, *J. Org. Chem.* **1994**, 59, 7517-7520.
- [58] A. Dondoni, M.-C. Scherrmann, *J. Org. Chem.* **1994**, 59, 6404-6412.
- [59] E. Locardi, M. Stöckle, S. Gruner, H. Kessler, *J. Am. Chem. Soc.* **2001**, 123, 8189-8196.
- [60] C. Vogel, P. Gries, *J. Carbohydr. Chem.* **1994**, 13, 37-46.
- [61] E. Kallin, *Meth. Enzymology* **1994**, 242, 221-226.
- [62] L. G. Revel'skaya, A. N. Anikeeva, S. N. Danilov, *Zh. Obshchei Khimii (Engl. Transl.)* **1973**, 43, 1624-1630.
- [63] G. Fodor, L. Ötvös, *Chem. Ber.* **1956**, 89, 701-708.
- [64] J. C. Irvine, D. McNicoll, A. Hynd, *J. Chem. Soc.* **1911**, 11, 250-261.
- [65] D. Mostowicz, M. Chmieliwski, *Carbohydr. Res.* **1994**, 257, 137-143.
- [66] K.-I. Kim, R. I. Hollingsworth, *Tetrahedron Lett.* **1994**, 35, 1031-1032.
- [67] S. J. Hecker, *J. Org. Chem.* **1990**, 55, 6051-6054.
- [68] M. F. Semmelhack, Y. Jiang, D. Ho, *Org. Lett.* **2001**, 3, 2403-2406.
- [69] A. G. Hedenetz, W. Schmidt, F. M. Unger, *A short synthesis of 2,3-diacetamido-2,3-dideoxy-D-mannuronic acid-derivatives*, Ges. Österr. Chem., Innsbruck, **2000**.
- [70] R. Hirschmann, K. C. Nicolaou, S. Pietranico, E. M. Leahy, J. Salvino, B. Arison, M. A. Cichy, P. G. Spoor, W. C. Shakespear, P. A. Sprengeler, P. Hamley, A. B. Smith III, T. Teisine, K. Raynor, L. Maechler, C. Donaldson, W.

- Vale, R. M. Freidinger, M. R. Cascieri, C. D. Strader, *J. Am. Chem. Soc.* **1993**, *115*, 12550-12568.
- [71] M. Bols, *Carbohydrate Building Blocks*, John Wiley & Sons, New York, **1996**.
- [72] T. Wunberg, C. Kallus, T. Opatz, S. Henke, W. Schmidt, H. Kunz, *Angew. Chem. Int. Ed.* **1998**, *37*, 2503-2505.
- [73] F. Schweizer, O. Hindsgaul, *Curr. Opin. Chem. Biol.* **1999**, *3*, 291-298.
- [74] R. Hirschmann, K. C. Nicolaou, S. Pietranico, J. Salvino, E. M. Leahy, P. A. Sprengeler, G. Furst, C. D. Strader, A. B. Smith, III, *J. Am. Chem. Soc.* **1992**, *114*, 9217-9218.
- [75] R. Hirschmann, W. Yao, M. A. Cascieri, C. D. Strader, L. Maechler, M. A. Cichy, J. H. Jr., R. D. v. Rijn, P. A. Sprengler, A. B. Smith III, *J. Med. Chem.* **1996**, *39*, 2441-2448.
- [76] R. H. Hirschmann, John, Jr.; Cichy-Knight, Maria A.; van Rijn, Rachel D.; Sprengeler, Paul A.; Spoor, P. Grant; Shakespeare, William C.; Pietranico-Cole, Sherrie; Barbosa, Joseph; Liu, Josephine; Yao, Wenqing; Rohrer, Susan; Smith, Amos B., III., *J. Med. Chem.* **1998**, *41*, 1382-1391.
- [77] C. Papageorgiou, R. Haltiner, C. Bruns, T. J. Petcher, *Bioorg. Med. Chem. Lett.* **1992**, *2*, 135-140.
- [78] A. B. Smith III, S. Sasho, B. A. Barwis, P. Sprengeler, J. Barbosa, R. Hirschmann, B. S. Cooperman, *Bioorg. Med. Chem. Lett.* **1998**, *8*, 3133-3136.
- [79] K. Kirshenbaum, R. N. Zuckermann, K. A. Dill, *Curr. Opin. Struct. Biol.* **1999**, *9*, 530-535.
- [80] M. J. Soth, J. S. Nowick, *Curr. Opin. Chem. Biol.* **1997**, *1*, 120-129.
- [81] P. H. Seeberger, *Solid support oligosaccharide synthesis and combinatorial carbohydrate libraries*, Wiley, New York, **2001**.
- [82] P. H. Seeberger, W.-C. Haase, *Chem. Rev.* **2000**, *100*, 4349-4393.
- [83] E.-F. Fuchs, J. Lehmann, *Chem. Ber.* **1975**, *108*, 2254-2260.
- [84] E. F. Fuchs, J. Lehmann, *Chem. Ber.* **1975**, *45*, 135-141.
- [85] E. F. Fuchs, J. Lehmann, *Carbohydr. Res.* **1976**, *49*, 267-273.
- [86] E. F. Fuchs, J. Lehmann, *Chem. Ber.* **1976**, *109*, 267-273.
- [87] J. Yoshimura, H. Ando, T. Sato, S. Tsuchida, *Bull. Chem. Soc. Jpn.* **1976**, *49*, 2511-2514.

- [88] C. Müller, E. Kitas, H. P. Wessel, *J. Chem. Soc. Chem. Commun.* **1995**, 2425-2426.
- [89] R. A. J. Goodnow, A.-R. Richou, S. Tam, *Tetrahedron Lett.* **1997**, 38, 3195-3198.
- [90] R. A. J. Goodnow, S. Tam, D. L. Pruess, W. W. McComas, *Tetrahedron Lett.* **1997**, 38, 3199-3202.
- [91] P. Fügedi, C. Peto, in *8th European Carbohydrate Symposium*, Sevilla, Spain, **1995**, p. Abstract A75.
- [92] P. Fügedi, C. Peto, L. Wang, in *9th European Carbohydrate Symposium*, Mailland, Italy, **1996**, p. Abstract B0 013.
- [93] C. Peto, P. Fügedi, K. Wlasichuk, in *8th European Carbohydrate Symposium*, Sevilla, Spain, **1995**, p. Abstract A 74.
- [94] P. Fügedi, C. J. Petö, L. Wang, in *9th European Carbohydrate Symposium*, Utrecht, Netherlands, **1997**, pp. A113-A114.
- [95] P. S. Ramamoorthy, J. Gervay, *J. Org. Chem.* **1997**, 62, 7801-7805.
- [96] J. Gervay, P. s. Ramamoorthy, N. N. Mamuya, *Tetrahedron* **1997**, 53, 11039-11048.
- [97] J. Gervay, T. M. Flaherty, C. Nguyen, *Tetrahedron Lett.* **1997**, 38, 1493-1496.
- [98] Y. Suhara, M. Izumi, M. Ichikawa, M. B. Penno, Y. Ichikawa, *Tetrahedron Lett.* **1997**, 38, 7167-7170.
- [99] C. M. Timmers, J. J. Turner, C. M. Ward, G. A. van der Marel, M. L. C. E. Kouwijzer, P. D. J. Grootenhuis, J. H. van Boom, *Chem. Eur. J.* **1997**, 3, 920-929.
- [100] S.-I. Nishimura, S. Nomura, K. Yamada, *Chem. Commun.* **1998**, 617-618.
- [101] R. M. van Well, H. S. Overkleeft, M. Overhand, E. Vang Carstensen, G. A. van der Marel, J. H. van Boom, *Tetrahedron Lett.* **2000**, 41, 9331-9335.
- [102] M. Stöckle, H. Kessler, in *11th European Carbohydrate Symposium*, Lisbon, **2001**, p. P157.
- [103] M. Stöckle, E. Locardi, S. Gruner, H. Kessler, in *20th International Carbohydrate Symposium* (Ed.: J. Thiem), LCI Publisher GmbH, Hamburg, **2000**, p. 124.
- [104] M. Bols, *Chem. Rev.* **2002**, special issue on Glycobiology.

- [105] G. W. J. Fleet, *Chem. Rev.* **2002**, special issue on Glycobiology.
- [106] R. A. Dwek, *Chem. Rev.* **2002**, special issue on Glycobiology.
- [107] K. H. Park, Y. J. L. Yoon, S. G., *J. Chem. Soc. Perkin Trans. 1* **1994**, 2621-2623.
- [108] K. S. Manning, D. G. Lynn, J. Shabanowitz, L. E. Fellows, M. Singh, B. D. Schrire, *J. Chem. Soc. Chem. Commun.* **1985**, 127.
- [109] I. C. di Bello, P. Dorling, L. Fellows, B. Winchester, *FEBS Lett.* **1984**, 176, 61-64.
- [110] Y. Nishimura, W. Wang, S. Kondo, T. Aoyagi, H. Umezawa, *J. Am. Chem. Soc.* **1988**, 110, 7249-7250.
- [111] Y. Nishimura, E. Shitara, H. Adachi, M. Toyoshima, M. Nakajima, Y. Okami, T. Takeuchi, *J. Org. Chem.* **2000**, 65, 2-11.
- [112] B. P. Bashyal, H.-F. Chow, G. W. J. Fleet, *Tetrahedron Lett.* **1986**, 27, 33205-33208.
- [113] Y. Igarashi, M. Ichikawa, Y. Ichikawa, *Tetrahedron Lett.* **1996**, 37, 2707-2708.
- [114] M. D. Smith, T. D. W. Claridge, G. E. Tranter, M. S. P. Sansom, G. W. J. Fleet, *Chem. Commun.* **1998**, 2041-2042.
- [115] T. D. W. Claridge, D. D. Long, N. L. Hungerford, R. T. Aplin, M. D. Smith, D. G. Marquess, G. W. J. Fleet, *Tetrahedron Lett.* **1999**, 40, 2199-2202.
- [116] T. K. Chakraborty, S. Jayaprakash, P. Srinivasu, M. G. Chary, P. V. Diwan, R. Nagaraj, A. R. Sankar, A. C. Kunwar, *Tetrahedron Lett.* **2000**, 41, 8167-8171.
- [117] E. Lohof, E. Planker, C. Mang, F. Burkart, M. A. Dechantsreiter, R. Haubner, H.-J. Wester, M. Schwaiger, G. Hölzemann, S. L. Goodman, H. Kessler, *Angew. Chem. Int. Ed. Engl.* **2000**, 39, 2761-2764.
- [118] S. Gruner, H. Kessler, in *26th European Peptide Symposium* (Eds.: J. Martinez, J.-A. Fehrentz), Editions Medicales et Scientifiques, Montpellier, France, **2000**, pp. 313-314.
- [119] S. Gruner, V. Truffault, G. Voll, E. Locardi, M. Stöckle, H. Kessler, *Chem. Eur. J.* **2001**, submitted.
- [120] S. A. W. Gruner, G. Kéri, R. Schwab, A. Venetianer, H. Kessler, *Org. Lett.* **2001**, 3, 3723-3725.

- [121] S. Gruner, H. Kessler, G. Kéri, A. Venetianer, in *2nd International/ 17th American Peptide Symposium* (Ed.: M. Lehel), American Peptide Society, San Diego, CA, USA, **2001**, p. accepted.
- [122] B. Aguilera, L. B. Wolf, P. Nieczypor, F. P. Rutjes, H. S. Overkleeft, J. C. van Hest, H. E. Schoemaker, B. Wang, J. C. Mol, A. Furstner, M. Overhand, G. A. van der Marel, J. H. van Boom, *J. Org. Chem.* **2001**, *66*, 3584-3589.
- [123] O. W. Griffith, *Ann. Rev. Biochem.* **1986**, *55*, 855.
- [124] W. Dürckheimer, J. Blumbach, R. Lattrell, K. H. Scheunemann, *Angew. Chem.* **1985**, *97*, 183-205.
- [125] G. Cardillo, C. Tomasini, *Chem. Soc. Rev.* **1996**, *25*, 117-128.
- [126] K. C. Nicolaou, W. M. Dai, R. K. Guy, *Angew. Chem. Int. Ed.* **1994**, *33*, 15-44.
- [127] J. M. Fernandez-Santin, S. Munoz-Guerra, A. Rodriguez-Galan, J. Aymami, J. Lloveras, J. A. Subirana, E. Giralt, M. Ptak, *Macromolecules* **1987**, *20*, 62-68.
- [128] J. M. Fernandez-Santin, J. Aymami, A. Rodriguez-Galan, S. Munoz-Guerra, J. A. Subirana, *Nature (London)* **1984**, *311*, 53-54.
- [129] H. Yuki, Y. Okamoto, Y. Taketani, T. Tsubota, Y. Marubayashi, *J. Polym. Sci., Polym. Chem. Ed.* **1978**, *16*, 2237-2251.
- [130] G. P. Dado, S. H. Gellman, *J. Am. Chem. Soc.* **1994**, *116*, 925-938.
- [131] K. R. Shoemaker, P. S. Kim, E. J. York, J. M. Stewart, R. L. Baldwin, *nature (London)* **1987**, *326*, 563-567.
- [132] P. C. Lyu, M. I. Liff, L. A. Marky, N. R. Kallenbach, *Science* **1990**, *250*, 669-673.
- [133] S. Marqusee, R. L. Baldwin, *Proc. Natl. Acad. Sci. USA* **1987**, *84*, 8898-8902.
- [134] K. T. O'Neil, W. F. DeGrado, *Science* **1990**, *250*, 646-651.
- [135] J. M. Scholtz, R. L. Baldwin, in *Peptides, Synthesis, Structures, and Applications*, Academic press, San Diego, **1995**.
- [136] R. P. Cheng, S. H. Gellman, W. F. DeGrado, *Chem. Rev.* **2001**, *101*, 3219-3232.
- [137] D. H. Appella, L. A. Christianson, I. L. Karle, D. R. Powell, S. H. Gellman, *J. Am. Chem. Soc.* **1996**, *118*, 13071-13072.
- [138] D. Seebach, M. Overhand, F. N. M. Kühnle, B. Martinoni, L. Oberer, U. Hommel, H. Widmer, *Helv. Chim. Acta* **1996**, *79*, 913.

- [139] D. Seebach, J. L. Matthews, *Chem. Commun.* **1997**, 2015-2022.
- [140] D. Seebach, S. Abele, K. Gademann, G. Guichard, T. Hintermann, B. Jaun, J. L. Matthews, J. V. Schreiber, L. Oberer, U. Hommel, H. Widmer, *Helv. Chim. Acta* **1998**, *81*, 932-982.
- [141] D. H. Appella, L. A. Christianson, D. A. Klein, D. R. Powell, X. Huang, J. J. Barchi Jr, S. H. Gellman, *Nature* **1997**, *38*, 381-384.
- [142] H.-S. Lee, F. A. Syud, X. Wang, S. H. Gellman, *J. Am. Chem. Soc.* **2001**, *123*, 7721-7722.
- [143] X. Wang, J. F. Espinosa, S. H. Gellman, *J. Am. Chem. Soc.* **2000**, *122*, 4821-4822.
- [144] J. J. Barchi, Jr., X. Huang, D. H. Appella, L. A. Christianson, S. R. Durell, S. H. Gellman, *J. Am. Chem. Soc.* **2000**, *122*, 2711-2718.
- [145] D. H. Appella, L. A. Christianson, D. A. Klein, M. R. Richards, D. R. Powell, S. H. Gellman, *J. Am. Chem. Soc.* **1999**, *121*, 7574-7581.
- [146] G. Quinkert, E. Egert, C. Griesinger, *Aspects of Organic Chemistry: Structure.*, VCH, Weinheim, **1996**.
- [147] M. A. Ondetti, J. Pluscec, E. R. Weaver, N. Williams, E. F. Sabo, O. Kocy, in *Am. Pept. Symp.*, 3rd (Ed.: J. Meienhofer), Ann Arbor Sci., Ann Arbor, Mich, **1972**, pp. 525-531.
- [148] T. Hintermann, D. Seebach, *Synlett* **1997**, *5*, 437-438.
- [149] D. Seebach, P. E. Ciceri, M. Overhand, B. Jaun, D. Rigo, *Helv. Chim. Acta* **1996**, *79*, 2043-2066.
- [150] D. Seebach, K. Gademann, J. V. Schreiber, J. L. Matthews, T. Hintermann, B. Jaun, *Helv. Chim. Acta* **1997**, *80*, 2033-2038.
- [151] R. Koradi, M. Billeter, K. Wüthrich, *J. Mol. Graphics* **1996**, *14*, 51-55.
- [152] D. Seebach, S. Abele, K. Gademann, B. Jaun, *Angew. Chem. Int. Ed.* **1999**, *38*, 1595-1597.
- [153] D. Seebach, J. L. Matthews, A. Meden, T. Wessels, C. Baerlocher, L. B. McCusker, *Helv. Chim. Acta* **1997**, *80*, 173-182.
- [154] H. S. Overkleeft, S. H. L. Verhelst, E. Pieterman, N. J. Meeuwnoord, M. Overhand, L. H. Cohen, G. A. van der Marel, J. H. van Boom, *Tetrahedron Lett.* **1999**, *40*, 4103-4106.

- [155] R. Haubner, H.-J. Wester, F. Burkhart, R. Senekowitsch-Schmidtke, S. L. Goodman, H. Kessler, M. Schwaiger, *J. Nucl. Med.* **2001**, *42*, 326-336.
- [156] R. Haubner, H.-J. Wester, W. A. Weber, C. Mang, S. I. Ziegler, S. L. Goodman, R. Senekowitsch-Schmidtke, H. Kessler, M. Schwaiger, *Cancer Res.* **2001**, *61*, 1781-1785.
- [157] B. Drouillat, B. Kellam, G. Dekany, M. S. Starr, I. Toth, *Bioorg. Med. Chem. Lett.* **1997**, *7*, 2247-2250.
- [158] D. F. Veber, R. M. Freidinger, D. S. Perlow, W. J. J. Paleveda, F. W. Holly, R. G. Strachan, R. F. Nutt, B. H. Arison, C. Homnick, W. C. Randall, M. S. Glitzer, R. Saperstein, R. Hirschmann, *Nature* **1981**, *292*, 55-58.
- [159] H. Kessler, M. Bernd, H. Kogler, J. Zarbock, O. W. Soerensen, G. Bodenhausen, R. R. Ernst, *J. Am. Chem. Soc.* **1983**, *105*, 6944-6952.
- [160] M. Aumailley, M. Gurrath, G. Müller, J. Calvete, R. Timpl, H. Kessler, *FEBS Lett.* **1991**, *291*, 50.
- [161] P. Brazeau, W. Vale, R. Burgus, R. Guillemin, *Can. J. Biochem* **1974**, *52*, 1067-1072.
- [162] P. Brazeau, W. Vale, R. Burgus, N. Ling, M. Butcher, J. Rivier, R. Guillemin, *Science* **1973**, *179*, 77-79.
- [163] J. Tamarit, J. Tamarit-Rodriguez, R. Goberan, M. Lucas, *Rev. Esp. Fisiol.* **1974**, *30*, 299-301.
- [164] S. E. Christensen, A. P. Hansen, J. Iversen, K. Lundbaek, H. Orskov, K. Seyer-Hansen, *J. Clin. Lab. Invest.* **1974**, *34*, 321-325.
- [165] G. Kéri, J. Erchegyi, A. Horváth, I. Mezo, M. Idei, T. Vántus, À. Balogh, Z. Vadásu, G. Bökönyi, J. Seprodi, I. Teplán, O. Csuka, M. Tejada, D. Gaál, S. Szegedi, B. Szende, C. Roze, H. Kalthoff, A. Ullrich, *Proc. Natl. Acad. Sci. USA* **1996**, *93*, 12513-12518.
- [166] I. Virgolini, *Eur. J. Clin. Invest.* **1997**, *27*, 793-800.
- [167] D. F. Veber, in *6th American Peptide Symposium* (Eds.: E. Gross, J. Meienhofer), Pierce Chem. Co., Rockford, Ill., **1979**, pp. 409-419.
- [168] P. S. Portoghese, *J. Med. Chem.* **1992**, *35*, 1927-1937.
- [169] P. S. Portoghese, M. Sultana, A. E. Takemori, *J. Med. Chem.* **1990**, *33*, 1714-1720.

- [170] G. B. Fields, R. L. Nobel, *Int. J. Pept. Protein Res.* **1990**, *35*, 161-214.
- [171] R. Knorr, A. Trzeciak, W. Bannwarth, D. Gillessen, *Tetrahedron Lett.* **1989**, *30*, 1927-1930.
- [172] J. C. Sheehan, S. L. Ledis, *J. Am. Chem. Soc.* **1973**, *95*, 875-879.
- [173] M. Barbacid, *Annu. Rev. Biochem.* **1987**, *56*, 779-827.
- [174] F. L. Zhang, P. J. Casey, *Annu. Rev. Biochem.* **1996**, *65*, 241-269.
- [175] M. Gurrath, G. Mueller, H. Kessler, M. Aumailley, R. Timpl, *Eur. J. Biochem.* **1992**, *210*, 911-921.
- [176] M. Pfaff, K. Tangemann, B. Müller, M. Gurrath, G. Müller, H. Kessler, R. Timpl, J. Engel, *J. Biol. Chem.* **1994**, *269*, 20233-22038.
- [177] R. Haubner, R. Gratias, B. Diefenbach, S. L. Goodman, A. Jonczyk, H. Kessler, *J. Am. Chem. Soc.* **1996**, *118*, 7461.
- [178] R. Haubner, D. Finsinger, H. Kessler, *Angew. Chem. Int. Ed. Engl.* **1997**, *36*, 1374-1389.
- [179] R. Haubner, D. Finsinger, H. Kessler, *Angew. Chem.* **1997**, *109*, 1440.
- [180] H. Kessler, B. Diefenbach, D. Finsinger, A. Geyer, M. Gurrath, S. L. Goodman, G. Hoelzemann, R. Haubner, A. Jonczyk, G. Müller, E. Graf von Roedern, J. Wermuth, *Lett. Pept. Sci.* **1995**, *2*, 155-160.
- [181] K. C. Nicolaou, J. I. Trujillo, K. Chibale, *Tetrahedron* **1997**, *53*, 8751-8778.
- [182] A. C. Bach, II, J. R. Espina, S. A. Jackson, P. F. W. Stouten, J. L. Duke, S. A. Mousa, W. F. DeGrado, *J. Am. Chem. Soc.* **1996**, *118*, 293-294.
- [183] R. Haubner, H.-J. Wester, M. Bock, R. Senekowitsch-Schmidtke, M. Herz, U. Reuning, B. Diefenbach, G. Stöcklin, H. Kessler, M. Schwaiger, *J. Lab. Compds. Radiopharm.* **1999**, *42*, 36.
- [184] S. Gruner, E. Locardi, M. Stöckle, H. Kessler, in *20th International Carbohydrate Symposium* (Ed.: J. Thiem), LCI Publisher GmbH, Hamburg, Germany, **2000**, p. B132.
- [185] S. Gruner, H. Kessler, in *GDCh Jahrestagung 2001, Vol. Symposium der Liebig-Vereinigung für Organische Chemie und Karl-Ziegler-Stiftungssymposium*, Media Process Management GmbH, Mainz, ISBN 3-924763-99-2, Würzburg, Germany, **2001**, p. 56.

- [186] L. N. Kulinkovich, V. A. Timoshchuk, *J. Gen. Chem. USSR (Engl. Transl.)* **1983**, *53*, 1917-1922.
- [187] M. Yamashita, Y. Kawai, I. Uchida, T. Komori, M. Koshaka, H. Imanaka, K. Sakane, H. Setoi, T. Teraji, *Tetrahedron Lett.* **1984**, *41*, 4689-4692.
- [188] L. Daley, C. Monneret, C. Gautier, P. Roger, *Tetrahedron Lett.* **1992**, *33*, 3749-3752.
- [189] H. H. Baer, Y. Gan, *Carbohydr. Res.* **1991**, *210*, 233-245.
- [190] J. M. G. Fernández, C. O. Mellet, J. L. J. Blanco, J. Fuentes, *J. Org. Chem.* **1994**, *59*, 5565-5572.
- [191] S. Gruner, H. Kessler, in *26th European Peptide Symposium*, Editions Médicales et Scientifiques, Montpellier, France, **2000**, p. P72.
- [192] L. A. Carpino, A. El-Faham, F. Albericio, *Tetrahedron Lett.* **1994**, *35*, 2279-2282.
- [193] L. A. Carpino, A. El-Faham, C. A. Minor, F. Albericio, *J. Chem. Soc. Chem. Commun.* **1994**, *2*, 201-203.
- [194] R. Bollhagen, M. Schmiedberger, K. Barlos, E. Grell, *J. Chem. Soc., Chem. Commun.* **1994**, *22*, 2559-2560.
- [195] D. Seebach, S. Abele, T. Sifferlen, M. Hänggi, S. Gruner, P. Seiler, *Helv. Chim. Acta* **1998**, *81*, 2218-2243.
- [196] K. A. Bode, J. Applequist, *Macromolecules* **1997**, *30*, 2144-2150.
- [197] J. Applequist, K. A. Bode, D. H. Appella, L. A. Christianson, S. H. Gellman, *J. Am. Chem. Soc.* **1998**, *120*, 4891-4892.
- [198] H. E. Stanger, S. H. Gellman, *J. Am. Chem. Soc.* **1998**, *120*, 4236-4237.
- [199] H. L. Schenck, S. H. Gellman, *J. Am. Chem. Soc.* **1998**, *120*, 4869-4870.
- [200] M. Brenner, D. Seebach, *Helv. Chim. Acta* **2001**, *84*, 1181-1189.
- [201] L. Braunschweiler, R. R. Ernst, *J. Magn. Reson.* **1983**, *53*, 521-528.
- [202] W. P. Aue, E. Bartholdi, R. R. Ernst, *J. Chem. Phys.* **1976**, *64*, 2229-2246.
- [203] L. Müller, *J. Am. Chem. Soc.* **1979**, *101*, 4481-4484.
- [204] A. Bax, M. J. Summers, *J. Am. Chem. Soc.* **1986**, *108*, 2093-2094.
- [205] J. Jeener, B. H. Meyer, P. Bachman, R. R. Ernst, *J. Chem. Phys.* **1979**, *71*, 4546-4553.

- [206] A. T. Brünger, in *x-plor*, 3.851 ed., Yale University Press, New Haven, CT, **1992**.
- [207] Discover,, 2.9.7 ed., Biosym/molecular Simulations, San Diego, CA, **1995**.
- [208] K. Möhle, R. Günther, M. Thormann, N. Sewald, H.-J. Hofmann, *Biopolymers* **1999**, *50*, 167-184.
- [209] R. Günther, H.-J. Hofmann, *J. Phys. Chem. B* **2001**, *105*, 5559-5567.
- [210] R. Günther, PhD thesis, University of Leipzig (Leipzig), **2001**.
- [211] C. A. G. Haasnoot, F. A. A. M. de Leeuw, H. P. M. de Leeuw, C. Altona, *Org. Mag. Reson.* **1981**, *15*, 43-52.
- [212] J. E. Kilpatrick, K. S. Pitzer, R. Spitzer, *J. Am. Chem. Soc.* **1947**, *69*, 2483-2488.
- [213] C. Altona, H. J. Geise, C. Romers, *Tetrahedron* **1968**, *24*, 13-32.
- [214] H. P. M. De Leeuw, C. A. G. Haasnoot, C. Altona, *Isr. J. Chem.* **1980**, *20*, 108-126.
- [215] J. L. Matthews, M. Overhand, F. N. M. Kühnle, P. E. Ciceri, D. Seebach, *Liebigs Ann. Chem.* **1997**, 1371-1379.
- [216] P. Brazeau, W. Vale, R. Burgus, N. Ling, M. Butcher, J. Rivier, R. Guillemin, *Science* **1973**, *179*, 77-79.
- [217] R. Guillemin, *Metabolism* **1993**, *41*, 1-4.
- [218] L. Pradayrol, H. Joernvall, V. Mutt, A. Ribet, *FEBS Lett.* **1980**, *109*, 55-58.
- [219] R. Benoit, F. Esch, H. P. J. Bennett, N. Ling, M. Ravazzola, L. Orci, E. J. Mufson, *Metab., Clin. Exp.* **1990**, *39*, 22-25.
- [220] Y. C. Patel, C. B. Srikant, *Trends Endocrinol. Metab.* **1997**, *8*, 398-405.
- [221] D. Damour, F. Herman, R. Labaudiniere, G. Pantel, M. Vuilhorgne, S. Mignani, *Tetrahedron* **1999**, *55*, 10135-10154.
- [222] D. Seebach, S. Abele, J. V. Schreiber, B. Martinoni, A. Nussbaum, H. Schild, H. Schulz, Hennecke, R. woessner, F. Bitsch, *Chimia* **1998**, *52*, 734-739.
- [223] K. Gademann, T. Kimmerlin, D. Hoyer, D. Seebach, *J. Med. Chem.* **2001**, *44*, 2460-2468.
- [224] T. Kimmerlin, D. Hoyer, D. Seebach, in *2nd International/ 17th American Peptide Symposium* (Ed.: M. Lehel), American Peptide Society, San Diego, CA, USA, **2001**.

- [225] L. Yang, S. C. Berk, S. P. Rohrer, R. T. Mosley, L. Guo, D. J. Underwood, B. H. Arison, E. T. Birzin, E. C. Hayes, S. W. Mitra, R. M. Parmar, K. Cheng, T.-J. Wu, B. S. Butler, F. Foor, A. Pasternak, Y. Pan, M. Silva, R. M. Freidinger, R. G. Smith, K. Chapman, J. M. Schaeffer, A. A. Patchett, *Proc. Natl. Acad. Sci. USA* **1998**, *95*, 10836-10841.
- [226] L. Yang, L. Guo, A. Pasternak, R. Mosley, S. P. Rohrer, E. T. Birzin, F. Foor, K. Cheng, J. Schaeffer, A. A. Patchett, *J. Med. Chem.* **1998**, *41*, 2175-2179.
- [227] M. Ankersen, M. Crider, S. Liu, B. Ho, H. S. Andersen, C. Stidsen, *J. Am. Chem. Soc.* **1998**, *120*, 1368-1373.
- [228] S. P. Rohrer, E. T. Birzin, R. T. Mosley, S. C. Berk, S. M. Hutchins, D.-M. Shen, Y. Xiong, E. C. Hayes, R. M. Parmar, F. Foor, S. W. Mitra, S. J. Degrado, M. Shu, J. M. Klopp, S.-J. Cai, A. Blake, W. W. S. Chan, A. Pasternak, L. Yang, A. A. Patchett, R. G. Smith, K. T. Chapman, J. M. Schaeffer, *Science* **1998**, *282*, 737-740.
- [229] Y. C. Patel, M. T. Greenwood, R. Panetta, L. Demchyshyn, H. Niznik, C. B. Srikant, *Life Sci.* **1995**, *57*, 1249-1265.
- [230] T. Reisine, G. I. Bell, *Endocrinol. Rev* **1995**, *16*, 427-442.
- [231] S. W. J. Lamberts, A.-J. van Der Lely, W. W. de Herder, L. J. Hofland, *N. Engl. J. Med.* **1996**, *334*, 246-254.
- [232] Y. C. Patel, *J. Endocrinol. Invest.* **1997**, *20*, 348-367.
- [233] Y. Yamada, S. Kagimoto, A. Kubota, K. Yasuda, K. Masuda, Y. Someya, Y. Ihara, Q. Li, H. Imura, S. Seino, Y. Seino, *Biochem. Biophys. Res. Commun.* **1993**, *195*, 844-852.
- [234] Y. Yamada, S. R. Post, K. Wang, H. S. Tager, G. I. Bell, S. Seino, *Proc. Natl. Acad. Sci. USA* **1992**, *89*, 251-255.
- [235] R. Panetta, M. T. Greenwood, A. Warszynska, L. L. Demchyshyn, R. Day, H. B. Niznik, C. B. Srikant, Y. C. Patel, *Mol. Pharmacol.* **1994**, *45*, 417-427.
- [236] J. F. Bruno, Y. Xu, J. Song, M. Berelowitz, *Proc. Natl. Acad. Sci. USA* **1992**, *89*, 11151-11155.
- [237] A. M. O'Carroll, S. J. Lolait, M. Koenig, L. C. Mahan, *Mol. Pharmacol.* **1992**, *42*, 939-946.

- [238] L. Rohrer, F. Raulf, C. Bruns, R. Buettner, F. Hofstaedter, R. Schuele, *Proc. Natl. Acad. Sci. USA* **1993**, *90*, 4196-4200.
- [239] Y. C. Patel, *Front. Neuroendocrinol.* **1999**, *20*, 157-198.
- [240] Y. C. Patel, K. K. Murthy, E. E. Escher, D. Banville, J. Spiess, C. B. Srikant, *Metab., Clin. Exp.* **1990**, *39*, 63-69.
- [241] J. C. Reubi, U. Horisberger, A. Kappeler, J. A. Laissue, *Blood* **1998**, *92*, 191-197.
- [242] A.-M. O'Carroll, K. Raynor, S. J. Lolait, T. Reisine, *Mol. Pharmacol.* **1994**, *46*, 291-298.
- [243] C. Liebow, C. Reilly, M. Serrano, A. V. Schally, *Proc. Natl. Acad. Sci. USA* **1989**, *86*, 2003+2007.
- [244] S. W. J. Lamberts, E. P. Krenning, J. C. Reubi, *Endocrinol. Rev* **1991**, *12*, 450-482.
- [245] L. J. Hofland, H. A. Visser-Wisselaar, S. W. J. Lamberts, *Biochem. Pharmacol.* **1995**, *50*, 287-297.
- [246] I. Lewis, in *2nd International Peptide Symposium in conjunction with the 17th American Peptide Symposium*, American Peptide Society, San Diego, CA, USA, **2001**, p. L68.
- [247] C.-C. Diaconu, M. Szathmári, G. Kéri, A. Venetianer, *Br. J. Cancer* **1999**, *80*, 1197-1203.
- [248] C. Scarpignato, I. Pelosini, *Chemotherapy* **2001**, *47*, 1-29.
- [249] V. T. Devita, *Principles of cancer management: Chemotherapy*, 5 ed., Lippincott Williams & Wilkins, Philadelphia, **1997**.
- [250] D. S. Fisher, K. M. Tish, H. J. Durivage, *The Cancer Chemotherapy Handbook*, St Louis, **1997**.
- [251] D. C. Baquiran, J. Gallagher, *Lippincott's Cancer Chemotherapy Handbook*, 5 ed., Lippincott Williams & Wilkins, Philadelphia, **1998**.
- [252] R. T. Skeel, *Handbook of Cancer Chemotherapy*, 5 ed., Lippincott Williams & Wilkins, Philadelphia, **1999**.
- [253] D. J. Kwekkeboom, E. P. Krenning, S. W. J. Lamberts, *Prog. Basic Clin. Pharmacol.* **1996**, *10*, 281-294.
- [254] K. J. O'Byrne, D. N. Carney, *Anti-Cancer Drugs* **1996**, *7*, 33-44.

- [255] G. A. Wiseman, L. K. Kvols, *Semin. Nucl. Med.* **1995**, *25*, 272-278.
- [256] E. P. Krenning, R. Valkema, P. P. Kooij, W. A. Breeman, W. H. Bakker, W. W. de Herder, C. H. van Eijck, D. J. Kwekkeboom, M. de Jong, S. Pauwels, *Ital. J. Gastroenterol. Hepatol.* **1999**, *31*, S219-S223.
- [257] H. Steller, *Science* **1995**, *267*, 1445-1449.
- [258] G. Kroemer, P. Petit, N. Zamzami, J.-L. Vayssiere, B. Mignotte, *FASEB J.* **1995**, *9*, 1277-1287.
- [259] S. Nagata, P. Golstein, *Science* **1995**, *267*, 1449-1456.
- [260] C. B. Thompson, *Science* **1995**, *267*, 1456-1462.
- [261] V. De Laurenzi, G. Melino, *nature* **2000**, *406*, 135-136.
- [262] S. Talapatra, C. B. Thompson, *J. Pharmacol. Exp. Ther.* **2001**, *298*, 873-878.
- [263] G. Kéri, I. Mezo, Z. Vadasz, A. Horvath, M. Idei, T. Vantus, A. Balogh, G. Bokonyi, T. Bajor, I. Teplán, J. Tamas, M. Mak, A. Horváth, O. Csuka, *Pept. Res.* **1993**, *6*, 281-288.
- [264] A. Stetak, A. Lankenau, T. Vantus, P. Csermely, A. Ullrich, G. Keri, *Biochem. Biophys. Res. Commun.* **2001**, *285*, 483-488.
- [265] W. Vale, M. Brown, C. Rivier, M. Perrin, J. Rivier, in *Brain Pept.: New Endocrinol., Proc. Argenteuil Symp., 4th* (Eds.: A. M. Gotto, Jr., E. J. Peck, Jr., A. E. Boyd, III.), Elsevier, Amsterdam, Neth, **1979**, pp. 71-88.
- [266] A. Janecka, M. Zubrzycka, T. Janecki, *J. Pept. Res.* **2001**, *58*, 91-107.
- [267] B. H. Arison, R. Hirschmann, D. F. Veber, *Bioorg. Chem.* **1978**, *7*, 447-451.
- [268] K. Hallenga, G. van Binst, M. Knappenberg, J. Brison, A. Michel, J. Dirx, *Biochim. Biophys. Acta* **1979**, *577*, 82-101.
- [269] W. Bauer, U. Briner, W. Doepfner, R. Haller, R. Huguenin, P. Marbach, T. J. Petcher, J. Pless, *Life Sci.* **1982**, *31*, 1133-1140.
- [270] H. Kessler, M. Bernd, I. Damm, *Tetrahedron Lett.* **1982**, *23*, 4685-4688.
- [271] H. Kessler, V. Eiermann, *Tetrahedron Lett.* **1982**, *23*, 4689-4692.
- [272] J. Pless, *Chemical Structure- Pharmacological profile of Sandostatin*, Springer, Berlin, **1989**.
- [273] G. Van Binst, D. Tourwe, *Pept. Res.* **1992**, *5*, 8-13.
- [274] J. Rivier, M. Brown, W. Vale, *Biochem. Biophys. Res. Commun.* **1975**, *65*, 746-751.

- [275] J. L. Fauchere, C. Thurieau, *Adv. Drug Res.* **1992**, *23*, 127-159.
- [276] D. F. Veber, F. W. Holly, R. F. Nutt, S. J. Bergstrand, S. F. Brady, R. Hirschmann, M. S. Glitzer, R. Saperstein, *nature (London)* **1979**, *280*, 512-514.
- [277] D. F. Veber, F. W. Holly, W. J. Paleveda, R. F. Nutt, S. J. Bergstrand, M. Torchiana, M. S. Glitzer, R. Saperstein, R. Hirschmann, *Proc. Natl. Acad. Sci. USA* **1978**, *75*, 2636-2640.
- [278] D. F. Veber, in *12th American Peptide Symposium* (Eds.: J. A. Smith, J. E. Rivier), ESCOM, Leiden, Cambridge, MA, USA, **1992**, pp. 3-14.
- [279] D. F. Veber, R. Saperstein, R. F. Nutt, R. M. Freidinger, S. F. Brady, P. Curley, D. S. Perlow, W. J. Paleveda, C. D. Colton, e. al., *Life Sci.* **1984**, *34*, 1371-1378.
- [280] W. A. Murphy, V. A. Lance, S. Moreau, J. P. Moreau, D. H. Coy, *Life Sci.* **1987**, *40*, 2515-2522.
- [281] J. E. Taylor, A. E. Bogden, J. P. Moreau, D. H. Coy, *Biochem. Biophys. Res. Commun.* **1988**, *153*, 81-86.
- [282] J. Tovari, B. Szende, J. Bocsi, A. Falaschi, A. Simoncsits, S. Pongor, J. Erchegy, A. Stetak, G. Keri, *Cell. Signalling* **1998**, *10*, 277-282.
- [283] C. Zhou, L. Guo, G. Morriello, A. Pasternak, Y. Pan, S. P. Rohrer, E. T. Birzin, S.-E. W. Huskey, T. Jacks, K. D. Schleim, K. Cheng, J. M. Schaeffer, A. A. Patchett, L. Yang, *Bioorg. Med. Chem. Lett.* **2001**, *11*, 415-417.
- [284] L. Yang, *Annu. Rep. Med. Chem.* **1999**, *34*, 209-218.
- [285] A. Pasternak, Y. Pan, D. Marino, P. E. Sanderson, R. Mosley, S. P. Rohrer, E. T. Birzin, Huskey, S.-E. Wu, T. Jacks, K. D. Schleim, K. Cheng, J. M. Schaeffer, A. A. Patchett, L. Yang, *Bioorg. Med. Chem. Lett.* **1999**, *9*, 491-496.
- [286] N. Marks, F. Stern, *FEBS Lett.* **1975**, *55*, 220-224.
- [287] S. R. Chhabra, B. Hothi, D. J. Evans, P. D. White, B. W. Bycroft, W. C. Chan, *Tetrahedron Lett.* **1998**, *39*, 1603-1606.
- [288] T. Shioiri, K. Ninomiya, S. Yamada, *J. Am. Chem. Soc.* **1972**, *94*, 6203-6205.
- [289] S. F. Brady, W. J. Paleveda, B. H. Arison, R. M. Freidinger, R. F. Nutt, D. F. Veber, in *8th Am. Pept. Symp.* (Eds.: V. J. Hruby, D. H. Rich), Pierce Chem. Co., Rockford, Ill, USA, Tuscon, Arizona, USA, **1983**, pp. 127-130.
- [290] A. Venetianer, Z. Pinter, A. Gal, *Cytogenet. Cell Genet.* **1980**, *28*, 280-283.

- [291] M. Pirity, A. Hever-Szabo, A. Venetianer, *Cytotechnology* **1996**, *19*, 207-214.
- [292] D. A. Scudiero, R. H. Shoemaker, H. Robert, K. D. Paull, A. Monks, S. Tierney, T. H. Nofziger, M. J. Currens, D. Seniff, M. R. Boyd, *Cancer Res.* **1988**, *48*, 4827-4833.
- [293] N. W. Roehm, G. H. Rodgers, S. M. Hatfield, A. L. Glasebrook, *J. Immun. Methods* **1991**, *142*, 257-265.
- [294] A. T. C. C. reference, in *American Type Culture Collection*, <http://phage.atcc.org/cgi-bin/searchengine/longview.cgi?view=ce,663682,CRL-1555&text=a-431>, **2001**, pp. <http://phage.atcc.org/cgi-bin/searchengine/longview.cgi?view=ce,663682,CRL-661555&text=a-663431>.
- [295] G. Kéri, J. Szolcsányi, E. Pintér, Z. Helyes, J. Érchehyi, A. Horváth, J. Horvath, I. Teplán, L. Örfi, in *A5013-9535-PT*, Biostatin, USA, **1998**.
- [296] E. Pinter, J. Szolcsanyi, *Neurosci. Lett.* **1996**, *212*, 33-36.
- [297] J. Szolcsanyi, in *Neurog. Inflammation* (Eds.: P. Geppetti, P. Holzer), CRC, Boca Raton, USA, **1996**, pp. 33-42.
- [298] J. Szolcsanyi, R. Porszasz, G. Pethö, in *Peripheral neurons in nociception: physio-pharmacological aspects* (Eds.: J. M. Besson, G. Gialbaud, I. Ollat), John Libbey, Eurotext, Paris, France, **1994**, pp. 109-124.
- [299] A. Lecci, C. A. Maggi, *Regul. Pept.* **2001**, *101*, 1-18.
- [300] C. A. Maggi, *Prog. Neurobiol. (Oxford)* **1995**, *45*, 1-98.
- [301] J. Szolcsanyi, in *Capsaicin Study Pain* (Ed.: J. N. Wood), Publisher: Academic, London, **1993**, pp. 1-26.
- [302] Z. Helyes, J. Nemeth, E. Pinter, J. Szolcsanyi, *Br. J. Pharmacol.* **1997**, *121*, 613-615.
- [303] J. Nemeth, Z. Helyes, T. Gorcs, J. Gardi, E. Pinter, J. Szolcsanyi, *Acta Physiol. Hung.* **1996**, *84*, 313-315.
- [304] L. D. Hall, D. C. Miller, *Carbohydr. Res.* **1976**, *47*, 299-305.
- [305] R. W. Binkley, M. G. Ambrose, D. G. Hehemann, *J. Org. Chem.* **1980**, *45*, 4387-4391.
- [306] A. Gomtsyan, I. Savelyeva, S. Belyakov, I. Kalvinsh, *Carbohydr. Res.* **1992**, *232*, 341-348.

- [307] A. L. Smith, J. Neduvélil, G., in *Solid-Phase Organic Syntheses, Vol. 1* (Ed.: A. W. Czarnik), John Wiley & Sons, New York, **2001**, pp. 113-120.